



**University of
Nottingham**

UK | CHINA | MALAYSIA

Specialty Natural Rubber Latex and Latex Foam Products Made Therefrom

by

ROSLIM BIN RAMLI @ LIM CHAI

Thesis submitted to the University of Nottingham
for the degree of **Doctor of Philosophy**

September 2022

Abstract

Specialty natural rubber (SpNR) latex is a modified form of natural rubber (NR) latex, a colloidal natural polymer harvested from rubber trees known as *Hevea brasiliensis*. To date, there is limited information on the use of SpNR latex in latex foam products, possibly due to low total solid content (TSC), of which, for the production of latex foam products, the minimum TSC of the latex should be at least 60 %. In this study, a new generation of SpNR latex has been developed. Unlike the traditional method, which requires a processed latex known as low-ammonia NR (LATZ) latex as the starting material, SpNR latex in this study is produced directly from freshly tapped NR latex. Two varieties of SpNR latex: deproteinized natural rubber (DPNR) latex and epoxidized natural rubber (ENR) latex were produced. DPNR latex is prepared via a heat enzymatic hydrolysis process, whilst ENR latex is prepared via an *in-situ* epoxidation chemical modification process. Afterward, both DPNR and ENR latex were concentrated to a TSC of 60% via ultrafiltration process using membrane separation technology. The physicochemical properties of the SpNR latex were determined, and found to be slightly different to the commercial LATZ latex. Nevertheless, the availability of SpNR latex at 60% TSC, allows SpNR latex to be used to produce latex foam. In this study, the foamability and subsequent stability of the SpNR latex were evaluated, and hence the compounding, foaming, and gelling formulations to produce latex foam were developed. Additionally, this study found that DPNR latex can be used to produce latex foams in the three intended densities of high, medium, and low-density. However, for ENR latex, only high- and medium-density latex foams have been successfully produced. The lower the density the softer the material. Therefore, these findings suggest that DPNR latex foam is a better choice compared to ENR latex foam for certain latex foam products, especially when the latex foam products require light-weight and soft properties.

Suitable latex foam products made from SpNR latex were identified. The first product developed is latex foam pillows from DPNR latex. Unlike conventional pillows, the DPNR latex foam pillows were produced in a cervical shape with a unique dual density. The purpose of producing pillows with such structures is to improve pressure-relief performance, which is an important feature for therapeutic pillows application to improve sleep quality. The extraordinary properties of DPNR latex foam, such as good support properties, pressure-relief are also beneficial for other cushioning product applications. Thus, seat cushions have been produced with aims to substitute the conventional seat cushions made from polyurethane used in the transportation industry. The developed DPNR latex foam shows good vibration isolation performance, suitable for seat cushions intended for the transportation industry that require the isolation of higher

frequency vibrations such as high-speed crafts, trains, and trucks. Apart from cushioning products, the porous structure of SpNR latex foam is also useful for noise and vibration control applications such as acoustic foam materials in buildings and the transportation industry. The results show that the acoustic properties of SpNR latex foam are comparable with those of commercial grade synthetic foam. Nevertheless, in order to utilize SpNR latex foam for buildings and the transportation industry, the thermal stability of SpNR latex foam must be improved to meet fire safety criteria. Oil palm fiber trunk biochar (OPTB) was incorporated as a flame-retardant agent into SpNR latex foam. The addition of OPTB to SpNR latex foam up to 24 phr improved the thermal stability of the material, but was not sufficient to meet fire rating requirements for building applications. However, the study found that the addition of OPTB to SpNR latex foam increased the dimensional stability, elongation at break and hardness of the SpNR latex foam. In addition to that, the OPTB/SpNR latex foam composite also has a high-damping property, making it appropriate for applications that require impact absorption, for example, in transportation industry, where a high level of crashworthiness is a key aspect to improve the safety of the transport vehicle.

It can be concluded that SpNR latex foam produced in this study is suitable to manufacture latex foam products. Cushioning products such as pillows and seat cushions have been successfully produced. The SpNR latex foam is also beneficial for sound and vibration control applications in the building and transportation industry, thus indicating that the application of latex foam can be broadened beyond its traditional bedding applications.

Acknowledgments

In the name of Allah, the Most Gracious and the Most Merciful.

Alhamdulillah. I thank God Almighty for the numerous mercies bestowed upon me in my times of tension, suffering, and ecstasy. My humblest gratitude to the holy Prophet Muhammad (Peace be upon him) whose way of life has been a continuous guidance for me. It would not be possible to finish this thesis without the help of many kind people surrounding me, especially when my PhD journey was interrupted by the pandemic COVID-19. I would like to gratefully acknowledge those who have contributed to this thesis and supported me during my PhD study.

First and foremost, I would like to thank my supervisor, Associate Professor Ir. Dr. Ai Bao Chai for her technical supervision, helpful assistance, and encouraging association throughout the period of my research work at the University of Nottingham, Malaysia. I am grateful to Associate Professor Dr. Jee Hou Ho, my co-supervisor, who is also the Director of Research Department in the Mechanical, Materials, and Manufacturing Engineering, University of Nottingham, Malaysia, for his advice and guidance throughout the research period. I am thankful to Associate Professor Dr. Davide S. A. De Focatiis, my co-supervisor from the Faculty of Engineering, University of Nottingham, United Kingdom, for his valuable discussions and constructive criticisms throughout this study. My sincere thanks to Dr. Shamsul Kamaruddin, my co-supervisor at the Malaysian Rubber Board, for his technical support, great discussions and continuous motivation. I am particularly thankful to Dr. Fatimah Rubaizah Mohd. Rasdi from the Malaysian Rubber Board and Professor Dr. Robert Thomas Bachmann from the Universiti Kuala Lumpur for their help and effort on our collaboration work. I also would like to thank Ahmad Syaheer Abu Aswad, Hishamudin Samat, Suhaimie Mohamed, Mohd. Yazid Suboh, and Mohd. Affarizan Zainal Anuar for their technical assistance during the duration of the study. I would like to express my gratitude to the Malaysian Rubber Board for providing the financial support during the period in which this research work was carried out. Finally, I want to thank my beloved parents, Siti Binti Elias and my late father Allahyarham Ramli @ Lim Chai Bin Abdullah for their love and inspiration. I also want to express my love and gratitude to my wife Siti Shuhada Binti Shuib and daughter, Raisha Rizqin Binti Roslim who have supported me and given me encouragement throughout the entire time of my study.

May Allah bless us.

Roslim Bin Ramli @ Lim Chai
September 2022

List of publications and contributions

Journal

1. Roslim Ramli, Chai Ai Bao, Shamsul Kamaruddin, Fatimah Rubaizah Mohd. Rasdi, Azira Abdul Aziz, Tan Kim Song, Mok Kok Lang, and Ho Jee Hou, (2020). Preliminary study on epoxidized natural rubber latex composites intended for shoe soles application. *International Journal of Emerging Trends in Engineering Research*.
<https://doi.org/10.30534/ijeter/2020/1781.22020>
2. Roslim Ramli, Chai Ai Bao, Shamsul Kamaruddin, Fatimah Rubaizah Mohd. Rasdi, Ho Jee Hou, and Davide S.A. De Focatiis, (2021). Preparation and characterization of specialty natural rubber latex concentrate. *Rubber Chemistry and Technology*.
<https://doi.org/10.5254/RCT.21.79945>
3. Roslim Ramli, Chai Ai Bao, Shamsul Kamaruddin, Fatimah Rubaizah Mohd. Rasdi, Ho Jee Hou, and Davide S.A. De Focatiis, (2021). Specialty natural rubber latex foam: Foamability study and fabrication process. *Rubber Chemistry and Technology*.
<https://doi.org/10.5254/rct.21.78938>
4. Roslim Ramli, Chai Ai Bao, Shamsul Kamaruddin, Fatimah Rubaizah Mohd. Rasdi, Ho Jee Hou, and Davide S.A. De Focatiis, (2021). Development of latex foam pillows from deproteinized natural rubber latex. *Journal of Rubber Research*.
<https://doi.org/10.1007/s42464-021-00130-7>
5. Roslim Ramli, Ai Bao Chai, Shamsul Kamaruddin, Jee Hou Ho, Davide S.A. De Focatiis and Kok Thai Goh. (2022). Natural rubber latex foam technology for bedding industry. *Science, Engineering and Health Studies*.
<https://li01.tci-thaijo.org/index.php/sehs/article/view/256626/175205>
6. Roslim Ramli, Ai Bao Chai, Shamsul Kamaruddin, Fatimah Rubaizah Mohd. Rasdi, Jee Hou Ho, and Davide S.A. De Focatiis. The acoustic properties of latex foam made deproteinized natural rubber latex and epoxidized natural rubber latex. *Journal of Rubber Research*.
<https://doi.org/10.1007/s42464-022-00178-z>
7. Roslim Ramli, Ai Bao Chai, Shamsul Kamaruddin, Fatimah Rubaizah Mohd. Rasdi, Jee Hou Ho, Davide S.A. De Focatiis, Siew Kooi Ong and Robert T. Bachmann. Effect of oil palm biochar on the thermal stability and acoustic properties of specialty natural rubber latex foam. Paper submitted to the *Journal of Rubber Research*. Manuscript ID:

JRUR-D-22-00069 under review.

Conference

1. Roslim Ramli, Ai Bao Chai, Shamsul Kamaruddin, Jee Hou Ho, and Davide S.A. De Focatiis. Development of deproteinized natural rubber latex foam for seat cushions. Paper presented at the 8th International Conference on Material Science & Smart Materials (MSSM2022), Brunel University of London, United Kingdom. 11–13 July 2022.
2. Roslim Ramli, Ai Bao Chai, Shamsul Kamaruddin, Jee Hou Ho, and Davide S.A. De Focatiis. Compressive stress-strain and rebound-resilience properties of a novel deproteinized natural rubber latex foam. Paper presented at the 8th International Conference on Material Science & Smart Materials (MSSM2022), Brunel University of London, United Kingdom. 11–13 July 2022.

Poster

1. Roslim Ramli, Chai Ai Bao, Shamsul Kamaruddin, Ho Jee Hou and Davide S.A. De Focatiis. Deproteinized natural rubber latex foam. Poster presented at the 8th *International Symposium on Applied Engineering and Science (SAES2020)*, Kyushu Institute of Technology, Fukuoka, Japan. Virtual Conference / 12-19 December 2020.
2. Roslim Ramli, Chai Ai Bao, Shamsul Kamaruddin, Ho Jee Hou and Davide S.A. De Focatiis. Natural rubber latex foam composites. Poster presented at the *University of Nottingham Postgraduate Showcase*, University of Nottingham, Malaysia. Virtual Showcase / 9 December 2021.

Award/Exhibition

1. **Gold Medal Award.** Roslim Ramli, Chai Ai Bao, Shamsul Kamaruddin, Ho Jee Hou and Davide S.A. De Focatiis. Development of latex foam pillows from deproteinized natural rubber latex. Video presented at the *Virtual Melaka International Intellectual Exhibition (V-MIIE2021)*, Melaka, Malaysia. Virtual exhibition / 2 - 3 July 2021.
2. **Gold Medal Award.** Roslim Ramli, Chai Ai Bao, Shamsul Kamaruddin, Ho Jee Hou and Davide S.A. De Focatiis. Acoustic foam material made of epoxidized natural rubber latex. Video presented at the *International EUREKA Innovation Exhibition 2021 (iEIE2021)*, Kedah, Malaysia. Virtual exhibition / 18 - 22 October 2021.
3. **IKM Research Prize in Polymer and Materials Science 2022.** Roslim Ramli. Best PhD. candidates. Institut Kimia Malaysia. 2 December 2022.

Contents

Abstract	i
Acknowledgements	iii
List of publications and contributions	iv
List of tables	xii
List of figures	xiv
List of abbreviation	xviii
1 Introduction	
1.1 Background and study justification	1
1.2 Problem statement	3
1.3 Aim and objectives	3
1.4 Conceptual framework and discussion of its novelty	4
1.5 Thesis outline	5
2 Literature review	
2.1 Introduction	9
2.2 Upstream sector	9
2.3 Midstream sector	10
2.3.1 Natural rubber latex concentrate	10
2.3.2 Specialty natural rubber latex	12
2.4 Downstream sector	13
2.4.1 Natural rubber latex products	14
2.4.2 Specialty natural rubber latex products	14

2.5	Natural rubber latex foam	15
2.5.1	NR latex foam technology for the bedding industry	15
2.5.1.1	The Dunlop NR latex foam process	16
2.5.1.2	The Talalay NR latex foam process	21
2.5.2	Current demand in NR latex foam technology	22
2.5.2.1	The vulcanization process	22
2.5.2.2	Physical properties of NR latex foam products	23
2.5.2.3	Environmental, health and hygiene issues	26
2.6	Potential application of NR latex foam	28
2.6.1	NR latex foam as seat cushions	28
2.6.2	NR latex foam for sound and vibration control	30
2.7	Summary	33
3	Methodology	
3.1	Introduction	35
3.2	Preparation of SpNR latex concentrates	35
3.2.1	Materials and collection of freshly tapped NR latex	35
3.2.2	Preparation of ENR latex concentrate	35
3.2.3	Preparation of DPNR latex concentrate	36
3.3	Characterization of SpNR latex concentrate	37
3.3.1	Determination of dry rubber content, total solid content, and alkalinity	37
3.3.2	Viscosity measurement	38
3.3.3	Measurement of mechanical stability	38
3.3.4	Determination of pH value	38
3.3.5	Determination of nitrogen content	38
3.3.6	Determination of epoxidation level via ¹ H-Nuclear Magnetic Resonance	39
3.3.7	Analyzing SpNR latex particle size using Brookhaven particle analyzer	39
3.3.8	Visualization of SpNR latex morphology via Scanning Electron Microscopy	39

3.3.9	Analysis of SpNR latex flow behavior using the Discovery Hybrid Rheometer	40
3.4	SpNR latex foamability and stability study	40
3.5	Chemical properties measurement	41
3.5.1	Determination of extractable proteins content	41
3.5.2	Determination of extractable residual chemicals	41
3.5.3	Determination of volatile organic compounds	42
3.6	Physical properties measurement	42
3.6.1	Determination of the dry density of latex foam	42
3.6.2	Determination of volume shrinkage	43
3.6.3	Visualization of the morphological structure of SpNR latex foam	43
3.6.4	Determination of shore F hardness	43
3.6.5	Pressure-relief performance evaluation	43
3.6.6	Measurement of physical properties for bedding products	44
3.7	Mechanical properties measurement	46
3.7.1	Acoustic properties measurement	46
3.7.2	Compression test	48
3.7.3	Ball-rebound resilience test	48
3.7.4	Vibration transmissibility test	49
3.8	Thermal properties evaluation	50
3.8.1	Thermogravimetric analysis	50
3.8.2	UL 94 horizontal burning test	50

4 Specialty natural rubber latex concentrate

4.1	Introduction	52
4.2	Characteristics of specialty natural rubber latex concentrate	53
4.2.1	Physicochemical properties	53
4.2.2	Epoxidation levels	54
4.2.3	Study on rubber particles	55

4.2.4 Rheological behavior	56
4.3 Conclusion	65
5 Specialty natural rubber latex foam	
5.1 Introduction	66
5.2 Specialty natural rubber latex foamability and stability study	66
5.2.1 Development of compounding formulation	66
5.2.1.1 Compounding process	66
5.2.1.2 Effect of compounding on viscosity and pH of the latex	67
5.2.2 Preliminary observation on foaming and gelling behavior	68
5.2.2.1 Foamability of latex and latex foam stability	68
5.2.2.2 Challenge during latex foam fabrication process	70
5.2.3 Development of foaming and gelling formulations	72
5.2.4 Specialty natural rubber latex foam fabrication process	77
5.2.5 SpNR latex foam appearance	78
5.2.6 Effect of density on volume shrinkage	79
5.3 Conclusion	80
6 Specialty natural rubber latex foam for cushioning applications	
6.1 Introduction	81
6.2 Development of cervical shape dual density latex foam pillows	83
6.2.1 Production of DPNR latex foam pillows prototype	83
6.2.1.1 Pillow production process	83
6.2.1.2 DPNR latex foam pillow's shape and structure	84
6.2.2 Properties of the latex foam pillows	84
6.2.2.1 Chemical properties	85
6.2.2.2 Physical properties	87
6.2.2.3 Morphological characteristics	90
6.2.2.4 Pressure-relief performance	92

6.3	Development of DPNR latex foam seat cushions	97
6.3.1	Production of DPNR latex foam seat cushions prototype	97
6.3.2	Properties of DPNR latex foam seat cushions	98
6.3.2.1	Density, hardness and morphological characteristics	98
6.3.2.2	Pressure-relief performance	99
6.3.2.3	Vibration transmissibility study	101
6.3.2.4	Compressive stress-strain behavior	102
6.3.2.5	Ball-rebound resilience properties	105
6.4	Conclusion	106
7	Specialty natural rubber latex foam for sound and vibration controls	
7.1	Introduction	108
7.2	Development of acoustic foam material from SpNR latex	109
7.2.1	Fabrication of SpNR latex foam for acoustic foam applications	109
7.2.2	Physical properties	109
7.2.3	Acoustic properties of SpNR latex foam	113
7.2.2.1	Effect of density on acoustic properties	113
7.2.2.2	Effect of thickness on acoustic properties	116
7.2.2.3	Effect of double-layer foam on acoustic properties	121
7.3	Study on the effect of oil palm trunk biochar as flame retardant filler	122
7.3.1	Preparation of OPTB/SpNR latex foam composite	123
7.3.1.1	Preparation of OPTB	123
7.3.1.2	Physical and thermal properties of OPTB	124
7.3.1.3	Fabrication process of OPTB/SpNR latex foam composite	128
7.3.1.4	The appearance of OPTB/SpNR latex foam composite	129
7.3.2	Morphological structures of OPTB/SpNR latex foam composite	130
7.3.3	Acoustic properties of OPTB/SpNR latex foam composite	131
7.3.4	Thermal stability of OPTB/SpNR latex foam composite	134
7.3.5	Physical and mechanical properties of OPTB/SpNR latex foam composite	138

7.3.5.1 Physical properties of OPTB/SpNR latex foam composite	138
7.3.5.2 Compressive stress-strain behavior	139
7.3.5.3 Rebound resilience behavior	143
7.3.5.4 Vibration-damping properties	145
7.4 Conclusion	148
8 Conclusions and recommendation for future work	
8.1 Summary	150
8.2 Study limitation and recommendation for future work	151
9 References	

List of tables

2.1	Compounding formulation used for NR latex foam	16
2.2	Gelling formulation used for NR latex foam	18
2.3	Physical properties of NR latex foam bedding products	24
4.1	Physicochemical properties of SpNR latex	53
4.2	Carreau-Yasuda parameters value	61
5.1	Compounding formulation used in this study	67
5.2	Effect of compounding on viscosity and pH of the latex	68
5.3	Wet density of the latex foam	73
5.4	Effect of compounding and density levels on pH of the latex foam	73
5.5	Effect of density on volume shrinkage	79
6.1	Physical properties of foam samples examined in this study	88
6.2	Pressure distribution, average peak pressure value and surface contact area	93
6.3	Pressure-relief performance of cervical shape pillows	95
6.4	Density and Shore F hardness of the foam sample	98
6.5	Pressure-relief performance of seat cushions	100
6.6	Vibration transmissibility characteristics of foam samples	102
7.1	Noise reduction coefficient of 20 mm latex foams	116
7.2	Effect of thickness levels on NRC value of latex foams	120
7.3	Effect of sandwich layer of latex foam on NRC value	122
7.4	Proximate analysis of OPTB produced at different temperatures	125
7.5	Data evaluated from TG and DTG thermograms of OPTB	128
7.6	Data evaluated from TG and DTG thermogram of SpNR latex foam composite	136
7.7	Burning rate of OPTB/SpNR latex foam composite	137
7.8	Stress value of the OPTB/SpNR latex foam at different strain	141
7.9	Effect of strain frequency on stress value	141

7.10	Effect of addition of OPTB on damping properties of SpNR latex foam	145
7.11	Effect of addition of OPTB on vibration characteristics of SpNR latex foam	147
7.12	Effect of addition of OPTB on damping ratio of SpNR latex foam	147

List of figures

1.1	Flow diagram of the study	4
2.1	Schematic diagram of the production of ENR via an <i>in-situ</i> epoxidation process	12
2.2	Schematic diagram of the production of DPNR through enzymatic reactions	13
2.3	Steps involved in the Dunlop batch process	17
2.4	NR latex foam gelling time	18
2.5	Steps involved in the Dunlop continuous process	19
2.6	NR latex foam continuous foaming machine	20
2.7	NR latex foam products molding process	20
2.8	Open-cell structures of NR latex foam	26
2.9	Polymer foams	31
2.10	The basic concept of sound absorption and sound transmission	31
3.1	Process for the production of ENR latex concentrate	36
3.2	Process for the production of DPNR latex concentrate	37
3.3	FoamScan [®] analyzer configuration	41
3.4	CONFORMat [™] pressure sensor system	44
3.5	Impedance tube model Kundt tube type SCS9020B	46
3.6	Schematic diagram of the impedance tube set up for STL test	47
3.7	Schematic diagram of the impedance tube setup for the SAC test	47
3.8	Configuration of ball-rebound resilience test	48
3.9	Configuration of vibration transmissibility test	49
4.1	¹ H-NMR chemical shift of ENR latex produced in this study	54
4.2	Particle size distribution of SpNR latex	55
4.3	SEM images of SpNR latex particles	56
4.4	Shear Stress as a function shear rate at 25 °C for LAT'Z, DPNR and ENR latex	57
4.5	Viscosity as a function of shear rate at 25 °C for LAT'Z, DPNR and ENR latex	57
4.6	Effect of storage properties of LAT'Z, DPNR and ENR latex	59

4.7	Application of a Carreau-Yasuda (C-Y) model to the rheological data	61
4.8	G' , G'' as a function of oscillation strain	63
4.9	G''/G' as a function of oscillation strain	65
5.1	Foam volume versus time for LATZ, DPNR and ENR	68
5.2	Foamability latex and the stability of latex foam	69
5.3	Failure during foaming process	71
5.4	Example of latex foam failure	72
5.5	Effect of SSF levels on gelling time of LATZ latex foam	74
5.6	Effect of SSF levels on gelling time of DPNR latex foam	75
5.7	Effect of SSF levels on gelling time of ENR latex foam	76
5.8	The different stages involved in the fabrication of SpNR latex foam	77
5.9	Appearance of LATZ, DPNR and ENR latex foam	78
6.1	The different stages involved in the production of NR latex foam pillows	83
6.2	Illustration of the shape and dimensions of the DPNR latex foam pillow prototype	84
6.3	Extractable protein content of latex foam pillow materials	85
6.4	Extractable residual chemicals of NR latex foam pillows	86
6.5	VOC concentrations of NR latex foam and memory foam pillows	87
6.6	Morphological structures of LATZ, DPNR, CNRL latex foam and PM foam	90
6.7	Distribution of pore size of the foam materials	91
6.8	Mean pore size of foam materials examined in this study	92
6.9	Modelling pillow conforming area under the head	94
6.10	Relationship between surface contact area and average peak pressure value	94
6.11	Modelling pillow conforming area under the neck	96
6.12	The different stages involved in the production of DPNR latex foam seat cushions	97
6.13	Morphological structures of DPNR latex foam, PU foam, and PM foam	98
6.14	Vibration transmissibility of DPNR latex foam, PU foam, and PM foam	101
6.15	Loading-unloading curve of foam materials examined in this study	103
6.16	Hysteresis loss ratio of DPNR latex foam, PU foam, and PM foam	105

6.17	Percentage of rebound height of DPNR latex foam, PU foam, and PM foam	106
7.1	Indentation hardness and density of the foams	110
7.2	Morphological structures of foam materials examined in this study	111
7.3	Average pore size of foam materials examined in this study	112
7.4	Mean pore area and porosity of foam materials examined in this study	112
7.5	Measurements of STL as a function of frequency on 20 mm thick latex foam	113
7.6	Measurements of SAC as a function of frequency on 20 mm thick latex foam	115
7.7	Effect of thickness levels on STL curve of HD foam	116
7.8	Effect of thickness levels on STL curve of MD foam	117
7.9	Effect of thickness levels on STL curve of LD foam	118
7.10	Effect of thickness levels on SAC curve of HD foam	118
7.11	Effect of thickness levels on SAC curve of MD foam	119
7.12	Effect of thickness levels on STL curve of MD foam	120
7.13	The effect of sandwich layer of latex foam on STL curve	121
7.14	The effect of sandwich layer of latex foam on SAC curve	121
7.15	Different stages involved in the preparation of OPTB	124
7.16	Effect of pyrolysis temperature on yield of OPTB	125
7.17	Effect of pretreatment and pyrolysis process of OPT	126
7.18	Thermogravimetric analysis of OPTB	127
7.19	The steps involve the fabrication of the OPTB/SpNR latex foam composite	129
7.20	Challenge in the fabrication process	129
7.21	The appearance of OPT/SpNR and OPTB/SpNR latex foam composites	130
7.22	Cross-section views of OPTB/SpNR latex foam composites	131
7.23	Effect of addition of OPTB on STL of SpNR latex foam	131
7.24	Effect of addition of OPTB on SAC of SpNR latex foam	132
7.25	Illustration of sound waves propagation in acoustic foam materials	133
7.26	Thermogravimetric analysis of the effect of OPT and OPTB on DPNR latex foam	135
7.27	Thermogravimetric analysis of the effect of OPT and OPTB on ENR latex foam	136

7.28	Burning rate versus OPTB loading concentration	137
7.29	Effect of addition of OPTB on physical properties of SpNR latex foam	138
7.30	Effect of addition of OPTB on stress-strain of SpNR latex foam	140
7.31	Hysteresis loss ratio of OPTB/SpNR latex foam composite	143
7.32	Effect of addition of OPTB on rebound resilience of SpNR latex foam	143
7.33	Effect of addition of OPTB on vibration transmissibility of DPNR latex foam	145
7.34	Effect of addition of OPTB on vibration transmissibility of ENR latex foam	146

List of Abbreviation

NR = Natural rubber
SR = Synthetic rubber
SpNR = Specialty natural rubber
ENR = Epoxidized natural rubber
DPNR = Deproteinized natural rubber
LATZ = Low ammonia latex
HA = High ammonia latex
CNRL = Commercial NR latex foam
PU = Polyurethane foam
PM = Polyurethane memory foam
OPT = Oil palm trunk
OPTB = Oil palm trunk biochar
MRB = Malaysian Rubber Board
PO = Potassium oleate
ZDEC = Zinc diethyl dithiocarbamate
ZDBC = Zinc dibutyl dithiocarbamate
ZMBT = Zinc 2-mercaptobenzothiazole
ZnO = Zinc oxide
DPG = Diphenyl guanidine
SSF = Sodium silicofluoride
phr = Part per hundred grams of rubber
kPa = Kilopascal
Hz = Hertz
mm = Millimeter
g = Gram
kg = Kilogram
µg = Microgram
mL = Milliliter
L = Liter
m = Meter
mm = Millimeter
s = Second

°C = Degree Celsius
DRC = Dry rubber content
MST = Mechanical stability time
TSC = Total solid content
VOC = Volatile organic compounds
ERC = Extractable residual chemicals
ERP = Extractable rubber proteins
SEM = Scanning electron microscopy
STL = Sound transmission loss
SAC = Sound absorption coefficient
NRC = Noise reduction coefficient
HD = High-density
MD = Medium-density
LD = Low-density
WBVS = Whole-body vibration syndrome
ASTM = American Society for Testing Materials
EN = European Standards
ISO = International Organization for Standardization
MS = Malaysian Standards

Chapter 1

Introduction

1.1. Background and study justification

Natural rubber (NR) consumption has been declining since the last few decades due to the increasing demand for synthetic rubber (SR)¹. This is due to the availability and easier processability of SR compared to NR. However, for specific applications such as bedding products, NR still retains its competitiveness, typically when elasticity, durability, and natural origin become people's choice. Additionally, with the growing awareness concerning the rising risk of global warming and fossil fuel depletion, agreements have been made world-wide to increase the use of natural and sustainable materials in many products' manufacturing processes. This has motivated researchers in the NR industry to develop modified NR, namely, specialty natural rubber (SpNR) latex, and thus broaden the applications of SpNR latex to innovative products².

There are two varieties of SpNR latex: epoxidized natural rubber (ENR) latex and deproteinized natural rubber (DPNR) latex. ENR is a chemically modified NR prepared by in-situ chemical reactions that convert part of the carbon-carbon double bonds of rubber chains into epoxy functional groups using performic acid. On the other hand, DPNR latex is a purified form of NR latex from which most of the components of the ash and protein components have been removed via enzymatic hydrolysis reactions. Products made from ENR have a high damping capacity, superior oil resistance, and excellent wet grip³⁻⁵. DPNR, on the other hand, exhibits low extractable protein content as well as good dynamic characteristics, low stress relaxation, and low creep⁶⁻⁸. However, the usage of SpNR latex in products was found to be limited. SpNR latex is used in the form of bulk rubber to produce dry rubber products such as tires and automotive parts. Even though SpNR has superior properties to normal NR, there is little information on its use in latex-based products, especially molded latex foam products. This could be due to a lack of scientific data on the properties of SpNR latex and the manufacturing process, which limit their potential applications. It will be more persuasive to apply and employ SpNR in a wider range of rubber product development applications if more technical data is produced.

On the other hand, synthetic polymer foams have been used in a wide range of applications, from automotive seats to bedding products and footwear applications, owing to their lightweight

and superior properties⁹⁻¹³. Synthetic polymer foams are also used as thermal and sound barriers in buildings and the transportation industry due to their excellent thermal and acoustic insulating properties¹⁴⁻¹⁶. Throughout the year, global demand for synthetic polymer foams has increased at a rapid rate. Synthetic polymer foams were valued at more than USD 100 billion in 2015 and are expected to be worth USD 150 billion by 2025¹⁷. However, it is well-known that synthetic polymer foams are made from petrochemical-based materials that have been linked to environmental and health issues, as well as contributing to challenging waste management and disposal problems^{10,18-20}. For example, polyurethane foam is made from a mixture of isocyanates and polyols that might cause occupational asthma due to excessive levels of exposure at work during manufacturing or by sensitization²¹. This has raised awareness among users of the possibility that synthetic polymer foams could, over time, release toxic gases that may cause health hazards²¹⁻²⁴. Further to that, with the growing awareness concerning the rising risk of global warming and fossil fuel depletion, as well as new legislation that has been implemented by several countries to encourage the use of 'green materials' in product manufacturing, it is both timely and necessary to develop foam materials made from less hazardous materials.

Considering the uniqueness and extraordinary properties of SpNR latex, as well as their 'green image' owing to their natural origin, it is essential to study the feasibility of SpNR latex as an alternative material for polymer foam product applications. This study intends to broaden the use of SpNR latex in molded latex foam products, such as therapeutic pillows for the bedding sector. Apart from its traditional use as bedding products, this study attempts to broaden the use of SpNR latex foam into new applications, such as sound and vibration control foam materials for buildings and the transportation industry. However, utilization of SpNR latex into latex foam products is not straightforward. Besides having a gap in knowledge on the physicochemical properties of SpNR latex, information on foamability and the subsequent stability of SpNR latex foam is still unsubstantial. Further to that, in order for the SpNR latex foam to be utilized either in beddings, buildings or the transportation industry, it is important for the latex foam to meet the products specifications and requirements. Besides that, the price of SpNR latex is also quite expensive compared to conventional synthetic polymer foams. Therefore, many factors should be taken into account to make sure the study achieved the goal. This includes investigating the possible approach to reduce the cost of SpNR latex, factors influencing foamability and subsequent stability of SpNR latex, and the optimal formulation for fabricating SpNR latex foam. Further to that, physical properties, mechanical properties, and vibro-acoustic properties of the fabricated SpNR latex foam should comply with the standard requirements. Knowledge gained from this study is important not only to provide a better understanding of the method and

procedure for the production of SpNR latex foam, but also to identify their prospective applications.

1.2. Problem Statement

Porous materials, especially polymer foams, have attracted significant interest among researchers and industry players due to their unique mechanical and acoustic properties, and have been widely used in various applications, including sound and thermal barriers, cushions, packaging, bedding, and health appliances. However, conventional polymer foams are made from synthetic materials that have been linked to environmental and health issues and contribute to challenging waste management and disposal problems. Additionally, with the increasing awareness of the rise of global warming and fossil fuel depletion, as well as new legislation implemented by several countries to encourage the use of 'green materials' in the manufacture of new products, it is timely and desirable to develop polymer foams from natural sources. SpNR latex is a natural material that could be used as a substitute for polymer foam products. To date, there is limited information on the use of SpNR latex in latex foam products, possibly due to the low total solid content (TSC), of which, for the production of latex foam products, the minimum TSC of the latex should be at least 60 %. Further to that, little is known about the physicochemical properties of SpNR latex, as well as the fundamental understanding of its foamability and stability. Such information is essential for developing compounding, foaming, and gelling formulations to produce SpNR latex foam. Additionally, chemical, physical, and mechanical properties of the SpNR latex foam should be characterized, and thus specific targeted applications can be identified.

1.3. Aim and objectives

The principal aim of this study is to diversify the applications of specialty natural rubber (SpNR) latex into latex foam products. However, to produce latex foam products from SpNR latex is not straightforward especially when physicochemical properties of SpNR latex differ from normal latex due to the modification process.

The objectives of the study are as follows:

- i. To characterize and build a good understanding on the physicochemical properties of SpNR latex concentrate that is prepared directly from freshly tapped NR latex.
- ii. To explore and evaluate factors that influence SpNR latex foamability and subsequent stability of the latex foam.
- iii. To develop compounding, foaming, and gelling formulations to produce SpNR latex foam.
- iv. To identify suitable latex foam products made from SpNR latex.

This study has identified three potential foam products. Therefore, objective iv also has the following four sub-objectives:

- a) To determine physical properties and pressure-relief performance of therapeutic pillows made from SpNR latex foam.
- b) To determine physical properties, vibration-damping and pressure-relief performance of latex foam seat cushions made from SpNR latex foam.
- c) To determine acoustic properties of acoustic foams made from SpNR latex foam.
- d) To investigate the effects of the incorporation of oil palm trunk biochar (OPTB) as a flame-retardant filler on the physical, mechanical, acoustic, and thermal properties of SpNR latex foam.

1.4. Conceptual framework and discussion of its novelty

This study involves fundamental and applied studies starting from preparation and characterization of the SpNR latex, to development of compounding, foaming and gelling formulations to produce SpNR latex foam, followed by development and characterization of chemical, physical, mechanical, and thermal properties of the potential SpNR latex foam products. Figure 1.1 shows the flow diagram of the study.

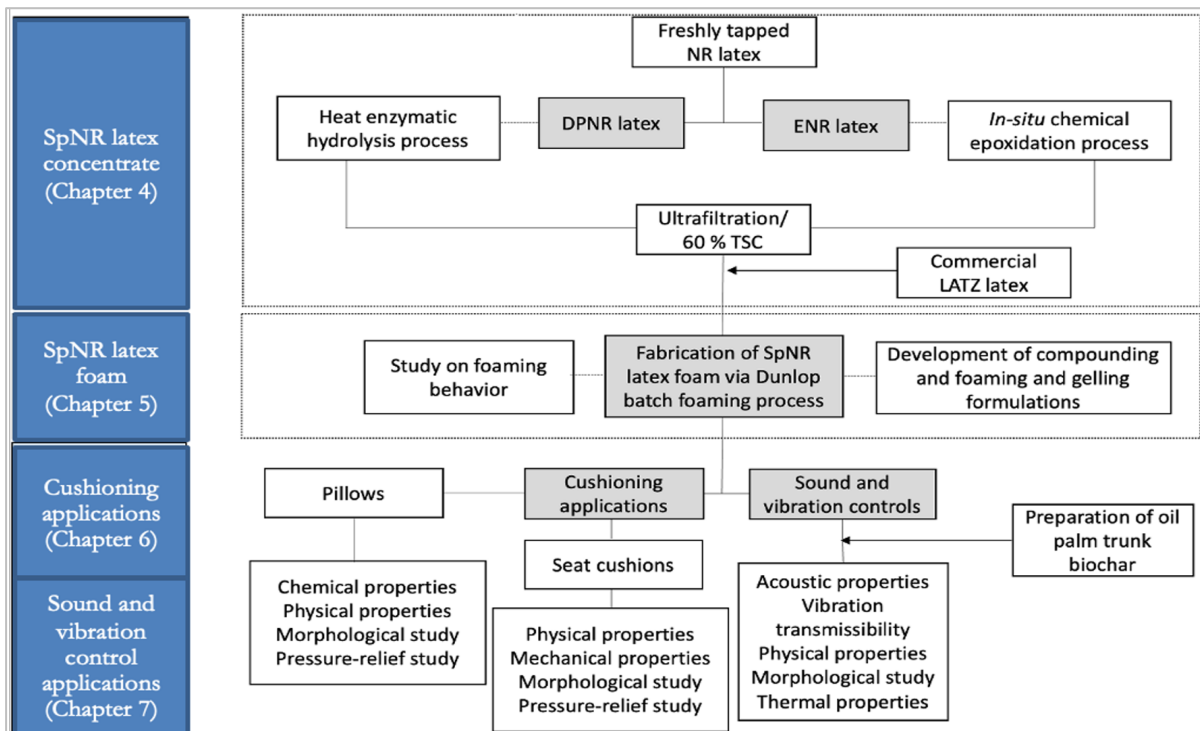


Figure 1.1: Flow diagram of the study

This study is the first to report the characteristics of SpNR latex that is prepared directly from freshly tapped NR latex. Physicochemical properties of SpNR latex concentrate that has been

produced through the ultrafiltration process using membrane separation technology were discussed in Chapter 4. The availability of SpNR latex with 60 % TSC has provided an opportunity to diversify the application of SpNR latex into latex foam products. In Chapter 5, the fundamental understanding on the foamability of SpNR latex and subsequent stability of the SpNR latex foam was evaluated in order to develop the novel compounding, foaming, and gelling formulations to produce SpNR latex foam. The challenges encountered in producing SpNR latex foam were explored and discussed. Following that, the compounding, foaming, and gelling formulations to produce SpNR latex foam were established. The potential applications of SpNR latex foam were identified, and they can be categorized into two groups: cushioning applications (Chapter 6) and sound and vibration control applications (Chapter 7). Although pillows are one of the traditional applications of NR latex foam, the pillow produced in this study is in cervical shape with a unique dual-density to improve pressure-relief performance, which is an important feature to improve sleep quality. Besides pillows, this study explores the potential application of SpNR latex for seat cushions, specifically for transportation industries that require the isolation of higher frequency vibrations such as high-speed crafts, trains, and trucks. Another novel application explored in this study is as sound and vibration control foam material. As far as the author is concerned, this is the first report on acoustic properties of SpNR latex foam. This study is also the first to report the effects of addition of oil palm trunk biochar as flame retardant filler on physical, mechanical, and thermal properties of SpNR latex foam.

1.5 Thesis outline

Chapter 1: Introduction.

This chapter specifies the background and motivation of the study. The flow of Chapter 1 includes background and study justification, problem statement, aim and objectives of the study, conceptual framework and discussion of its novelty.

Chapter 2: Literature review.

This chapter explores the three main sectors of the natural rubber industry: upstream, midstream, and downstream. The NR plantation industry is upstream, the NR processing industry is midstream, while the NR product manufacturing industry is downstream. The literature review focuses on the production of NR latex and current technology used to produce NR latex foam products. The difference between two varieties of SpNR latex, namely deproteinized natural rubber (DPNR) latex and epoxidized natural rubber (ENR) latex, were described. This followed by discussion on potential applications of SpNR latex as latex foam products.

Section 2.5 was written in a journal paper format and submitted for publication in Science, Engineering and Health Studies. Title of the paper: Natural rubber latex foam technology for bedding industry. Roslim Ramli, Ai Bao Chai, Shamsul Kamaruddin, Jee Hou Ho, Davide S.A. De Focatiis and Kok Thai Goh. (2022). *Science, Engineering and Health Studies*. <https://li01.tci-thaijo.org/index.php/sehs/article/view/256626/175205>

Chapter 3: Methodology.

This chapter can be divided into seven sections: Preparation of SpNR latex, characterization of SpNR latex, fabrication process of SpNR latex foam, characterization of chemical properties, physical properties, mechanical properties, and thermal properties of the SpNR latex foam.

Chapter 4: Preparation and characterization of specialty natural rubber latex concentrate.

This chapter describes the novel method to prepare SpNR latex. The physicochemical properties, deproteinization and epoxidation levels, rubber particles, and the rheological behavior of SpNR latex were evaluated.

This chapter was written in a journal paper format and is published in Rubber Chemistry and Technology. Title of the paper: Preparation and characterization of specialty natural rubber latex concentrate. Roslim Ramli, Chai Ai Bao, Shamsul Kamaruddin, Fatimah Rubaizah Mohd. Rasdi, Ho Jee Hou, and Davide S.A. De Focatiis, (2021). *Rubber Chemistry and Technology*. <https://doi.org/10.5254/RCT.21.79945>

Chapter 5: Specialty natural rubber latex foam: Foamability study and fabrication process

This chapter describes the study of the foamability of SpNR latex and the subsequent stability of the latex foams. The challenges in producing SpNR latex foam, the defects observed, and the factors that caused the latex foam defects were evaluated. In this chapter, compounding, foaming, and gelling formulations to produce SpNR latex foam were established.

This chapter was written in a journal paper format and is published in Rubber Chemistry and Technology. Title of the paper: Specialty natural rubber latex foam: Foamability study and fabrication process. Roslim Ramli, Chai Ai Bao, Shamsul Kamaruddin, Fatimah Rubaizah Mohd. Rasdi, Ho Jee Hou, and Davide S.A. De Focatiis, (2021). *Rubber Chemistry and Technology*. <https://doi.org/10.5254/rct.21.78938>

Chapter 6: Specialty natural rubber latex foam for cushioning applications

In this chapter, DPNR latex foam was used to produce therapeutic pillows and seat cushions. This chapter explains how the unique dual-density and cervical shape of the pillow contribute to higher pressure-relief performance compared to conventional pillows. Besides complying with the physical properties requirements stipulated in the standard method, the DPNR latex foam pillows

is also hypoallergenic thus fulfilling the current demands in the bedding industry. On the other hand, for seat cushions, the results show that DPNR latex foam has excellent pressure-relief, vibration isolation, and rebound resilience properties, making it an ideal candidate material for seat cushions intended for the transportation industry, typically for transportation that involve high frequency vibrations.

Section 6.2 was written in a journal paper format and is published in the *Journal of Rubber Research*.

Title of the paper: Development of latex foam pillows from deproteinized natural rubber latex. Roslim Ramli, Chai Ai Bao, Shamsul Kamaruddin, Fatimah Rubaizah Mohd. Rasdi, Ho Jee Hou, and Davide S.A. De Focatiis, (2021). *Journal of Rubber Research*.

<https://doi.org/10.1007/s42464-021-00130-7>

Section 6.3.2.1, Section 6.3.2.1 and Section 6.3.2.3 were written in a conference paper format and is presented at 8th International Conference on Material Science & Smart Materials (MSSM2022), Brunel University of London, United Kingdom. 11–13 July 2022.

Title of the paper: Development of deproteinized natural rubber latex foam for seat cushions. Roslim Ramli, Ai Bao Chai, Shamsul Kamaruddin, Jee Hou Ho, and Davide S.A. De Focatiis.

Section 6.3.2.4 and Section 6.3.2.5 were written in a conference paper format and is presented at 8th International Conference on Material Science & Smart Materials (MSSM2022), Brunel University of London, United Kingdom. 11–13 July 2022.

Title of the paper: Compressive stress-strain and rebound-resilience properties of a novel deproteinized natural rubber latex foam. Roslim Ramli, Ai Bao Chai, Shamsul Kamaruddin, Jee Hou Ho, and Davide S.A. De Focatiis.

Chapter 7: Specialty natural rubber latex foam for sound and vibration control applications

This chapter investigates the feasibility of using SpNR latex foam for noise and vibration control applications. Research findings revealed that the density, thickness and morphological structures of SpNR latex foam play the major role in influencing the sound transmission loss and sound absorption performance of the latex foam. In order to meet the fire safety requirement as acoustic foam for building applications, oil palm trunk biochar (OPTB) was added as a flame-retardant agent. The addition of OPTB to SpNR latex foam up to 24 phr improved the thermal stability of the material, but was not sufficient to meet fire rating requirements for building applications. However, the study found that the addition of OPTB to SpNR latex foam increased the dimensional stability, elongation at break, hardness, and vibration-damping property, making it appropriate for applications that require impact absorption, for example, in the transportation

industry, where a high level of crashworthiness is a key aspect to improve the safety of the transport vehicle.

Section 7.2.1 was written in a journal paper format and is published in the Journal of Rubber Research. Title of the paper: The acoustic properties of latex foam made from deproteinized natural rubber latex and epoxidized natural rubber latex. Roslim Ramli, Ai Bao Chai, Shamsul Kamaruddin, Fatimah Rubaizah Mohd. Rasdi, Jee Hou Ho, and Davide S.A. De Focatiis. (2022). *Journal of Rubber Research*.

<https://doi.org/10.1007/s42464-022-00178-z>

Section 7.2.2 was written in journal paper format and submitted to the Journal of Rubber Research. Title of the paper: Effect of oil palm biochar on the thermal stability and acoustic properties of specialty natural rubber latex foam. Roslim Ramli, Ai Bao Chai, Shamsul Kamaruddin, Fatimah Rubaizah Mohd. Rasdi, Jee Hou Ho, Davide S.A. De Focatiis, Siew Kooi Ong and Robert T. Bachmann.

Manuscript ID: JRUR-D-22-00069 under review.

Chapter 8: Conclusions and recommendations for future work

This chapter concluded that a new generation of SpNR has been successfully developed. The latex foam made from SpNR latex is a strong contender for the next generation of environmentally friendly therapeutic pillows, seat cushions and acoustic foams for noise control applications in buildings and the transportation industry. This chapter also states the limitations of the study and the recommendation for future work.

Chapter 2

Literature Review

2.1 Introduction

Natural rubber (NR) latex is a high molecular weight hydrocarbon polymer of isoprene (C_5H_8), whereas one double bond unit exists for each C_5H_8 group². NR latex occurs in the free-flowing milky cytoplasmic exudates of the commercial rubber trees known as *Hevea brasiliensis*. This tree is originally found growing in the Amazon basin of South America but now grown in the plantations of rubber producing nations such as Malaysia, Indonesia, Vietnam and Thailand. The NR industry in Malaysia has been established since the 1950's and has contributed significantly to the country's socio-economic development^{2,25}. The NR industry is divided into three sectors: upstream, midstream and downstream. The NR plantation industry is upstream, the NR processing industry is the midstream, while the NR product manufacturing industry is downstream. This chapter provides overviews of each sector and identifies relevant areas of study that demand further research or improvement. Existing research articles related to the present study are explored, compared and correlated in this chapter.

2.2 Upstream sector

There are about eight *Hevea* plant species from the *Euphorbiaceous* family known to produce NR latex, but only *H. brasiliensis* species is economically exploited. In 1888, Henry Nicholas Ridley developed a tapping method to extract NR latex from the trees. The NR latex is obtained from the tree by removing a thin slice of the bark with a special tapping knife. The NR latex flows slowly through the latex vessels found in the bark of the rubber tree out into a collecting cup placed below. This method triggered the beginning of large-scale rubber plantations. Rubber trees are now planted in over 20 countries around the world. Nevertheless, 80% of total rubber plantation areas in the world today are in Asia, with Malaysia, Indonesia, Vietnam and Thailand covering almost 70% of the total NR production.

Rubber trees take about six to seven years to grow to a point where it is economical to harvest (to tap) the latex. Rubber trees normally reach 20-30 meters in height on rubber plantations. Economical life span of a rubber tree is between 10 to 20 years, but may extend past 25 years in the hands of a skilled tapper and bark consumption. Tapping process usually takes

place in the early hours of the morning. NR latex will flow for approximately 1 to 3 hours after which time the vesicles become plugged with coagulum. Each rubber tree usually produces NR latex about a quarter of the cup per day. The dry rubber content (DRC) in the NR latex varies from 25 to 45 percent depending on the clones, seasons, soil and farm management.

NR price has fluctuated over the year, a situation that is linked to the impact of global market uncertainties¹. For the past 10 years the price of NR has been declining. The declined trend of NR prices has placed many rubber tappers and smallholders' livelihood at risk because of the increasing living expenses. Various approaches have been implemented by the government in the NR producing countries to assist rubber smallholders affected by low productivity and the decline in rubber prices. These measures include the provision of incentives and subsidies, development of high yielding rubber clones, introduction of enhanced intercropping techniques, improved farm management and the development of high value-added products²⁵.

2.3 Midstream sector

NR is used extensively in many applications and products. Depending on its products and application the tapped latex is either collected or left to coagulate in the cup. The latex that coagulates in the cup is called cup lump. Acidic materials are used to accelerate the coagulation process. This is to avoid total loss of the NR due to unexpected rain during or after tapping operation has completed. Cup lump is collected by the rubber tapper during next visits to the tree to tap it again. The cup lump is transferred to the collection center for further process. Cup lump is used in the manufacture of Standard Malaysian Rubber (SMR), such as SMR10 and SMR20 grade rubbers. Processing for these grades is a size reduction and cleaning process to remove contamination and prepare the material for the final stage of drying.

A higher quality grade of NR is produced from the NR latex. The tapped latex is collected and transferred into coagulation tanks for the preparation of dry rubber or transferred into air-tight containers with sieving for ammonization. Ammonization preserves the NR latex in a colloidal state for longer periods of time. NR latex is generally processed into either latex concentrate for manufacture of dipped goods or coagulated under controlled, clean conditions using formic acid. The coagulated NR latex can then be processed into the higher-grade, technically specified block rubbers such as SMR L or SMR CV or used to produce Ribbed Smoked Sheet grades.

2.3.1 Natural rubber latex concentrate

NR latex is quite fluid after tapping from the tree. NR latex is a colloid material made up of a dispersed phase containing rubber particles and other non-rubber constituents in trace amounts,

as well as a dispersing medium (water) containing several organic substances and mineral salts that give the natural rubber latex its chemical and physical properties. The NR latex that has just been tapped has a pH of 6.5-7.0 and a density of 0.98 g/cm³ ². Rubber particles are formed by the aggregation of rubber hydrocarbon molecules and are encased by a negatively charged membrane made up of proteins, lipids, and other non-rubber substances that separate the hydrophobic and hydrophilic phases. The rubber particles are spherical or oval in shape and range in size from 0.1 to 2.0 µm in diameter². In order to maintain the NR latex fluid, a small amount of preservative, such as ammonia solution, must be added to protect the protein-lipid layer around the rubber particles^{2,25}. However, for long-term storage, it is common practice to treat NR latex with a strong preservative that prevents bacteria from producing acid that causes the NR latex to coagulate. As a result, freshly tapped NR latex is often collected and transported to a centralized processing facility for preservation treatment. The freshly tapped NR latex is then processed into NR latex concentrate.

Upon arrival at the centralized processing plant, the freshly tapped natural rubber latex is blended and sieved to remove dirt and rubber bark. The blending process is important to ensure that clonal variations in properties are eliminated. NR latex concentrate is made by concentrating freshly tapped NR latex approximately from 25%-45% DRC to a maximum of 60% DRC. This process also reduces the concentration of non-rubber substances such as water, minerals, proteins etc., resulting in a more uniform quality of NR latex. Furthermore, it is economical to transport NR latex concentrate with a higher dry rubber percentage from the processing plant to the product factory than it is to transport NR latex with a low dry rubber content.

It should be noted that the preservatives used in the concentration process must be able to prevent bacteria from generating acid and, at the same time, contribute to the colloidal stability of the NR latex by raising the charge on the rubber particles. The high ammonia latex (HA) system is currently the most important industrially relevant preservation system used in the concentration process. This HA system has been widely employed due to its high effectiveness and low cost. The disadvantages of the HA system, on the other hand, derive from health concerns caused by exposure to fumes in the proximity of the working area, as well as factory building corrosion. Alternatively, there are three other preservative systems used to produce NR latex concentrate, namely the low ammonia tetramethyl-thiuram disulphide-ZnO system, the low ammonia-zinc diethyl-dithiocarbamate system, and the low ammonia-boric acid system. The availability of NR latex concentrate permits the use of rubber in a liquid form which may be spread, dipped or whipped into a foam. For beddings industry, low ammonia latex (LATZ) is a commonly used NR latex concentrate for producing latex foam products such as mattresses and pillows due to its

reduced ammonia content, which offers a safer manufacturing environment as well as minimizes corrosion of mold used for producing mattresses and pillows^{26,27}. Nevertheless, certain manufacturers choose to use HA latex for specific manufacturing reasons. However, the concentration of the ammonia in HA latex was also reduced from 0.7% to 0.2% during the maturation process before being subjected to the latex foam manufacturing process. Certain manufacturers also add chemical additives to the NR latex concentrate to give it the necessary qualities.

2.3.2 Specialty natural rubber latex

Specialty NR (SpNR) latex is a modified NR latex. There are two varieties of SpNR latex: Epoxidized natural rubber (ENR) latex and deproteinized natural rubber (DPNR) latex. ENR latex is a chemically modified NR latex prepared by *in-situ* chemical reactions that convert a part of the carbon–carbon double bonds of rubber chains into epoxy functional groups using performic acid (Figure 2.1)³.

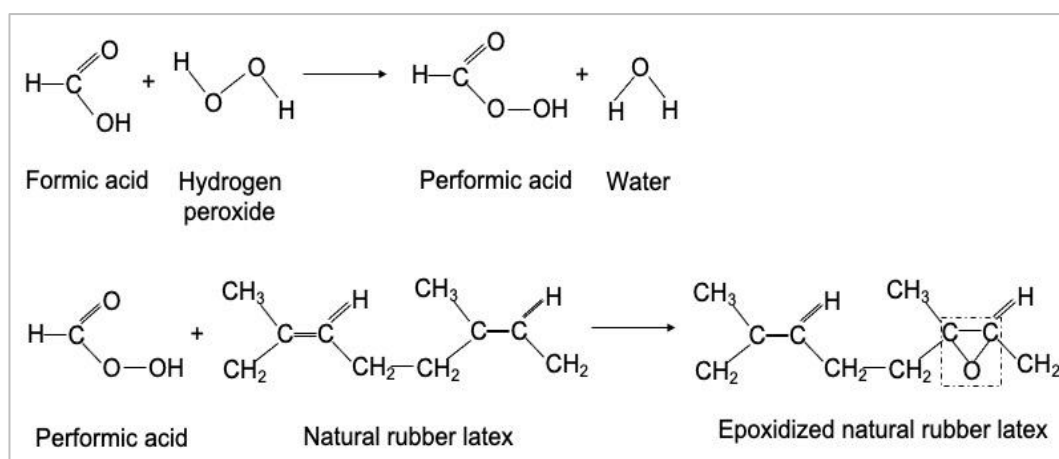


Figure 2.1: Schematic diagram of the production of ENR via an *in-situ* epoxidation process. Adapted from³.

The introduction of epoxy groups onto rubber chains was found to occur randomly along the rubber chains while retaining NR's high stereoregularity²⁸. ENR possesses excellent properties such as high damping, wet grip, gas permeability and oil resistance compared to normal NR, but retaining the intrinsic rubber elasticity³⁻⁵. On the other hand, DPNR latex is a purified form of NR latex from which most of the ash and protein components have been removed via enzymatic hydrolysis reactions (Figure 2.2). Products made from DPNR exhibit good dynamic properties, low stress relaxation, low creep and lower extractable protein content compared to normal NR⁶⁻⁸. Despite its unique properties, product applications of SpNR are relatively limited. SpNR is normally used in the form of block rubber to manufacture dry rubber products such as tires and automotive parts. To date, there is limited information concerning the use of SpNR to manufacture

latex-based products. The high cost of SpNR latex remains the challenging issue in manufacturing latex-based products. One of the reasons for the high cost of the existing SpNR latex is that it is produced from LATZ latex.

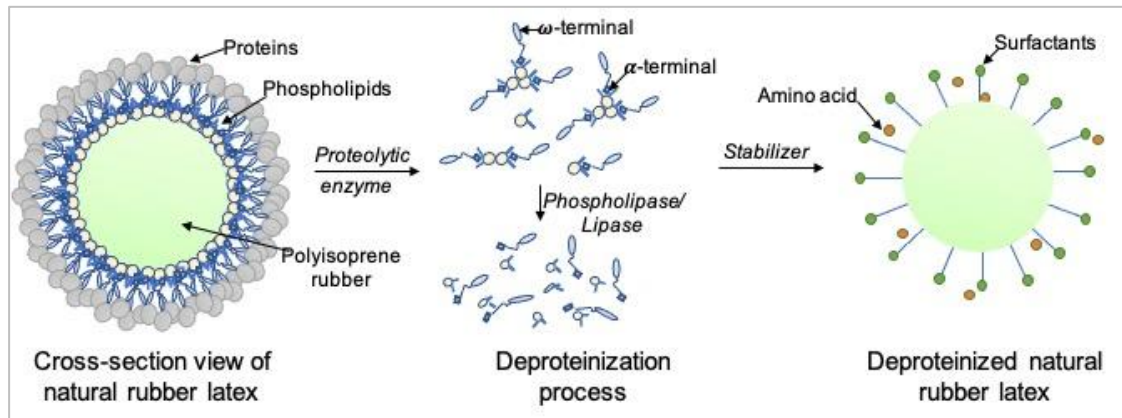


Figure 2.2: Schematic diagram of the production of DPNR through enzymatic reactions. Adapted from^{29,30}.

Generally, LATZ latex is prepared from freshly tapped NR latex. The freshly tapped NR latex is first treated with chemicals and undergoes a centrifugation process to remove ash and non-rubber content, to improve the quality and uniformity of the latex. In order to produce SpNR latex, the LATZ latex was treated with specific chemical reactions and processes, and then underwent similar centrifugation procedures to improve the quality and uniformity of the latex. Therefore, when LATZ is used as the source of SpNR latex, the production cost of SpNR is high because of the additional chemical treatments and repeating the centrifugation process. Hence, to overcome this issue, one of the objectives of this study is to investigate the feasibility of producing SpNR latex directly from freshly tapped NR latex. In such a way, the cost of the material could be minimized.

2.4 Downstream sector

The NR products manufacturing in Malaysia started in the 1910s but only began to expand after the 1970s. The sudden increase in the manufacturing sector of NR products was catalyzed by research and development conducted by the Malaysian Rubber Board (MRB) formerly known as Rubber Research Institute of Malaysia (RRIM), which identified the prospective rubber-based products²⁵. As a result, the NR industry has evolved from an agriculturally based industry toward a product manufacturing industry.

The NR product manufacturing industry falls into two categories: dry NR products and NR latex products^{2,25}. Dry NR products are products manufactured from treated bulk rubber, i.e., SMR L and SMR CV. Dry NR products include footwear, tires, hoses, engine mountings, dock fenders, and seismic bearings. On the other hand, NR latex products are those manufactured from treated latex, i.e., high ammonia (HA) and low ammonia (LATZ) latex concentrates. Examples of NR

latex products are gloves, balloons, toys, condoms, catheters, latex threads, and latex foam products.

2.4.1 Natural rubber latex products

NR latex has become material of choice for many thin film products such as surgical and examination gloves, catheters, balloons, condoms, etc. due to its intrinsic elasticity and durability, while being a natural and biodegradable material^{31,32}. NR latex is also used in producing foam material known as latex foam. The main application of latex foam is bedding products such as mattresses and pillows².

Currently, Malaysia is the world's leading exporter of NR latex gloves, accounting for over 60% of the global glove market^{33,34}. The total export value of NR latex gloves is estimated to grow at a rate of more than 10% per year owing to the prevalence of infectious diseases such as influenza A (H1N1), Ebola, and, most recently, the pandemic coronavirus known as COVID-19. Nevertheless, NR latex gloves face increasing competition from synthetic rubber (SR) latex such as nitrile, neoprene, polyisoprene, and vinyl^{31,35,36}.

Beside NR latex gloves, NR latex foam is another latex-based product that is gaining popularity due to its elasticity, durability, and cushioning support properties^{27,37}. According to the Malaysian Rubber Council (MRC)³⁴, the value of Malaysian NR latex foam products exported in 2020 was RM 154.5 million, an increase of 3.3% over the previous year. This suggests that, despite the fact that the world has experienced poor economic development in 2020 as a result of COVID-19, demand for this product remains high and has a promising future. This is mainly due to the unique elasticity, durability, and cushioning support properties of NR latex foam that no other foam material can match.

2.4.2 Specialty natural rubber latex products

Currently, SpNR latex is mostly used in the form block rubber to produce dry rubber products such as tire and automotive parts. Dry rubber products made from ENR possesses excellent properties such as high damping, wet grip, gas permeability and oil resistance compared to normal NR, but retaining the intrinsic rubber elasticity³⁻⁵. On the other hand, products made from DPNR exhibit good dynamic properties, low stress relaxation, and low creep compared to normal NR⁶⁻⁸.

Currently, attempts have been made by many researchers, typically at MRB to diversify the application of SpNR latex. For example, Rohani and Asrul³⁸ developed adhesives from ENR latex. The adhesives exhibited comparable peel strength, odor concentration to commercial synthetic-based adhesive. Additionally, pigments were added to the ENR latex adhesives to impart additional function of adhesive for example as a medium for art and paint. However, to commercialize

adhesives made from ENR latex is not straightforward. This is because the cost of the material is quite expensive compared to adhesives made from synthetic material. On the other hand, many studies were conducted to examine the possibility of using the DPNR latex for dipped goods such as gloves³⁸⁻⁴⁰. The research finding is beneficial to address healthcare issues that are related to those who have an allergy (*Type I* hypersensitivity) to rubber proteins. However, as far as the author is concerned, gloves made from DPNR latex are not yet available in the market. This could be the lower physical properties such as tensile strength of gloves made from DPNR latex compared to normal latex³⁸⁻⁴⁰.

2.5 Natural rubber latex foam

NR latex foam is an open-cell structured foam material. The foams are either completely interconnected, partially interconnected, or both completely interconnected and partially interconnected, giving it unique porous structures. NR latex foam is a versatile material due to its physical properties such as elastic, soft, good support, and porous structures. Such properties make NR latex foam one of the best materials for use in bedding products such as mattresses and pillows. However, the application of NR latex foam should not be limited to bedding products. It is believed the application of NR foam can be broadened beyond its traditional bedding applications to innovative applications, including buildings, transportation, and the footwear industry.

2.5.1 Natural rubber latex foam technology for bedding industry

NR latex foam was first introduced by Schidrowitz and Goldsbrough in late 1914²⁷. However, a method known as the Dunlop foaming process, introduced in the 1920s, has been considered the major breakthrough in the NR latex foam industry^{15,41}. Although new technologies have been developed by industry players to improve the manufacturing process, these processes remain company secrets and most are not well documented. On the other hand, new research findings published by universities or government research institutes are based on the laboratory scale, and no further attempt is generally made to transfer the technology to the industry so it can be used in factory-scale processes⁴². Surprisingly, most of the information related to the science and technology of NR latex foam was elucidated by Madge in 1962⁴¹ and Blackley in 1997²⁷. Therefore, there is a necessity to review such information and the current developments in NR latex foam technology. Furthermore, current issues should be discussed, such as the hygiene and environmental concerns related to the bedding industry.

This section reviews the NR latex foam technology and chemistry used for producing mattresses and pillows. Current issues focus on the process of manufacturing these items and the

demand for NR latex foam mattresses and pillows to contain certain properties. This section also highlights the need to establish international standards and specifications for NR latex foam mattresses and pillows. The effects of filler on the properties of NR latex foam and the feasibility of diversifying the applications of NR latex foam into new products (other than mattresses and pillows) have also become subjects of discussion.

2.5.1.1 The Dunlop NR latex foam process

NR latex has been used to manufacture bedding products such as mattresses and pillows because items made from this material can provide good support and extra comfort to users. Currently, two types of NR latex foam manufacturing processes are utilized: the Dunlop process and the Talalay process. Both have advantages, but the vulcanization process principle is based on the sulfur vulcanization system. In the Dunlop process, NR latex foam can be produced using either a batch foaming process or a continuous process. Briefly, the batch process is suitable for R&D purposes whilst the continuous process is more suitable for commercialization or production. Using either Dunlop foaming process, NR latex is first matured using sulfur vulcanizing agents to impart elastic properties using crosslinking reactions²⁷. Table 2.1 shows the sulfur vulcanized compounding formulation used to produce NR latex foam.

Table 2.1: Compounding formulation used for NR latex foam²⁶

Ingredient	TSC (%)	Dry weight (phr)
NR latex (LATZ)	60	100
Potassium oleate	20	1.50 - 3.50
Sulphur dispersion	60	2.00 - 3.00
Zinc diethyl dithiocarbamate dispersion	50	0.75 - 1.50
Zinc 2-mercaptobenzothiazole dispersion	50	0.75 - 1.50
Antioxidant dispersion (Wing stay-L)	50	1.00 - 1.50

phr = part per hundred grams of rubber; TSC = total solid content

During the compounding process, potassium oleate is first added to the NR latex as a stabilizer and foaming agent, while the NR latex is being stirred slowly at approximately 60 rpm. The stirring process should continue for at least an hour to ensure a homogenous mix of NR latex and potassium oleate is obtained. Meanwhile, a premixed sulfur vulcanizing agent is prepared, comprising sulfur, zinc diethyl dithiocarbamate, zinc 2-mercaptobenzothiazole and antioxidants. According to Blackley²⁷, sulfur and zinc diethyl dithiocarbamate together play the main role in the crosslinking of the rubber molecular chains to produce vulcanized NR latex material, whilst the presence of zinc 2-mercaptobenzothiazole as the secondary accelerator helps to increase the compression modulus and reduce the compression set of the NR latex foam products. A combination of these two accelerators is important to increase the elastic modulus of the NR latex

foam rather than the rate of vulcanization^{27,41}. However, in this respect, to the best of the authors' knowledge, no quantitative study has been conducted to clarify the effects of varying levels of sulfur and accelerators on the degree of vulcanization and the physical properties of NR latex foam. As a result, data in this field is critical, particularly in determining whether specific compositions result in specific features and benefits. After the NR latex and potassium oleate have been well mixed, the premixed sulfur vulcanizing agent is added slowly into the NR latex. The speed of the mixer is increased to up to 100 rpm to ensure the premixed sulfur vulcanizing agent is comprehensively dispersed in the latex system. After an hour, the mixer speed is decreased to 50 rpm, and the NR latex compound is left at room temperature for at least 16 hours for the maturation process to begin.

After the maturation process, the matured NR latex is subjected to a foaming process. As mentioned above, there are two ways of performing this in the Dunlop process, the batch foaming process (Figure 2.3) and the continuous foaming process (Figure 2.5)²⁷. The batch foaming process is conducted in a Hobart foam mixer comprising a metal bowl and a wire whisk, which whips the NR latex into latex foam. The batch foaming process is suitable for small production units or when miscellaneous products of varying density and/or color are required^{43,44}. Examples of products made using the batch foaming process are shoe insoles, U-shaped neck pillows and dual-density pillows.

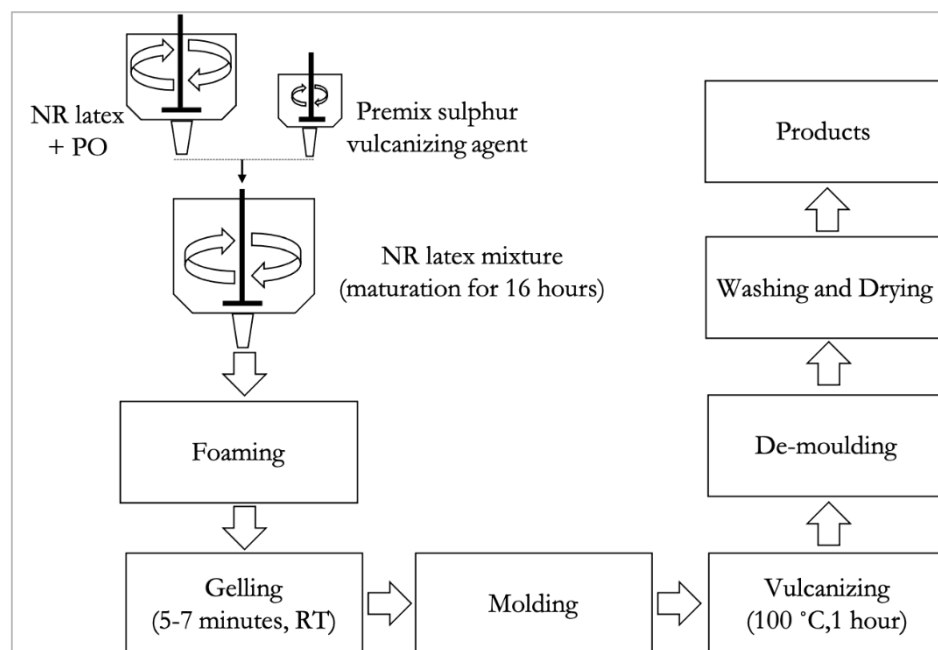


Figure 2.3: Steps involved in the Dunlop batch process. Adapted from²⁷.

In this process, the matured NR latex is whipped in the bowl mixer using the wire whisk in a planetary direction until a targeted volume is achieved. During the whipping process, the presence of potassium oleate in the latex system enhances the growth of bubbles, changing the NR latex

from the liquid phase into the latex foam phase. Technically, the initial whipping process is performed at high speed to allow air to be incorporated into the NR latex until the targeted latex foam wet density has been achieved. Latex foam wet density is crucial in latex foam product manufacturing because different products require specific density levels. For example, shoe insoles require high-density NR latex foam, whilst U-shaped neck pillows require low-density NR latex foam. After the targeted latex foam wet density has been reached, the mixer speed is reduced to a medium rate to refine the foam cell structures. After fine foam cell structures have been obtained, gelling agents are added to set the foam cell structures by means of the gelling process⁴⁴. Table 2.2 shows the gelling formulation used for making NR latex foam. Technically, the initial whipping process is performed at high speed to allow air to be incorporated. Although sodium silicofluoride is usually prepared at 50% TSC, to avoid sudden gelling reactions, it may be an advantage to dilute it to 15% TSC or to pH 7 using sodium hydroxide prior to its addition to the latex foam.

Table 2.2: Gelling formulation used for NR latex foam²⁶

Ingredient	TSC (%)	Dry weight (phr)
Zinc oxide dispersion	60	3.50 – 5.50
Diphenyl guanidine dispersion	40	0.30 - 0.50
Sodium silicofluoride dispersion	50	0.50 - 1.50

phr = part per hundred grams of rubber; TSC = total solid content

At this point, sodium silicofluoride is gradually hydrolyzed as shown in Equation 2.1⁴⁵. The sodium silicofluoride hydrolyzes into silicic acid and hydrofluoric acid, which gel the NR latex foam^{27,41,45}. The presence of hydrofluoric acid causes the pH value to drop gradually (Figure 2.4).

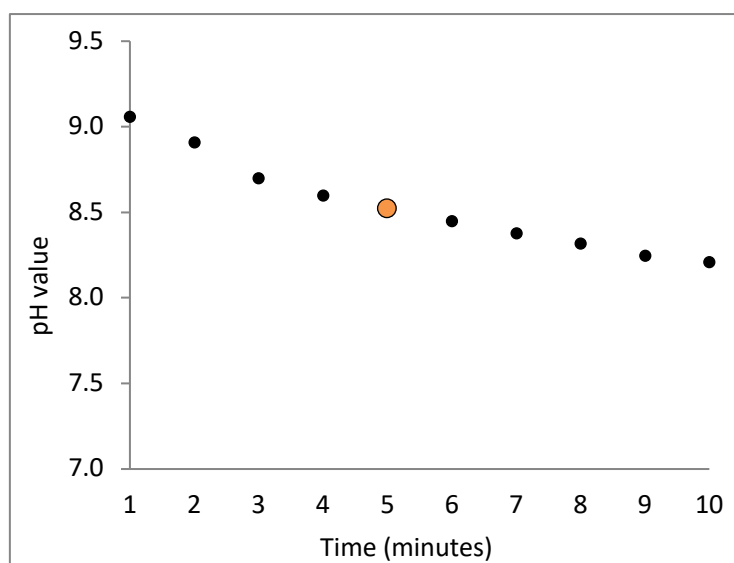
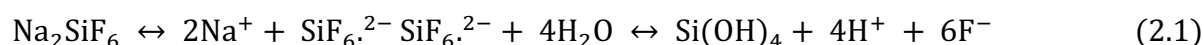


Figure 2.4: NR latex foam gelling time. Adapted from⁴⁶. Orange point indicates NR latex foam gelling time

Normally, the NR latex foam gelling process occurs at pH 8.0 - 8.5^{27,46}. Approximately four to six minutes is required to set the foam cell structures, hence the NR latex foam should be transferred into the product's mold within that period. After filling the mold with the NR latex foam, the mold lid is closed and the NR latex foam is left to stand for another five minutes to allow the gelation to be completed. The NR latex foam is then heated either in a hot air or steam oven to allow vulcanization to occur. After the vulcanization process, the NR latex foam is peeled out from the mold, washed and dried.

For high production volumes requiring large quantities of products with a fixed NR latex foam density, such as mattresses and pillows, a continuous foaming machine equipped with a mold conveyor system is used. Figure 2.5 shows the setup and overall stages of the Dunlop continuous foaming process.

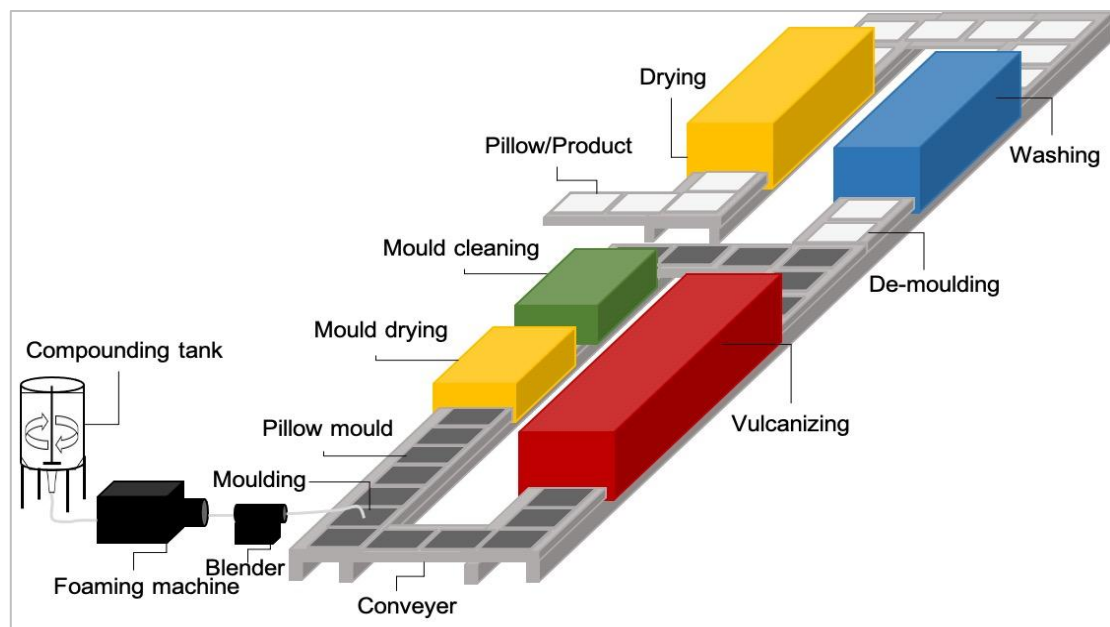


Figure 2.5: Steps involved in the Dunlop continuous process. Adapted from⁴⁷.

In a continuous foaming machine, the matured NR latex and air are metered under pressure into an Oakes foaming head consisting of a rotor enclosed by two stators (Figure 2.6a). The rotor and stators feature many protruding lugs with clearances small enough to provide sufficient shear to foam the NR latex when the rotor revolves. The NR latex foam is generated continuously in the foaming head, where compressed air and the NR latex are mixed at the desired ratio to achieve the required wet (liquid) foam density. It is claimed that NR latex foam with specific gravity as low as 0.06 g/cm³ can be produced using a continuous foaming machine²⁷. Subsequently, the NR latex foam is passed through a length of hose to a dynamic blender machine (Figure 2.6b), into which gelling agents are metered and mixed with the NR latex foam.

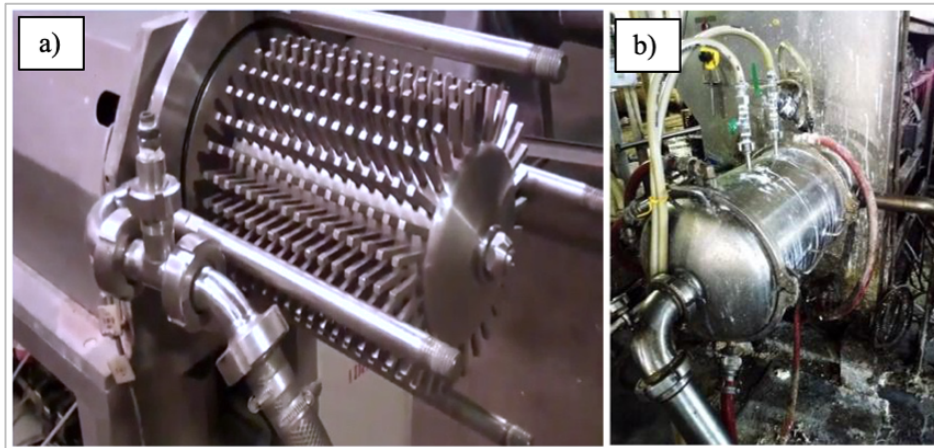


Figure 2.6: NR latex foam continuous foaming machine.
 a) The Oakes foaming head; b) Blender machine
 (Source with permission: LSK Latex Sdn. Bhd. factory)

From the blender, the NR latex foam is discharged into molds designed to produce finished products with the desired shape and size (Figure 2.7). After gelation, the foam is vulcanized by heating it for 30 - 60 minutes at 100 °C in a steam oven. At this stage, the foam cell structure is solidified and the strength of the NR latex foam is further improved.

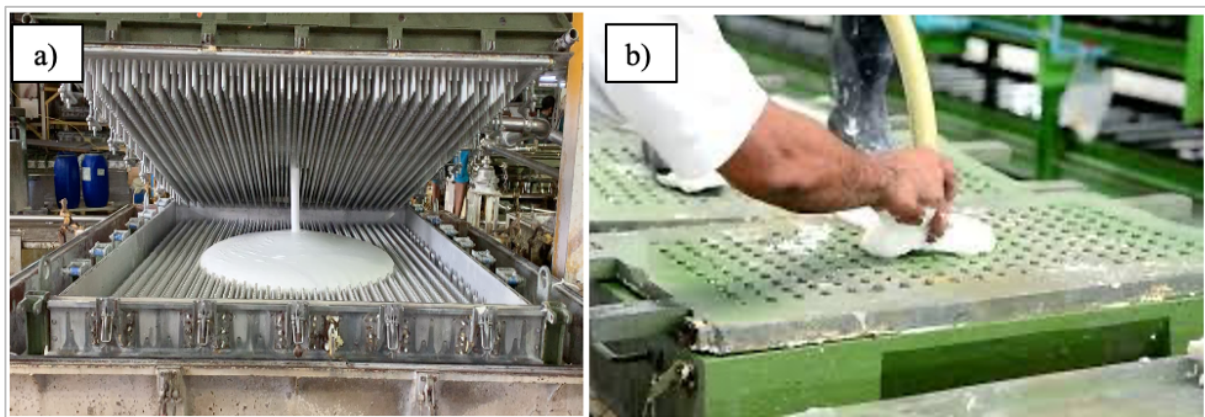


Figure 2.7: NR latex foam products molding process.
 a) Mattress; b) Pillow
 (Source with permission: LSK Latex Sdn. Bhd. factory)

After vulcanization, the mold is opened and the wet NR latex foam is removed. It should be noted that the removal of NR latex foam from the mold should be facilitated as much as possible because the tensile and tear strength of the wet NR latex foam are lower than those of the dry NR latex foam. The wet vulcanized foam is then subjected to a washing process with running water by squeezing and hydro extraction to remove the excess soap and unreacted chemicals, thus improving the hygiene of the end products. After the excess chemicals have been removed, the NR latex foam is dried, either in a continuous tunnel dryer or a batch chamber heated by hot air, radio frequency or a far infra-red frequency system. It is theorized that during the gelling process, the zinc complexes react vigorously with the potassium oleate, subsequently dissociating to form

amine ions and hydrated zinc ions. The resultant free zinc ions interact with the latex-stabilizing component to form water-insoluble zinc derivatives, thus destabilizing the NR latex and causing the rubber particles in the latex foam to gelate into a cellular structure. A secondary gelling agent is necessary as a gel sensitizer to increase the uniformity of the porous structures. The secondary gelling agent enhances the stability of the air interface of the latex foam cell so that the rubber interphase is destabilized first; this produces latex foam gel during the gelling process. Many types of secondary gelling agents are available but the most commonly used is diphenyl guanidine. However, there are health concerns related to the use of diphenyl guanidine in rubber product manufacturing because diphenyl guanidine contains an aromatic amine, aniline^{48,49}. This is a toxic chemical and may have mutagenic and carcinogenic effects⁴⁸. Therefore, research⁴² has been conducted to address this issue, which has included using carrageenan as an alternative, natural-based secondary gelling agent to replace diphenyl guanidine in the NR latex foam process. Although this paper has been published, the research findings remain an experimental laboratory output and have not been adopted by industry players. There are two main reasons for this. First, the newly developed technology needs to be further assessed before it can be used commercially. For example, in pillow production, the wet density of NR latex foam should be low (below 0.09 g/cm³). At this low density, the use of a secondary gelling agent is important to stabilize the latex foam cell structure. Therefore, an alternative secondary gelling agent should be capable of ensuring the stability of the latex foam cell structure during the gelling process. Meanwhile, few attempts have been made to collaborate with industry players on transferring the technology from the laboratory scale to the factory scale due to complex legal issues. On the other hand, it is relatively difficult for industry players to use this new technology because the standard technology is considered well established.

2.5.1.2 The Talalay NR latex foam process

The Talalay process, an advanced NR latex foam process, has become a key development in the NR latex foam manufacturing industry. However, establishing a bedding factory using the Talalay process might require higher financial resources because this technology involves freeze-vacuum equipment. The compounding formulation of NR latex in the Talalay process is almost identical to that of the Dunlop process. However, in the Talalay process, the compounded NR latex is converted into high-density pre-foam without prior maturation. A carefully metered amount of this pre-foam is then transferred into aluminum molds, which are specially designed to allow the circulation of heat-transfer fluids within them. However, interestingly, the NR latex foam partially filled the molds. The molds are sealed by closing their lids. Then, the NR latex foam is expanded to fill the mold, with the application of a vacuum. Once the NR latex foam is fully expanded, the

foam is quickly cooled to a temperature of $-20\text{ }^{\circ}\text{C}$ to prevent it from collapsing and ensure consistent foam cell structures. Carbon dioxide gas is pushed through the NR latex foam to increase the zinc oxide solubility through the formation of ammonium ions of carbonic acid ($\text{CO}_2 + \text{H}_2\text{O} \rightarrow \text{H}_2\text{CO}_3$). Much like the addition of sodium fluorosilicate (Na_2SiF_6) in the Dunlop process, the carbonic acid lowers the pH, thereby causing gelation. The mold is then warmed, so the NR latex foam is thawed and vulcanized by fluids circulating within the body of the mold. Like the Dunlop process, the NR latex foam is removed from the mold and subjected to washing and drying. It is claimed that Talalay NR latex foam is lighter and softer than Dunlop NR latex foam. This is because the latex foam has narrower cell walls and a lower density than the Dunlop NR latex foam. The drawback is that Talalay NR latex foam may break down faster than Dunlop NR latex foam because less raw NR material is used in this type of latex foam. Nevertheless, no quantitative or comparative studies have been conducted on the advantages and disadvantages of the two processes and the properties of products made from either Dunlop or Talalay NR latex foam. This could be due to the complexity of the equipment setup, while it is impractical for an R&D institution (i.e., MRB) to employ both systems in one laboratory. On the other hand, initiating a collaborative study between R&D institutions and factories is also complex because Talalay process factories are commonly found in Western countries, whilst Asian companies prefer to use the Dunlop process.

2.5.2 Current demand for NR latex foam technology

2.5.2.1 The vulcanization processes

NR latex foam technology has experienced slow growth in terms of vulcanization, with most NR latex foam product manufacturers using technology dating from the 1920s²⁷. The use of the hot air or steam oven in the Dunlop process and the freeze-vacuum in the Talalay process for vulcanization consume high levels of energy and time, later reflected in the high usage of electricity or fuel. Therefore, there is substantial demand to develop an alternative technology that can improve the current vulcanization technology and accelerate the vulcanization process, because the primary cost of NR latex foam products is due to the processing technology. So far, infra-red and radio frequency are among the alternative vulcanization and drying technologies that have been developed by industry players. Radio frequency vulcanizing using a drying oven, developed by STALAM⁴⁷, is one such example. According to STALAM⁴⁷, radio frequency technology does not rely on heat transmission, so even thick, dense and variable shapes and thicknesses of NR latex foam can be dried quickly with no surface overheating or yellowing effects. Furthermore, through this technology, the use of conventional aluminum molds in NR latex foam product manufacturing can be replaced by polycarbonate molds. This is because radio frequency waves can penetrate the

polycarbonate mold so the vulcanization process can occur. It is anticipated that a combination of polycarbonate molds and radio frequency technology would accelerate the NR latex foam process, thus proportionally reducing the space required to attain a certain production capacity and being considerably more efficient, leading to energy savings of over 50%. However, no scientific report can be identified to support these claims. Therefore, collaborative studies between R&D institutions and NR latex foam manufacturers are essential to provide scientific data and reports in order to develop the technology that can reduce energy consumption and accelerate the manufacturing process. Meanwhile, there is considerable demand from industry players for technology that would enable a shift from using ample human labor into automation, robotic and/or digital means of advancing the manufacturing process. This would reduce not only labor costs but also the dependence of NR latex foam products manufacturers on human skills to complete certain tasks.

2.5.2.2 Physical properties NR latex foam products

In many product applications, a material's physical properties are becoming the focal point because they are directly related to the product's performance and lifespan. Currently, numerous methods have been developed to examine the physical properties of foam materials including bedding products such as the European Standards (EN) 1957⁵⁰, the International Organization for Standardization (ISO) 2439⁵¹ and the American Society for Testing Materials (ASTM) D3574⁵². Moreover, in-house methods have also been developed by specific institutions - such as Germany's Landesgewerbeamt (LGA), or QualiTest GmbH - to examine the quality of foam products. Surprisingly, these standard methods and product specifications were developed for synthetic foam materials, such as polyurethane foam. No international standard specifications and methods of classifying the quality of NR latex foam products have been developed.

Nevertheless, some countries have developed a national standard. For instance, in Malaysia, the Department of Standards Malaysia, together with the Malaysian Rubber Board, developed Malaysian Standard (MS) 679⁵³ as a quality measure of NR latex foam bedding products such as mattresses. This standard specification forms a guide for Malaysian bedding products manufacturers to commercialize and market their products locally and globally. Table 2.3 shows the requirements of Malaysian Standard (MS) 679⁵³, while the importance of such requirements is discussed below. Compression set is a static fatigue measurement that assesses the degree of irreversible deformation under a specific load⁵⁴. Compression set is also often correlated with the degree of vulcanization of NR latex foam⁵⁵. When the compression set value of NR latex foam is greater than 6%, the NR latex foam is considered under-vulcanized; thus, it does not meet the NR latex foam product specifications^{53,55}.

Table 2.3: Physical properties of NR latex foam bedding products⁵³

Properties	MS679 standard requirements
Compression set (%)	6 (max)
Pounding Change in thickness (%)	5 (max)
Pounding Change in hardness index (%)	20 (max)
Indentation hardness index (N)	100 < (Soft)
	101-170 (Middle Firm)
	> 170 (Firm)
Elongation at break (%)	Min 150
Accelerated aging (%)	±20

Pounding indicates the lifespan of NR latex foam products, which is estimated to be equivalent to 10 years of daily (8 hours per day) usage. Pounding test is measured based on changes in hardness index and thickness after the latex foam receives a total of 250,000 compression poundings at a rate of four times per second. The elongation at break value refers to the physical strength of the latex foam. A higher elongation at break value indicates that the latex foam can be stretched for longer before breaking. If the elongation at break value of the latex foam does not meet the requirements, this indicates that the material will tear easily, so extra care is needed during product handling. On the other hand, the subjective individual perceptions of the hardness of foam products such as mattresses has led to the development of the classification of indentation hardness. There are three classifications: soft, middle firm and firm based on the indentation hardness (IH) value. In NR rubber product industries, the aging test is used to estimate the durability or life span of NR latex foam products in years. Accelerated aging is the measurement of the IH value of the NR latex foam after the NR latex foam has aged. The effect of aging on NR latex foam should be 20%.

Besides these physical measures, the density of NR latex foam also plays a major role in the physical performance of mattresses and pillows made from this material. The NR latex foam density is calculated using the mass and volume of the material. The density of NR latex foam products can vary from 0.12 g/cm³ to 0.05 g/cm³, depending on the targeted applications. For example, the density of NR latex foam mattresses is normally in the range of 0.12 g/cm³ to 0.08 g/cm³, whilst the equivalent for pillows ranges from 0.05 g/cm³ to 0.08 g/cm³. It should be noted that to comfortably support the body and neck during sleep, the density of an NR latex foam mattress should be greater than that of a pillow. This is because the body is heavier than the head, so the mattress density should be higher to support the body's weight and promote the spine's natural alignment. On the other hand, an NR latex foam pillow requires low-density foam material because this type of foam is softer, so it should offer more comfortable support to the neck joints

and shoulders during sleep. Previous studies^{20,56} stated that a soft material with characteristics that offer effective support for the cervical spine and neck appears to be the optimum choice of material for pillow fabrication. A comparative study by Gordon *et al.*⁵⁷ found that NR latex foam pillows appear to be the best type of pillow for providing decent spinal alignment, leading to the least muscle activity and extra comfort. NR latex pillows are also recommended to relieve headaches or scapular/arm pains, as well as reduce awakening symptoms.

On the other hand, the current expansion of the middle classes in Asian countries has resulted in higher demand for health and wellness products. This has led to research into pillow and mattress materials and designs that could reduce sleep disruption events such as neck pain, snoring and awakening^{13,58,59}. Gordon *et al.*⁵⁷ stated that the key function of a pillow during sleep is to support the neck and head in a position that maintains the cervical spine in its neutral posture while sleeping. The human neck naturally curves slightly forward to sustain the weight of the head when upright, and it is important to maintain this curve during sleep⁵⁷⁻⁵⁹. Therefore, Lin and Wu¹³ proposed a solution to contour the neck's natural curves, owing to the pillow's prominence under the neck region. Previous studies^{13,60,61} stated that a cervical-shaped pillow can offer better support to the cervical spine, thus restoring cervical lordosis and avoiding neck and shoulder pain while sleeping. However, evidence indicating the benefits of cervical-shaped pillows remains disputed. Some studies^{13,60-63} demonstrated that cervical-shaped pillows could maintain the spine in a neutral posture and thus allow the joints and muscles to achieve the optimal resting state. However, other studies^{24,64,65} found that a cervical-shaped pillow induced hyper-extension of the neck and was poorly tolerated. Jeon *et al.*⁶⁵ stated that although cervical-shaped pillows increased cervical lordosis with firm support, the feeling of firm support might be a negative outcome of increased comfort among users. Therefore, future studies must identify which pillow design factors influence pressure-relief and sleeper comfort.

Another important property of NR latex foam mattresses and pillows that influences sleep quality is their thermal characteristics⁶³. A study by Liu *et al.*⁶³ suggested that using a cool material that can reduce sweating and whole-body temperature would indirectly improve sleep quality. This is because the heat generated by the brain's metabolism during sleep is transferred from the skin surface to the pillow and dissipates into the environment¹¹, making sleepers comfortable overnight. It is widely known^{37,44,65} that NR latex foam is a porous material with open-cell structures (Figure 2.8). The porous structures of the foam not only influence the softness of the pillow but also offer better ventilation properties than normal pillows. Technically, the open-cell structures of NR latex foam contain air and can easily become deformed under pressure (e.g., when pressed by an object)³⁷. In other words, NR latex foam with open-cell structures would allow air to pass through

it, thus providing better airflow than conventional pillows. Therefore, NR latex foam is the optimum choice for mattresses and pillows because of the material's capacity to provide better air flow during overnight sleep. Therefore, the material is currently gaining greater re-acceptance by consumers and retailers as a premium bedding product.

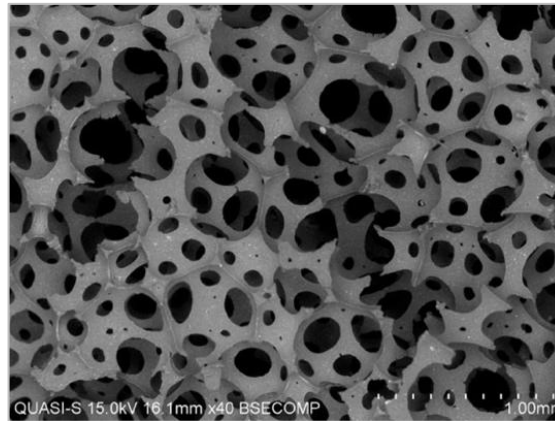


Figure 2.8: Open-cell structures of NR latex foam³⁷.

2.5.2.3 Environmental, health and hygiene issues

Most bedding products available in the market, such as mattresses and pillows, are made from petrochemicals-based foams using polyurethane or polyester because of their versatility and ease of handling. However, it is widely recognized that such materials contribute to environmental issues, such as carbon emissions during manufacturing and waste management problems^{10,19,20,66}. Petrochemicals-based foam can also cause human health hazards. For example, isocyanates, one of the chemicals used to produce polyurethane, has been recognized to induce occupational asthma caused by high exposure to it at work or sensitization^{21,67,68}. The presence of isocyanates in materials used for mattresses and pillows has also raised awareness among users that such mattresses and pillows could release toxic gasses that may cause health hazards²¹⁻²⁴. Furthermore, the growing awareness of the risks of global warming and fossil fuel depletion has led several countries to encourage foam-based product manufacturers to use alternative green materials in the manufacturing process^{67,68}. NR latex foam is one such potential green material.

Previous study⁶⁹ has reported that the global NR latex foam mattress market size was valued at USD 7.8 billion in 2018 and was expected to expand at a high compound annual growth rate (CAGR) of 7.3% from 2019 to 2025. The study also stated that the consumer preference for high-end lifestyle products is a key factor driving the demand for mattresses and pillows made from NR latex foam. Moreover, mattresses and pillows made from NR latex foam are safer and have proven to be comfortable and durable. Nevertheless, NR latex foam mattresses and pillows are expensive because of the limited availability of the raw materials and the complexity of the manufacturing process. Consequently, some bedding manufacturers are now blending NR latex

with synthetic latex to produce NR latex foam products with a 'green image'. This blending has become a common approach of industry players since it offers the advantage of higher profits, with synthetic latex being cheaper than NR latex. Interestingly, bedding manufacturers claim that the blending process incorporates the best qualities of each latex type⁷⁰. Furthermore, some manufacturers or retailers are labelling such products as "contains NR latex", while others simply (but falsely) claim them to be "made from natural origin". It should be stressed that the blending process is not the proper way to produce NR latex foam mattresses and pillows. The blending process not only leads to incorrect perceptions that it is a 'green material' but also affects the properties of NR latex foam. This is because bedding products made from blended latexes exhibit poor durability, poor physical properties and higher heat retention compared to NR latex foam⁷⁰. Moreover, extra chemical additives are required to improve the homogeneity between the synthetic latex and the NR latex. Meanwhile, manufacturers might need to add antibacterial agents to avoid the growth of bacteria and fungus.

To address these issues, the MRB has developed a Malaysian Standard, MS 2623, to distinguish between pure 100% NR latex foam and blended latex foam, which has been accredited for national use by the Department of Standards Malaysia⁷¹. This test method is used to identify β -sitosterol in NR in its raw and vulcanized form. Principally, the polymer can be characterized using Fourier Transform Infrared Spectroscopy. Cis-1,4-polyisoprene (rubber) can be found in both NR and synthetically prepared rubber. However, β -sitosterol is only present in NR. Therefore, the presence of β -sitosterol can be used to confirm that a cis-1,4-polyisoprene rubber is of natural origin. Nevertheless, as with Malaysian Standard MS 679, Malaysian Standard MS 2623 is not yet accredited by global standards organizations such as the International Organization for Standardization (ISO). Therefore, the Malaysian Rubber Board submitted a draft to the ISO Technical Committee (ISO/TC45) so that the standard can become accredited and used worldwide. However, acceptance or accreditation by an international body might take several years due to the complexity of the process.

Besides blending NR latex with synthetic latex, the addition of filler is another method that has been practiced by bedding manufacturers to reduce material costs. The most commonly used low-cost material is calcium carbonate dispersion. However, the unexpected detection of VOCs and radon in NR latex foam mattresses has recently elevated awareness among users that NR latex foam products, over time, might release toxic gasses and potentially cause health hazards^{24,72-74}. Lavin *et al.*²⁴ revealed that radon was detected in the NR latex foam made by an unrevealed company due to the use of filler, namely monazite, in the latex foam. Besides monazite, radon emissions from NR latex foam mattresses are thought to be linked to the usage of a uranium-

polluted filler such as calcid (chalk). Therefore, it is important for the bedding manufacturer to carefully select the type of filler added into the latex foam. On the other hand, the possible reason for the detection of VOCs is that they are widely used as chemical additives in the production of vulcanizing ingredients. For example, β -sodium naphthalene sulfonate formaldehyde is used during the preparation of sulfur dispersion to change sulfur from powder form into dispersion. Meanwhile, NR latex has been recognized to contain proteins, high fatty acids, phospholipids and a small amount of surfactant, all of which could aid in the detection of VOCs, particularly when they are degraded.

Apart from the negative effects of fillers and blending techniques on the quality of NR latex foam, there is now a great demand for hypoallergenic NR latex foam mattresses and pillows. This is due to the increased prevalence of clinical sensitivity to NR latex products^{39,40}. NR latex products contain extractable rubber proteins, which, when they come into contact with human sweat, can cause latex allergies or *Type I* (immediate) hypersensitivity reactions^{75,76}. Latex allergy symptoms can be mild, such as redness of the skin and itching, or severe, such as wheezing, mucosal swelling and anaphylactic shock^{75,77}. Although no evidence has been reported of NR latex foam mattresses and pillows causing latex allergies, as is the case with NR latex gloves, the latex allergy issue has raised awareness among users of the potential risks of using other products, including mattresses and pillows, made from NR latex foam^{6,40,78,79}.

As mentioned earlier DPNR latex is a modified form of NR latex. Deproteinization is a process of treating the NR latex with a proteinase enzyme to hydrolyze proteins in the latex system, which are then eliminated through a concentration process². Therefore, the resultant products exhibit lower extractable proteins compared to normal NR latex products, as well as being odorless (they less smell of rubber)^{37,80}. DPNR latex could be the optimum alternative NR latex for producing NR latex foam mattresses and pillows with improved hygiene or hypoallergenic properties. However, the manufacturing technology has not yet been established; this would include compounding, foaming and gelling formulations to produce NR latex foam mattresses and pillows especially within a continuous foaming process for high production volumes. Therefore, this area should become a focal point for researchers in the near future.

2.6 Potential applications of NR latex foam

2.6.1 NR latex foam as seat cushions

Seat is one of the most critical parts in a transportation vehicle where they are always in contact with the occupant when the vehicle is used. Therefore, the desire of occupant for comfort in vehicle seats are continuously rising. There are two key types of comfort: static and dynamic. Static

comfort is known as the frame and support given by the seat itself. Dynamic comfort on the other hand, is identified with the level of vibrations experienced by the occupant sitting in a vehicle seat.

NR latex foam is a versatile material due to its physical properties such as elastic, soft, good support and porous structures. Such properties make NR latex foam one of the best materials for use in bedding products such as mattresses and pillows. However, the application of NR latex foam should not be limited to bedding products. This is due to the fact that physical properties of NR latex foam are also beneficial for other cushioning products including seat cushions in the transportation industry.

Previous studies⁸¹⁻⁸³ revealed that a person sitting on a hard surface can have interface pressures of more than 200 kPa in the posterior area, especially at the bony prominence area. Another study⁸¹ stated that long-time sitting can cause various complexities including impeding the bloodstream, which can cause redness or soreness. Body weight in sitting posture causes pressure of the perianal region of the body, which restricts the blood-stream to the urethra, bladder, prostate, and legs. A good seat cushion should have interface pressures approximately between 60 kPa to 120 kPa system. Utilization of the seat cushion is crucial, as it is directly responsible for the comfort and safety of the occupant while sitting⁸⁴. The capability of NR latex foam to redistribute the body weight pressure over a larger area, and thus relieving pressure on stress points of the body is therefore, useful for seat cushions application, typically to reduce pain at the posterior area (buttock-thigh area) upon sitting especially during long-distance travel.

Besides cushioning properties, NR foam is beneficial to reduce vibration transmission from the transportation vehicle to the human body. Previous study⁸⁵, revealed that exposure to vibration generated by the transportation vehicle may lead to adverse health effects known as whole-body vibration syndrome (WBVS). WBVS is characterized by disorders of the muscles, nerves, bone, joints, and circulatory systems. WBVS exposures are associated with transportation where the occupant is exposed to mechanical disturbances and impacts while traveling. Vibration is usually transmitted through seat surfaces, backrests, and through the floor. Although many measurements include higher frequencies, humans are most sensitive to vibration within the frequency range of 2 to 20 Hz. Besides WBVS, vibration also causes motion sickness. Motion sickness can occur when a person is exposed to real or apparent low-frequency motion (below 1 Hz).

It is well-known that vibrations are emitted from the source to another area through a structure-borne and airborne system⁸⁶⁻⁸⁸. In simple terms, structure-borne is the transmission of mass particles (vibrations) through solid structures, such as steel, wood, concrete, stone etc. On the other hand, airborne air consists of sound pressure waves propagating through air. In the last

few decades, the variety of specialized vibration materials has increased greatly⁸⁵. Nevertheless, porous structures material known as polymer foam material has been widely used to minimize vibration pollution due to its versatility such as light-weight, flexible and high strength⁸⁹⁻⁹¹. The irregular foam cell structures of polymer foam materials allow pressure waves to interact with membranes so that the energy is transformed into heat, thus absorbing an extent of the vibration^{91,92}.

However, the production of polymer foam materials contributes to the emission of greenhouse gasses into the atmosphere. Furthermore, environmental issues such as sustainability of materials and eco-efficiency have received much attention in recent years^{67,68}. This has led to research concerning the utilization of residual materials obtained from agricultural industries such as natural fibers to substitute polymer foam materials^{93,94}. Various natural fibers, such as flax, hemp, jute, sisal, palm oil, kenaf, banana, and coconut have been studied to be used as vibration-damping material^{95,96}. In fact, natural fibers have advantages over polymer foam materials such as low cost, abundance, comparable specific properties, renewability and biodegradability^{94,97}. Nevertheless, the performance of natural fiber as an alternative material for vibration-damping materials is not as good as polymer foam materials. Therefore, many research works are being tailored to incorporate natural fiber into polymer foam materials, thereby producing polymer foam composite materials with enhanced biodegradability^{19,67,68,93,94}. Although the incorporation of natural fiber into polymer foam materials offers a solution in minimizing the use of synthetic polymer hence reducing environmental impact, they are still associated with health hazards whereas there is a possibility of the materials over time, releasing toxic gases²¹⁻²⁴. Therefore, there is a necessity to develop vibration-damping material entirely made from a natural material, for example, SpNR latex foam.

2.6.2 NR latex foam for sound and vibration control

Acoustic foam materials have been installed on walls, ceilings, doors of a recording studio, auditorium, cinema, ball room, etc. to control noise and unwanted sound, as well as to mitigate noise transmission from one area to another^{90,98-101}. Acoustic foam materials can be made from different types of materials but polymer foams have become the material of choice because of their lightweight and simple manufacturing process. Polymer foams can be categorized either as closed-cell foam or open-cell foam structures (Figure 2.9)¹⁰². Both closed-cell and open-cell foams have their advantages and disadvantages; and are normally tailor-made for specific applications. Open-cell polymer foams are interconnected with each other. They have a spongier appearance and are softer than closed-cell polymer foams. Open-cell polymer foams provide better sound absorptive capability compared to closed-cell polymer foams and are incredibly effective as a noise absorber for middle and high-frequency ranges. On the other hand, for closed-cell polymer foams,

the foam cells are isolated from each other and cavities are surrounded by complete cell walls. Generally, closed-cell foam has lower permeability, leading to better noise insulation properties. Therefore, the selection of a suitable type and properties of polymer foams is crucial because each of them possesses specific characteristics to perform its own function and is not capable of carrying out both tasks.

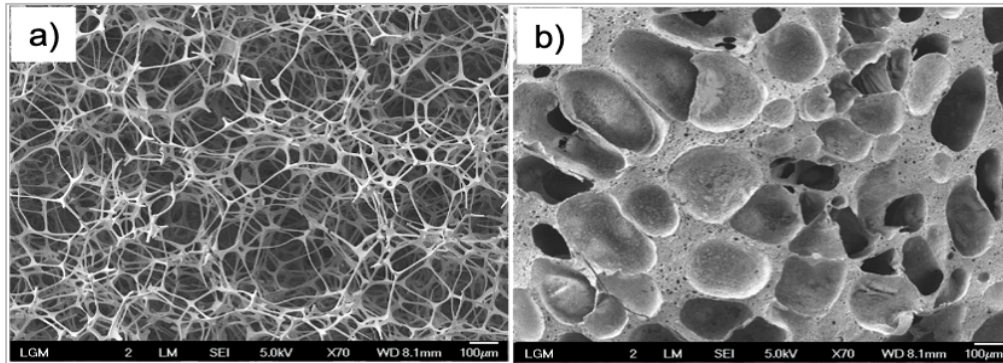


Figure 2.9: Polymer foams⁴⁵.

a) Open-cell structures of melamine; b) Closed-cell structures of styrene butadiene rubber.

Normally, for a recording studios, theaters, and cinemas, acoustic foam materials made from open-cell foam materials are mounted to absorb the unwanted sound or control echoes. On the other hand, for building and construction applications, acoustics foam materials made from closed-cell foam materials are installed onto a wall as a barrier to dampen the noise propagation from one area to another. The sound insulation or sound transmission loss of a wall is that property that enables it to resist the passage of noise or sound from one side to the other. This should not be confused with sound absorption which is that property of a material that permits sound waves to be absorbed, thus reducing the noise level within a given space and eliminating echoes or reverberations¹⁰³. Figure 2.10 shows the basic concept of sound absorption and sound insulation characteristics of acoustics foam materials.

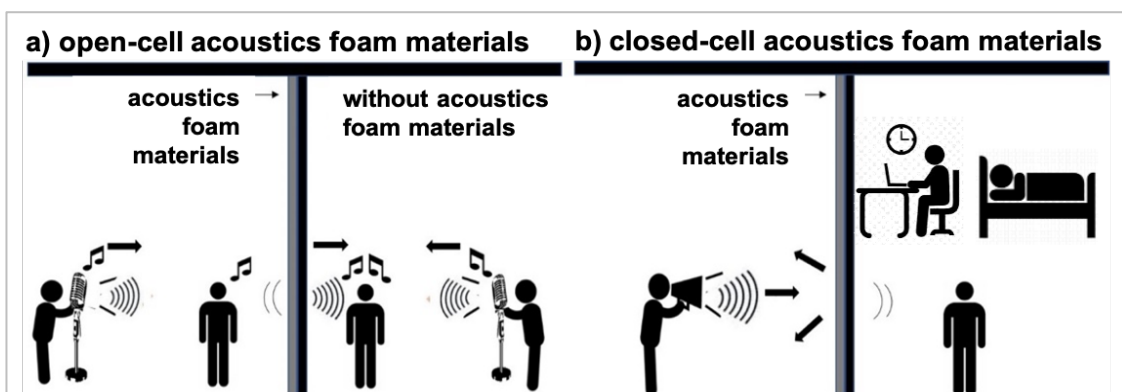


Figure 2.10: The basic concept of sound absorption and sound transmission. Adapted from¹⁰⁴.

a) open-cell foam absorbed echoes and reverberations; (b) closed-cell foam reduced noise propagation from one room to another

Figure 2.10a illustrates that, when sound waves strike on the acoustics foam materials, the porous open-cell structures permit the sound energy to enter into the material through numbers of pores and small cell openings. The open-cell structures allow sound waves energy to interact with membranes. The sound waves energy is then trapped in the porous structures, and forced to change direction several times. Each time the sound wave energy changes its direction, a part of the sound energy is absorbed by conversion to heat. The main purpose of open-cell acoustics foam materials is to control the sound reverberation level inside a confined space, creating a pleasant acoustics environment. On the other hand, Figure 2.10b shows that, when sound waves strike the sound insulation panel, the energy of the sound waves propagates into and through the porous structures. When the energy of the sound wave reaches a reflective surface, it will be reflected or forced to change direction to exit the material. Part of the energy of the sound wave will travel a long-distance before passing completely through the porous materials. Therefore, some of the noise will be reflected into the room, and some will be transmitted into the adjacent room through the wall¹⁰⁵. The main function of closed-cell acoustics foam materials is to reduce the sound intensity to a level that is not harmful to the human ear. Nevertheless, besides foam-cell structures, the effectiveness of sound absorption/insulation also depends on other factors such as thickness, density, and intrinsic properties of the materials¹⁰⁶.

Besides buildings or entertainment industries, acoustics foam materials also have been utilized to control noise in the transportation industry, for example automotive industry^{100,101}. The automotive industry typically has seen rapid evolution over the past few decades focusing on vehicle exterior design. However, in recent years the market radically has changed, with a focus on technologies, new features and advanced materials that could provide safety, extra comfort, and better quality of the driver and passenger experience. As a result, vehicle interiors have received great attention as a differentiator that can differentiate a vehicle model from its competitors. According to Chen¹⁰⁷, the passenger vehicle cabin is the only space for drivers and passengers to enjoy their driving or traveling. Therefore, the interior quality of a vehicle is often becoming an important factor in influencing customers' purchase decisions. Customers appraise the vehicle interior quality not only by visual assessment such as surface style and color, but also by acoustical assessment such as quietness, noise, vibration, and harshness (NVH). NVH cancellation of passenger vehicles is an important invisible factor for vehicle comfort that will leverage consumers' preferences in the decision-making process.

To support the increasing demand for acoustic foam material for NVH cancellation, in the transportation industry, manufacturers are now developing superior grade materials having better noise absorption and vibration-damping characteristics. Additionally, this material is expected to

show acceptable physical and mechanical properties, and to comply with the interior body of the vehicle specifications. Further to that, with the growing awareness concerning the rising risk of global warming and fossil fuel depletion, as well as new legislations that have been implemented by several countries typically in European countries to utilize ‘green materials’ in products manufacturing, it is essential to develop acoustic foam material from natural-based material. One of possible solution is by using SpNR latex foam as the material. However, manufacturers are facing the challenge of developing acoustic foam material from SpNR latex because this material should offer a tailored design and higher performance without any negative impact on material cost. Additionally, the material should be a lightweight material so that it would not increase fuel consumption.

2.7 Summary

Most foam products, such as bedding, shoe insoles, and seat cushions, are made from synthetic polymer foams, i.e., polyurethane, polyester, and ethylene vinyl acetate. However, synthetic polymer foams have been linked to environmental and health issues and have contributed to challenging waste management and disposal problems. Additionally, with increasing awareness of the rise of global warming and fossil fuel depletion, as well as new legislation implemented by several countries to encourage the use of ‘green materials’ in the manufacture of new products, it is timely and desirable to develop foam products from natural resources. NR latex foam is a natural and porous material made from NR latex concentrate that was harvested from rubber trees. NR latex foam can be produced through the Dunlop process or the Talalay process. Although there are new developments in the NR latex foam processing technology, the Dunlop process is considered the main technology used in the latex foam industry. The unique open-cell porous structures, soft, elastic and good support properties of NR latex foam making them suitable for bedding products such as pillows and mattresses. However, the application of NR latex foam should not be limited to bedding products since such properties are also beneficial for other applications, including seat cushions and sound and vibration control in the building and transportation industries. Further to that, NR latex that was harvested from rubber trees can be modified to improve its properties, which later impart the properties of the end products. There are two types of modified NR latex, namely ENR latex and DPNR latex. However, the current applications of ENR and DPNR latex are in the form of bulk rubber to produce dry rubber products such as tires and automotive parts. There is limited information on the use of ENR and DPNR latex in latex-based products, typically in latex foam products. This is mainly due to the lack of information on the physicochemical properties of ENR latex and DPNR latex, as well as

the fundamental understanding of the foamability and stability of the latex foam. Additionally, the compounding, foaming, and gelling formulations to produce ENR latex foam and DPNR latex foam have not yet been established. Further to that, due to the lack of information on the chemical, physical, and mechanical properties of ENR latex foam and DPNR latex foam, their potential application in the foam industry is limited.

Chapter 3

Methodology

3.1 Introduction

This chapter presents the research methodologies employed at different stages of the research. Its primary purpose is to highlight the linkages between the methods and the individual chapters. Methods which have not been described in detail in this chapter are discussed in the individual chapter to ensure a better understanding of the research.

3.2 Preparation of SpNR latex concentrate

3.2.1 Materials and collection of freshly tapped NR latex

SpNR latex concentrate was prepared from freshly tapped NR latex collected from the MRB plantation in Kota Tinggi, Johor. The collected freshly tapped NR latex was preserved first using an ammonia solution to avoid coagulation before being transferred to the MRB Experimental Station at Sg. Buloh, Selangor for further process. All chemicals used in this work are commercially available. Formic acid (95%), hydrogen peroxide (30%), ammonium laurate (30%), ammonia solution (25%), alcalase (99%) and hydroxylamine neutral sulphate (99%) were purchased from Sigma-Aldrich (M) Sdn. Bhd.

3.2.2 Preparation of ENR latex concentrate

ENR latex was prepared in accordance with a standard process and formulation described elsewhere^{3,28,108,109}. The process involves *in-situ* chemical reactions of hydrogen peroxide and formic acid which substitutes the double bond structure to generate an epoxy group onto the rubber molecules. In this study, the epoxidation process of freshly tapped NR latex is conducted in a jacketed reactor. Figure 3.1 illustrates the overall process of producing ENR latex concentrate. In general, the composition for producing ENR latex comprises freshly tapped NR latex, a non-ionic surfactant, formic acid and hydrogen peroxide. Preferably, the freshly tapped NR latex should have a TSC of 30%. The process starts with the addition of 2.0% non-ionic surfactant containing fatty alcohol ethoxylated groups into the latex under slow stirring. The mixture was stirred for 30 minutes to achieve a homogeneous mixture. Formic acid (0.75 mol) and hydrogen peroxide (1.00

mol) solutions were added slowly and mixing was carried out for approximately 10 minutes between each addition to ensure homogeneity.

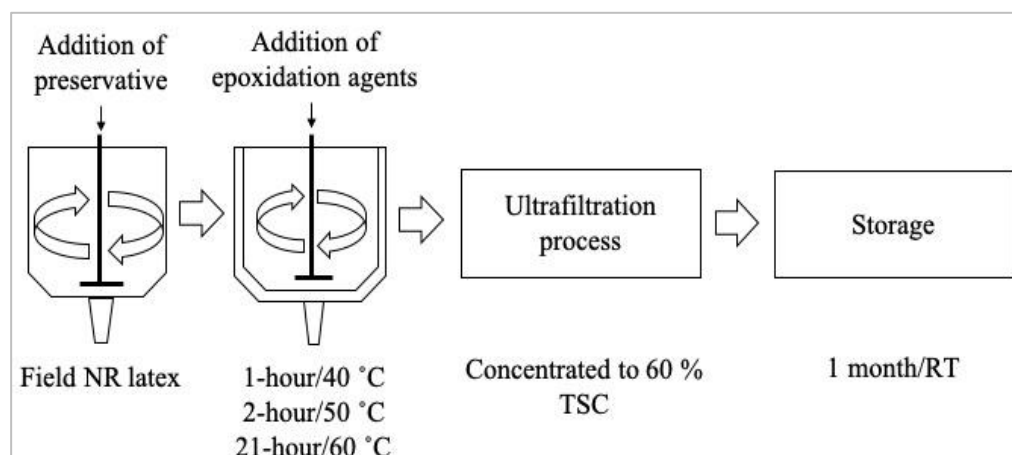


Figure 3.1: Process for the production of ENR latex concentrate.

Once all the addition was completed, the NR latex mixture was heated at the temperature of 40 °C for an hour, 50 °C for 2 hours and 60 °C for a further 21 hours for the epoxidation reactions to take place. During the heating process, the NR latex mixture was stirred at 50 rpm to allow efficient heat distribution during the reaction. Once the targeted time for epoxidation process was achieved, the reacted NR latex mixture was cooled down to room temperature and the epoxidation reaction was terminated by neutralizing the latex ammonia solution until it reached a pH of 7. The production of the ENR latex concentrate involves continuously pumping the preserved ENR latex into a series or parallel ultrafiltration membrane arrangement according to the method patented in PI 2012004868¹¹⁰, wherein the ultrafiltration technology comprises multi-tubular ceramic membranes having pore a size between 50 and 100 nm. This ultrafiltration technology uses pressure (300 to 400 kPa) as the driving force and separation depends on the pore size of the membrane applied. Therefore, it is essential to ensure that the process is maintained below 40 °C to avoid blockage of the membrane system¹¹⁰⁻¹¹². More importantly, to obtain an ENR latex concentrate having a TSC content of more than 60%, the preserved ENR latex (having a TSC about 30%) is passed through the multi-tubular ceramic membranes in a continuous manner until 50% by weight of a clear serum is obtained. The clear serum is removed as permeate, leaving behind a retentate having a TSC of approximately 60%.

3.2.3 Preparation of DPNR latex concentrate

For the preparation of DPNR latex concentrate, the deproteinization of freshly tapped NR latex was carried out via heat enzymatic hydrolysis reactions. Enzymatic hydrolysis reaction is a well-known technique for deproteinization of NR latex²⁹. Conventionally, the NR latex is mixed with proteinase enzyme and surfactants; and left at room temperature for 72 hours for the enzymatic

hydrolysis reactions to take place. However, this procedure is a time-consuming process. Therefore, to accelerate the enzymatic hydrolysis reactions, this study introduces a novel approach by heating the NR latex mixture to a high temperature in a jacketed reactor. After that, an ultrafiltration process using membrane separation technology is adopted to concentrate the DPNR latex. Figure 3.2 illustrates the overall process of producing DPNR latex concentrate. In general, the composition to produce DPNR latex comprises freshly tapped NR latex, proteinase enzyme and non-ionic surfactant. Preferably, the freshly tapped NR latex should have a TSC of 30%. The method starts with the addition of 2.0% non-ionic surfactant followed by 0.15% alcalase and 0.15% hydroxylamine neutral sulphate; mixing was carried out for approximately 10 minutes between each addition to ensure homogeneity. Once all the additions were completed, the NR latex mixture was heated to a temperature of 60 °C for 6 hours using a jacketed reactor. During the heating process, the NR latex mixture was stirred at 50 rpm to allow efficient heat distribution during the reaction. After the completion of the heat enzymatic hydrolysis reactions, the reacted NR latex mixture was cooled down to room temperature and preserved with ammonium laurate and ammonia at levels of 0.1% and 0.4% respectively. The preserved NR latex was then pumped into the ultrafiltration membrane separation system to obtain an DPNR latex concentrate having a TSC content approximately of 60%, similarly to the ENR latex process¹¹³.

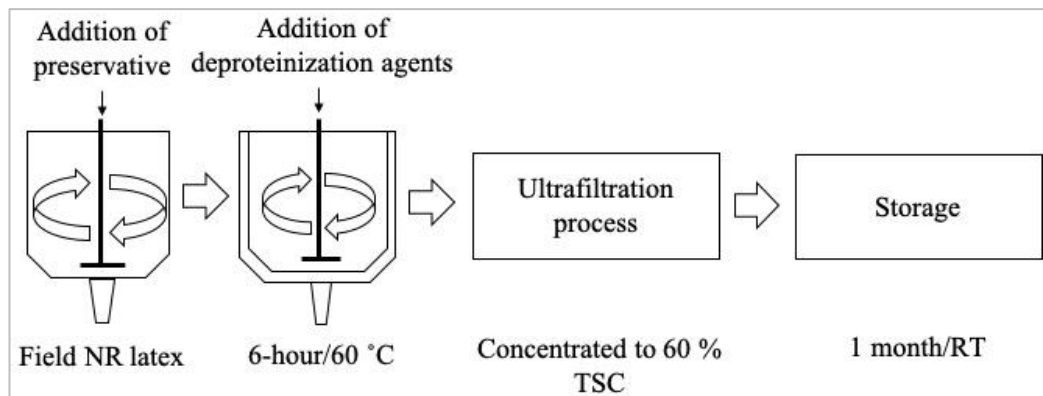


Figure 3.2: Process for the production of DPNR latex concentrate.

3.3 Characterization of SpNR latex concentrate

3.3.1 Determination of the dry rubber content, total solid content and alkalinity

In this work, a modern and fast technology developed by MRB known as RRIMETER[®] was used. The determination of dry rubber content (DRC), total solid content (TSC) and alkalinity (NH₃) was carried out according to an MRB *in-house* method developed through calibration and comparison to the standard latex testing method¹¹⁴. Approximately 20 mL of latex was poured into

the RRIMETER[®] container and placed in the RRIMETER[®] slots. DRC, TSC and alkalinity values of the latex were analyzed automatically using the instrument and recorded.

3.3.2 Viscosity measurement

The viscosity of the latex was measured at specified time periods using a Brookfield viscometer (model LVF) with spindle No. 3 at 60 rpm in accordance with ISO 1652:2011 standard¹¹⁵.

3.3.3 Measurement mechanical stability time

The mechanical stability time (MST) was examined using a KLAXON latex stability test machine in accordance with ISO 35:2004 standard¹¹⁶.

3.3.4 Determination of pH value

A glass electrode of a pH meter model HANNA Instruments 2210 was placed into the latex. The test principle is based on the direct determination of hydrogen ion concentration in the solution.

3.3.5 Determination of nitrogen content

Nitrogen content is a measurement of the deproteinization level of DPNR latex. The nitrogen content was determined in accordance with the Kjeldahl method¹¹⁷. A $w = (0.1 \pm 0.05)$ g quantity of sample was weighted and placed into the Kjeldahl flask, followed by the addition of 0.65 g of catalyst and 2.5 mL of concentrated sulphuric acid. The mixture was boiled until the solution turned into a clear green or almost colorless liquid. Next, the mixture was cooled down and diluted with 10 mL distilled water; and transferred to the distillation apparatus. After that, 10 mL of sodium hydroxide was added into the apparatus and washed down again with distilled water. In another conical flask, 10 mL of boric acid was added into the flask with three drops of methyl red indicator and placed at the receiver vessel tip. At this stage, it is important to ensure the receiver tip reaches the boric acid mixture. Once the boric acid turned green and 5 minutes had elapsed, the conical flask was adjusted until the receiver tip position was well above the solution. Further to this, the distillation process was allowed to continue for a further 1 minute. Finally, after 1 minute, the end of the receiver was washed using distilled water. The distillate collected was titrated with sulphuric acid until the color turned from green to light violet. The titrate value was recorded, and the nitrogen fraction was calculated using Equation 3.1:

$$Nf = \frac{(V_1 - V_2) \times N \times 0.014}{w} \quad (3.1)$$

where Nf is nitrogen fraction, V_1 is the volume of sulphuric acid required for titration of the contents in the conical flasks, V_2 is the volume of sulphuric acid required for titration of the blank, N is the normality of the sulphuric acid and w is weight of the samples.

3.3.6 Determination of epoxidation level via ^1H nuclear magnetic resonance

The determination of ENR structure using the ^1H -NMR method was developed by Durbetaki and Miles^{118,119}. The percentage of epoxidation level (El) of ENR was estimated from the intensity ratio signals presented in Equation 3.2.

$$El = \frac{I_2}{I_1 + I_3 + I_4} \quad (3.2)$$

The determination of the El was performed based on the olefinic and epoxy methane protons at $\delta = 5.3\text{-}5.0$ ppm (I_1) and $\delta = 2.9\text{-}2.6$ ppm (I_2) respectively. For the determination of ring opening, the measurement was carried out using integration peaks of $\delta = 3.5\text{-}3.2$ ppm (I_3) and $\delta = 4.0\text{-}3.7$ ppm (I_4). For both determination methods mentioned above, tetramethyl silane (TMS, $\delta = 0.0$ ppm) was used as the standard. In this work, Bruker AMX 400 Wide Bore nuclear magnetic resonance (NMR) spectrometer ($^1\text{H} = 400$ MHz) was used to perform the analysis. An *in-house* method developed by MRB¹²⁰ was followed. The procedure involved dissolving approximately 25 ± 5 mg of rubber in 2 mL of deuterated chloroform solvent. The mixture was kept in a specimen vial at room temperature in a dark area for 24 hours. Then, 1 mL of the sample solution was pipetted and transferred into a 5 mm NMR tube which was sealed with a tube stopper and placed inside the NMR chamber for analysis.

3.3.7 Analyzing SpNR latex using Brookhaven particle analyzer

The particle diameters of all latexes were measured using a Brookhaven Particle Size Analyzer (90Plus/BI-MAS). Dynamic light scattering (DLS) provides a simple and fast method for micron and nanoparticle sizing. In this technique, spectroscopy of quasi-elastically scattered light intensity fluctuations arising from the Brownian motion of particles is analyzed by autocorrelation to provide both mean size and polydispersity. All latexes were diluted to 0.01 % by weight prior to the particle size analysis.

3.3.8 Visualization SpNR latex morphology using Scanning Electron Microscopy

The latex was diluted with distilled water to 3 wt.%, and then stirred with a magnetic stirrer. A few drops of the diluted latex were then transferred to a vial containing a solution of 2 wt.% osmium tetroxide solution and left to stand for 30 minutes, followed by centrifugation at 5000 Hz for 10 minutes. The supernatant was removed and distilled water was poured into the vial. The process of centrifuging, removing the supernatant and adding distilled water was repeated until the latex and osmium tetroxide mixture became colorless. After that, a few drops of the final mixture were

pipetted onto the specimen stub and left to dry at room temperature. The stub was then mounted onto a stub holder, which was placed into the field emission scanning electron microscope (JEOL FESEM JSM-6701F). The images were observed at a magnification of 5000 \times , under an acceleration voltage of 5 keV.

3.3.9 Analysis of SpNR latex flow behavior using Discovery Hybrid Rheometer

The flow behavior of SpNR latex was characterized using a Discovery Hybrid Rheometer (DHR) from TA Instruments. Two types of experiments were carried out: steady-state and dynamic (oscillatory), both performed at 25 $^{\circ}$ C using a Peltier concentric cylindrical geometry couette cell. In this work, approximately 23 ml of sample was poured into the cylindrical geometry. The viscosity as a function of shear rate, which varied between 0.001 and 1000 s^{-1} , was determined by using a flow ramp protocol. To study the viscoelastic properties of the SpNR latex, an oscillatory test was carried out at a fixed angular frequency of 10 $rad\ s^{-1}$ and a strain amplitude of 0.001% to 100%.

3.4 SpNR latex foamability and stability study

This part was conducted to evaluate the foamability of the SpNR latex and subsequent stability of the latex foam over time. Foamability is the ability of the latex to change from colloid/liquid phase into latex foam phase when subjected to a constant rate of shear. On the other hand, stability refers to the durability of the latex foam to retain the foam-cell structure before drainage (a tendency of the latex foam to change back into liquid phase). In this work, a FoamScan[®] analyzer from Teclis, France was used. Figure 3.3 shows the instrument configuration. To the best of our knowledge, a study on foamability and stability NR latex using FoamScan[®] analyzer is not yet established, thus experimental parameters were set in this particular study. In this work, 60 mL of latex was injected into a glass tube with an inner diameter of 35 mm. Latex foam was generated through a whipping process using a high-speed rotary spin located at the bottom of the tube. A constant rate of 1000 rpm was set to foam the latex, under a controlled temperature of 25 $^{\circ}$ C. The latex foaming process stopped automatically when the foaming time reached 600 seconds. Then, the latex foam stability was observed for another 600 seconds. An integrated camera was used to capture images of the foams microscopically throughout the experiment. Foamability and stability of the latex were quantified in terms of volume expansion and foam decays respectively. The foaming process of latex foam using FoamScan[®] analyzer is slightly different compared to the actual foaming process using Kenwood mixer, especially the design of the rotary blade and the speed of the whipping process. Nevertheless, FoamScan[®] analyzer is the only instrument available that allows researchers

to visualize microscopically the transition of latex from liquid phase into foam phase, thus allowing further study on foamability and subsequent stability of SpNR latex foam.

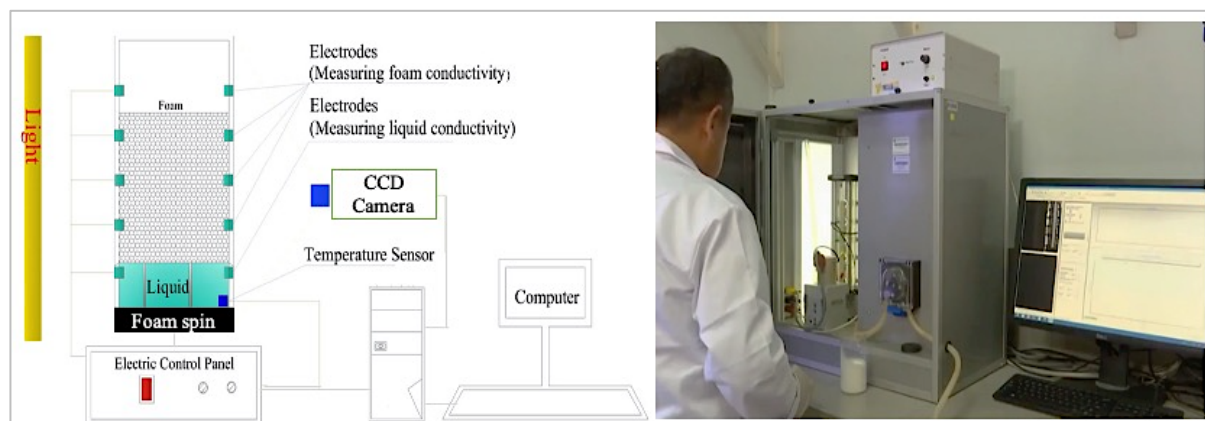


Figure 3.3: FoamScan[®] analyzer configuration.

3.5 Chemical properties measurement

3.5.1 Determination of extractable proteins content

Exposure to extractable rubber proteins (ERP) can cause *Type I* immediate hypersensitivity reactions such as urticaria, facial swelling and asthma^{75,76}. Therefore, the ERP content of SpNR, LATZ and commercial NR (CNRL) latex foam samples was investigated. The American Society for Testing Materials (ASTM) D5712 standard method was used to determine the level of extractable protein content of the latex foam samples. Approximately 5 g of latex foam was cut from the sample. The test specimen was extracted in phosphate-buffered saline (0.025 M) (1 g/ 5 ml) at 25 °C for 2 hours. The limit of detection for the ASTM D5712¹²¹ assay was 2.2 µg/mL and the limit of quantification was 11.0 µg/gm.

3.5.2 Determination of extractable residual chemicals

Exposure to extractable residual chemicals (ERC) can cause *Type IV* delayed hypersensitivity reactions (48-96 hours after contact) such as vesiculation, erythema, swelling, cracking and itching of the skin at the site of contact^{79,122}. Therefore, the ERC content of SpNR, LATZ and CNRL latex foam samples was determined. For the specific purpose of this study, similar compounding ingredients were used to produce both the SpNR and the LATZ latex foams. The compounding formulation used to produce SpNR latex foam will be described in detail in Table 5.1 at Section 5.2.1.1. On the other hand, the compounding ingredients for the CNRL foam are unknown as this is a commercial product. In this study, extractable of three chemicals that are normally used as vulcanizing agents and are also roots of *Type IV* allergy were examined: zinc diethyl dithiocarbamate (ZDEC); zinc dibutyl dithiocarbamate (ZDBC); and zinc 2-

mercaptobenzothiazole (ZMBT)¹²³. To determine the extractable residual chemicals, An *in-house* method developed by MRB¹²⁴ was followed. Approximately, 3-5 g of the test specimens were extracted and boiled for one hour in 100 mL of deionized water. The water was further extracted via liquid-liquid extraction by using methylene chloride. The concentrations of the extracted chemicals were individually determined using high performance liquid chromatography (HPLC) by comparing them to reference materials. The detection limit of the HPLC were 2 µg/g for ZDEC and ZDBC, and 10 µg/g for ZMBT¹²⁴.

3.5.3 Determination of volatile organic compounds

In recent years, concern has been raised about the smell of rubber and its possible health implications due to the emission of volatile organic compounds (VOCs) from foam materials used for bedding products^{23,24}. Additionally, odor-less foam materials with reduced emissions of VOCs have become desirable in the bedding industries^{125,126}. Unlike ERP and ERC, where allergic reactions can occur when the substances are in contact with skin, VOCs are chemicals that move to the gaseous phase, particularly at higher temperatures. Exposure to VOCs at high concentrations in a closed space may cause health hazards^{21–24,72,127}. Although there is no regulatory standard for VOCs, the levels of VOC emission are typically classified into four levels: low, acceptable, marginal and high¹²⁸. Low VOC concentration levels are considered to be less than 300 mg/m³; acceptable levels of VOC range from 300 to 500 mg/m³; from 500 to 1000 mg/m³ of VOC is considered to be marginal; and above 1000 mg/m³ is classed as high. The VOCs of SpNR, LATZ, CNRL latex foams and of PM foam were tested using thermal desorption gas chromatography with mass spectrometric detection (TDS-GC/MS) and high-performance liquid chromatography with a diode-array detector (HPLC-DAD) in accordance to MS300-55 (2018-06)¹²⁹. The method detection limit was 10 µg/m³.

3.6 Physical properties measurement

3.6.1 Determination of dry density of latex foam

During the foaming process, approximately 250 mL of latex foam was poured into a 250 mL square container. Then, the latex foam sample was subjected to vulcanization, washing and drying processes. The dry density of the latex foam was determined in accordance with Equation 3.3.

$$Dd = \frac{Ms}{Vs} \quad (3.3)$$

where Dd is dry density, Ms is mass of the specimen and Vs is the volume of the specimen.

3.6.2 Determination of volume shrinkage

Volume shrinkage is an important property in latex foam technology as it determines the size of the finished latex foam products. Volume shrinkage was calculated as a percentage and measured from the difference in dimension between the mold and the fabricated foam⁷⁰ (Equation 3.4).

$$Vsh = \frac{Mz - Lfz}{Mz} \quad (3.4)$$

where Vsh is volume shrinkage, Mz is mold size and Lfz is the latex foam size.

3.6.3 Visualization of the morphological structure of SpNR latex foam

Hitachi SU1510 low-vacuum scanning electron microscopy (SEM) was used to visualize the morphological structures of the latex foam samples. A test portion of 5 mm × 5 mm × 5 mm (length × width × thickness) was cut from the sample using a razor blade and attached to a sample stub using carbon double-sided tape. The specimens were visualized using back-scattered electrons operating at an accelerating voltage of 2.0 keV. SEM images were captured at ×40, ×70, and ×100 magnification. In this work, no metallic coating was required. Images obtained from SEM were then analyzed using ImageJ software to quantify the porosity and pore size of the latex foams.

3.6.4 Determination of shore F hardness

The Shore F durometer was used to measure the hardness of the foam samples. The measurement was carried out according to standard durometer measurement procedures, ASTM D 2240¹³⁰. A square sample size of 200 mm × 200 mm with a thickness of 40 ± 5 mm was used. Measurements were taken at five different locations at least 6.0 mm apart from each sample. The highest and lowest readings were then discarded, and the hardness value was calculated from the average of the remaining three readings.

3.6.5 Pressure-relief performance evaluation

Pressure mapping technology is a valuable clinical tool that has been used to measure pressure-relief performance of a material as a cushioning material. In this study, pressure-relief performance of pillows and seat cushion of latex foam was examined using a CONFORMat™ pressure sensor system from Tekscan, USA (Figure 3.4). For the pillow, the pressure sensor mat was placed first on top of the pillow. Then, a 4.5 kg mannequin head was used to simulate the human head in a reproducible way. The weight of the mannequin head was matched to the average weight of an adult human head¹²⁷. The pressure distribution pattern was visualized via a color map where the maximum pressure appears as a red color, and the minimum as a dark blue color. The peak pressure value and surface contact area were quantified using the Tekscan software system. A

similar method was used to evaluate pressure-relief performance of the seat cushions. A mannequin was used to assess the differences in pressure distribution during sitting on latex foam and conventional polyurethane foam.

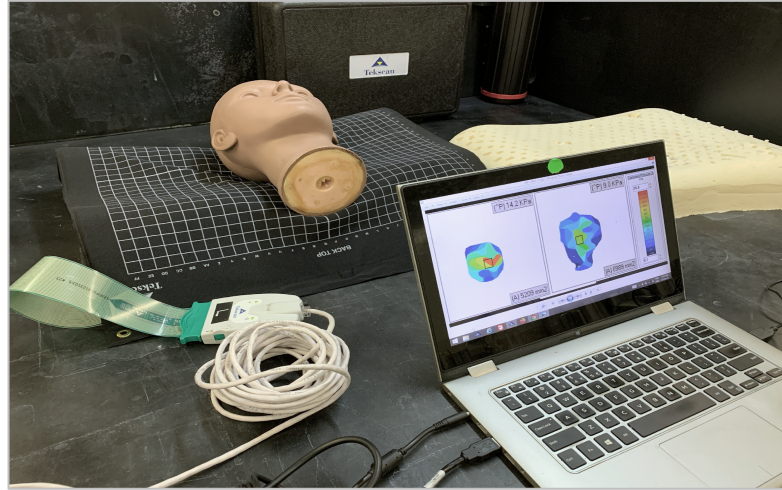


Figure 3.4: A CONFORMat™ pressure sensor system.

3.6.6 Physical properties measurement for bedding products

The physical properties of the latex foams were measured in accordance with the Malaysian Standard MS 679⁵³. This includes density, compression set, indentation hardness, accelerated aging, pounding and elongation at break.

Compression set - Compression set is a static fatigue measurement which measures the degree of irreversible deformation under a specific load⁵⁴. Compression set is also often correlated with the degree of vulcanization of latex foam⁵⁵. When the compression set value of latex foam is greater than 6 %, the latex foam is considered under-vulcanized, and thus does not meet the latex foam product specifications^{53,55}. The compression set value was determined using a compression device consisting of two flat steel plates between which the latex foam specimen was compressed. Each test specimen was compressed to 50% of its original thickness. The compression was maintained for 72 hours at room temperature (approximately 23 °C). At the end of the test period, the test specimen was removed, and the thickness was measured after 30 minutes of rest at room temperature. The compression set was then calculated as

$$Cs = \frac{\Delta h}{h_0} \quad (3.5)$$

where Cs is the compression set, h_0 is the initial thickness and Δh is the change in thickness.

Pounding effect - The pounding test machine consists of a pounding plate connected to two push rods, one at each side, and held in a horizontal position locking the nuts. The initial thickness (h_0) of the sample was determined. The sample was placed with the cavities face resting on the perforated plate. The pounding machine was adjusted such that the stroke of the compression

plate is equal to 20% of the measured thickness of the sample and that, at the top of its stroke, the plate compresses the sample by 40% (and therefore by 60% at the bottom of the stroke). After pounding the sample for 60 seconds at a rate of 4 Hz (240 poundings) the initial indentation hardness index is recorded (H_0). The sample was returned to the pounding machine so that the sample received a total of 250,000 poundings. On completion of the required pounding, the sample is removed and left to recover in an unloaded state for 30 minutes. After this time, the sample is again measured for its thickness (t_1) and indentation hardness index (H_1). The resistance of the latex foam sample to pounding is determined through two measurements: change in thickness (CIT) and change in hardness index (CHI).

$$CHI = \frac{H_0 - H_1}{H_0} \quad (3.6)$$

$$CIT = \frac{t_0 - t_1}{t_0} \quad (3.7)$$

Elongation at break - The elongation at break value is a measure of the physical strength of the latex foam. A higher elongation at break value indicates that a latex foam can be stretched more before breakage occurs. If the elongation at break value of the latex foam does not meet the requirements, this indicates that the material is easy to tear and thus extra care is needed during product handling. The elongation at break of the latex foam was determined using an Instron universal machine. Parallel-sided test samples having cross-sectional dimensions of 10 mm × 12.7 mm and 150 mm in length were pulled at a constant rate of 500 mm/min until the failure of the test specimen. The elongation of the gauge length to the ultimate breaking point of test sample was recorded, and the elongation at break was determined from

$$EB = \frac{L_1 - L_0}{L_0} \quad (3.8)$$

where EB is elongation at break, L_0 is the undeformed gauge length and L_1 is the gauge length at break.

Indentation hardness - Individual perception of hardness of foam products such as pillows can be very subjective. Therefore, MS679⁵³ was developed to classify latex foam into three different categories which are soft, middle firm, and firm based on an indentation hardness (IH) value. The hardness of the latex foam was determined using this indentation test. The indenter foot was brought into contact with the top surface of the test specimen, and the test sample was then indented to 40% of its initial thickness. The corresponding force in Newtons was recorded as the indentation hardness index.

Accelerated aging - In NR latex product industries, an aging test is used to estimate the durability or life span of the latex foam products. This is generally achieved by accelerated aging followed by a

measurement of the IH value of the latex foam after the aging process. According to MS679⁵³, the effect of aging on the IH of latex foam should be $\pm 20\%$. In this test, the test specimen was placed in a heated air oven at a temperature of 70 °C for seven days. After the exposure period, the test specimen was allowed to cool to room temperature and rest for at least 16 hours. The test specimen was then subjected to an indentation test following a similar procedure. The age hardening was then calculated according to the following formulation.

$$Ah = \frac{H_0 - H_a}{H_0} \quad (3.9)$$

where Ah is age hardening, H_0 is the initial hardness index and H_a is the hardness index after aging.

3.7 Mechanical properties measurement

3.7.1 Acoustics properties measurement

The acoustic properties of the DPNR, ENR and LATZ latex foam samples were evaluated by measuring sound transmission loss (STL), sound absorption coefficient (SAC), and noise reduction coefficient (NRC) using an impedance tube model, Kundt tube type SCS9020B in accordance with ISO 10534-2¹³¹. The impedance tube is made up of two combination tubes, two microphones (type GRAS-40BP, ¼ in, for pressure and type GRAS-26AC, ¼ in, for the preamplifier), a two-channel data acquisition system with 0.1 dB resolution, and SCS-90 software, as illustrated in Figure 3.5.

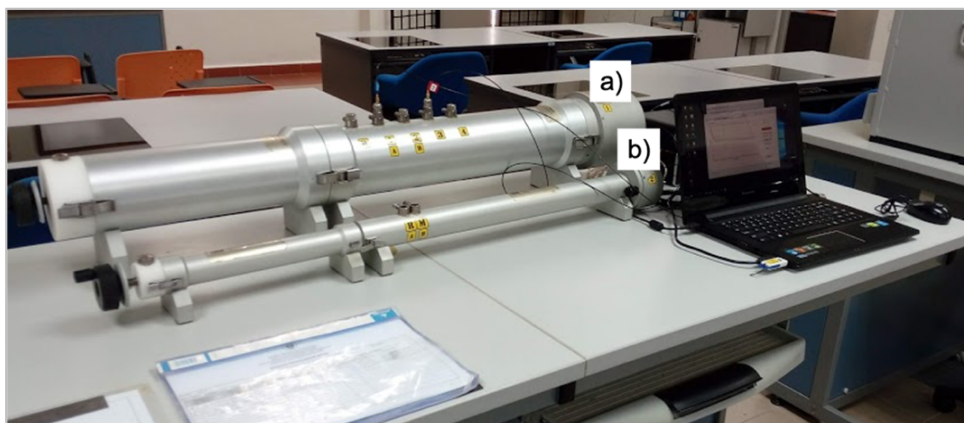


Figure 3.5: Impedance tube model Kundt tube type SCS9020B.

a) a 100 mm diameter test tube; b) a 28 mm diameter test tube

The calibrator used was a Larson-Davis CAL 200. The impedance tube system used in the experiment includes a large tube with an inner diameter of 100 mm and a small tube with an inner diameter of 28 mm to measure the absorption coefficients at both low frequencies (160 - 1600 Hz) and high frequencies (1600 - 6300 Hz), respectively. The full frequency range for the sound absorption coefficients presented in this report is a combination of the values measured in the large tube and the small tube, which gives the measured frequency range of 160 - 6300 Hz. The test samples varied in thickness from 10 mm to 20 mm and up to 40 mm. A circular die cutter was

used to cut the samples into cylindrical shapes that matched the size of the impedance tube. Additionally, a comparison was made between 20 mm single-layer foams and 10 mm double-layer foam sandwiches. To make a 20 mm double layer foam sandwich, needle pins were used to join two 10 mm foams. STL is a measure of the loss of energy from sound waves experienced as the wave passes through the material, as shown schematically in Figure 3.6, and is calculated using the ratio of the power of the incident wave energy, W_i , to the power of the transmitted wave energy, W_t , as decibel (dB)¹³². According to previous studies^{128,129} noise reduction of at least 10 dB is essential for sound insulation. A material that has an STL of 33 dB or greater would be adequate for a noise barrier in any application.

$$STL = 10 \log_{10} \left(\frac{W_i}{W_t} \right) \quad (3.10)$$

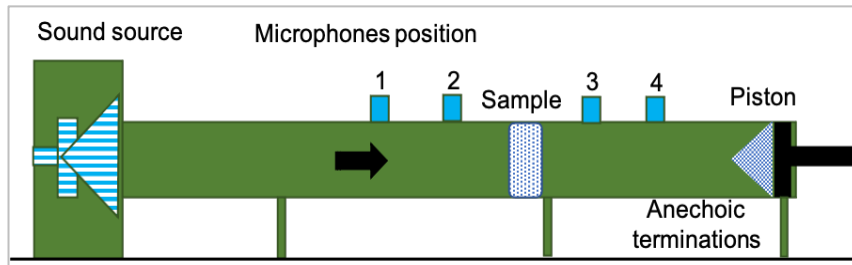


Figure 3.6: Schematic diagram of the impedance tube set up for STL test. Adapted from¹³³.

SAC is a measure of the sound energy that is absorbed after incidence on a material surface, as shown schematically in Figure 3.7, and is defined as

$$SAC = 1 - \left(\frac{I_r}{I_i} \right) \quad (3.11)$$

where I_r is the reflected sound intensity and I_i is the incident sound intensity. The SAC of the materials varies in the range of 0 to 1. An SAC of 0 means that the sound is completely reflected by the material, whereas an SAC of 1 means that the sound is completely absorbed by the material. Therefore, a higher SAC represents better sound absorption.

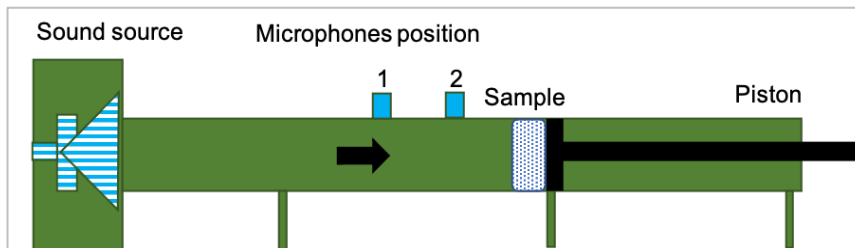


Figure 3.7: Schematic diagram of the impedance tube setup for the SAC test. Adapted from¹³³.

NRC is defined as the arithmetic mean of the SAC at frequencies 250, 500, 1000, 2000 and 4000 Hz¹³¹, and represents a measure of the ability of a material to absorb broad-spectrum sound.

3.7.2 Compression test

Compressive stress-strain response generally indicates the resistance of the material from being compressed. A compression test is normally used to evaluate the compressive stress-strain behavior and hysteresis loss^{123,134}. In this study, compressive stress-strain behavior of the latex foam was carried out using a 25 kN servo-hydraulic MTS Multi-Axis testing machine. A sample size of 200 mm × 200 mm × 40 mm (length × width × thickness) was used. The compression testing method was created in accordance with the method suggested by previous studies^{123,134} utilizing the machine software program Blue Hill[®]. To measure the stress-strain of the sample, the specimen was placed between two square platens. The upper plate was brought down slowly until it touched the specimen. A maximum preload of 9 N should be applied to the initial height of each specimen. The specimen was compressed up to 50% from its initial height. The loading and unloading processes were set to run for five consecutive cycles at a rate of 0.2 Hz. An assumption was made that there was no separation between the platen and the specimen during the loading and unloading process of the tests. The output from the testing machine was obtained in the form of load and displacement. The output data was analyzed to plot a compressive stress-strain curve.

3.7.3 Ball-rebound resilience test

The rebound resilience (R_r) of latex foam samples was measured using a simple ball-rebound device fabricated in-house (Figure 3.8). The experiment was carried out in accordance with ASTM D3574⁵².

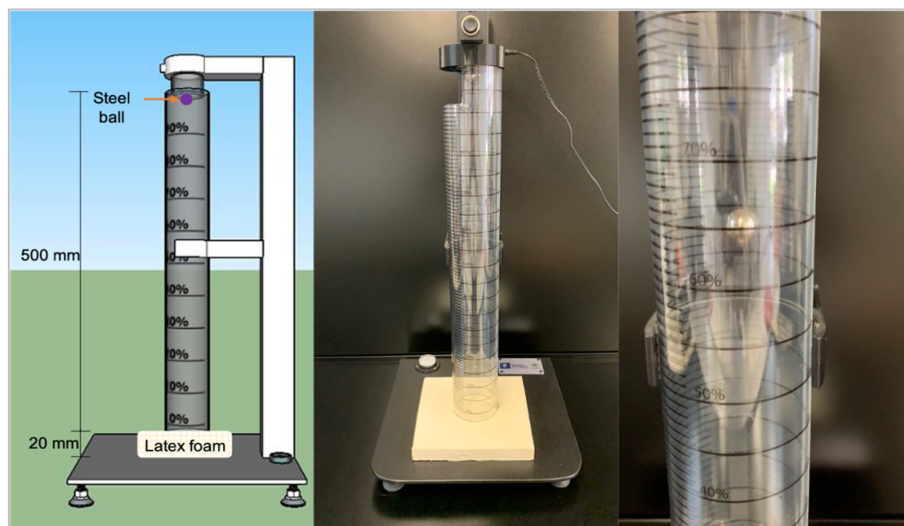


Figure 3.8: Configuration of ball-rebound resilience test.

A magnetic steel ball with a diameter of 16 ± 0.2 mm and weight of 16.3 ± 0.2 g was vertically dropped from a height of 500 mm on a sample size of 200 mm × 200 mm × 40 mm (length × width × thickness). The maximum ball-rebound height (h_{final}) was measured from recorded videos.

The rebound resilience was calculated as the percentage of the ball-rebound height over the initial drop height (h_{max}) as shown in Equation 3.12⁵².

$$RS = \frac{h_{final}}{h_{max}} \quad (3.12)$$

3.7.4 Vibration transmissibility test

The vibration transmissibility of the latex foam samples was measured using the UCON vt-9008 vibration test machine (Figure 3.9). The test was performed according to ASTM D3580-95¹³⁵ under vertical linear motion. A sample size of 40 mm × 40 mm × 40 mm (width × length × thickness) was used, and the weight of each foam block was measured before being placed between the base plate and a moveable block. Two cylindrical blocks were loaded onto the moveable top plate and locked on the sliding top plate. The vibration transmissibility test was generated at a base excitation level of 1 mm and a frequency range from 3 Hz and 30 Hz. Two Kistler accelerometers were initially attached to the base and sliding top plates to measure the vibration amplitude of the base plate (input) and the response of mass (output) to the base excitation.

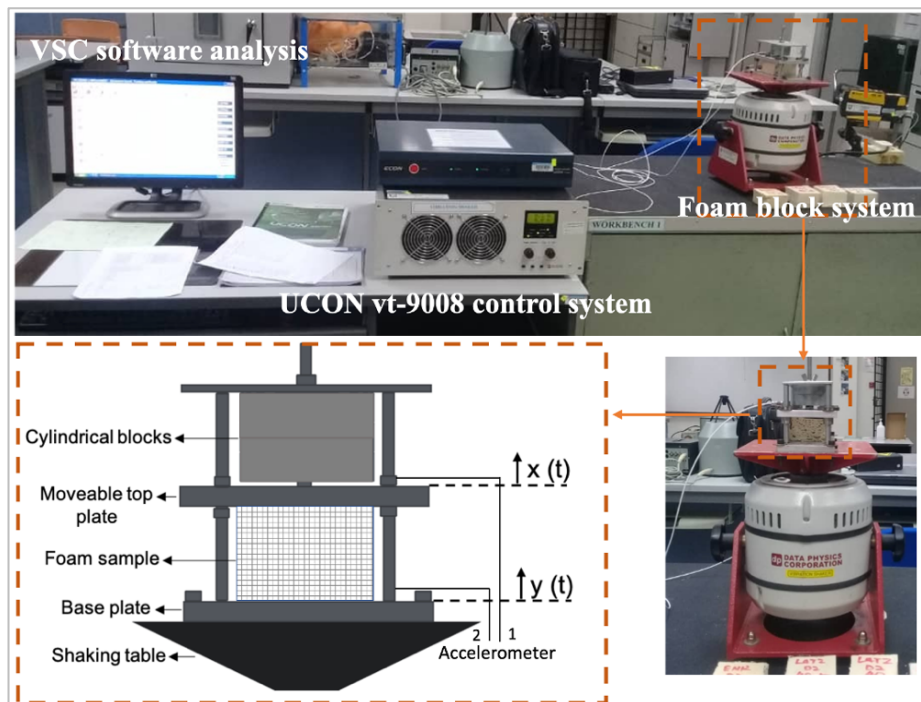


Figure 3.9: Configuration of vibration transmissibility test.

In this system, a vertical amplitude, $y(t)$ was initially given at the shaking table but the total amplitude, $x(t)$ received by the cylindrical blocks (mass) was read from the moveable top plate. The vibration transmissibility curve between two amplitude signals at the driving frequency was obtained from the data acquisition system and analysis package (VSC software). The vibration damping test system shown in Figure 3.9 is a single degree of freedom (SODF) system, which means that the vibration system is only allowed to move in one vertical direction. The vertical

linear motion and the transmissibility of the system from the base to the moveable top plate can be defined as shown in Equations 3.13 and 3.14,

$$M\ddot{x} + C\dot{x} + Kz = 0 \quad (3.13)$$

$$Tr = \frac{x}{y} = \left[\frac{1 + (2\xi r)^2}{\sqrt{(1 - r^2)^2 + (2\xi r)^2}} \right]^{\frac{1}{2}} \quad (3.14)$$

where Tr is the transmissibility, M is the mass of the block system, \ddot{x} is the acceleration, C is the damping, \dot{x} is the velocity K is the stiffness coefficient, z is equal to $(x-y)$, x is the amplitude from the top plate, y is the amplitude from the base, ξ is the total damping in the system, and r is the frequency ratio. It has been reported that flexible foam could be represented by a model with nonlinear stiffness (K) and damping (C) owing to its nonlinear and viscoelastic behavior^{136,137}. Thus, Equation 3.14 was used to calculate the total damping (ξ total) that occurred in system at resonance.

3.8 Thermal properties evaluation

3.8.1 Thermogravimetric analysis

Thermogravimetric analysis (TGA) was performed to determine the thermal decomposition behavior of the latex foam samples. Samples of ~ 10 mg were heated in a Mettler-Toledo TGA through a temperature range from 35 °C to 850 °C, at a heating rate of 10 °C/min, under a nitrogen flow rate of 20 ml/min^{138–140}. The mass of the sample was recorded as a function of temperature and time. The residual weight (TG) and its derivative (DTG) with respect to temperature were evaluated.

3.8.2 UL 94 horizontal burning test

The flammability of the latex foam composite was evaluated using the horizontal burning foamed material test (UL 94 HBF) according to ISO 9772¹⁴¹. Briefly, five specimens per sample were prepared with 150 mm \times 50 mm \times 13 mm (length \times width \times thickness) size. Each sample was marked along its length at 25 mm, 60 mm, and 125 mm and placed horizontally on a metallic grid. The samples were burned for 60 s using a methane burner with a flame height of 38 mm. The burner was placed in the corner of the sample closest to the 25 mm mark. The time taken for the flame to move from the 25 mm gauge mark to the 125 mm was recorded using a video camera. The burning velocity V was calculated from,

$$V = \frac{L_d}{t_b} \quad (3.15)$$

where V denotes the burning velocity rate (mm/min), L_d is the distance between the 25 mm gauge mark and the point where the flame stopped or passed the 125 mm gauge mark and t_b is the time elapsed between the flame passing the 25 mm gauge mark to the flame stopping or reaching the 125 mm gauge mark. A material passes the UL 94 HBF criteria if it does not have a burning rate exceeding 40 mm/min over a 100 mm span or if ceases to burn before the flame reaches the 125 mm mark.

Chapter 4

Specialty natural rubber latex concentrate

4.1. Introduction

The conventional procedure of producing SpNR latex is merely complex. First, the freshly tapped NR latex is collected from the rubber field and subjected to a centrifugation process using centrifuge equipment operated at high rotational speeds, typically 700 rpm²⁵. The centrifugation process separates the freshly tapped NR latex into two main fractions: one fraction contains the concentrated latex of 60% total solid content (TSC), whilst the other contains unwanted materials and 4-6% of rubber material^{2,25}. The concentrated NR latex is then diluted to 30 % TSC before being subjected to deproteinization process to produce deproteinized natural rubber (DPNR) latex, or epoxidation process to produce epoxidized natural rubber (ENR) latex. DPNR latex is prepared via an enzymatic hydrolysis process, whilst ENR latex is prepared via an *in-situ* epoxidation chemical modification process²⁷. It should be noted that it is important to dilute the NR latex concentrate to 30 % TSC to ensure adequate chemical reactions or a successful deproteinization process, as well as a successful epoxidation process. Further to that, non-ionic surfactant is used to stabilize and preserve the latex from coagulation after the modification process. The presence of the non-ionic surfactant in the SpNR latex system has restricted the centrifugation method thus SpNR latex is prepared below 30 % TSC^{111,142}. The low TSC of SpNR latex restrains the application of SpNR latex into latex foam products. This is because, for the production of latex foam products, the minimum TSC of the latex should be at least 60 %^{27,41}. Additionally, the multiple steps of producing SpNR latex led to high cost of the material, thus remaining a challenging issue in manufacturing latex products.

In order to produce SpNR latex concentrate, a possible approach is to use an ultrafiltration process employing membrane separation technology^{113,143}. On the other hand, in order to reduce the cost, it is proposed to prepare SpNR latex directly from freshly tapped NR latex. As the study aims to diversify the application of SpNR latex into latex foam products, information on the physicochemical properties of SpNR latex is important because it relates to the foamability and subsequent stability of the latex foam⁷⁰. Therefore, in this chapter, physicochemical properties of

SpNR latexes (DPNR and ENR) such as mechanical stability time (MST), viscosity, total solid content (TSC), dry rubber content (DRC), and pH were characterized and compared to commercially available NR latex concentrate, namely low-ammonia NR (LATZ) latex. It should be noted that the latex foam process involves a high-speed whipping process to incorporate air into the latex, to change the SpNR latex from a liquid phase into a latex foam phase. Therefore, knowledge of the rheological behavior of SpNR latex is also important. In this chapter, the rheological behavior of SpNR latex typically, the viscosity and viscoelasticity properties are discussed.

4.2. Characteristics of specialty natural rubber latex concentrate

4.2.1 Physicochemical properties

Table 4.1 shows the physicochemical properties of ENR, DPNR and LATZ latex examined in this study. It is clear that the TSC and DRC of both DPNR and ENR latex produced in this study achieved the targeted value of 60%. The alkalinity level of LATZ was found to be 0.29%. On the other hand, for ENR and DPNR latex, the alkalinity level was purposely adjusted to be approximately 0.35%, as suggested by a previous study³. The viscosity of ENR and DPNR is higher than LATZ. It should be noted that the higher the viscosity value the thicker the material. The high viscosity of ENR could be due to the presence of non-ionic surfactants in the latex system which increase the flow resistance of the latex.

Table 4.1: Physicochemical properties of SpNR latex

Parameters	LATZ	DPNR	ENR
TSC (%)	61	63	63
DRC (%)	60	61	63
Alkalinity (%)	0.29	0.36	0.35
Viscosity (cP)	70	115	300
MST (s)	1380	240	1800
Nitrogen content (%)	0.29	0.11	0.25

The MST value of ENR latex was found to be greater than that of the LATZ latex, implying a high stability of ENR latex, most likely due to the presence of the surfactants used in the ENR latex. However, the MST value of the DPNR latex was found to be much lower than that of the LATZ. The reason behind this is not clear, but could possibly be due to the removal of the protein-phospholipid layer that normally covers the rubber particles, and the consequent destabilization of the latex aggregation^{144,145}. In future studies, other types of surfactants will be investigated to

identify an effective surfactant that can improve the stability of DPNR latex during high-speed shear.

Table 4.1 also shows that the nitrogen content of ENR, DPNR and LATZ latex examined in this study was 0.25 %, 0.11 % and 0.29 % respectively. According to Blackley² and Nawamawat *et al.*¹⁴⁴, the amount of protein in NR latex can be estimated in terms of the nitrogen content value. The studies also stated that the nitrogen content of freshly tapped NR latex and concentrated NR latex is about 0.65% and 0.30 % respectively. The nitrogen content of the LATZ and ENR examined in this study was similar to the 0.30 % value reported by Blackley² and Nawamawat *et al.*¹⁵⁵. On the other hand, the nitrogen content value of the DPNR examined in this study is significantly lower, confirming the success of the deproteinization process. Furthermore, the reduction of nitrogen content is considerably high, which is approximately 80 %. Therefore, it can be concluded that the deproteinization process of freshly tapped NR latex via a synergistic effect between the proteinase enzyme and the heat treatment is highly effective.

4.2.2 Epoxidation levels

NR structure consists of a long molecular chain made of cis-1,4-polyisoprene repeat units. Chemical modification of the rubber chain through epoxidation reactions produced epoxy groups along the molecule. The success of this process can be estimated through epoxidation and ring opening levels via ¹H-NMR spectrum measurements (Figure 4.1).

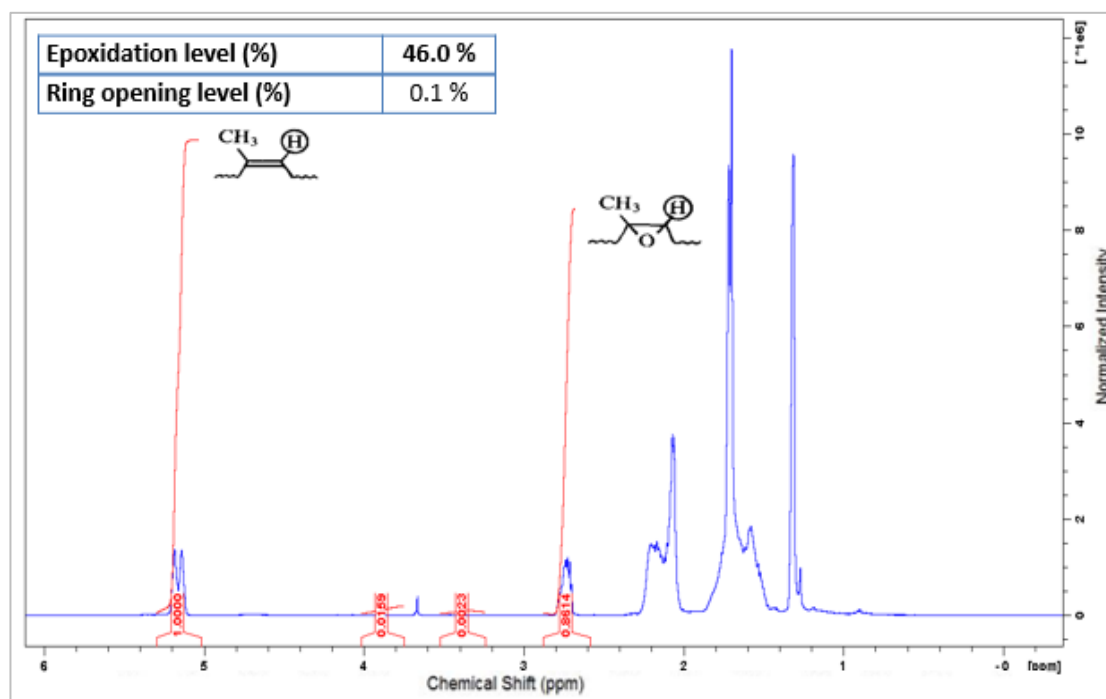


Figure 4.1: ¹H-NMR chemical shift of ENR latex produced in this study.

The determination of the epoxidation level was performed based on the olefinic and epoxy methane proton integration peaks at $\delta = 5.3-5.0$ ppm and $\delta = 2.9-2.6$ ppm respectively.

Determination of ring opening was carried out using integration peaks of $\delta = 3.5-3.2$ ppm and $\delta = 4.0-3.7$ ppm. At these peaks, the epoxidation level of ENR latex produced in this study was found to be 46.3 mol%, with a very low level of ring opening of 0.1 mol%. Although the epoxidation level of ENR latex was slightly lower than the targeted value of 50 mol%, this study has proved that ENR latex concentrate can be produced directly from freshly tapped NR latex through the method proposed in Section 3.2.2.

4.2.3 Study on rubber particles

Figure 4.2 shows particle diameter and distribution of freshly tapped NR latex (a), LAT'Z latex (b), DPNR latex (c) and ENR latex (d). It can be observed that the particle size distributions are in the range between 50 to 3000 nm in diameter.

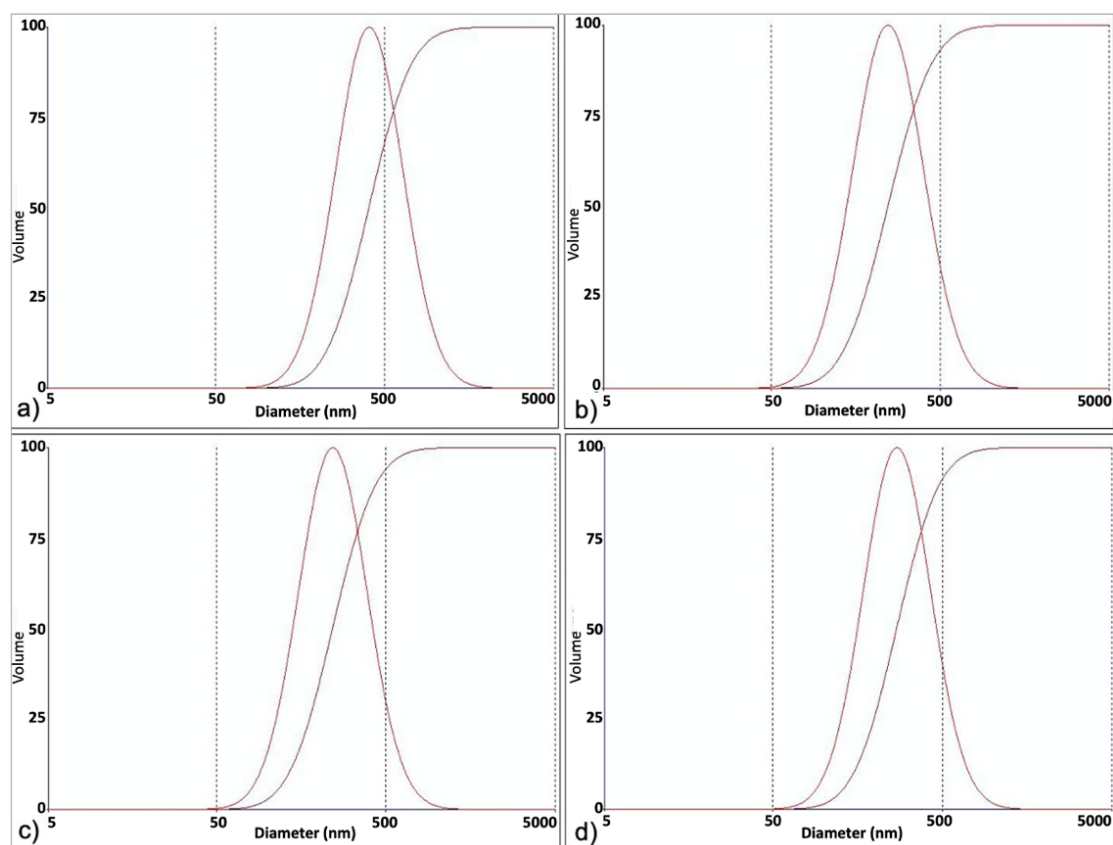


Figure 4.2: Particle size distribution of NR latex.

a) = Freshly tapped NR latex; b) = LAT'Z latex; c) = DPNR latex; d) = ENR latex

The mean particle diameters of freshly tapped NR latex, LAT'Z, DPNR and ENR latex were examined as 683 nm, 415 nm, 436 nm and 453 nm respectively. The mean particle size of freshly tapped NR latex is larger than that of the other latexes. This could be due to non-rubber materials adsorbed on the surface of the latex particles. The non-rubber materials were removed during the concentration process¹⁴⁶, producing smaller mean particle diameters in the LAT'Z, DPNR and ENR latexes.

Figure 4.3 shows the morphological structures of freshly tapped NR latex, LATZ latex, DPNR latex, and ENR latex at $\times 5000$ magnification. The SEM images confirm that the rubber particles are spherical in shape, and of varied size. However, the largest particle size visualized through SEM does not necessarily represent the actual size of the rubber particle. This is due to the potential of smaller rubber particles to agglomerate to form a bigger particle during sample preparation. Nevertheless, the SEM images illustrate that freshly tapped NR latex appeared to be slightly different compared to LATZ latex, DPNR latex and ENR latex. This could again be due to the presence of non-rubber materials in the latex system which could influence the surface structure of the rubber particles¹⁴⁷.

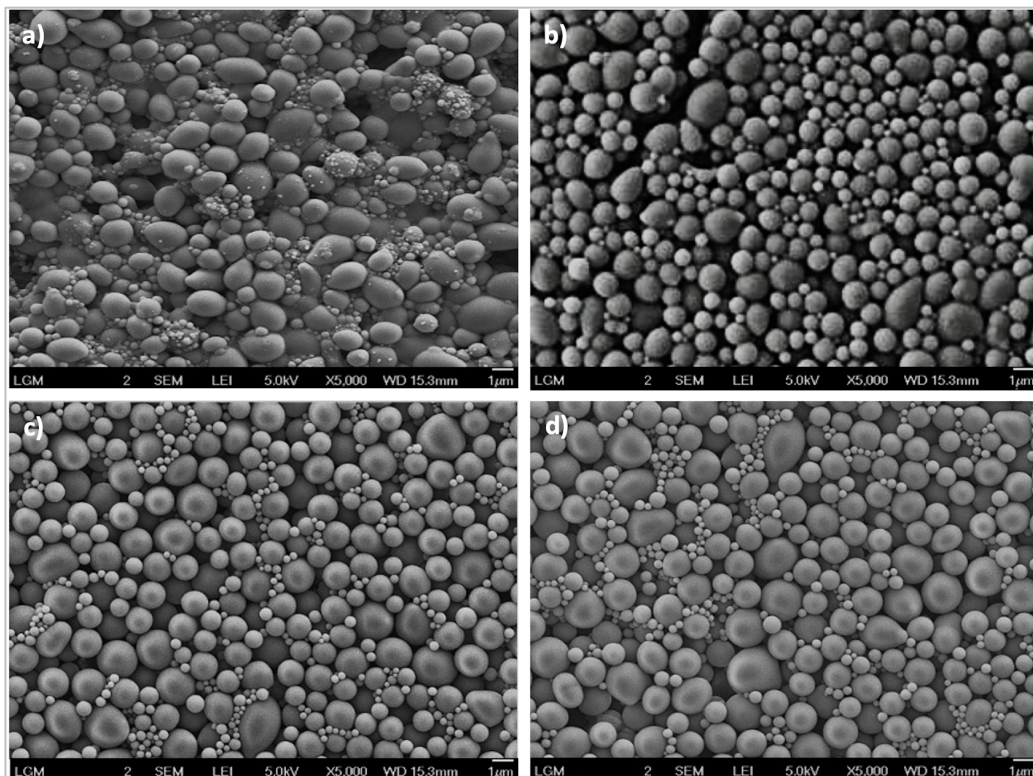


Figure 4.3: SEM images of NR latex particles.

a) = Freshly tapped NR latex; b) = LATZ latex; c) = DPNR latex; d) = ENR latex

4.2.4 Rheological behavior

In this work, rheology was used to evaluate the flow behavior (viscosity) and the structure (viscoelasticity) of SpNR latex. A method to measure the viscosity and viscoelasticity of SpNR latex and its aging characteristics is through rotational rheometry. Viscosity is the resistance to flow. The more complex the structure of SpNR latex, the greater the resistance to flow. To determine the dynamic (apparent) viscosity (η) of LATZ, DPNR and ENR latex examined in this study, shear stress (σ) was measured as a function of shear rate ($\dot{\gamma}$), and the apparent viscosity was

calculated from $\sigma/\dot{\gamma}$. Figure 4.4 shows the shear stress as a function of shear rate at 25 °C, whilst Figure 4.5 shows viscosity as a function of shear rate, for LATZ, DPNR and ENR latex.

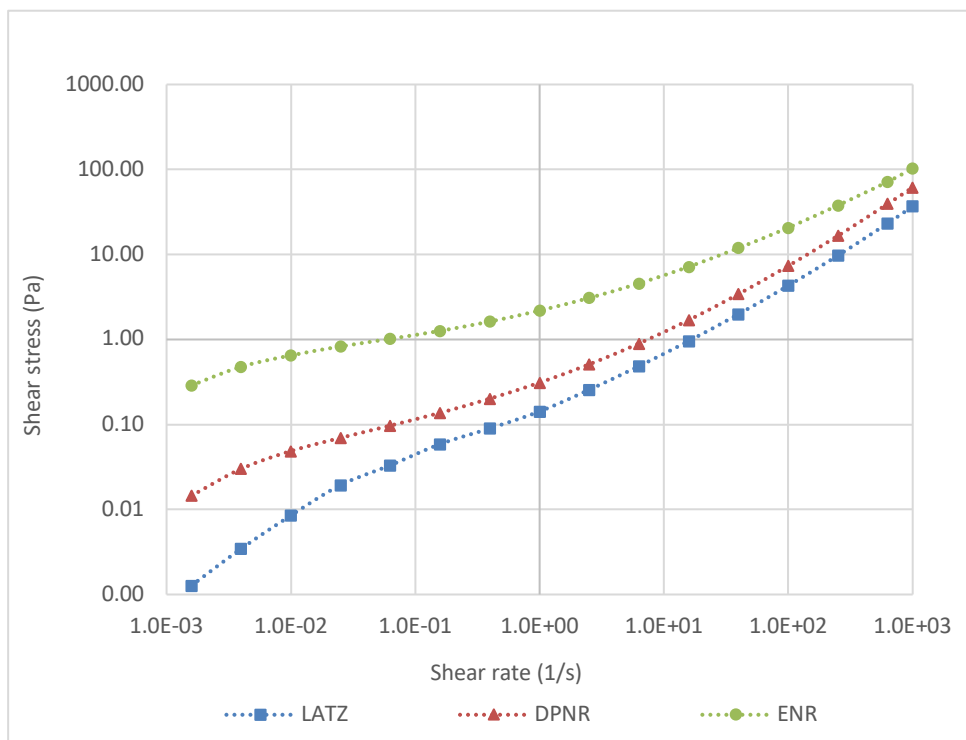


Figure 4.4: Shear Stress as a function shear rate at 25 °C for LATZ, DPNR and ENR latex.

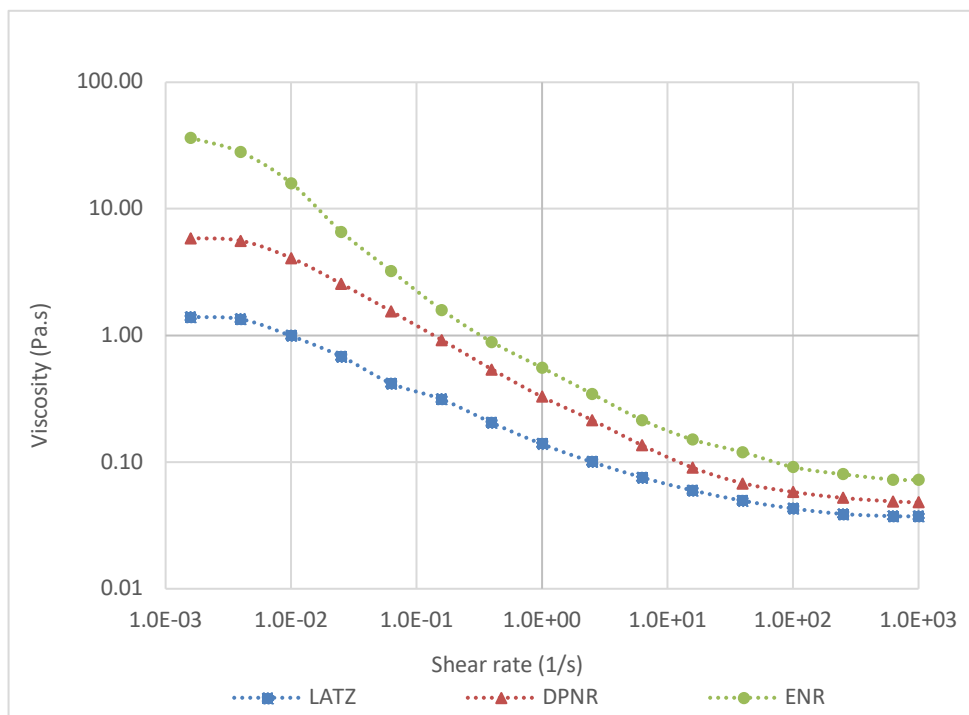


Figure 4.5: Viscosity as a function of shear rate at 25 °C for LATZ, DPNR and ENR latex.

It is evident from Figure 4.4 that the shear stresses of all latices examined in this study increased with shear rate. The results show that ENR latex demonstrates the highest shear stress followed by DPNR and LATZ latex, at all shear rates examined. This could be due to the high concentration

of the latex which contributes to particle–particle interaction (repulsion), chemical additives (i.e., non-ionic surfactant, steric) and changes to the material properties of ENR latex due to the epoxidation process¹⁴⁸. Figure 4.5 shows a comparison of viscosity between LATZ, DPNR and ENR latex. The ENR latex exhibits the highest viscosity, followed by DPNR and LATZ latex, and is approximately 30 times higher than LATZ latex and six times higher than DPNR latex at the lower shear rates. The higher viscosity can be explained by a higher interaction within the ENR latex system. The addition of a non-ionic surfactant that was used as a stabilizer to protect the rubber particles from destabilizing during the preparation and modification process may be responsible for a strong repulsive interaction between the particles and thus increase the viscosity. This result is in agreement with a previous study¹⁴⁸ where the presence of surfactant adsorbed on the surface of the rubber particles was observed to lead to restriction in the flow of the latex, hence increasing the viscosity. Figure 4.5 also clearly indicates shear-thinning behavior, where the viscosity is decreasing with increasing shear rates¹⁴⁹. Shear thinning is commonly observed in high molecular weight polymers. As indicated by Jatuporn¹⁵⁰, NR latex is a high molecular weight polymer where rubber molecules are always entangled and randomly oriented when at rest. When sheared, rubber molecules start to stretch and align with the flow, which facilitates disentanglement and causes the viscosity to drop. The degree of disentanglement of rubber molecules will depend on the shear rate and stability of the latex. Figure 4.5 also shows that at low shear rates the viscosity tends to a constant, known as the zero-shear viscosity. Brownian motion caused the rubber molecules to vibrate and rotate, and they interact strongly with one another, resulting in a higher viscosity¹⁵⁰. As the shear rate increases, the rubber molecules disentangle, reducing the viscosity until a second plateau was observed at high shear rate. DPNR and ENR latex prepared in this study show a similar pattern as the LATZ, and from a rheological perspective are comparable to LATZ latex. Nevertheless, the presence of a non-ionic surfactant in the ENR latex system leads to a higher viscosity in the ENR latex¹⁵¹. As stated in previous studies^{152,153}, the drawback of a higher viscosity is that the latex can be too stable, which hinders film formation and thus can be an issue in dipped film products such as for the gloves manufacturing process. As far as latex foam production is concerned, there is limited information on the effect of viscosity and stability of ENR latex in the literature. Nevertheless, latex with high viscosity is expected to cause a slower growth of the foam (foam-cell formation) during foaming process. Therefore, a study on achieving the right balance between the type and level of stabilizer of ENR latex is crucial in future work.

The viscosity of the latexes was monitored at monthly intervals for a period of three months. It was found that the viscosity of ENR latex increased during storage, whereas the viscosity of the

DPNR was mostly constant, increasing only at the lowest shear rates, and that of the LATZ latex was mostly constant and decreased a little at the lowest shear rates with time (Figure 4.6).

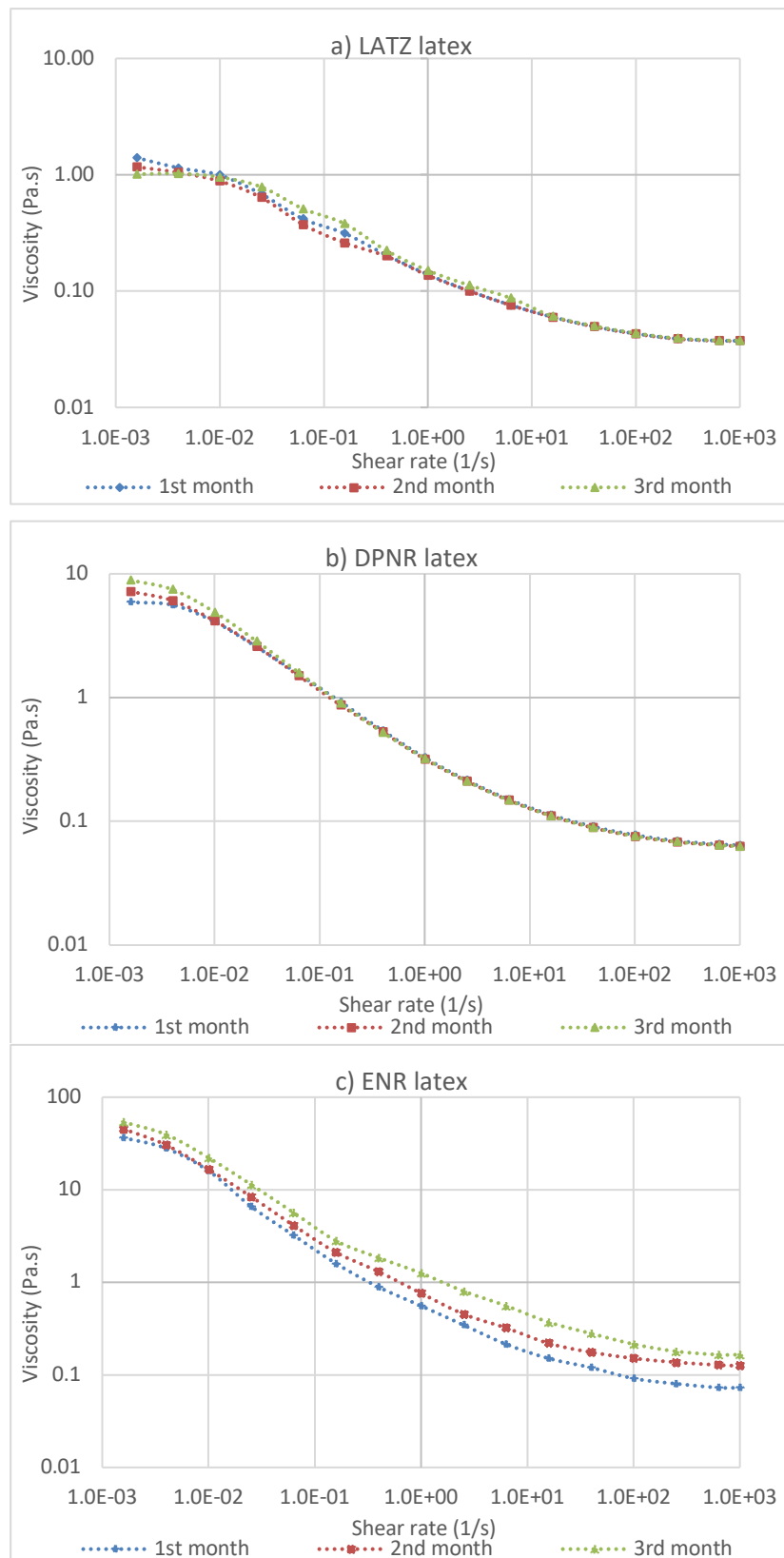


Figure 4.6: Effect of storage properties of LATZ, DPNR and ENR latex.

The increase in viscosity of the ENR and DPNR latex during storage could be due to a storage hardening effect. This correlates with findings revealed by previous studies^{7,154} where a strong interaction between epoxy groups and non-rubber substances including non-ionic surfactants in the latex system was observed to take place during storage, thereby increasing the viscosity of the latex. Further to that, the significant increase in viscosity of the ENR latex could be due to the presence of epoxy groups on the rubber chain inducing an interaction with the non-rubber substances, which could lead to gel formation^{151,154}. The substantially higher viscosity of the ENR latex compared to LATZ and DPNR latex could also be due to the molecular structure of the ENR latex. It is well described in the previous studies^{109,154,155} that NR chemical structure contains double bonds and hydrocarbon polymers that are hydrophobic. The chemical modification at double bonds and introduction of epoxy group which is hydrophilic along the NR backbone could improve the properties of NR. Additionally, ENR that contains both hydrophobic and hydrophilic end structures as a result of the epoxidation modification process can be used in widespread applications. However, the epoxidation modification process might also continue to take place during storage, which result in storage hardening. The storage hardening of ENR latex produced in this study may result through a series of chemical interactions between the rubber chains and the active component in the epoxy group^{7,154}. According to previous studies^{7,154,156}, the storage hardening phenomenon in modified NR (i.e. ENR) has long been recognized as a factor not only affecting the processing properties but also the physical and mechanical properties of the end products. Therefore, this study advised using ENR latex within a month of the processing or manufacturing date to prevent problems with product manufacturing as well as discrepancies in the quality of the finished goods.

A variety of mathematical rheological models such as Maron–Pierce, Bingham, Krieger–Dougherty, Carreau-Yasuda and Herschel-Bulkley can be fitted to rheological data^{148,150,151}. Among these models, the Carreau-Yasuda model has been extensively used to predict the rheological behavior of entangled polymers and other shear thinning fluids, and was found to be particularly suitable for the trends observed here. The Carreau-Yasuda equation is given as follows:

$$\eta = \eta_{\infty} + (\eta_0 - \eta_{\infty}) [1 + (\lambda \dot{\gamma})^2]^{\frac{n-1}{2}} \quad (4.1)$$

where η is the viscosity, η_0 is the zero-shear viscosity, η_{∞} is the viscosity at infinite shear rate, $\dot{\gamma}$ is the shear rate, λ is the relaxation time, and n is the power-law index describing the slope of the viscosity curve with respect to shear rate in the shear-thinning region.

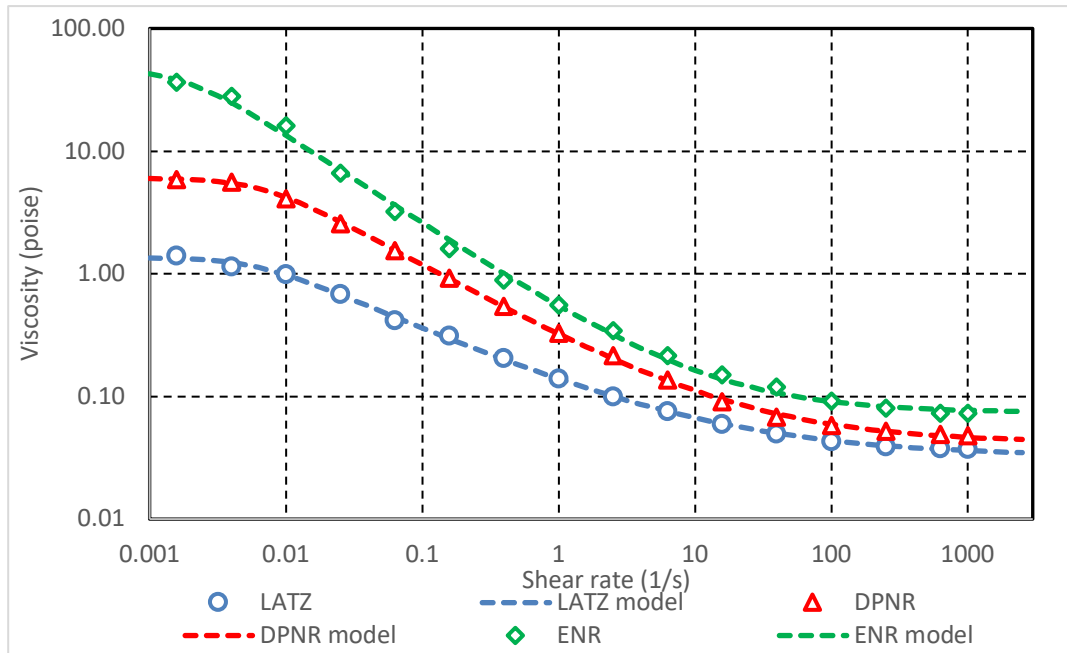


Figure 4.7: Application of a Carreau-Yasuda (C-Y) model to the rheological data.

Figure 4.7 shows fits to the Carreau-Yasuda model achieved using the Solver add-in in Microsoft Excel. The quality of fit is excellent, with R^2 values >0.998 in all cases. Table 4.2 reports the Carreau-Yasuda parameters obtained. In all cases n values are below 1, which implies that the latexes are shear-thinning fluids. It was observed that the relaxation time λ of ENR latex exhibits the highest value, followed by LATZ and DPNR latex. The inverse of λ represents the critical shear rate at which the viscosity begins to decrease with the shear rate, and the data suggest that the ENR latex requires a smaller shear rate in order to start to shear thin. This could be due to modification effects on the ENR latex, although the effect is not very significant.

Table 4.2: Carreau-Yasuda parameters value

Parameter	LATZ	DPNR	ENR
η_0 (Poise)	1.355	6.025	47.14415
η_∞ (Poise)	0.03255	0.04222	0.07405
λ (s)	170.9	152.1	561.8
n (-)	0.5104	0.3920	0.2747
R^2	0.9993	0.9998	0.9986

Soft materials such as NR exhibit both elastic and viscous responses to deformation and are therefore called viscoelastic¹⁴⁹. Figure 4.8 shows viscoelastic behavior of LATZ, DPNR and ENR latex. The magnitude of the elastic part of the response is characterized by a storage modulus (G'), which is associated with solid-like, recoverable deformation. The magnitude of the viscous part of the response is characterized by a loss modulus (G''), which is associated with liquid-like, dissipative behavior. Determination of these two parameters is important because the storage

modulus is an indicator of the degree of entanglement and the ability of the material to store energy during deformation, whilst the loss modulus indicates the ability of the material to dissipate energy during deformation as heat. Figure 4.8 shows amplitude sweeps at fixed frequency and temperature for all latex materials. In LATZ latex, the loss modulus is greater than the storage modulus at all amplitudes. In DPNR latex, the moduli are almost identical until a shear strain of 1%, after which the storage modulus drops faster than the loss modulus. For ENR latex, the storage modulus is greater than loss modulus until a cross-over at a shear strain of $\sim 20\%$. Comparison of the storage modulus of LATZ, DPNR and LATZ latex shows that ENR latex exhibits the highest storage modulus followed by DPNR and LATZ latex, suggesting a greater ability to store elastic energy compared to DPNR and LATZ latex.

A previous study¹⁵⁷ revealed that reduction of proteins and phospholipids lowered the storage modulus of bulk DPNR (dry rubber). The same study also found remarkable restriction of proteins and phospholipids within entanglements of the microstructure of bulk rubber, which influences the modulus and the viscoelastic behavior of the bulk rubber. The results obtained in this study suggest instead that the removal of proteins through heat enzymatic reactions increases the storage modulus of DPNR latex. This is likely due to the colloidal behavior of the latex. Another reason is the presence of a thick layer of non-ionic surfactant on the rubber particles, which may also increase the storage modulus of DPNR latex¹⁵¹. As indicated in reference¹⁵⁷, removal of proteins and phospholipids during deproteinization process could reduce strain-induced crystallization, therefore lowering the mechanical properties of an eventual DPNR latex foam. Additionally, Tangpakdee and Tanaka¹⁵⁸ stated that the non-rubber components in NR, mainly proteins and phospholipids, are believed to be the reason why NR has much better mechanical properties than synthetic polyisoprene. In future studies it may be useful to compare the rheological characteristics of SpNR latex with those of dried SpNR latex foam, to study the effect of deproteinization and epoxidation process on mechanical properties of SpNR latex foam. Figure 4.8 also shows that in ENR latex the storage modulus is greater than the loss modulus for most of the amplitude range explored, suggesting that the material is predominantly elastic in its deformation behavior. Results obtained from this work correlate to those in the study by Manroshan and Fatimah Rubaizah¹⁵¹ who observed that ENR latex exhibits elastic-dominated deformation, whilst LATZ and DPNR latex exhibit viscous-dominated deformation. They suggested that the presence of non-ionic surfactant at the outer layer of the rubber particles contributes to a high storage modulus. However, increasing the oscillation strain beyond 10% produces a cross-over where the viscous response becomes the dominant one.

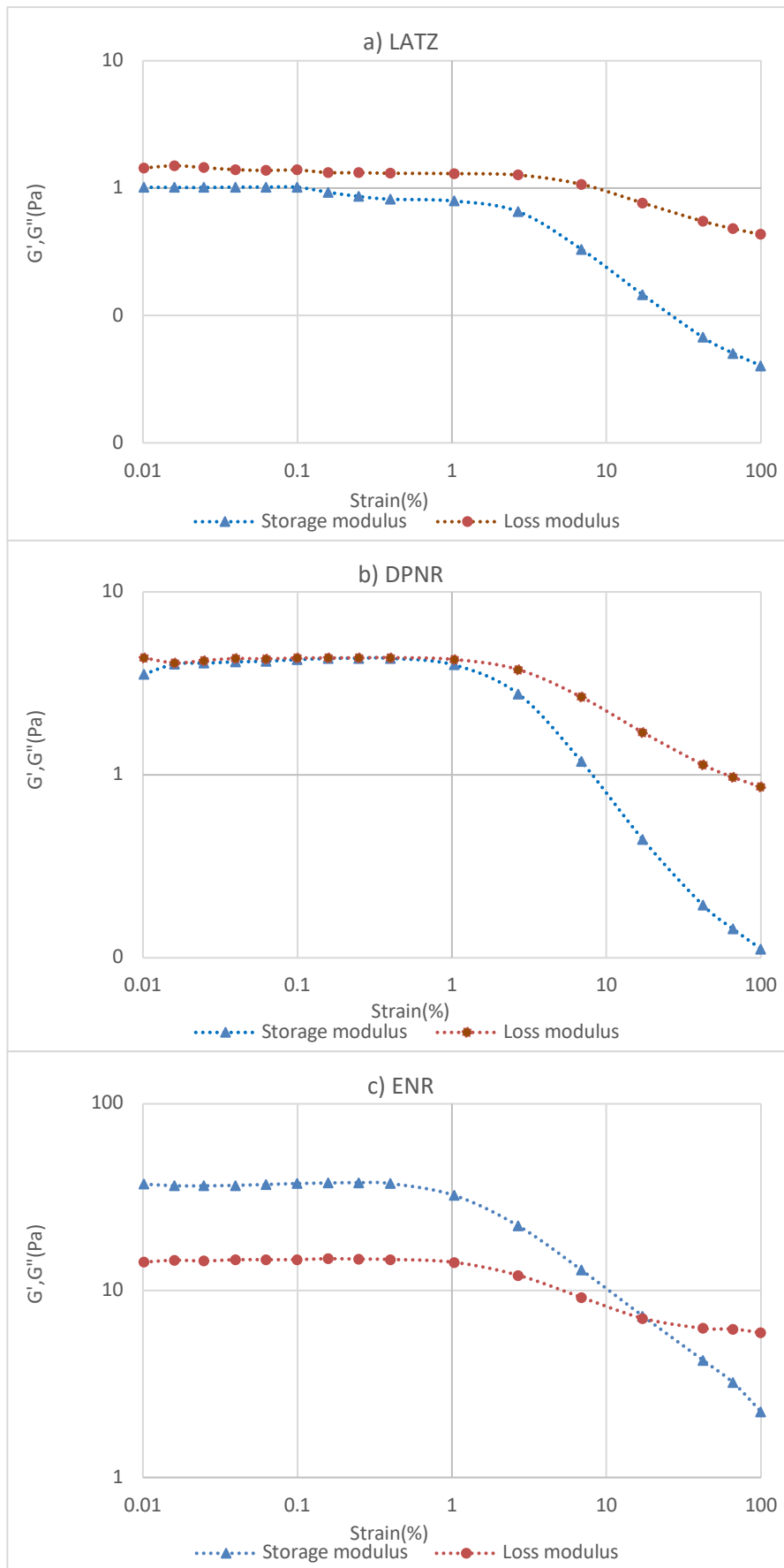


Figure 4.8: G' , G'' as a function of oscillation strain.
 (a) LATZ, (b) DPNR and (c) ENR latex

For LATZ latex, the loss modulus is higher than the storage modulus value at all strain levels, suggesting that this material is composed mainly of individual rubber particles. However, it should be noted that the difference between storage and loss modulus of DPNR latex is very small, and there are likely significant inter-particle interactions. It is presumed that the removal of the protein layer at the outer phase of the rubber particles allows the rubber particles to interact more with each other. It was also observed that the loss tangent (i.e., the ratio of loss modulus to storage modulus) of all latex examined in this study was relatively constant through to 0.1% strain. Beyond this critical strain value, both storage modulus and loss modulus values decreased simultaneously, with the storage modulus falling more sharply. This is probably indicative of a reduction in particle-particle interactions corresponding to a breakdown of structure.

According to Daniel *et al.*¹⁴⁹, the internal microstructure of polymers is linked together by permanent bonds that prevent relative motions of the polymers. Cross-linked networks are different from entangled networks, which are held together only by physical entanglements between chains. Entangled networks possess mechanisms of stress relaxation that are absent in cross-linked networks. The most important of these mechanisms is the thermal motion known as reptation, in which stress relaxation occurs via diffusion^{149,159}. In cross-linked networks, this regime is absent because cross-linking prevents reptation (and hence stress relaxation), leading to a predominantly elastic (storage modulus greater than loss modulus) response. Therefore, from the evidence obtained in this study it is probable that the ENR latex behaves more like a cross-linked network, presumably due to the presence of epoxy groups in the rubber chains. However, at 10% strain a cross-over point was observed, indicating that the material can flow and that the corresponding internal microstructure collapses, and is therefore not fully cross-linked.

To further confirm the influence of microstructure of rubber particles on viscoelastic response, the ratio of G'' to G' ($\tan \delta$) was determined. This study found that (Figure 4.9) when the strain value increased, the $\tan \delta$ also increased. For ENR latex alone, at low oscillation strains the loss tangent is less than unity, suggesting more elastic behavior. However, when the oscillation strain increases, the response of all materials becomes increasingly viscous. For ENR, the shift from elastic to viscous behavior occurs at $\sim 20\%$ strain, where $\tan \delta = 1$. The transition might be due to interpenetration and compression of the adsorbed non-ionic surfactant layer. This result correlates well to a previous study¹⁵¹ where it was suggested that high oscillation strains could lead to compression of the adsorbed non-ionic surfactant layer, leading to a shift from elastic to viscous behavior.

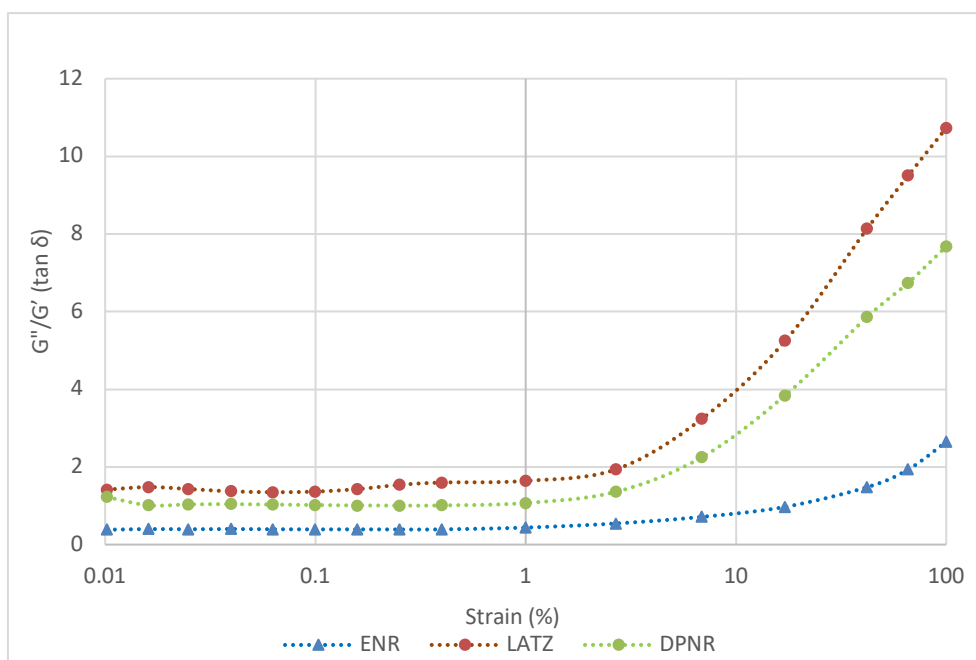


Figure 4.9: G''/G' as a function of oscillation strain.
 (a) LATZ, (b) DPNR and (c) ENR latex

4.3. Conclusion

This study has shown that SpNR latex concentrate can be produced directly from freshly tapped NR latex by using a novel method. The physicochemical properties of the different types of latex produced are slightly different from each other. ENR latex exhibits highest viscosity followed by DPNR and LATZ. This study also concluded that LATZ and DPNR latex behave more like viscous liquids, whilst ENR latex is more like an elastic solid. The non-ionic surfactant used during the preparation and modification process influenced the flow and deformation behavior of the ENR and DPNR latex.

Chapter 5

Specialty natural rubber latex foam

5.1 Introduction

Currently, there are two main types of NR latex that have been used to manufacture latex foam products, namely low ammonia NR (LATZ) latex and high ammonia NR (HA) latex. LATZ latex is the commonly chosen NR latex for producing bedding products such as mattresses and pillows due to its reduced ammonia content which offers a safer manufacturing environment^{26,27}. Utilization of SpNR latex in latex foam products is almost impossible due to their low total solid content (TSC) which is only 30% TSC. This is because low TSC of latex leads to high volume shrinkage and variable physical properties, which is a great challenge in latex foam products manufacturing process⁷⁰. SpNR latex with higher TSC has been produced through the ultrafiltration process using membrane separation technology^{113,143} as presented in Chapter 3. The physicochemical properties of SpNR latex have been characterized and discussed in Chapter 4. The availability of SpNR latex with 60 % TSC has provided an opportunity to diversify the application of SpNR latex into latex foam products. However, there are few challenges to develop latex foam from SpNR latex. First, there is a gap in knowledge on foamability and subsequent stability of SpNR latex. Second, the physicochemical properties of SpNR latex differ from the LATZ latex. Therefore, the compounding, foaming and gelling formulations to fabricate SpNR latex foam is expected to be differ from the one used for LATZ latex. In this chapter the foamability and stability of SpNR latex is discussed. The compounding, foaming and gelling formulations to produce SpNR latex foam are established.

5.2 Specialty natural rubber latex foamability and stability study

5.2.1 Development of compounding formulation

5.2.1.1 Compounding process

SpNR latex of 60 % TSC as prepared in Section 3.3 was used. It should be noted that both ENR and DPNR latex concentrate were kept for one month at room temperature to improve

homogeneity². Table 5.1 shows the compounding formulation used in this work. The compounding formulation is adapted from the commonly-used sulphur-vulcanized system²⁷. However, small changes were made in this study, whereas zinc oxide (ZnO) and zinc dibutyl dithiocarbamate (ZDBC) were used as part of the vulcanizing ingredients. Both chemicals were used to improve the pre-vulcanization process of the latex compound which helps to accelerate the vulcanization process and to reduce the volume shrinkage of the end products. Further to that, all vulcanizing agents were mixed first and allowed to activate at room temperature for 30 minutes. During the compounding process, potassium oleate (PO) was added first into the SpNR latex, followed by the pre-mixed vulcanizing agents, all while the NR latex was being stirred at 100 rpm. The mixing process was carried out for two hours. After that, the speed of the stirrer was reduced from 100 rpm to 45 rpm and left at room temperature for a further 16 hours to allow efficient maturation of the DPNR latex compound⁴³. The DPNR latex compound should be continuously stirred to prevent sedimentation of the vulcanizing agents, but at a low speed to avoid latex destabilization (coagulate) due to shear.

Table 5.1: Compounding formulation used in this study

Ingredient	TSC (%)	Dry weight (phr)
NR latex ^{a, b, c}	60	100
Potassium oleate	20	1.50
Sulphur dispersion	60	2.50
Zinc oxide (ZnO) dispersion	60	0.15
Zinc diethyl dithiocarbamate (ZDEC) dispersion	50	0.75
Zinc dibutyl dithiocarbamate (ZDBC) dispersion	50	0.25
Zinc 2-mercaptobenzothiazole (ZMBT) dispersion	50	1.0
Antioxidant dispersion (Wing stay-L)	50	1.0

^a = LATZ latex; ^b = DPNR latex; ^c = ENR latex; phr = parts per hundred rubber

5.2.1.2 Effect of compounding on viscosity and pH of the latex

Table 5.2 shows the effect of compounding on viscosity and pH value of the latexes. It is clear that pH value of all latexes was decreased, whilst viscosity was increased. The decrease of pH value could be due to the evaporation of ammonia from the latex during overnight maturation process. On the other hand, the increased viscosity of the latex could be due to the chemical reactions of the vulcanizing ingredients. The viscosity of pre-vulcanized NR latex is correlates with colloidal stability of the material, in which depends on many factors such as pre-vulcanization temperature and time, the amount and type of stabilizers and the dosage of vulcanizing ingredients, as well as the TSC and particle size of the latex itself. Previous study¹⁶⁰ indicated that, pre-vulcanization

process has little effect on viscosity of the latex compound. Contradictorily, another study¹⁶¹ stated that viscosity of NR latex increases due to the thickening effect resulting from the chemical reaction between soaps (in this case PO) and ZnO in the presence of ammonia in the latex system. This was further supported by Mathew and Varghese¹⁶² whereas, the soluble soaps converted into insoluble material due to reaction with ZnO, thus increasing viscosity value. Further to that, the presence of ZMBT as a secondary accelerator also can cause latex thickening (increase in viscosity) because ZMBT is slightly acidic and thus neutralizes alkaline in the latex system¹⁶³.

Table 5.2: Effect of compounding on viscosity and pH value of the latex

Stage of latex	LATZ pH/viscosity	ENR pH/viscosity	DPNR pH/viscosity
Latex concentrate	9.70/ 70	9.50/ 500	9.61/ 115
Compounded latex	9.46/ 135	9.20/ 500	9.35/ 175

5.2.2 Preliminary observation on foaming and gelling behavior

5.2.2.1 Foamability of latex and latex foam stability

Figure 5.1 shows that the foam volume of all latexes gradually increased with time due to the mechanical agitation process. In this experiment, the agitation process was automatically stopped after 600 seconds to elucidate the foamability of each latex. The results show that all latexes can be foamed. However, the foamability of each latex is different.

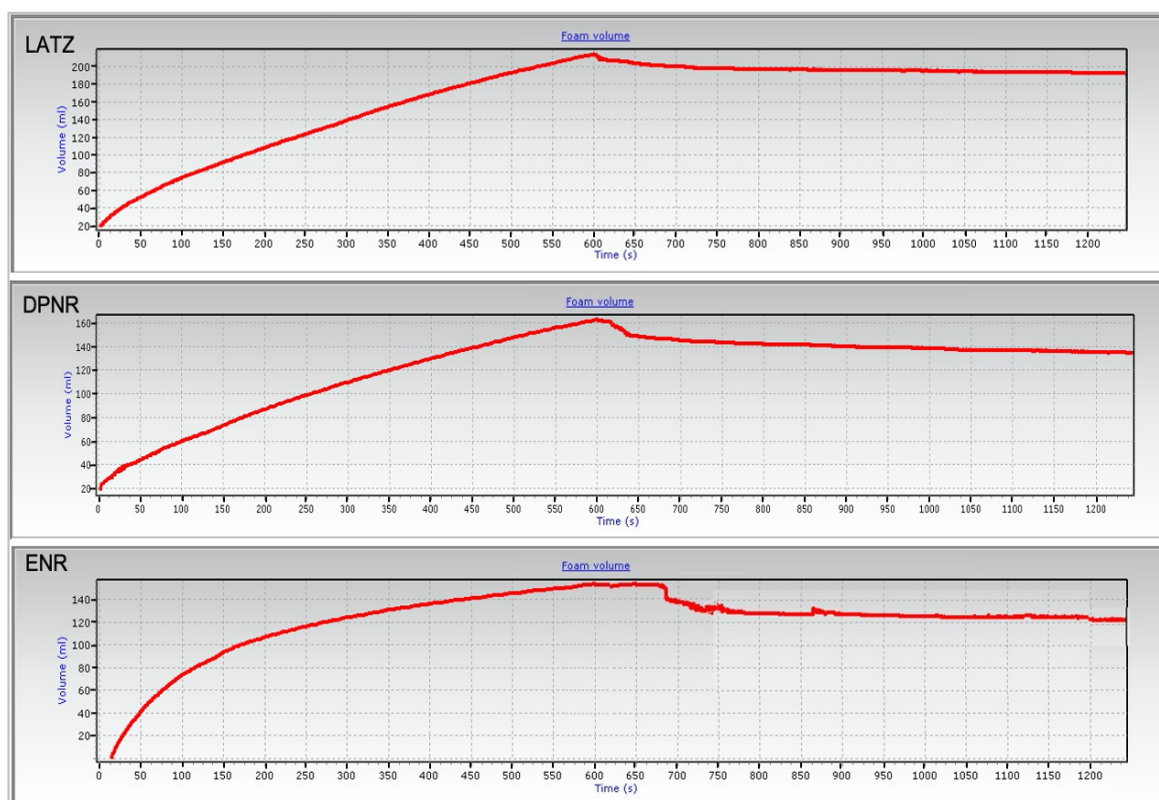


Figure 5.1: Foam volume versus time for LATZ, DPNR and ENR latex.

The study found that the LATZ, DPNR and ENR latex was foamed from 60 mL to 200 mL, 160 mL and 140 mL latex foam respectively. This indicates that LATZ latex exhibits the highest foamability followed by DPNR and ENR latex. According to Sun et al.¹⁶⁴, the thicker the liquid, the slower the growth speed, in other words the slower the transition of the material from a liquid phase to foam phase. Therefore, the foamability of each NR latex examined in this study might be influenced by the viscosity of the latex, whereas higher viscosity was less foamability of the latex. This correlates with viscosity results shown in Table 5.2 whereas, the viscosity of ENR latex is the highest, followed by DPNR and LATZ latex. Nevertheless, Figure 5.1 demonstrates that all latex foams are thought to be stable because the drainage volume over time is less than 15%, indicating that each latex is suitable for the production of latex foam products.

Figure 5.2 shows foaming images of the latex foams that were captured by the integrated camera. The gray area represents the gas-phase encapsulated by latex film, whilst the darker area is the latex phase. The images show that at 300 seconds all latex foams are still at the foaming stage. LATZ exhibits the highest number of bigger foam-cell size, followed by DPNR and ENR latex foam. This correlates with Figure 5.1, whereas LATZ shows the fastest foams grow compared to DPNR and ENR latex foam.

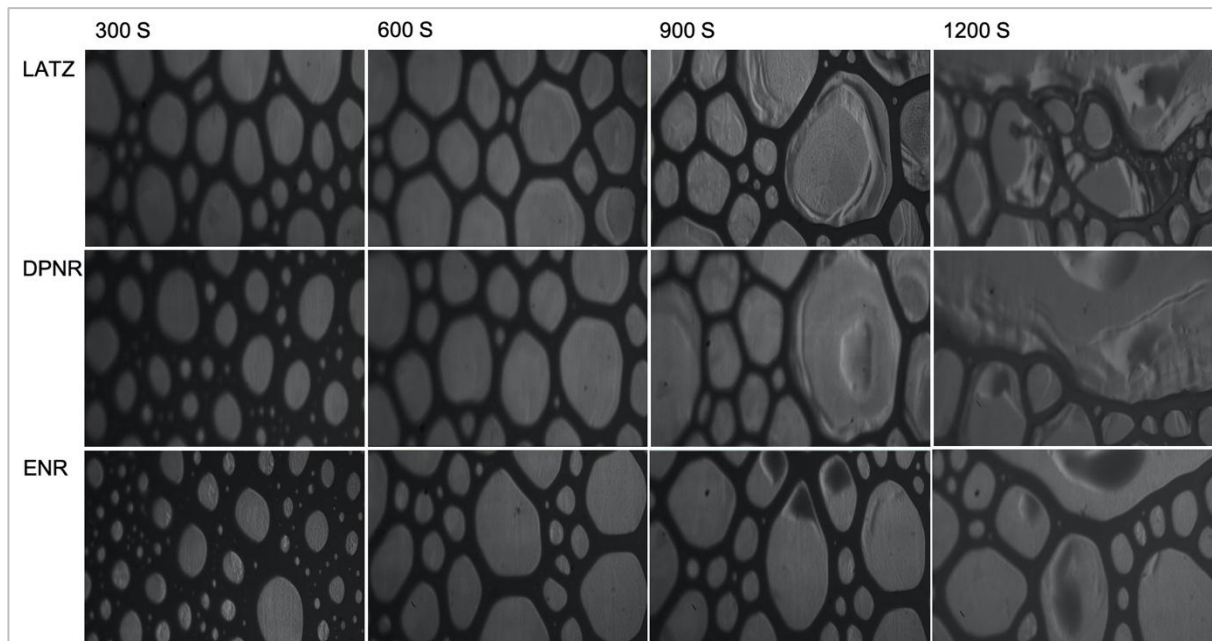


Figure 5.2: Foamability latex and the stability of latex foam.

After the mechanical agitation automatically stopped at 600 seconds, the foam-cell size of each latex was visually compared. Assessing from the liquid film thickness (dark area) and foam-cell size, LATZ and DPNR latex exhibit a moderately even liquid film thickness but unequal foam-cell size, thus the foam-cell structure of LATZ and DPNR latex is categorized as polynomial foams¹⁶⁴. On the other hand, for ENR latex foam, it can be seen the liquid film thickness are varied, and

there is much small foam-cell structure that can be observed. This study assumed that the liquid film thickness and foam-cell size of ENR latex foam can be more equivalent by the addition of foaming agents. Figure 5.2 also demonstrates the foam-cell structure started to collapse after 900 seconds. This is due to the pressure difference between foam-cells and the gravitational force that causes the liquid film to drain out of the foam. This phenomenon has been explained by Sun *et al.*¹⁶⁴ whereas, a pressure difference between smaller and bigger foam-cell has driven gas molecules trapped in the smaller foam-cell to diffuse into bigger foam-cell through liquid film. Gas molecules diffuse from a smaller foam-cell into a bigger foam-cell because the pressure in the smaller foam-cell is higher than the bigger foam-cell. Therefore, the bigger foam-cells continue to grow bigger, and eventually the liquid film ruptures and the foams collapse. Nevertheless, different types of latex might have different foam stability. It can be seen in Figure 5.2, that after 900 seconds the foam-cell structure of ENR latex is more stable compared to LATZ and DPNR latex foam. The reason behind this phenomenon is unclear but possibly due to the physicochemical properties (i.e., total solid content, dry rubber content, mechanical stability time, viscosity) of each latex. Previous study¹⁵¹ revealed that the presence of non-ionic surfactant in the ENR latex system contributes to a high stability of the material. Additionally, the presence of non-ionic surfactant in the ENR latex system was observed to increase the viscosity of the latex. Previous study¹⁶⁵ cited that, a viscosity of a liquid affects foam stability whereas, higher viscosity exhibits higher flow resistance of the fluid, consequently reducing foam drainage tendency. Thereby, the foam produced from higher viscosity exhibits more stable foam. Table 5.1 indicated that, each latex has different viscosity, and ENR latex shows the highest viscosity followed by DPNR and LATZ latex. Therefore, ENR latex foam demonstrates a stable foam compared to LATZ and DPNR latex foam. This phenomenon can be observed in Figure 5.1 and microscopically visualized in Figure 5.2. Nevertheless, it should be noted that, the different viscosity of each latex is influenced by the composition in the latex system, whereas both DPNR and ENR latex contain non-ionic surfactant to stabilize and preserve the latex from coagulation after the modification process. Further to that, as indicated in Figure 5.1, the volume expansion of ENR latex foam is lower compared to LATZ latex foam and DPNR latex foam. However, at 1200 seconds all latex foams were observed to collapse.

5.2.2.2 Challenge during latex foam fabrication process

The first step of the Dunlop batch foaming process is compounding the latex with a vulcanizing agent together with a stabilizer which also acts as a foaming agent. Second, is to foaming the latex, whereas the latex changes from the liquid phase into the latex foam phase. This is followed by the addition of gelling ingredients to set the foam-cell structure. This study observes that to produce SpNR latex foam, it is crucial to determine relevant parameters controlling foaming and gelling

behaviors of SpNR latex. The study observed that foam collapses and foam coagulate are two main challenges in producing SpNR latex foam (Figure 5.3). It was noticed that there are few factors that lead to foam collapse such as volume expansion too high, levels of gelling agent not being suitable and latex foam too stable to be gel due to excessive stabilizer or surfactants. On the other hand, foam coagulates mainly due to insufficient foam stabilizers and excessive gelling agent.

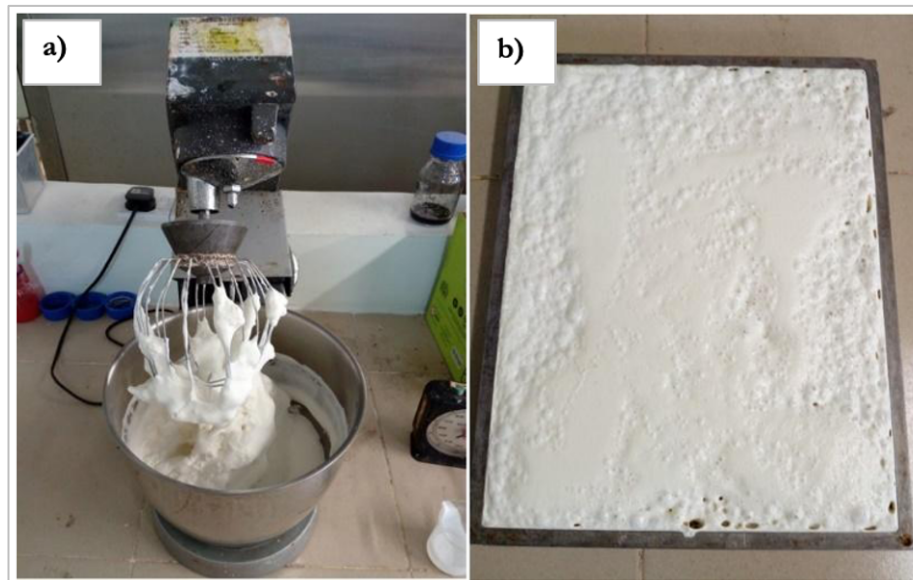


Figure 5.3: Failure during the foaming process.

a) Foam coagulate; b) Foam collapse

This study also found that lower foam density requires additional PO to function as a foaming agent. However, the presence of a higher level of PO requires additional sodium silico fluoride (SSF) to balance the gelling system. In a well-balanced latex foam foaming and gelling formulation, the latex foam required about five to seven minutes to set, and this must be regarded as the upper limit of time that is available for transferring the latex foam from the bowl to the mold¹⁶³. Normally, a secondary delayed-gelling agent such as diphenyl guanidine (DPG) can be added to stabilize the foam-cell structure². Nevertheless, it should be noted that many other factors might contribute to foam process failure such as viscosity, total solid content, chemical stability of the latex as well as the type of chemical stabilizer used in the latex system²⁷. Besides foam collapse and foam coagulate, surface defects such as wrinkles, rat holes, coarse structure, flow marks and phase separation may occur if the gelling formulation is incorrect. Figure 5.4(a) shows surface wrinkles caused by an imbalance between zinc soap and an acidic gelling agent, typically insufficient SSF. Figure 5.4(b) demonstrates a thick layer of skin that appeared at the bottom part of the latex foam. This is because the liquid foam that has been drained back into the liquid phase coalesce to become latex film. To address these issues, additional SSF should be added to set the latex foam-cell or locking latex foam at a consistent foam-cell structure. However, it is important to keep in mind that too much SSF causes the latex foam to coagulate in a very short period.

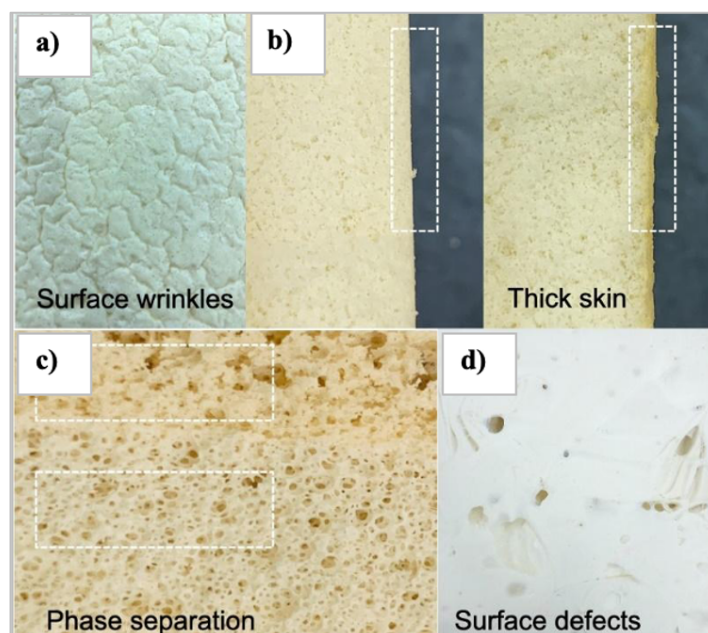


Figure 5.4: Examples of latex foam failure.

a) Surface wrinkles; b) Thick skin; c) Phase separation; d) Surface defects

Figure 5.4(c) shows an example of phase separation whereas the foam-cell size at the bottom part of the latex foam sample appeared to be smaller than the upper part. According to Blackley²⁷, phase separation is a consequence of foam drainage caused by long gelling time. This is a situation where the latex foam-cell structure slowly collapses due to the pressure difference between foam cells and gravitational forces. Figure 5.4(d) demonstrates surface defects such as rat holes, coarse structure and flow marks. This is a consequence of an incorrect gelling system whereas the gelling reaction occurred at low pH due to an acidic gelling agent⁴¹. Therefore, determination of the actual dosage of SSF is important, especially in this study when different types of latex are used.

5.2.3 Development of foaming and gelling formulations

In this section, three wet latex foam densities which are 0.16 g/cm³, high-density (HD), 0.12 g/cm³, medium-density (MD) and 0.09 g/cm³, low-density (LD) were prepared as variables. During the foaming process LATZ latex can be foamed to the targeted volume expansion within five minutes. Thus, the targeted wet density of HD, MD, and LD were achieved. For DPNR latex, it was observed that, for HD, the latex can be foamed to the targeted volume expansion within five minutes. But, for MD and LD, the growth of the latex foam was found to be slightly slower, thus unable to reach the targeted volume expansion within five minutes. Although the foaming time has been extended to eight minutes, the latex foam is still unable to reach the targeted volume expansion. The latex foam was observed to reach only $\frac{3}{4}$ of the targeted volume expansion. Therefore, in this work, an additional dosage of PO was added into the DPNR latex to improve its foamability. Thus, to produce MD and LD DPNR latex foam, additional 0.25 phr and 0.5 phr of PO was added respectively. Similar to DPNR latex, ENR latex is unable to reach the targeted

volume expansion within the targeted time. Therefore, additional 0.25 phr, 0.5 phr and 0.75 phr of PO were added to the latex to produce HD, MD and LD foam respectively. This study suggests that the addition of additional volume of PO as a foaming agent helps to improve the foamability of DPNR and ENR latex.

During the foaming process, the latex foam sample was taken out from the bowl mixer and poured into a 50 mL beaker to determine the wet density of the latex foam, to ensure each batch of latex achieved the targeted latex foam wet density. The wet density was calculated in accordance with Equation 5.1.

$$Wd = \frac{Ms}{Vb} \quad (5.1)$$

where Wd is the wet density, Ms is mass of the sample and Vb is the volume of the beaker.

Table 5.3 shows that the targeted wet density of ENR (LD) latex foam was found slightly higher than the targeted wet density. The reason behind this is still unclear and needs further investigation. After the latex foam achieved the desired degree of volume expansion, the speed of the foam mixer was reduced to refine the foam-cell structure. Then, zinc oxide (ZnO) and DPG were added. The latex foam was allowed to be continuously stirred for one minute to ensure ZnO and DPG are well dispersed in the latex foam. Then, the pH value of the latex foam was recorded.

Table 5.3: Wet density of the latex foam

Parameters	LATZ Wet density (g/cm ³)	ENR Wet density (g/cm ³)	DPNR Wet density (g/cm ³)
HD	0.16	0.16	0.16
MD	0.12	0.12	0.12
LD	0.09	0.10	0.09

Average of three replicates. Values in brackets represent the standard deviation.

Table 5.4 shows that the pH value of the latex foam was reduced after the foaming process. The reduced pH value of the latex foam could be due to a chemical reaction between the ZnO + DPG and the latex and also due to the frothing process. According to Madge⁴¹, during the foaming process, a certain amount of ammonia has been lost to the atmosphere, thus changing the acidity of the latex foam. Therefore, this study agreed with a report made by Madge⁴¹.

Table 5.4: Effect of compounding and density levels on pH of the latex foam

Stage of latex	LATZ (pH)	ENR (pH)	DPNR (pH)
Compounded latex	9.46	9.41	9.35
Latex foam + DPG + ZnO	9.37 ^a /9.20 ^b /8.75 ^c	9.38 ^a /9.30 ^b /8.99 ^c	9.28 ^a /9.15 ^b /8.99 ^c

^a = HD; ^b = MD; ^c = LD

Further to that, this study observed that the lower the density of the latex foam the further the pH value was decreased. A similar trend was observed on each type of latexes used in this study. The latex foam fabrication process was continued by the addition of SSF as the gelling agent. In this work, the effects of SSF on pH value and gelling time of latex foam produced at different density levels were investigated. Figure 5.5, Figure 5.6 and Figure 5.7 show the results for LATZ, DPNR and ENR latex foam respectively. For LATZ, a gradual drop of pH value was observed after the addition of SSF.

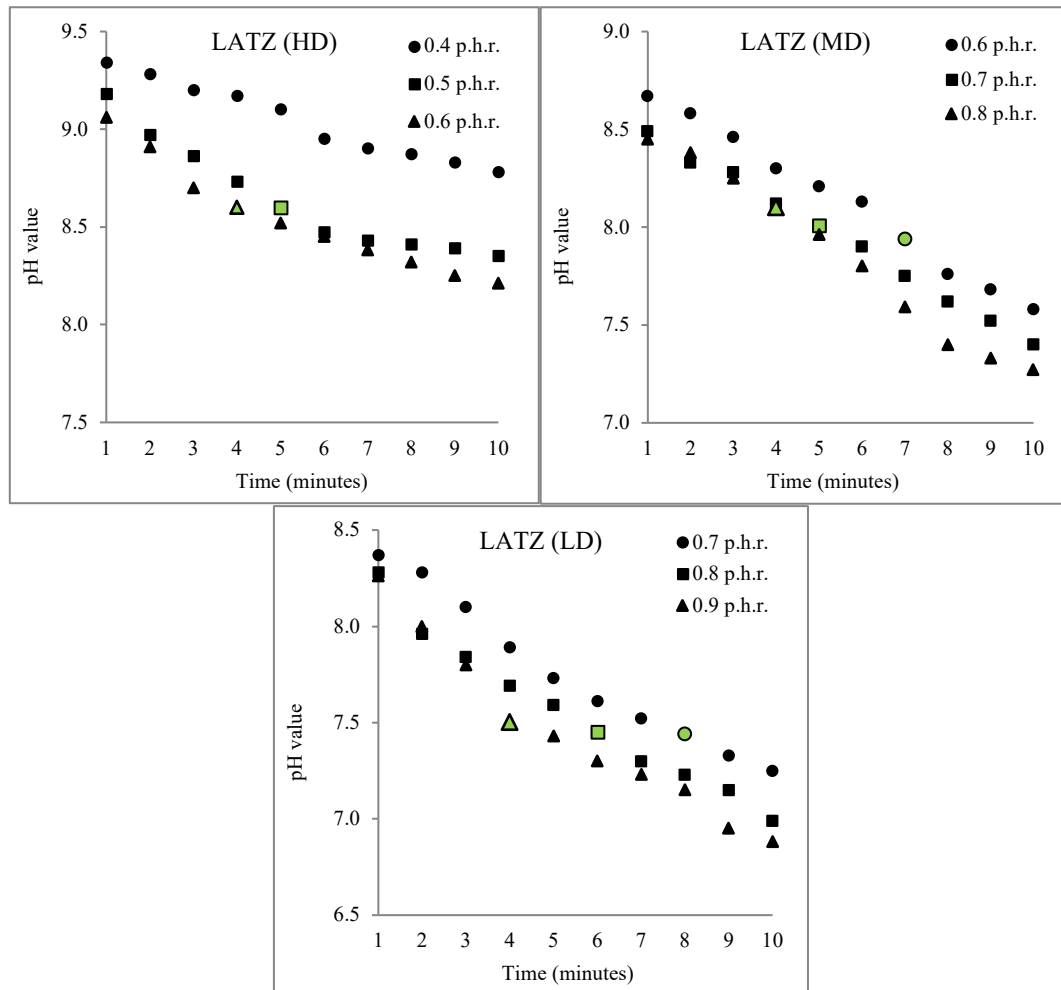


Figure 5.5: Effect of SSF levels on gelling time of LATZ latex foam. Green color indicates the gelling time.

This study also observed that a higher level of SSF leads to a bigger drop in pH value. However, this study observed that the addition of 0.4 phr of SSF into HD LATZ latex foam, was unable to gel the latex foam even after the latex foam was left to gel for 10 minutes. Consequently, the latex foam tended to collapse. This indicates that 0.4 phr of SSF used is too low. Therefore, the level of SSF was increased. This study found that the addition of 0.5 phr and 0.6 phr of SSF was able to gel the latex foam within five and four minutes respectively. Both samples were observed to gel at pH 8.6, almost similar to the gelling pH value of 8.5 recorded by the previous study⁷⁰. Comparison

between 0.5 phr and 0.6 phr, gelling time 0.6 phr is slightly faster than 0.5 phr. According to a previous study⁴¹, in a well-balanced latex foam formulation, latex foam required about five to seven minutes to set or completely gel. This is regarded as the time for transferring the latex foam from the bowl into the mold.

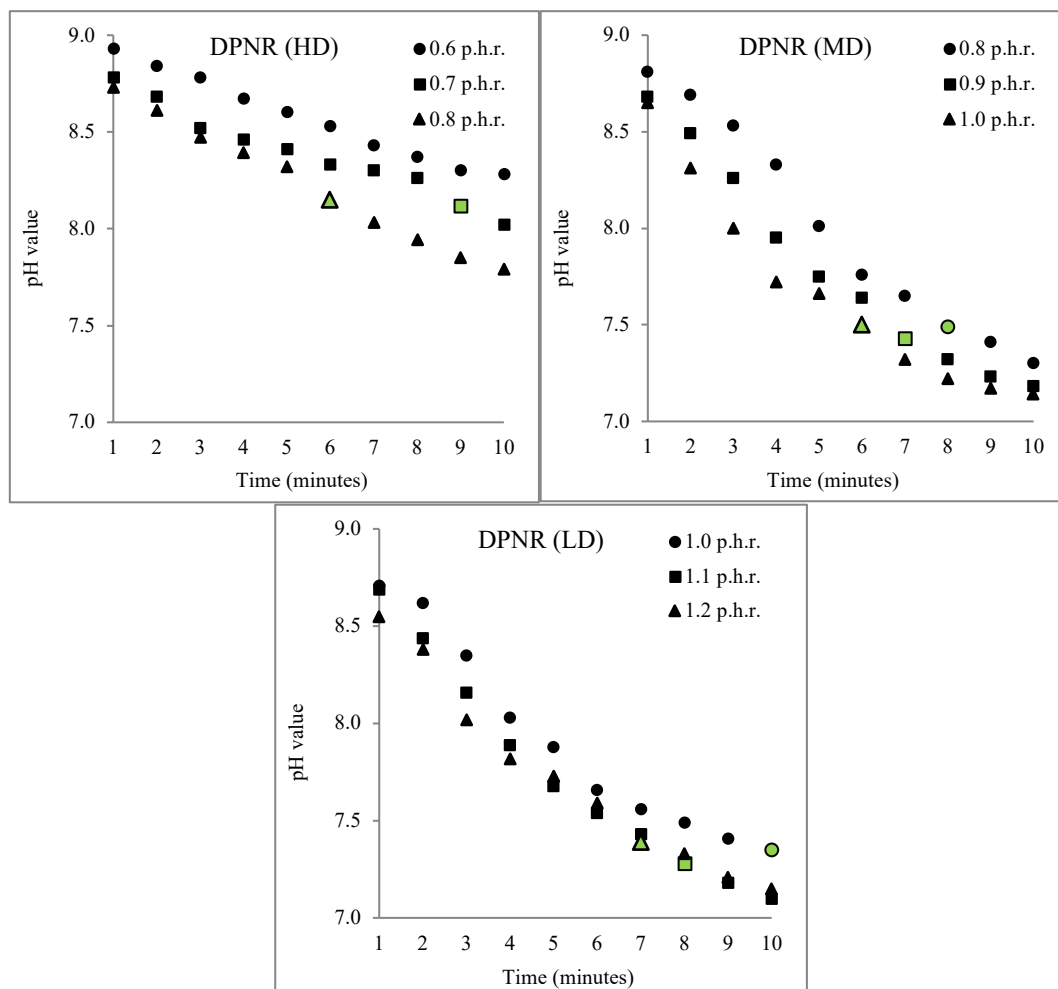


Figure 5.6: Effect of SSF levels on gelling time of DPNR latex foam. Green color indicates gelling time

Therefore, this study suggested that the best dosage of SSF for HD LATZ latex foam is 0.5 phr. Nevertheless, Figure 5.5 revealed that different density levels require a different dosage of SSF whereas, LATZ latex foam MD and LD requires 0.7 phr and 0.8 phr of SSF respectively. Accordingly, the gelling time for MD and LD LATZ latex foam was recorded at five and six minutes respectively. On the other hand, the gelling pH was recorded for MD and LD LATZ latex foam was recorded at pH 8.0 and pH 7.5. Generally, it can be observed that gelling time and gelling pH are influenced by the levels of SSF added. The level of SSF required depends on the density levels of the latex foam.

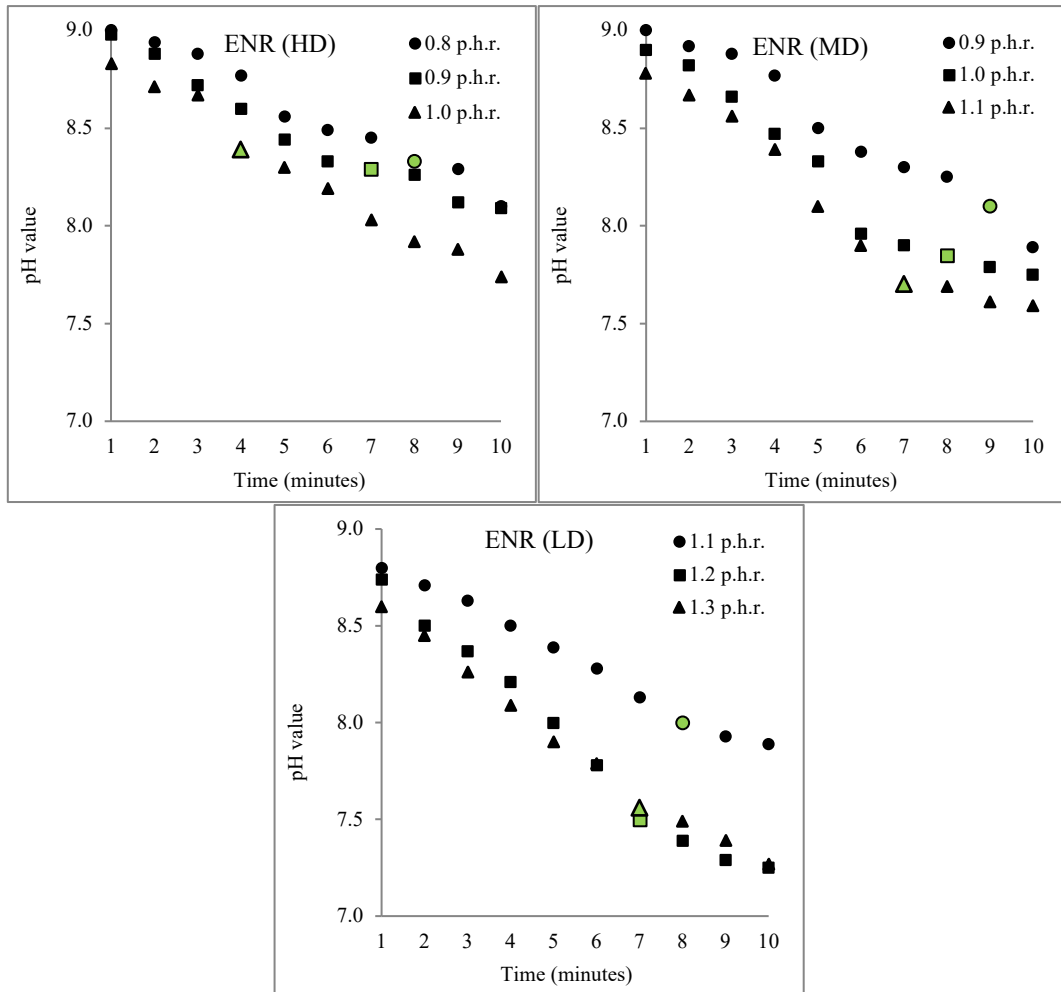


Figure 5.7: Effect of SSF levels on gelling time of ENR latex foam. Green color indicates gelling time

Similar to LATZ latex foam, Figure 5.6 shows gradual drops of pH by time in each density level of DPNR latex foam after SSF was added. Nevertheless, results shown in Figure 5.6 indicated that DPNR latex requires higher levels of SSF to reach the gel state compared to LATZ latex foam. For example, 0.5 phr SSF is required to gel HD LATZ latex foam, but for HD DPNR latex foam, 0.8 phr of SSF is required. This could be due to the presence of non-ionic surfactants in the DPNR latex system reacting with the chemical gelling agents thus preventing and delaying the gelling process¹⁶⁶. In addition, gelling pH of HD DPNR latex was observed lower than HD LATZ latex foam. A similar trend was observed on each density level of DPNR latex foam. Figure 5.6 shows that HD, MD and LD of DPNR latex foam were gel at pH 8.15, pH 7.50 and pH 7.40, at gelling time of six, six and seven minutes using SSF levels of 0.8 phr, 1.0 phr and 1.2 phr respectively. On the other hand, ENR latex shows a longer gelling time than LATZ and DPNR latex foam (Figure 5.7). HD MD and LD of ENR latex foam were observed to gel at the gelling time of seven minutes, at pH 8.29, pH 7.70 and pH 7.50, using SSF levels of 0.9 phr, 1.10 phr and 1.20 phr respectively. This could be due to different chemical compositions in the ENR latex system as a result of the

epoxidation process. Further to that, it should be noted that NR latex is stabilized by protein molecules, fatty acid soaps, and surfactants (carboxylic anions) adsorbed on the surface of rubber particles². This negative charge produces repulsive forces and ensures the absence of aggregation. Reduction in pH by the addition of an acid gelling agent reduces ionization of adsorbed anions and decreases the repulsive forces due to which gelation takes place^{26,41}. Therefore, the slower rate of gelation of ENR latex foam in comparison to LATZ foam might be due to the presence of additional stabilizers or surfactants (i.e., ammonium laurate, potassium oleate).

5.2.4 Specialty natural rubber latex foam fabrication process

The fabrication of latex foam in this work is similar to the conventional Dunlop batch foaming process^{27,43} which involves compounding, foaming, gelling, molding, vulcanizing, washing and drying process (Figure 5.8). After a suitable level of SSF was added (Section 5.2.3), the latex foam was poured into a square shape mold of 200 × 200 × 40 mm (length × width × height).



Figure 5.8: The different stages involved in the fabrication of SpNR latex foam.

In this work, the latex foam was allowed to gel and rest at room temperature for five minutes before being transferred into a hot air oven at a temperature of 100 °C and vulcanized for 60 minutes. Vulcanization is a chemical reaction that gives the latex foam its final fixed and elastic shape. After vulcanization, the mold is opened, and the vulcanized latex foam is peeled out from the mold and then subjected to a washing process to remove excessive soap, extractable proteins and residual chemicals. The washing operation is not critical, but this process is important to

ensure that elasticity is retained and to counter aging due to chemical residues. A typical process is by soaking the latex foam in warm water (45 °C), and then squeezed out the water through squeeze rollers. Then, the latex foam was subjected to a drying process.

5.2.5 SpNR latex foam appearance

Figure 5.9 shows the appearance of LATZ, DPNR and ENR latex foam produced in this study. The color of the dried latex foam appeared slightly different, whereas LATZ and DPNR latex foam were visualized as off-white color, but ENR latex foam was visualized as creamy-yellow color. The creamy-yellow color of ENR latex foam could be due to epoxidation reactions as well as a heating process that was conducted at elevated temperatures for 24 hours. It should be noted that all latexes are able to be foamed at three different density levels and labeled as HD, MD and LD foams.

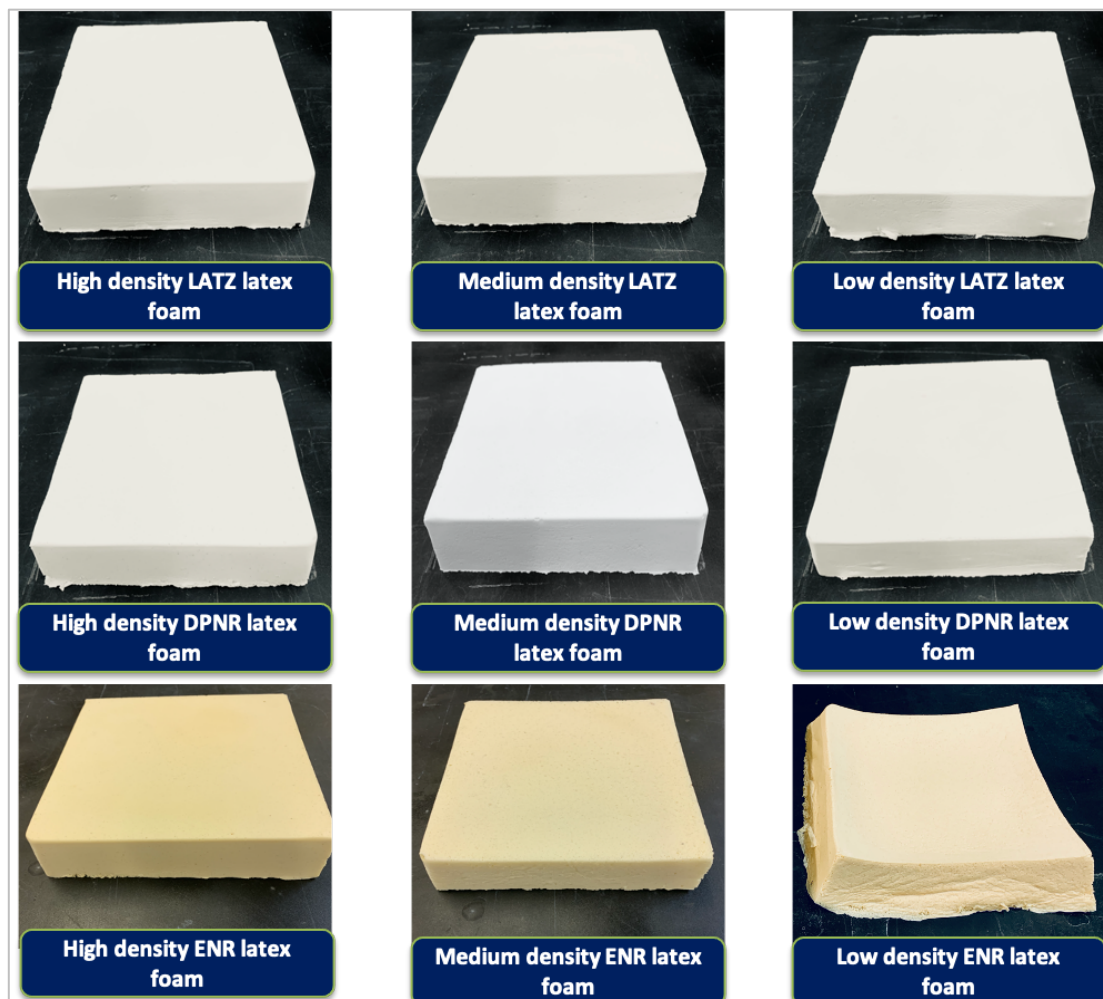


Figure 5.9: Appearance of LATZ, DPNR and ENR latex foam.

However, after the vulcanization process, only LATZ and DPNR latex foam were successfully fabricated at three density levels. For ENR latex, ENR (LD) foam was observed to flop down to the center of the latex foam sample like a crater after the vulcanization process. The reason behind

this is not clear but possibly due to the poor wet gel strength of the material, as a result of the high level of stabilizer presence in the latex system. During the vulcanization process, the mold is closed with a lid. The lid has been manufactured with a small hole to allow vaporize materials including water and ammonia to evaporate from mold leaving a solid latex foam material. However, during the evaporation process, the wet latex foam suffered from pressure differences in between the lid and top surface of the latex foam. At this stage, the foam-cell structure of the latex foam has not solidified, therefore, the pressure tends to push the latex foam to flop down. Latex foam LD is a low-density latex foam, thus expected to have low wet strength compared to latex foam HD and MD. Therefore, this study assumes that the weak wet gel strength of ENR (LD) is unable to oppose the pressure, thus leading the latex foam to flop down creating a crater during the vulcanization process.

5.2.6 Effect of density on volume shrinkage

Table 5.5 shows the dry density and volume shrinkage of latex foam fabricated in this study. It can be seen that, the dry density of all latex foams fabricated in this study was decreased to almost half of the wet density value.

Table 5.5: Effect of density levels on volume shrinkage

Samples	LATZ		ENR		DPNR	
	Dry density (g/cm ³)	Volume shrinkage (%)	Dry density (g/cm ³)	Volume shrinkage (%)	Dry density (g/cm ³)	Volume shrinkage (%)
HD	0.102	12	0.111	13	0.103	12
	(0.003)		(0.009)		(0.006)	
MD	0.084	11	0.090	12.5	0.084	11
	(0.004)		(0.001)		(0.002)	
LD	0.063	10	N/A	N/A	0.064	11
	(0.006)				(0.006)	

Average of three replicates. Values in brackets represent the standard deviation.

This study also found that higher density latex foam exhibits higher volume shrinkage. No significant difference in volume shrinkage between LATZ and DPNR latex foam was observed. However, the volume shrinkage of ENR latex foam is higher than LATZ and DPNR latex foam. The reason behind this is not clear, but possibly due to chemical epoxidation reactions on the molecular structure of rubber which lead to changes in physical properties of the rubber material including volume shrinkage. Additionally, the higher volume shrinkage of ENR latex foam also might be due to higher SSF added during gelling process^{26,41}.

5.3 Conclusion

This study proved that SpNR latex concentrate can be used to produce latex foam. The foamability of SpNR latex is lower compared to normal latex (LATZ). Foam collapse and foam coagulate are two main challenges in the fabrication of SpNR latex foam which can be solved by altering the foaming levels and gelling ingredients. Each type of latex requires different quantities of gelling ingredients. Gelling time and gelling pH are influenced by latex foam density and gelling agent added. This work identifies ideal compounding, foaming and gelling formulations for the fabrication of SpNR latex foam via Dunlop batch foaming process. It was found that DPNR latex can be used to produce low-density latex foam similar to LATZ latex foam. On the other hand, ENR latex can only be used to produce medium and high-density latex foam.

Chapter 6

Specialty natural rubber latex foam for cushioning applications

6.1 Introduction

Most of the bedding products available in the market are made from synthetic polymers (petrochemicals). It is well-known that petrochemicals-based products contribute to environmental and health issues, as well as challenging waste management and disposal problems^{67,68}. Therefore, many countries have implemented new legislation to restrict the utilization of synthetic polymers, and at the same time to promote the utilization of 'green materials' in the products manufacturing process¹⁶⁷⁻¹⁶⁹. Natural rubber (NR) latex foam is the best alternative material for bedding applications, not only because NR is a natural material, but also because of its high degree of elasticity, softness and durability compared to petrochemical-based bedding products⁵⁴. Bedding products made from NR latex also exhibit anti-microbial and dust-mite resistant properties, and have been identified as suitable for people susceptible to asthma^{2,10,170}.

Nevertheless, bedding products made from NR latex foam have been linked to latex allergy issues^{39,40}. NR latex products contain extractable rubber proteins, which, when in contact with human sweat, can cause latex allergy or *Type I* (immediate) hypersensitivity reactions^{75,76}. Latex allergy symptoms can be mild, such as redness of skin and itching, or severe, such as wheezing, mucosal swelling and anaphylactic shock^{75,77}. Although there is no evidence reported of NR latex foam bedding products causing latex allergies, as is the case with NR latex gloves, the latex allergy issue has raised awareness among users of the potential risks of using products made from NR latex^{6,40,78}.

Deproteinized natural rubber (DPNR) latex is a purified form of NR latex from which most of the ash and protein components have been removed. This is achieved by treating the NR latex with a proteinase enzyme to hydrolyze proteins in the latex system, which are then eliminated through a concentration process². Previous studies^{37,80} found that the resultant end products exhibit reduced levels of extractable proteins as well as being odor-less when compared with normal NR products. However, to date there is limited information concerning the utilization of

DPNR in latex foam bedding products. The reason behind this is unclear but it could be due to the lack of studies in this area.

The primary objective of the study is to produce pillows from SpNR latex. However, it is important to understand that for cushioning applications, typically pillows, the degree of softness of the material influences the degree of comfort for users. A previous study³⁷ demonstrated that the lower the density of latex foam, the softer the material. The inability of ENR latex to produce low-density latex foam shown in Chapter 5, suggesting that ENR latex foam is not suitable for cushioning applications. Therefore, in this study, the development of pillows from DPNR latex becomes a focal point. Three crucial criteria are assessed in this study because they affect the quality of the pillow and the comfort of sleep. These characteristics are the chemical, physical, and pressure-relief performance of the pillow^{13,59,171}. In this study, a comparison has been made between a latex foam pillow made from DPNR latex foam and two types of commercial pillows, namely commercial NR latex foam (CNRL) and memory foam (PM). However, since the compounding formulation used to produce CNRL is unknown, comparisons on chemical properties between DPNR latex foam and CNRL foam have limitations. Therefore, for a comparative study of chemical properties, LATZ latex foam was produced using a similar method and composition used for DPNR latex foam.

On the other hand, it should be noted that the excellent properties of NR latex foam such as a high degree of elasticity, soft and durable are also beneficial for other cushioning applications such as seat cushions for the transportation industry. Therefore, the second objective of the study is to investigate the feasibility of producing seat cushions from DPNR latex. The pressure relief performance and vibration transmissibility characteristics of the DPNR latex foam become the focal points, since they are related to the comfort and safety that the seat cushions can provide^{81,172}.

In order to accomplish these objectives, the development of compounding, foaming and gelling formulations to produce DPNR latex foam is essential. This chapter demonstrates the process of producing DPNR latex foam pillows and seat cushions. Factors influencing pressure-relief performance, vibration transmissibility and physical properties of the DPNR latex foam are discussed. Further to that, a comparative study has been made between the developed DPNR latex foam pillows and seat cushions with pillows and seat cushions purchased from Goodfoam Sdn. Bhd.

6.2 Development of cervical shape dual density latex foam pillows

6.2.1 Production of DPNR latex foam pillows prototype

6.2.1.1 Pillows production process

There are two options to produce DPNR latex foam pillows: the Dunlop batch foaming process, and the continuous foaming process^{27,43}. In this work, the batch foaming process was chosen because this technique is better suited to small-scale production and research and development purposes, especially when density is varied^{43,44}. Figure 6.1 shows the different stages in the DPNR latex foam pillow production process using the Dunlop batch foaming technique. The compounding, foaming and gelling formulations used in this work are similar to those that have been described in Section 5.2. However, for the foaming process a Hobart mixer is used instead of a Kenwood mixer because the high volume of latex foam is required to produce latex foam pillows. The compounded DPNR latex is whipped in a Hobart mixer where the stirrer rotates in a planetary motion at high speed (400 rpm) to entrap air into the DPNR latex compound. Three varieties of latex foam density were evaluated in this study: 0.16 g/cm³, high-density (HD); 0.12 g/cm³, medium-density (MD); and 0.09 g/cm³ low-density (LD). This was done by controlling the volume expansion of the latex foam during the foaming process. In this work, the volume of the latex foam bowl mixer is 15,000 ml. Therefore, approximately 2400 g, 1800 g and 1400 g of compounded DPNR latex was whipped until the latex foam reached the marked level of the bowl, to produce the HD, MD and LD latex foam respectively.

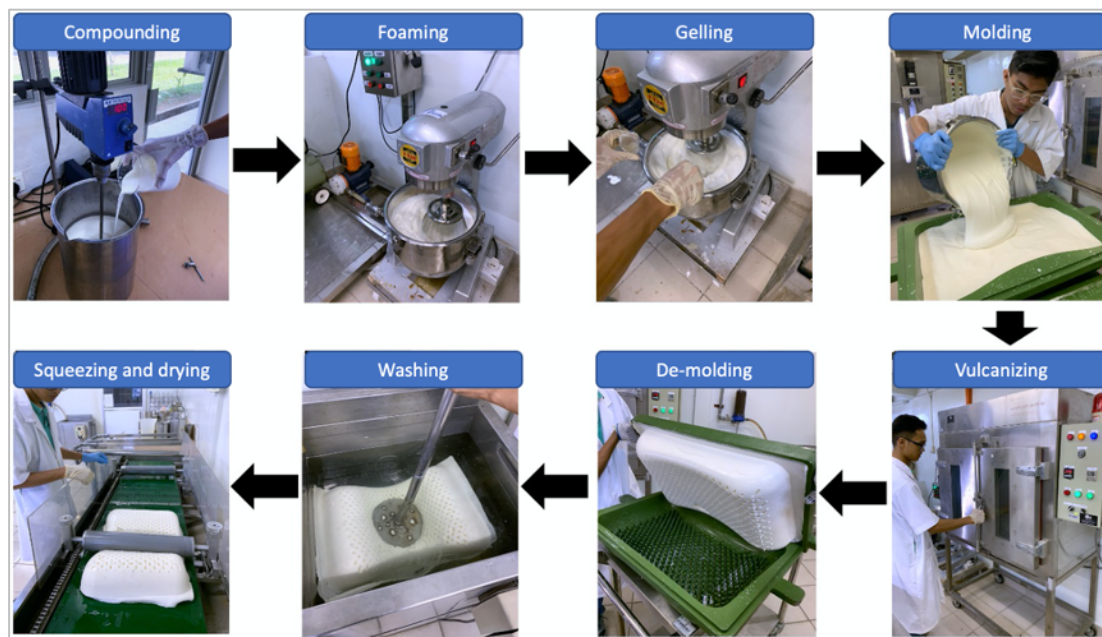


Figure 6.1: The different stages involved in the production of NR latex foam pillows.

After the latex foam achieved the targeted wet density level, the gelling ingredients were added. It should be noted that sodium silicofluoride (SSF) dosage was varied due to the different foaming and gelling behavior between density and types of latex that have been investigated in Section 5.2. After that, the latex foam is transferred into an aluminum pillow mold. Approximately, 5 to 6 minutes are required to set the foam cell structures. After the gelling process was completed in the aluminum pillow mold, the mold lid was closed and the DPNR latex foam was subjected to the vulcanization process in a hot air oven at 100 °C for 60 minutes. After the vulcanization process, the DPNR latex foam pillow was peeled out of the mold and subjected to washing and drying processes.

6.2.1.2 DPNR latex foam pillow's shape and structure

In this chapter, two different pillow shapes were investigated: a standard pillow, and a cervical shape pillow. For the cervical shape pillow, a novel cervical shape dual density DPNR latex foam pillow prototype was produced, whereas the pillow has a lower density at the upper part and a higher density at the lower part. In this work, the dual-density pillow was produced by first pouring the LD latex foam until it reached the marked level in the pillow mold, followed by pouring MD latex foam. It should be noted that the pillow mold is upside down, thereby, a dual density pillow with LD at upper part (curvy-shaped) and MD at the bottom part was obtained. The dimensions of the cervical shape pillow are shown in Figure 6.2. In addition, two commercially available pillows, one NR latex foam (CNRL) and one memory foam (PM), were purchased from Goodfoam Sdn. Bhd. for comparison.

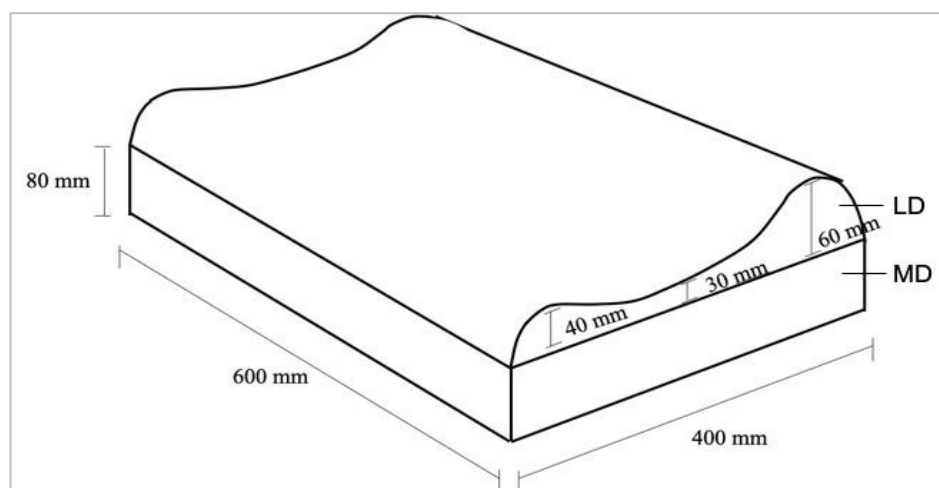


Figure 6.2: Illustration of the shape and dimensions of the DPNR latex foam pillow prototype.

6.2.2 Properties of latex foam pillows

The properties of DPNR latex foam pillows and LATZ latex foam pillows produced in this study were compared to commercially available NR latex foam (CNRL) pillows and polyurethane

memory foam (PM) pillows purchased from Goodfoam Sdn. Bhd. This is to ensure that the developed DPNR latex foam pillows are comparable to commercial products available in the market.

6.2.2.1 Chemical properties

Figure 6.3 reports the extractable protein content (ERP) content for LATZ, DPNR and CNRL foams, and shows that DPNR latex foam exhibits the lowest ERP content followed by CNRL foam and LATZ latex foam. This implies that DPNR latex is a suitable material to produce hypoallergenic pillows without changing the existing NR pillow's production technology. Overall, the ERP contents detected are low. The intensive washing process, where the latex foams underwent hot water washing treatment during the production process may have removed most of the water-soluble substances including ERPs.

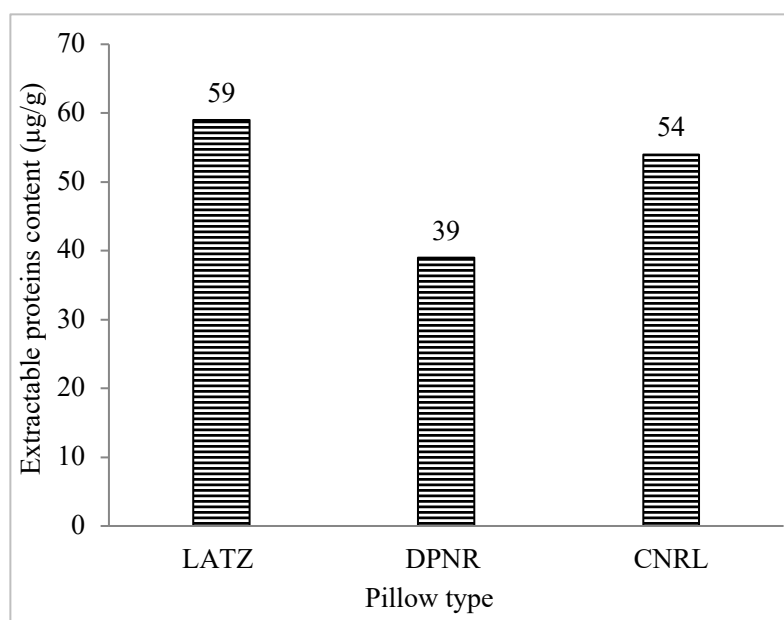


Figure 6.3: Extractable protein content of latex foam pillow materials.

Figure 6.4 reports the extractable residual chemicals (ERC) for LATZ, DPNR and CNRL foams. The ERC of ZDEC and ZDBC content of both DPNR and LATZ latex foams are very low, and almost invisible in the bar chart. CNRL latex foam exhibits a higher extractable ZDEC and ZMBT content compared to DPNR and LATZ latex foam, but no extractable ZDBC was detected. For ZMBT, DPNR latex foam exhibits slightly higher extractable ZMBT residue compared to LATZ latex foam but slightly lower than CNRL latex foam.

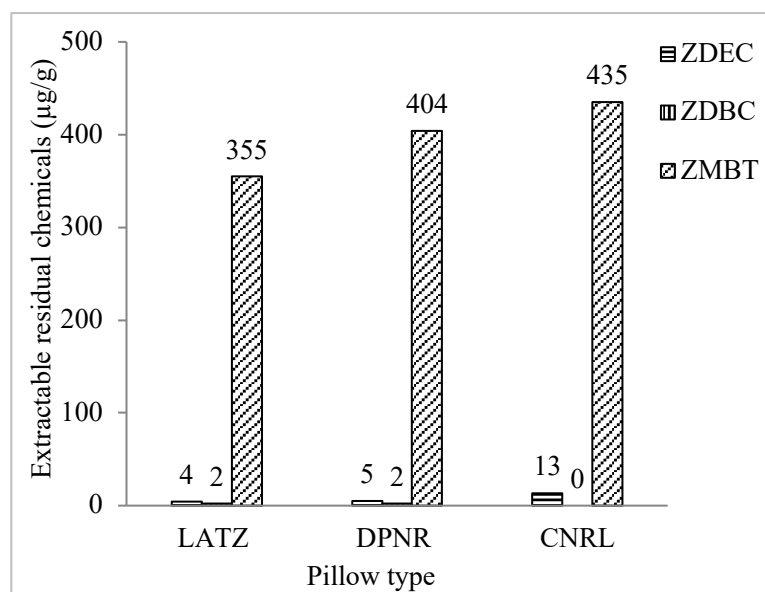


Figure 6.4: Extractable residual chemicals of NR latex foam pillows.

It should be noted that, there is no standard specification of ERP for NR latex foam products, thus the result shown is for research purpose especially when *Type IV* allergies issue has raised awareness among users of the potential risks of using pillows made from NR latex. The study revealed that, although the washing process may have removed most of the water-soluble substances, there are still remaining quantities of chemicals within the NR latex foam. Nevertheless, the test was conducted in boiling water to force extract as much water-soluble residues as possible, which may not be extracted in real practice. Further to that, pillows are usually covered by two layers of fabric to prevent direct contact between user and pillow. Therefore, the likelihood of the material causing *Type IV* allergies is considered low.

Figure 6.5 shows the concentration of (volatile organic compound) VOCs in each sample examined in this work. It is clear from the figure that PM produces the highest VOC emission, which is classified as high. This could be due to degradation of PM material that is made from polyurethane. This is in agreement with previous study¹⁷³ whereas bedding products made from polyurethane foam is a significant source of VOC emission. Although VOC emission also was observed in all NR latex foam samples, the detected amount is below than $500 \mu\text{g}/\text{m}^3$ thereby free from health risk⁷³. It is well-known that NR is a natural material obtained from rubber trees. Other than that, the rubber latex contains proteins, higher fatty acids, phospholipids and a very small portion of surfactant which could all contribute to a small volume of VOC, the slightly high volume of VOC detected on NR latex foam examined in this work could be due to the use of chemicals during the NR latex preparation process, as well as during the NR latex foam production process. Additionally, the use of chemical additives, for example β -sodium naphthalene sulphonate formaldehyde during the preparation of the vulcanizing ingredients (i.e., to change the sulphur

from powder form into dispersions) might also contribute to VOCs because during sampling condition, latex foam sample was heated up to 65 °C for two hours. Therefore, further investigation should be conducted to clarify the source of VOCs in NR latex foam samples in the future study.

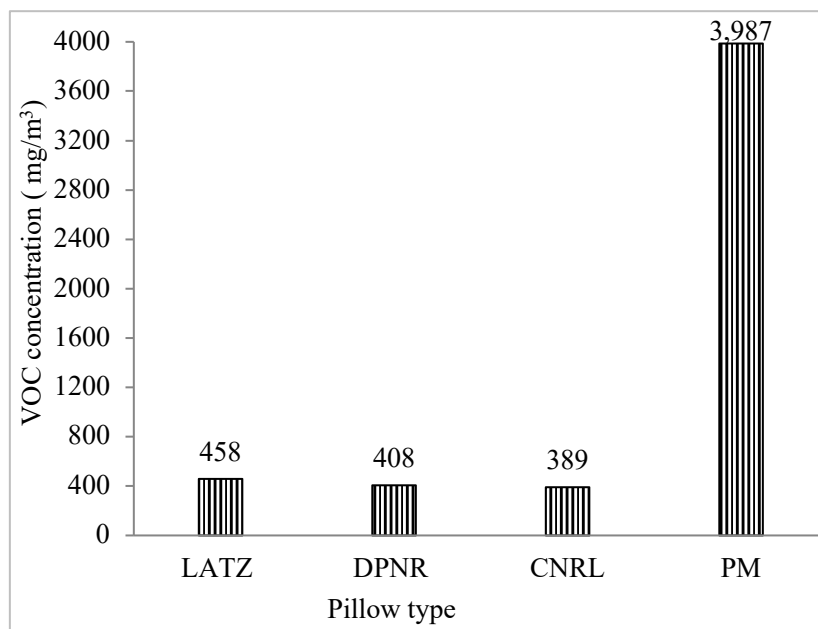


Figure 6.5: VOC concentrations of NR latex foam and memory foam pillows.

6.2.2.2 Physical properties

Table 6.1 shows a summary of the physical properties of all foam materials examined in this work, including samples from the commercial CNRL and PM pillows. The results show that the dry density of both DPNR and LATZ latex foams can be manipulated by controlling the wet density of the latex foam during the foaming process. Both LATZ and DPNR latex foams obtained a similar density value at each targeted density level. Table 3 also shows that the dry density of both CNRL and PM was 0.08 g/cm³, similar to the MD of LATZ and DPNR latex foams produced in this work. The compression set value of all samples examined complied with the requirements stipulated in the standard specifications. Although the compression set of DPNR (MD) is higher than HD and LD, the difference is not considered significant³⁷. Also, the recovery of PM was observed at 100 %. For elongation at break, no significant differences between the elongation at break values of CNRL, LATZ and DPNR latex foam samples was observed, indicating that DPNR latex foam is comparable to CNRL and LATZ latex foam in these terms. The elongation at break of PM, however, did not meet the standard requirement. This could be due to the soft nature of the material, leading to faster damage of the material compared with NR latex foam^{172,174,175}.

Table 6.1: Physical properties of foam samples examined in this study

Properties	MS679 specifications	LATZ			DPNR			CNRL	PM
		HD	MD	LD	HD	MD	LD	MD	MD
Wet density (g/cm ³)		0.16 (0.004)	0.12 (0.007)	0.09 (0.002)	0.16 (0.006)	0.12 (0.005)	0.09 (0.006)	N/A	N/A
Dry density (g/cm ³)	-	0.10 (0.003)	0.08 (0.004)	0.06 (0.006)	0.10 (0.006)	0.08 (0.002)	0.06 (0.006)	0.08 (0.009)	0.08 (0.001)
Compression set (%)	6 (max)	2.2 (0.6)	2.2 (0.6)	1.1 (0.7)	2.1 (0.8)	3.1 (1.2)	2.1 (1.7)	2.9 (0.3)	0 (0)
Elongation at break (%)	150 (min)	270 (15)	250 (6)	230 (6)	260 (20)	270 (17)	230 (35)	270 (10)	130 (20)
Indentation hardness (N)	<100 (Soft) 101-170 (Middle firm) >170 (Firm)	203 (2)	105 (4)	89 (1)	186 (2)	91 (4)	70 (2)	97 (2)	39 (1)
Accelerated aging (%)	±20 (max)	5 (1.0)	11 (1.0)	16.5 (0.8)	2 (1.0)	-8.5 (3.2)	-13 (3.6)	6.2 (0.2)	50.6 (4.5)
Pounding Change in thickness (%)	5 (max)	0 (0)	2.5 (0)	2.3 (0.1)	0 (0)	2.3 (0.1)	3.7 (0.1)	0 (0)	3.3 (0.1)
Pounding Change in hardness index (%)	±20 (max)	-1.2 (0.3)	-3.1 (5.2)	-1.8 (0.1)	-1.5 (6.5)	6.3 (0.1)	6.6 (0.2)	0.2 (0.1)	10.2 (2.6)

N/A = not available.

Average of three replicates. Values in brackets represent the standard deviation.

Table 3 clearly shows that decreasing the density levels of both DPNR and LATZ latex foams decreases the IH value. For LATZ latex foam, HD, MD and LD are as categorized firm, middle firm and soft respectively. For DPNR latex foam, HD, MD and LD are categorized as firm, soft and soft respectively. IH of DPNR latex foam is lower compared to LATZ latex foam. The reason behind this is unclear but possibly due to the removal of proteins that act as non-rubber reinforcing material in NR^{29,157,176}. On the other hand, both CNRL latex foam and PM foam are categorized as soft foam materials. Table 6.1 also shows a significant aging effect on PM, where the IH value of the PM increased by more than 50%. This result is in agreement with a previous study¹⁶¹ where PM materials were observed to become harder after prolonged use leading to less cushioning support. On the other hand, the pounding test is one of the testing methods to measure the lifespan of NR latex foam products, which is estimated to be equivalent to 10 years of daily (8 hours per day) usage. The comparative study between LATZ and DPNR latex foams found that, at equivalent density levels, LATZ latex foam exhibits slightly better pounding resistance compared to DPNR latex foam, whereas change in thickness (CIT) and change in hardness index (CHI) of LATZ are lower than DPNR latex foam. Although the CHI is observed to change from -3.1 to -

1.2 to 1.8 as the foam density goes from HD to MD to LD, these values are all considered to be small and within the experimental uncertainty.

Generally, this study observed that DPNR latex foam samples complied with the standard requirements of the accelerated aging test. However, it is interesting to observe the opposite effect of aging between LATZ and DPNR latex foams, whereas after aging LATZ shows an increase in hardness whilst DPNR shows a decrease in hardness, although their compounding formulation is the same. The effect of thermal aging of NR vulcanizate has been studied by many researchers¹⁷⁷⁻¹⁸³, but the effect of thermal aging on NR latex foam has not been explored. Special methods are needed to investigate this phenomenon which is beyond the scope of this paper. Nevertheless, it is possible to suggest some reasons for this unusual behavior based on literature. According to Gui Yang and Koenig¹⁸², thermal oxidation will either cause hardening or softening, depending on the microstructure of the diene elastomer. However, the process is very complex and involves several intermediates and side reactions. Azura¹⁸¹ and Samsuri¹⁸⁴ suggested that the effect of thermal oxidation on the physical properties of NR vulcanizate is governed by two competitive factors. One, oxidative and post vulcanization crosslinking reactions which increases hardness. Second, oxidative chain scission reactions and reversion which decreases hardness. Previous studies^{178,182,183} stated thermal oxidation of NR leads to main-chain modifications of various types of crosslinks (e.g., poly-sulphidic, di-sulphidic, mono-sulphidic, cyclic sulphidic, conjugated dienes and trienes, etc.) Samsuri¹⁸⁴ stated, sulphur-vulcanized NR vulcanizates may hardens before chain scissions take place. This hardening is due to crosslinking associated with oxidative reactions of sulphur species in the molecular network. Hardening is much due to the formation of new crosslinks, thus an overall increase in crosslink density would be expected thereby, would increases the IH of the foam material. Additionally, the increased of IH of the foam material also could be contributed by the presence of non-rubber components (proteins, phospholipids, etc.) which act as filler, as well as residual chemicals (soap, vulcanizing agents, etc.) possibly act as catalysts under aging conditions (70 °C for seven days) used in this work that harden the latex foam material^{177,180,184}.

On the other hand, the reduction of IH observed on the DPNR foams may well be associated with oxidative scission during aging. It is well-understood^{182,184}, that, NR is an unsaturated rubber, subjected to degradation due to the attack of heat, ozone, oxygen and ultraviolet light. It should be noted that, for NR latex foam the scission reactions could occur throughout the foam material for a longer time because NR latex foam contains an additional source of oxygen, the air within the foam-cell structures. Further to that, Lucille¹⁷⁷ stated that proteins play an important role in heat resistance and aging properties of DPNR vulcanizate.

Removal of proteins may result in the reduction of thermal-oxidative stability, thus inducing degradation of the physical properties of the DPNR vulcanizate^{177,179}. Additionally, Surakit *et al.*¹⁸⁰ stated that the deproteinization process leads to a reduction of naturally occurring antioxidants (i.e., phospholipids), thus enhancing the deterioration process, which, under the influence of heat, could accelerate the oxidation of rubber chains, thus rendering the material softer. The study also observed a correlation between density levels and aging effects, where decreasing the density levels increases the accelerated aging value. Therefore, it is suggested that increasing the density levels would improve the durability of the latex foam material.

6.2.2.3 Morphological characteristics

The effect of density levels on the physical properties of DPNR latex foam was further investigated through scanning electron microscopy (SEM). Figure 6.6 demonstrates morphological characteristics of LATZ, DPNR, CNRL and PM foams. Apparently, PM foam exhibits a visibly different foam-cell structure compared to CNRL, DPNR and LATZ latex foam. PM appears to have elongated pores which are less circular than those observed in the other CNRL, DPNR and LATZ latex foams.

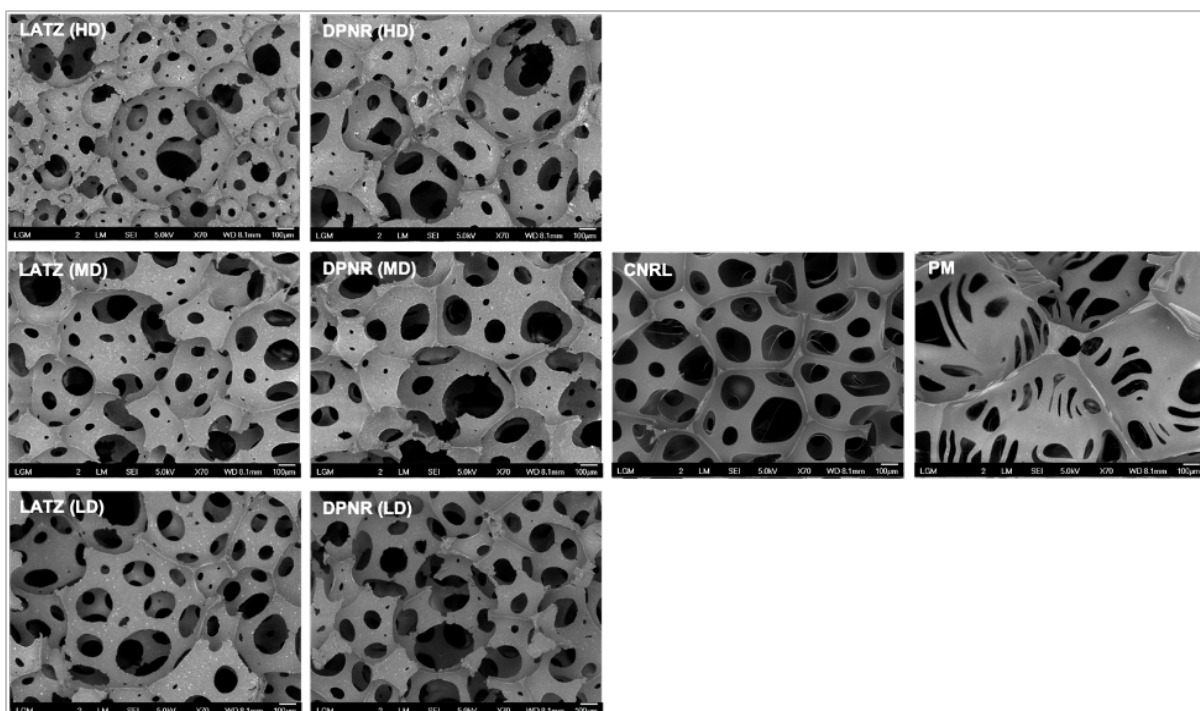


Figure 6.6: Morphological structures of LATZ, DPNR, CNRL latex foam and PM foam.

CNRL latex foam exhibits a more uniform pore size compared to DPNR and LATZ latex foam. This could be due to different foaming processes used between CNRL latex foam and DPNR and LATZ latex foams. The CNRL latex foam was produced using a commercial continuous foaming process in which air is metered under controlled pressure into an Oakes foaming head. On the other hand, DPNR and LATZ latex foams were produced using a batch foaming process where

the air is introduced through whipping the latex in a Hobart mixer. For DPNR and LATZ latex foams, it can be observed that the pore size of HD latex foam is smaller compared to that of MD and LD. To further investigate the effect of density on pores size of the latex foams, ImageJ software was used to quantify the pore size distribution from the images. Figure 6.7 shows the distribution of pores size of LATZ, DPNR, CNRL latex foams and PM foam.

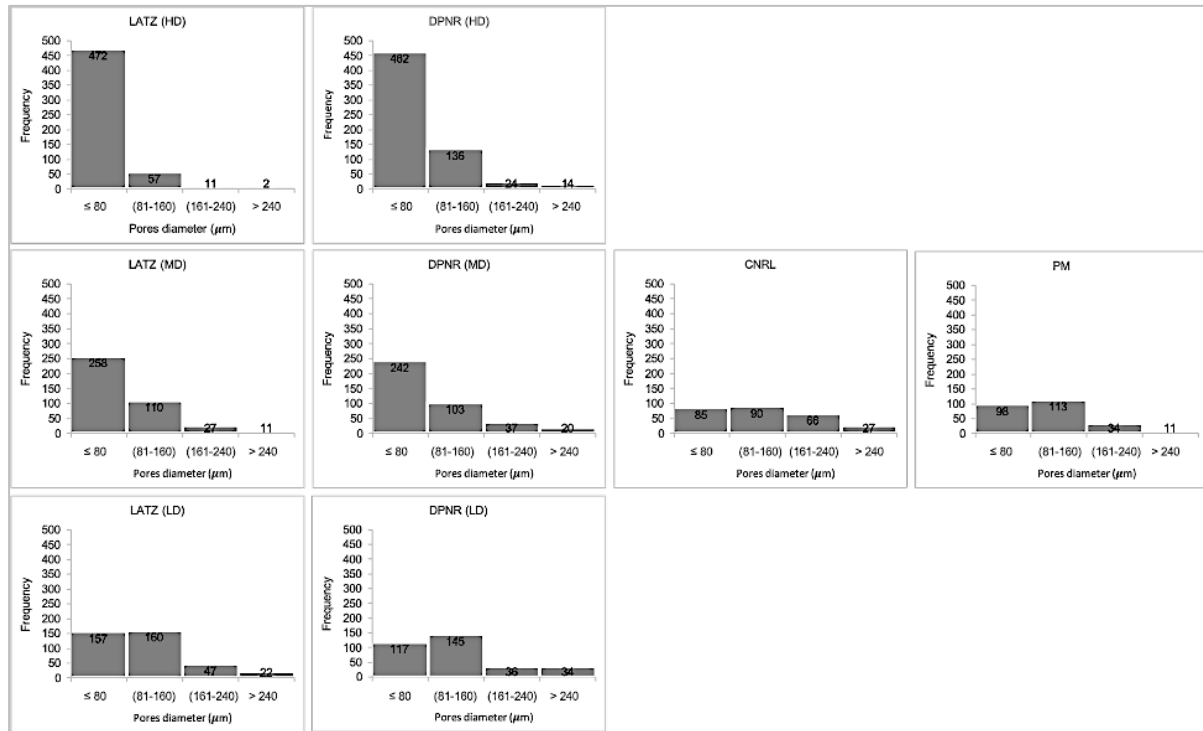


Figure 6.7: Distribution of pore size of the foam materials.

It is clear that the dominant pore size is 80 μm and below in the HD foam of both LATZ and DPNR latex foam. Decreasing the density from HD to MD and to LD has the effect of shifting the distribution to larger pore sizes. For CNRL, the fraction of pore size of 80 μm and below is similar to that of pore size of 80-160 μm and of pore size of more than 160 μm. For PM, the fraction of pore size of 80 μm and below is slightly lower than that of pore size of more than 80 μm.

Figure 6.8 shows the mean pore size of LATZ, DPNR, CNRL latex foams and of PM foam. LATZ (HD) demonstrates the smallest mean pore size compared to the other foam type examined in this work. Figure 6.8 also shows that perhaps unsurprisingly, decreasing the density levels of both LATZ and DPNR latex foam from HD to MD and to LD leads to an increase in the mean pores size of the latex foams. The study also observed that although PM foam, CNRL, LATZ (MD) and DPNR (MD) all have a similar density level (0.08 g/cm³), they exhibit different mean pore sizes. This could be due to different processes of production between each foam. Technically PM foam is a different material compared to the other foams, and is produced by chemical reactions between polyols and isocyanates. Thus, the morphological characteristics,

including the pore size of PM, are expected to be different to the other foams. On the other hand, CNRL, LATZ (MD) and DPNR (MD) latex foam are basically NR latex, but the foaming mechanism between CNRL latex foam and LATZ (MD) and DPNR (MD) latex foam is different. The effects of the foaming mechanism on morphological characteristics of NR latex foam have been described in previous studies^{41,174,185}.

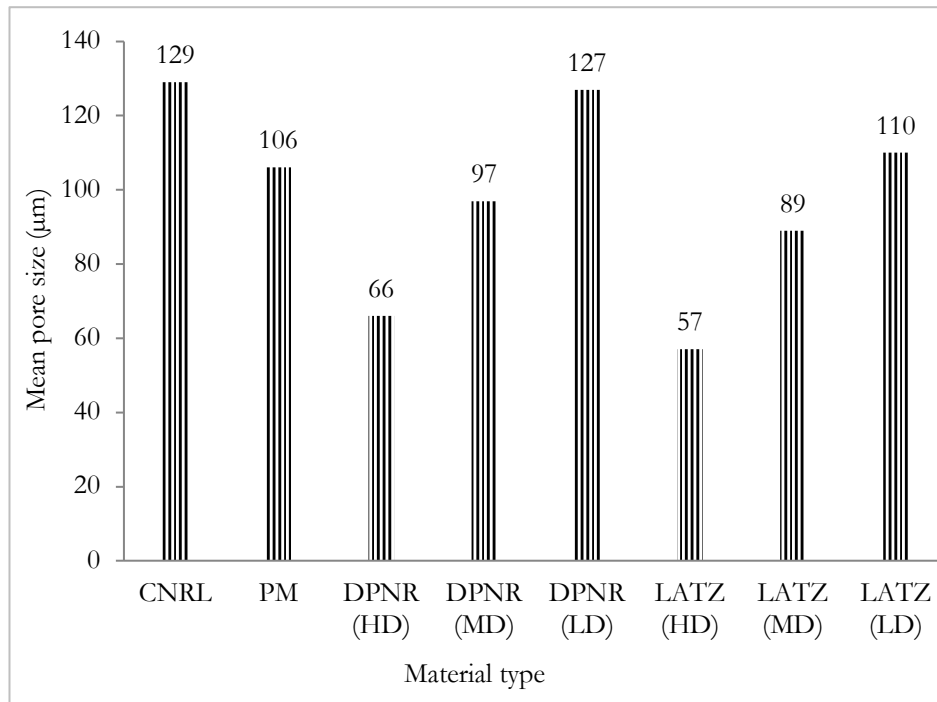


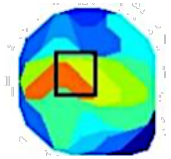

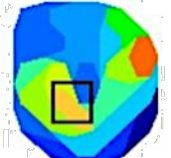


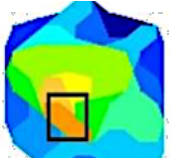
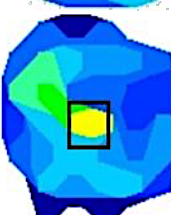
Figure 6.8: Mean pore size of foam materials examined in this study.

6.2.2.4 Pressure-relief performance

This section can be divided into two parts. First, the study investigated whether there was a remarkable difference in the pressure-relief performance of a normal flat-shaped pillow made from DPNR latex foam and LATZ latex foam. It should be noted that similar manufacturing processes and compounding formulations were used to produce both the LATZ and DPNR latex foam pillows. On the other hand, the second part evaluates whether the cervical shape could enhance the pressure-relief performance. The second part also evaluates whether the dual-density structure is efficient in enhancing the pressure-relief performance of the pillow.

Table 6.2 shows snapshots from real-time measurements of pressure distribution, surface contact area and average peak pressure values of LATZ and DPNR latex foam pillows when a mannequin head was placed on the top of the pillow. It should be noted that, peak pressure is the peak interface pressure or physical loading between the mannequin head and the foam material.

Table 6.2: Pressure distribution, average peak pressure value and surface contact area

Type	Pressure distribution*	Surface contact area (mm ²)	Average peak pressure value (kPa)	Pressure scale
LATZ (HD)		5209	15.6	
LATZ (MD)		6511	14.2	
LATZ (LD)		7464	11.0	
DPNR (HD)		5860	15.4	
DPNR (MD)		6729	13.8	
DPNR (LD)		7596	10.9	

*Black square box located the average peak pressure

Previous studies^{61,186} stated that, such physical loading caused tissue deformation at a cellular level and thus prevents arterial vessels from resupplying tissues with oxygen leading to ischemia (disrupts of blood circulation). Therefore, it is important to optimize the interface pressure distributions. In this work, irregular color intensities and contours of the mannequin head in each type of pillow, shown as a red box in Figure 6.9 were observed. The results indicate dissimilar physical responses of the pillows to the loading of the mannequin head. This implies that the physical properties of the pillows affect the pressure distribution pattern.

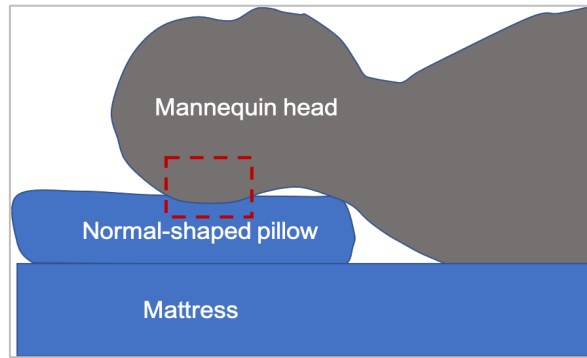


Figure 6.9: Modeling pillow conforming area under the head.

Table 6.3 also demonstrates that decreasing the density levels from high-density (HD) to medium-density (MD) and low-density (LD) increases the surface contact area value. A comparison between LATZ and DPNR latex foam pillows indicates that, at similar density levels, DPNR latex foam pillows produce a larger surface contact area than LATZ latex foam pillows. The results also indicated there is an inter-relationship between surface contact area and average peak pressure value, illustrated in Figure 6.10.

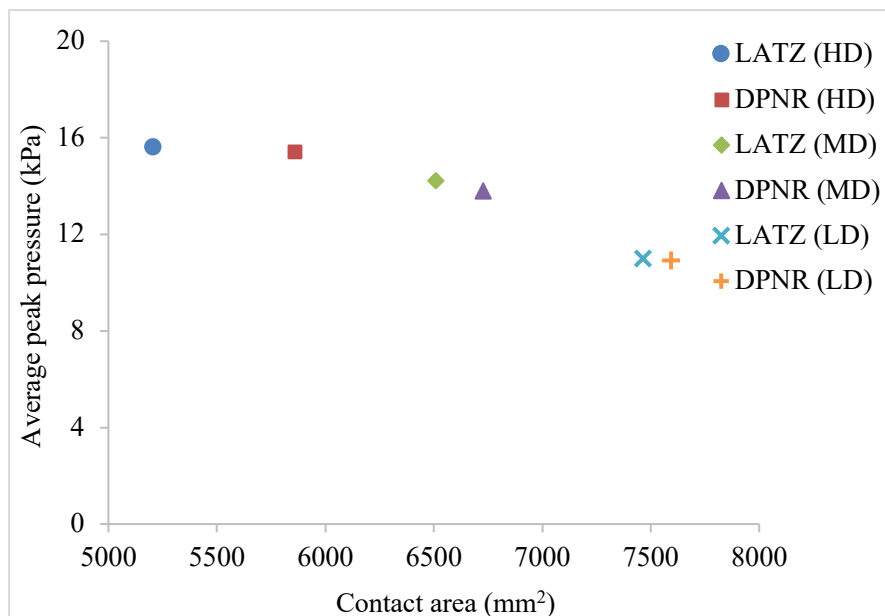



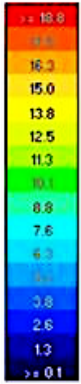
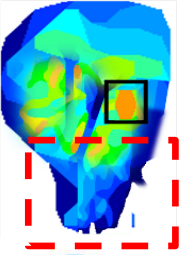
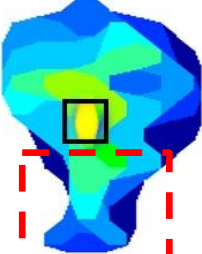

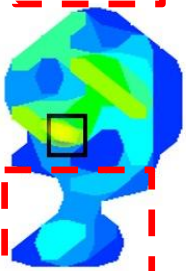
Figure 6.10: Relationship between surface contact area and average peak pressure value.

It can be seen in the graph that increasing the surface contact area decreases the average peak pressure value. Empirically, there is evidence linking material with higher surface contact area able to optimize interface pressure distribution, hence reducing the average peak pressure value. It is clear that LD pillows of both DPNR and LATZ latex foam produce the highest surface contact area followed by MD and HD pillows, and thus LD pillows exhibit the lowest average peak pressure value followed by MD and HD pillows. This is directly proportional to the hardness of the material whereas, LD pillows exhibit a low IH value. Therefore, it can be concluded that density

levels and hardness of both LATZ and DPNR latex foam play an important role in the capability of the material to improve the pressure-relief performance of the pillows.

The dependence of pressure-relief performance on surface contact area and average peak pressure of a pillow was investigated. Table 6.3 shows pressure-relief performance of normal-shaped and cervical-shaped pillows.

Table 6.3: Pressure-relief performance of cervical shape pillows

Type	Pressure distribution*	Surface contact area (mm ²)	Average peak pressure value (kPa)	Pressure scale
Normal-shaped DPNR latex foam pillow (MD)		6729	13.8	
Cervical-shaped DPNR latex foam pillow (MD)		7901	10.4	
Cervical-shaped DPNR latex foam pillow (MD+LD)		8681	9.2	
Cervical-shaped CNRL latex foam pillow (MD)		8064	10.2	
Cervical-shaped PM foam pillow (MD)		8549	9.3	

*Black square box located the average peak pressure; the red rectangular box indicates the region under the neck.

The cervical-shaped dual-density DPNR latex foam pillow exhibits the highest surface contact area followed by the cervical-shaped PM foam pillow, cervical-shaped DPNR (MD+LD) latex foam pillow, cervical-shaped CNRL latex foam pillow, cervical-shaped DPNR (MD) latex foam pillow and normal-shaped DPNR latex foam pillow. A clear increase of surface contact area at the region under the neck, shown as a red box in Figure 6.11, was observed. The results indicate that an increase in surface contact area at the region under the neck leads to a decrease in the average peak pressure value. This finding suggests that cervical-shaped pillows could provide a better neck support and pressure-relief performance compared to normal-shaped pillows. This is in agreement with previous studies^{13,60,61} where the ability of cervical-shaped pillows to contour the neck's natural curve has been shown to offer a better support to the cervical spine and restore cervical lordosis, and therefore, provide relief to neck and shoulder pain.

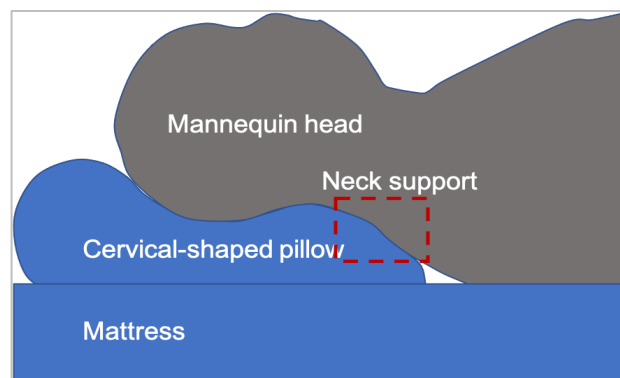


Figure 6.11: Modeling pillow conforming area under the neck.

Comparisons between the cervical-shaped dual-density DPNR pillow and the cervical-shaped single-density pillow indicate that the dual-density pillow exhibits a lower peak pressure value, indicating a better pressure-relief performance. The LD foam part at the upper part of the pillow is expected to provide extra comfort to users, and it is encouraging that the pillow exhibits the lowest average peak pressure value. On the other hand, the MD foam at the lower part of the pillow is expected to provide a firmer feeling and superior neck support. It should be noted that LD foam is soft, and thus, when the pillow is overloaded, the foam will be flattened (bottoming out), and thus will no longer be able to provide its important pressure distribution feature, something that has been observed before in some PM foam pillows^{172,174,175}. The bottoming out issue not only affects pressure-relief performance but also reduces its durability over time. Therefore, the combination of LD and MD foam, namely dual-density DPNR foam, is designed not only to offer a good pressure-relief performance but also to address the bottoming out issue, as well as to be more durable than single-density (LD) pillow. Comparisons between the cervical-shaped dual-density DPNR pillow with other pillows, indicate that the average peak pressure value of the dual-density cervical-shaped DPNR latex foam pillow is similar to that of the cervical-

shaped PM pillow. The excellent pressure-relief performance of PM foam pillows is expected due to its low hardness and has been observed elsewhere^{10–13}. This study has shown a cervical-shaped dual-density DPNR pillow is also capable to offer excellent pressure-relief performance as PM foam pillow do. It should be noted that dual density as well as multiple density foam combination approach has already been applied in mattresses^{187–189} to provide uniform and enhanced body support and extra comfort to users, but to the authors’ knowledge has not been applied to pillows. This present study attempts to provide some initial information, but due to the limitations of time and materials, there is no conclusive data to support the view that multiple density DPNR latex foam pillows could enhance the pressure-relief performance as well as increase uniformity and durability, something which should be the focal point of a future study.

6.3 Development of latex foam seat cushions

6.3.1 Production of DPNR latex foam seat cushions prototype

The compounding, foaming and gelling formulations used to produce DPNR latex foam seat cushions are similar to the one used for the production of DPNR latex foam pillows. For the transportation industry, a low-weight material for seat cushion is important to ensure effective energy consumption of the vehicle.

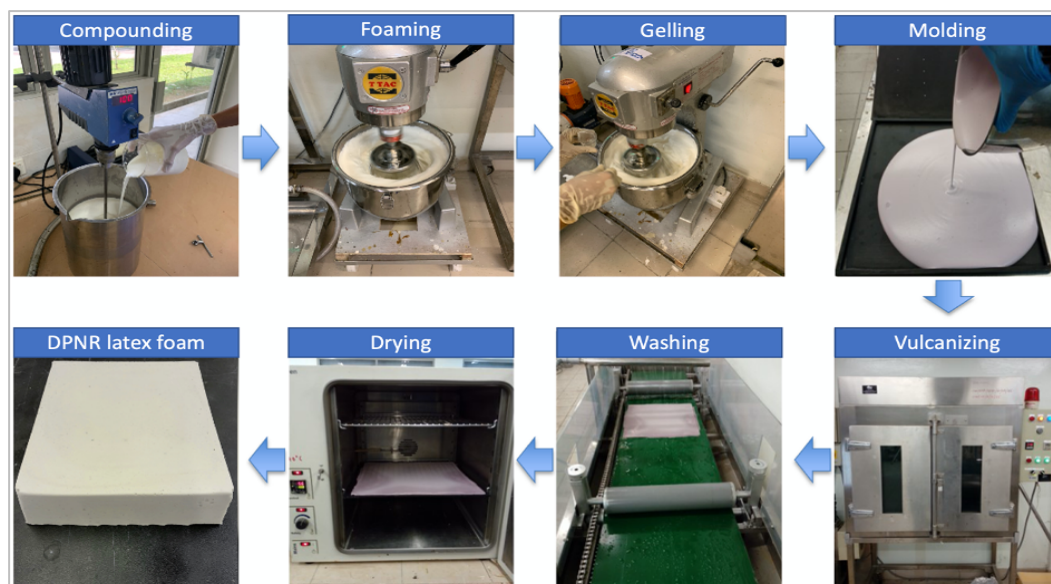


Figure 6.12: The different stages involved in the production of DPNR latex foam seat cushions.

Therefore, the wet density of DPNR latex foam was targeted at 0.09 g/cm^3 , to produce low-density DPNR latex foam seat cushions. Figure 6.12 shows the steps involved in the production of the DPNR latex foam seat cushions. The production process is also similar to the DPNR latex foam pillows, but the shape of the mold is different. In this part a square mold of $500 \text{ mm} \times 500 \text{ mm} \times$

40 mm (length × width × thickness) was used. This also suggested that DPNR latex foam can be used to produce many other foam products through similar a formulation and manufacturing process. The only change that requires is the mold. The mold used in the manufacturing process should be in the shape of the intended foam products.

6.3.2 Properties of DPNR latex foam seat cushions

This section evaluates the performance of the DPNR (LD) latex foam as seat cushions for the transportation industry. In order to gain a better understanding on the feasibility of DPNR (LD) latex foam as an alternative foam material for seat cushions, the properties of the material were compared to those of commercially available foams, such as polyurethane foam (PU) and polyurethane memory foam (PM).

6.3.2.1 Density, hardness and morphological characteristics

The morphological structure of DPNR (LD) latex foam, PU foam, and PM foam at ×70 magnification is shown in Figure 6.13. Each foam is a structured open-cell foam, interconnected by struts. However, each foam demonstrates different characteristics of the foam cell. The pores of the DPNR (LD) latex foam are elliptical with a size of less than 300 microns. PM foam appears to have elongated-shaped pores that are less circular than those observed in DPNR (LD) latex foam. On the other hand, PU foam has a foam-cell structure of springy coils. It can be seen in the SEM images that PM foam has a thicker cell wall thickness compared to DPNR (LD) latex foam and then PU foam. Table 6.4 shows the average cell wall thickness of each foam. The thickest cell wall is observed in PM foam, followed DPNR latex foam, and finally PU foam.

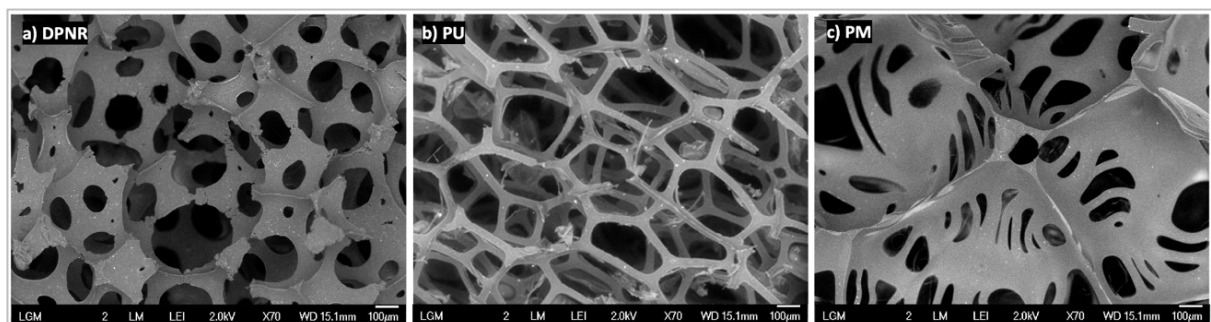


Figure 6.13. Morphological structures of DPNR latex foam, PU foam, and PM foam.

Table 6.4: Density and Shore F hardness of the foam sample

Parameter	DPNR	PU	PM
Cell wall thickness (µm)	84.99 (36.10)	33.26 (9.43)	151.86 (99.55)
Dry density (g/cm ³)	0.064 (0.006)	0.040 (0.004)	0.080 (0.004)
Shore F hardness	25.7 (0.96)	34.2 (0.85)	17.1 (0.32)

Average of three replicates. Values in brackets represent the standard deviation.

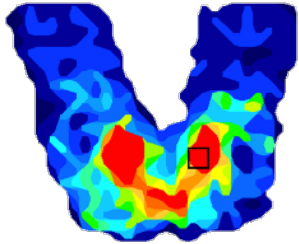
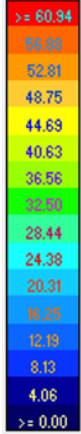
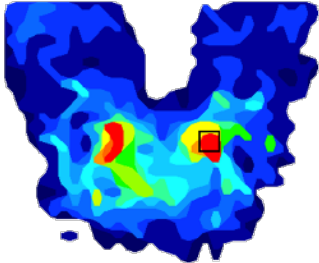
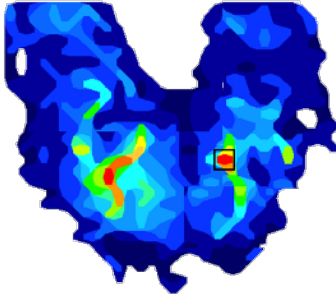
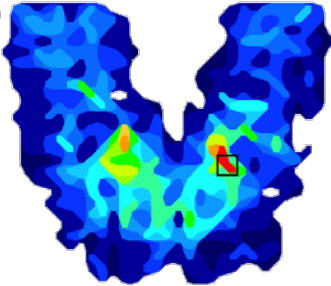
Table 6.4 also shows the density and Shore F hardness of DPNR (LD) latex foam, PU foam, and PM foam. The highest density is found in PM foam, followed by DPNR (LD) latex foam and then PU foam. It should be noted that polymer foams are complex composites consisting of an air phase and a solid phase. Because the density of the polymer foams is influenced by the proportion of the solid phase rather than the air phase, this study suggests that the higher the cell wall thickness of the foam, the higher the density of the foam material. Although PU foam has the lowest density and the thinnest cell walls, this foam has the highest hardness value. This is because PU foam is rigid, whilst PM foam and DPNR (LD) latex foam are viscoelastic materials. Rigid material is often harder than viscoelastic material. Generally, the hardness of the material depends on the formulation used and the intrinsic property of the material, such as the crystallinity and cross-link networks of polymer chains¹⁹⁰.

6.3.2.2 Pressure-relief performance

Table 6.5 shows snapshots of real-time measurements of pressure distribution, surface contact area, and average peak pressure values of PU foam, PM foam, and DPNR (LD) latex foam seat cushions when a mannequin was seated on the top of the seat cushions. Irregular color intensities and contours of the posterior area of the mannequin were observed in each type of seat cushion. This indicates dissimilar physical responses of the seat cushions to the loading of the mannequin. It is clear that without a seat cushion, the average peak pressure value is high compared to the use of seat cushions. A black square box locating the peak pressure area was observed in the middle of the posterior of the mannequin. According to studies^{37,61,186,191}, the stress point (peak pressure area) is the area where humans feel pain during sitting, especially due to long-distance travel. It is important to relieve pressure at the stress points in the posterior area to prevent the development of pressure ulcers. This is due to the fact that continuous pressure or compression on skin tissues, especially at stress points in the posterior area, leads to endothelial damage to the arterioles, followed by necrosis of skin structures. Optimizing the pressure distributions at the interface area between the seat system and the posterior area by using seat cushions is common practice in the transportation industry. Table 6.5 indicates that the use of PU foam as the seat cushion reduces the average peak pressure value by more than half the average peak pressure value without cushions. On the other hand, when PM foam or DPNR (LD) latex foam is used, the average peak pressure value is reduced by more than two-thirds of the average peak pressure value without cushions. This indicates that PM foam and DPNR (LD) latex foam exhibit higher pressure relief performance than PU foam. This could be due to the softness of the materials, which allows the foam to conform to the shape of the posterior, resulting in a larger interface (surface contact area) between the seat and the posterior area, thus reducing the peak pressure at the stress points. The

dependence of the average peak pressure value on the surface contact area is observed in Table 4, while the higher the surface contact area, the lower the average peak pressure value. This finding also suggests that the developed DPNR (LD) latex foam has excellent pressure relief performance similar to that of PM foam, making it suitable for seat cushion applications in the transportation industry.

Table 6.5: Pressure-relief performance of seat cushions

Type	Pressure distribution*	Surface contact area (mm ²)	Average peak pressure value (kPa)	Pressure scale
Without foam		86596	238	
PU foam		106563	96	
PM foam		114376	66	
DPNR (LD) latex foam		114159	68	

*The black square box locates the average peak pressure value. The area with a pressure higher than 60.94 kPa appeared in red.

6.3.2.3 Vibration transmissibility study

Figure 6.14 shows the vibration transmissibility of DPNR (LD) latex foam, PU foam, and PM foam. The transmissibility of vibrations was plotted as a function of frequency. The vibration transmissibility characteristics of the foams were studied through the resonance peak, resonance frequency, and attenuation frequency. Two regions were identified: the amplification region, where the value of the vibration transmissibility response is greater than one, and the isolation region, where the vibration transmissibility response is less than one¹⁹². Table 6.6 shows the resonance peak value, resonance frequency value, and attenuation frequency value of the foam materials examined in this study. According to Chan *et al.*¹³⁶, the resonance peak corresponds to the vibration-damping property of the material, while the lower the resonance peak, the higher the vibration-damping property. Table 6.6 indicates that PM foam has the lowest resonance peak compared to DPNR (LD) latex foam and PU foam.

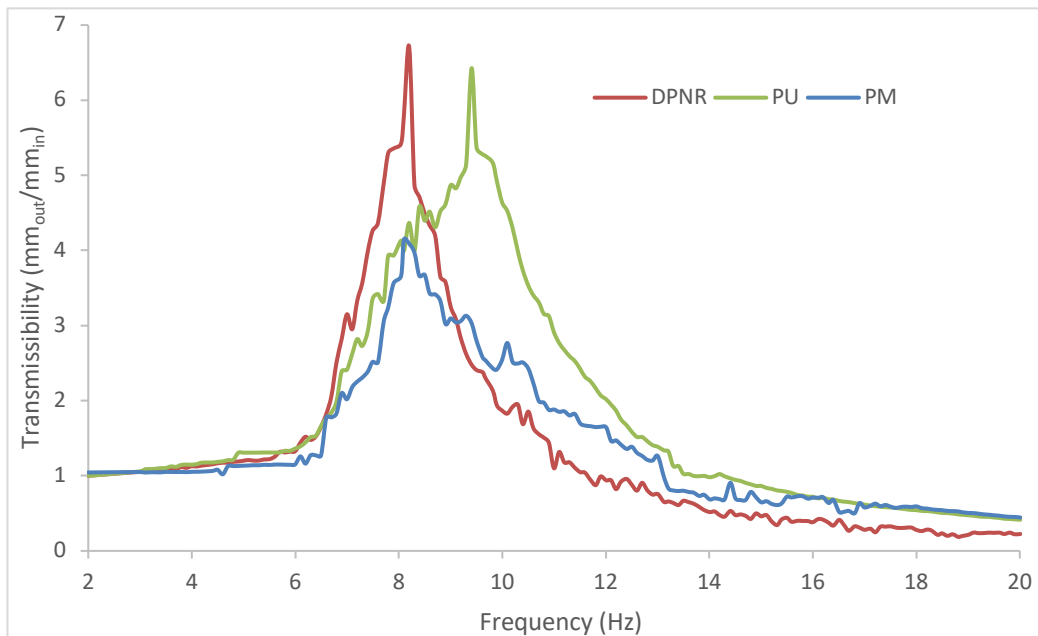


Figure 6.14: Vibration transmissibility of DPNR (LD) latex foam, PU foam, and PM foam.

Table 6.6 also indicates that PU foam has the highest resonance frequency compared to PM foam and DPNR (LD) latex foam. Previous studies^{136,193,194} stated that the harder the material, the higher the resonance frequency. This is in correlation with the results shown in Table 6.4, which found that the PU foam has the highest Shore F hardness value. The results indicate that PM foam exhibits a better damping property compared to PU foam in the amplification region. The excellent damping property of PM foam could be due to its viscoelastic properties and higher density of PM foam than that of PU foam. It should be noted that PM foam was designed by NASA in the 1960s to serve as an impact absorber for their astronauts¹⁶. Due to its unique viscoelastic behavior that enables the absorption of impact, PM foam is now used in a wide variety of foam products,

including seat cushions for luxury vehicles. The comparison between PM foam and PU foam is somewhat straightforward because both materials are made from polyurethane.

Table 6.6: Vibration transmissibility characteristics of foam samples

Type of material	Resonance peak (mm _{out} /mm _{in})	Resonance frequency (Hz)	Attenuation frequency (Hz)
DPNR (LD) latex foam	6.71	8.20	11.70
PU foam	6.42	9.30	13.70
PM foam	4.14	8.05	13.10

On the other hand, the comparison between PM foam, PU foam and DPNR (LD) latex foam is merely complex because DPNR (LD) latex foam is made of rubber. It is well-known that rubber is a highly elastic material, and thus exhibits a different response to vibration. Although the DPNR (LD) latex foam has a higher density than the PU foam, the material exhibits a higher resonance peak. As shown in Table 6.4, DPNR (LD) latex foam is harder than PM foam. Therefore, the resonance frequency of the DPNR latex foam is expected to be higher than that of the PM foam. However, the results show that there are not many differences in resonance frequency between DPNR (LD) latex foam and PM foam. Table 6.6 also shows that DPNR (LD) latex foam has the lowest attenuation frequency, which could be related to the material's low stiffness and high resilience properties. Starting at a frequency 9.50 Hz, DPNR (LD) latex foam exhibits lower resonance than the other two foams and reaches vibration isolation at a frequency 11.70 Hz, lower than PM foam. Previous studies^{85,195} stated that vibrations of frequencies above 12 Hz led to a health effect on particular parts of the human body (e.g., legs, arms, shoulders, head). Research findings in this chapter suggested that DPNR (LD) latex foam exhibits a better damping property compared to PU and PM foams in the isolation region, thus an ideal foam material for seat cushions that require isolation of higher frequency vibrations. Various types of vehicles, including motorcycles, high-speed crafts, trains, and trucks, are very often subjected to high-frequency vibrations¹⁹⁶. Therefore, DPNR (LD) latex foam could be the alternative foam material for seat cushions in such vehicles.

6.3.2.4 Compressive stress-strain behavior

The cyclic compressive stress-strain responses of DPNR (LD) latex foam, PU foam, and PM foam are shown in Figure 6.15. To study the stress-strain behavior of the foams, the first and third cycle loading and unloading curves were plotted. The gap between the loading and unloading curves (hysteresis loop) indicates the ability of the foam to recover after being compressed¹⁹⁷. In this study, the third cycle was chosen because it was recommended as the most stable curve for the hysteresis loop research¹⁹⁸. The finding showed that the loading and unloading curves of each foam

are influenced by the mechanical properties of the material when subjected to compressive forces. Figure 6.15 shows that PM foam has the biggest gap between the loading and unloading curves, indicating that the recovery rate of PM foam is slower than that of PU foam and DPNR (LD) latex foam. According to previous research works^{197,199} during loading, the foam cell walls are bent and come into contact with specific friction and air escapes from the foam cell. During unloading, the air is sucked back into the foam cell. The recovery rate of the foam cell depends on the breathability of the porous cells and the relaxation behavior of the material. Previous studies^{2,200,201}, stated that the T_g of PM foam ranges from -10 to 20 ° C, while the T_g of PU foam and DPNR (LD) latex foam are -46 ° C and -70 ° C, respectively. The high T_g of PM foam restricted the mobility of the chain network. This resulted in slow air take-up and re-expansion to its original dimension during unloading; thus, a slow-recovery (memory) property was observed. Therefore, the PU and PM foams have larger hysteresis loops compared to DPNR (LD) latex foam. This also resulted in a significant loss of stress between the first and third cycles of loading curves in PU and PM foams.

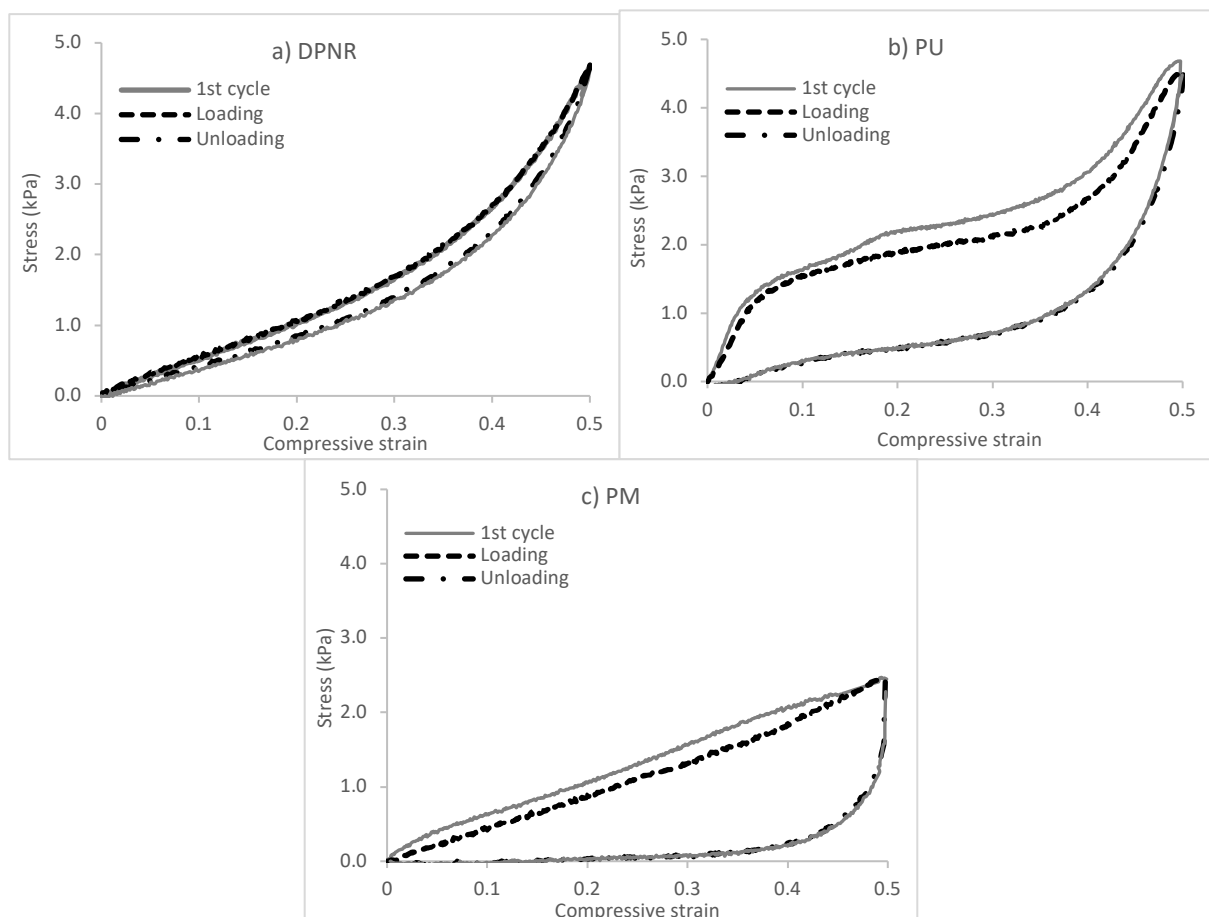


Figure 6.15: Loading-unloading curve of foam materials examined in this study. a) DPNR (LD) latex foam, b) PU foam, and c) PM foam. The solid line represents the first cycle, the dashed line represents the third cycle

On the other hand, DPNR (LD) latex foam exhibits the smallest hysteresis loop, and the low loss of stress gap between the first and third cycles could be related to the high resilience and low

stiffness property of the material. On the other hand, previous studies^{16,202,203} stated that the small hysteresis loop could also be related to the dimensional stability of the material against sagging or bottom out during in use, which implies that the DPNR (LD) latex foam can withstand high load pressures or heavy loads. This characteristic is important for cushioning applications. In addition to that, similar studies^{16,202,203} also suggested that the deformation characteristics of foam caused by compression may be correlated with the durability of the material, that is the lower the deformation, the longer the life span of the foam. Although in this study the durability test and dimensional stability study were not conducted, the results obtained from the compression test and review of the literature could be used to suggest that DPNR (LD) latex foam is suitable for heavy-duty industrial applications, e.g., seat cushions for the transportation industry.

It is well understood that in a hysteresis loop, the area under the loading curve is the total mechanical energy input while the area under the unloading curve is the return of stored energy and the area between the two curves is the dissipated energy that is converted to heat^{197,204}. The importance of the hysteresis study is that it provides a strong indicator of the ability of the material to absorb energy and/or relief pressure. The hysteresis loss ratio equation is given as follows:

$$Hlr = \frac{H}{E} \quad (6.1)$$

where Hlr is the hysteresis loss ratio, H is the amount of hysteresis (dissipated energy, given by the difference between the area under the uploading and the unloading curve) and E is the energy supplied during uploading (given by the area under the uploading curve). Figure 6.16 shows the hysteresis loss ratio of the foam materials examined in this study. It can be seen that PM foam exhibits the highest hysteresis loss ratio, followed by PU foam and DPNR (LD) latex foam. DPNR (LD) latex foam is a predominantly elastic material and thus able to store a high amount of energy due to deformation. On the other hand, it is well understood that PM foam is a viscoelastic material, which does not store energy under deformation^{56,205}. The energy will be dissipated as heat. This explained the low hysteresis loss ratio of DPNR (LD) latex foam compared to PM and PU foams. Furthermore, hysteresis loss is associated with the energy-consuming mechanisms of foam cell collapse and possibly by friction between the various structural elements of the collapsing foam cell²⁰³. Previous studies^{199,200} stated that during compression, the foam cell network produces a resilient force. The resilient force depends on the reverse effect, namely the relaxation effect, the pneumatic effect, and the adhesive effect. The relaxation effect is the mobility of the chain network that is related to the T_g value and intrinsic elasticity of the material. The pneumatic effect depends on the morphological characteristics of the foam material, typically porosity. On the other hand, the adhesive effect is the force between the struts and the foam structure that causes friction. This

suggested that the hysteresis loss ratio of each foam examined in this study is very dependent on the behavior of the viscoelasticity and the morphological structure.

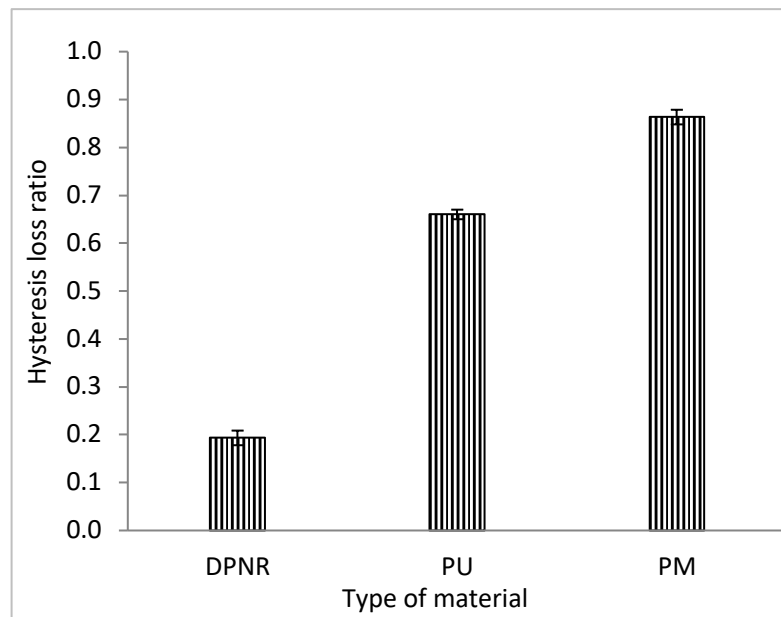


Figure 6.16: Hysteresis loss ratio of DPNR latex foam, PU foam, and PM foam.

6.3.2.5 Ball-rebound resilience properties

Figure 6.17 shows the percentage of rebound height after the ball was dropped onto the surface of the foam materials. DPNR (LD) latex foam exhibits the highest degree of bounce, followed by PU foam and PM foam. This indicated that DPNR (LD) latex foam exhibits the highest resilience property in which the foam material pushes the ball back into the air with most of its energy obtained from potential energy from the height of the drop point, as well as the kinetic energy they gained from the fall. On the contrary, PM foam is a unique viscoelastic foam material designed by NASA in the 1960s as an impact absorber for their astronauts¹⁶. According to previous studies^{16,206}, PM foam has little upward pressure and less ability to bounce back the ball due to its slow recovery property. In fact, for the viscoelastic material, the mechanical energy/force from the ball was absorbed and dissipated as thermal energy. Therefore, PM foam was expected to show the lowest degree of bounce. On the other hand, PU is a normal polyurethane foam, and thus it is expected to exhibit a higher rebound height compared to PM. The result also indicated that the rebound height of the PU is lower than that of the DPNR latex foam. It should be noted that the lower the ball-rebound height indicates the higher capacity of the foam material to relief pressure. This study concluded that PM foam exhibits a higher capacity to absorb energy and relief pressure, followed by PU foam and DPNR (LD) latex foam. From the other point of view, the ball-rebound height is also proportional to the degree of resilience of the material. A previous study²⁰² revealed that the resilience property is correlated with the dimensional stability and durability properties, while a higher resilience is associated with the improved dimensional stability and durability of foam

materials. Therefore, DPNR (LD) latex foam is potentially more durable than PU foam and PM foam, which is an important feature in heavy-duty cushion applications such as automotive seats.

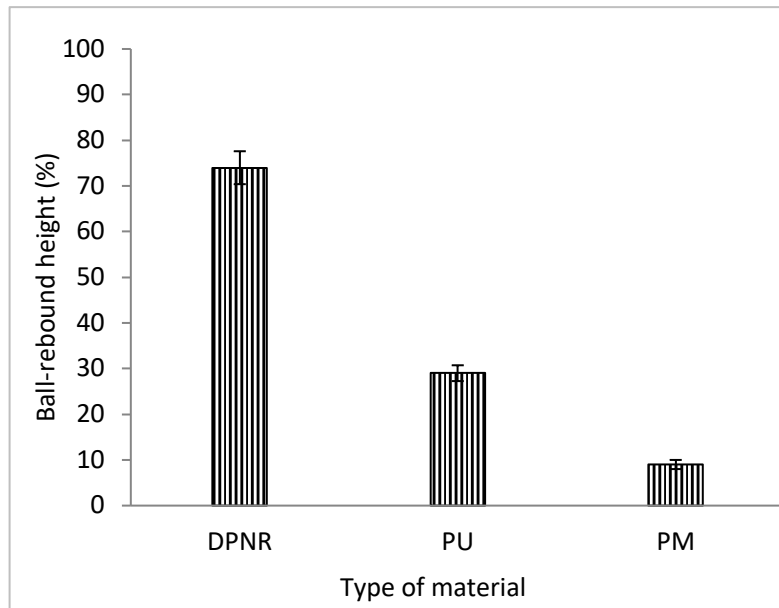


Figure 6.17: Percentage of rebound height of DPNR (LD) latex foam, PU foam, and PM foam.

6.4 Conclusion

This study has shown that DPNR latex can be used to produce hypoallergenic DPNR latex foam pillows and seat cushions without changing the existing latex foam products production technology. It was found that DPNR latex foam exhibits open-cell foam structures, and decreasing the density levels from HD to MD and to LD leads to an increase in the mean pore size of the DPNR latex foam. In the pillow study, the properties of DPNR latex foam were shown to be influenced by the density of the latex foam, where the lower the density the softer the latex foam. Also, there is a correlation between density levels and aging effects, where decreasing the density levels increases the effect of accelerated aging. This study also found that lower-density foams exhibit lower average peak pressure values when subjected to the loading of a mannequin head. There is an inter-relationship between surface contact area and average peak pressure value where high surface contact area leads to lower average peak pressure values. It was also shown that the surface contact area of a cervical-shaped pillow is higher than that of a normal-shaped pillow. Thus, a cervical-shaped pillow is expected to offer better pressure-relief performance compared to a normal-shaped pillow. In the seat cushions study, DPNR (LD) latex foam exhibits high elasticity and support properties. It was observed that the DPNR (LD) latex foam has a peak pressure value comparable to those of the PM foam. This is due to the softness of the materials, which results in a high interface between the seat and the posterior area of the mannequin, thus

lowering the peak pressure at the stress point. This study also found that DPNR (LD) latex foam has the lowest attenuation frequency, resulting in greater vibration isolation compared to PU foam and PM foam. This could be related to the material's low stiffness and high resilience. DPNR (LD) latex foam maintains excellent bounce-back and load-distribution features. DPNR (LD) latex foam has the lowest hysteresis loss ratio, followed by PU foam and PM foam. The advantage of DPNR (LD) latex foam over PU and PM is that DPNR (LD) latex foam is softer than PU but has a better return-to-form than PM, which is beneficial for seat cushions in the transportation industry. The ball-rebound test indicates that DPNR (LD) latex foam has a higher resilience property compared to PU foam and PM foam, thus DPNR (LD) latex foam is suitable for padding applications. It can be concluded that DPNR (LD) latex foam has both excellent pressure-relief and vibration-isolation performance, suitable for seat cushions intended for the transportation industry that require isolation of higher frequency vibrations such as high-speed crafts, trains, and trucks.

Chapter 7

Specialty natural rubber latex foam for sound and vibration controls

7.1 Introduction

Noise and vibration pollution generated from many mechanical systems, including industrial machines, transportation, construction, home appliances, etc., has a negative effect on human health^{207,208}. According to Groothoff²⁰⁹, noise and vibration are often considered as one and the same discipline because they are both analyzed as a wave phenomenon, whereas noise is defined as sound waves propagating through the air, whilst vibrations travel through the solid material also in the form of waves. Previous studies^{98,210,211} have shown that long-term exposure to noise pollution can result in hearing loss, psychological stress and mental fatigue. These adverse health effects can lead to workplace accidents and injuries. The adverse effect of exposure to vibration can range from muscular-skeletal pain disorders to harmful effects to the functions of the organs and body system, and subsequently, reduced work performance⁸⁵.

The evolution in structural engineering studies has resulted in a particular interest in the development of foam materials for sound and vibration controls for the building and transportation industry. Previous studies^{1,85} revealed that foam materials work in three mechanisms: absorbing, insulating and damping. A noise absorbing foam material is essential to control sound propagation within a closed room. On the other hand, the noise insulating foam material is essential to prevent sound transmission from outside to the room, as well as from a room emitted to the surrounding environment. If wave energy propagates from a source of vibrations that transmit through the solid material, then vibration-damping foam material is required²¹².

In Chapter 5, SpNR latex foam has been successfully developed, whilst Chapter 6 revealed that SpNR latex foam has an open-cell foam structure. The latex foam also exhibits excellent physical properties and low volatile organic compounds. Such properties are beneficial for sound and vibration control applications, to minimize noise propagation in a closed room as well as to dampen vibration transmission from one area to the adjacent area. Therefore, this chapter investigates the possibility of diversifying the application of SpNR latex foam into sound and

vibration control applications, typically for building and the transportation industry. The effect of density, hardness and morphological structure of the foam material on sound and vibration transmissibility becomes focal points. In this study, a PM foam with a density of 0.08 g/cm³ that is normally used as acoustic foam, supplied by Goodfoam Sdn. Bhd., Malaysia was used as a benchmark to evaluate the acoustic performance of the latex foams.

7.2 Development of acoustic foam material from SpNR latex

7.2.1 Fabrication of SpNR latex foam for acoustic foam applications

The formulations and manufacturing process to produce SpNR latex foam for acoustic foam application is similar to Section 5.2. Generally, to produce HD, MD, and LD latex foams, approximately 800 g, 600 g, and 450 g of compounded SpNR latex were whipped using Kenwood mixer until it reached the desired volume marked on the bowl, fixed at 5 L. However, as indicated in Chapter 5, for ENR latex foam, the ENR(LD) latex foam collapses after the vulcanization process. Therefore, in this section, only ENR (HD) and ENR (MD) latex foams were produced. On the other hand, for DPNR latex foam, the DPNR latex foam was produced at HD, MD and LD latex foams. Similar to the fabrication process demonstrated in Chapter 5, after the latex foam reached the targeted density, the latex foam was poured into the mold. In this part, the latex foam was poured into 200 mm × 200 mm × 40 mm (length × width × thickness) square molds with different thickness: 10 mm, 20 mm, and 40 mm. Subsequently, the mold lid was closed and the latex foam was subjected to the vulcanization process in a hot air oven at 100 °C for 60 minutes. After the vulcanization process, the latex foam was peeled out of the mold, followed by a washing and drying process. All samples were kept dry at room temperature before testing.

7.2.2 Physical properties

Figure 7.1 shows that ENR exhibits the hardest foam material followed by LATZ and DPNR latex foams. This could be due to the presence of epoxy group in the rubber chains which increased the stiffness of the material. On the other hand, the lower indentation hardness value of DPNR latex foam compared to LATZ could be due to the removal of proteins in the latex system, which has been identified to act as filler that increases the stiffness of the latex foam^{149,158}. Figure 7.1 also shows that the indentation hardness value of the latex foams decreases in tandem with the density levels. The density of the latex foams has a substantial impact on the indentation hardness value, whereas the higher the density the harder the material. ENR (HD) is the hardest foam material,

which could be owing to the epoxy group's presence in the rubber chains. On the other hand, the lower indentation hardness value of DPNR latex foam compared to LATZ could be related to the elimination of proteins from the latex system, which has previously been indicated to act as fillers that increase the stiffness of the latex foam^{29,157,176}. PM on the other hand is a different class of material made from polyurethane that is specifically formulated to has low hardness properties.

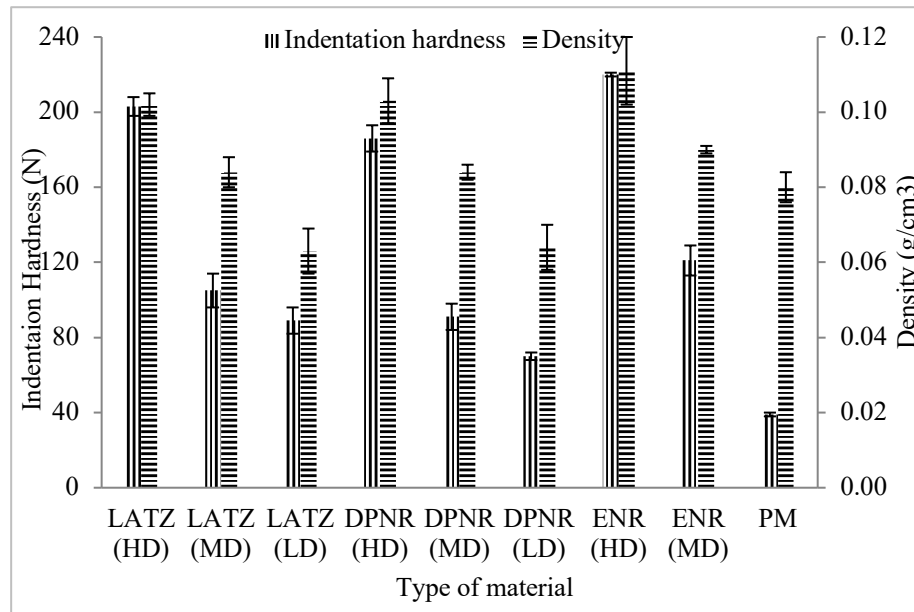


Figure 7.1: Indentation hardness and density of the foams.

Figure 7.2 shows SEMs of the morphological structures of the foam materials investigated in this study. Two regions were visualized under SEM, the top and bottom of the samples. Minor morphological differences can be observed between the top and bottom regions of the samples. PM foam exhibits a distinct foam cell structure compared to LATZ, DPNR, and ENR latex foam. The pores in PM foam appear to be elongated, while the pores in LATZ, DPNR, and ENR latex foam are more circular. The different morphological properties between PM and NR (LATZ, DPNR, ENR) are likely due to the different interplay between the rheology and surface tension during the foaming process. PM is produced through chemical reactions of two reactants; reactant A (polyols, chain extenders, blowing agents, gelling and blowing catalysts, surfactants, etc.) and reactant B (isocyanates), as raw materials²¹³. On the other hand, NR latex foam is produced through mechanical agitation, where the compounded NR latex is whipped in a Kenwood mixer where the stirrer rotates in a planetary motion at high speed to entrap air into the NR latex compound. The different morphological structures of the foam materials, in particular between the NR foams and the PM foams, are expected to show different acoustic performance. Previous studies^{1,214,215} have explored how morphological characteristics such as pore size and the percentage of pores

(porosity) have their own significant absorbing impact at low and high frequencies. In this study, ImageJ software was used to measure the pore size, pore area and porosity.

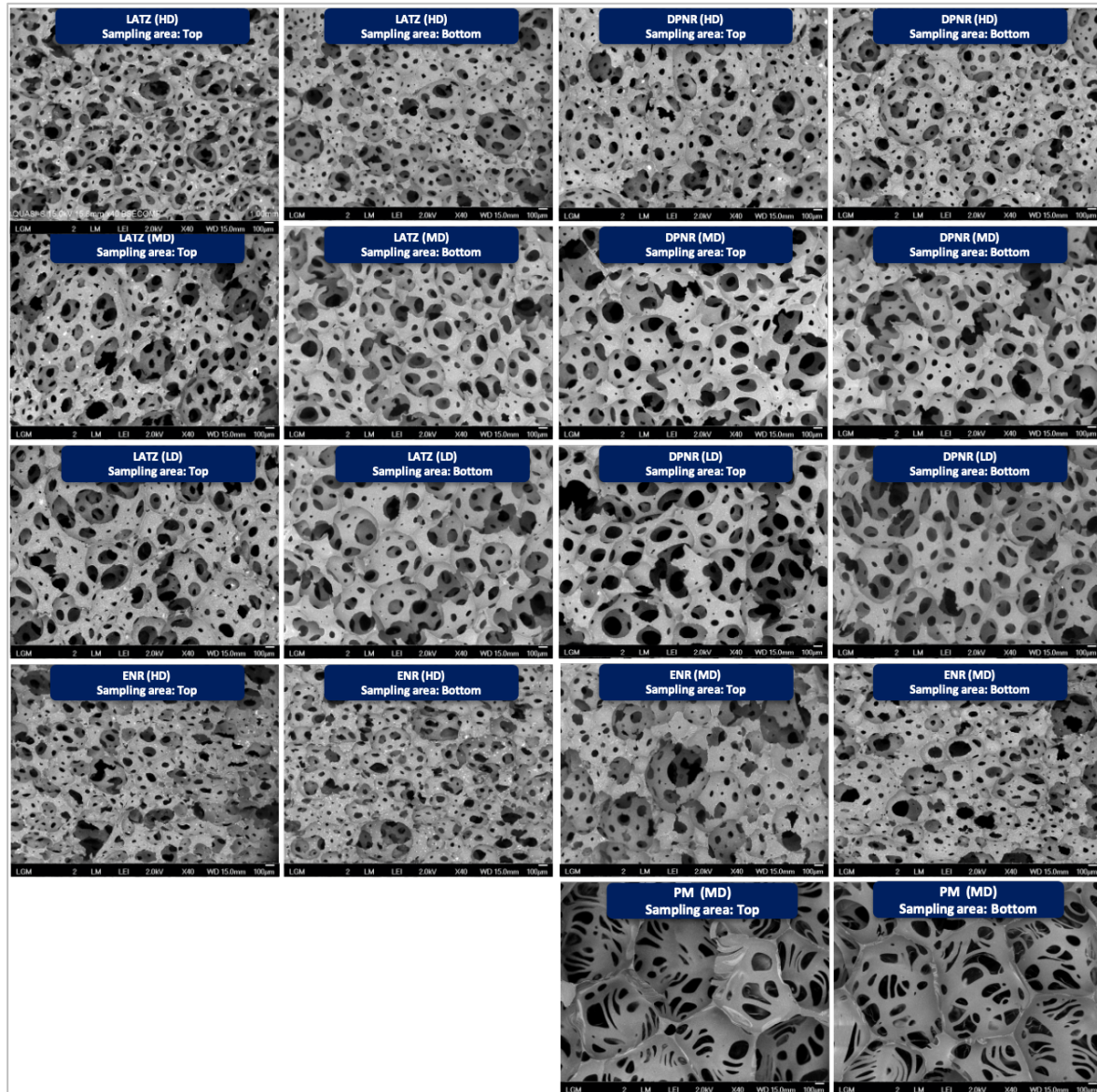


Figure 7.2: Morphological structures of foam materials examined in this study.

Figure 7.3 shows the average pore size of the foam materials examined in this study. It can be seen that LD foam has a larger average pore size compared to MD foam, followed by HD foam. This is expected because the lower the density, the higher the air phase to solid phase ratio of the material. The DPNR (LD) foam has the largest pore size, while the ENR (HD) foam has the smallest pore size. As mentioned above, PM foam has a density of 0.08 g/cm^3 , which is similar to that of DPNR (MD) foam and LATZ (MD) foam. In comparison with similar density levels, PM foam has the largest pore size, followed by DPNR (MD) foam and LATZ (MD) foam.

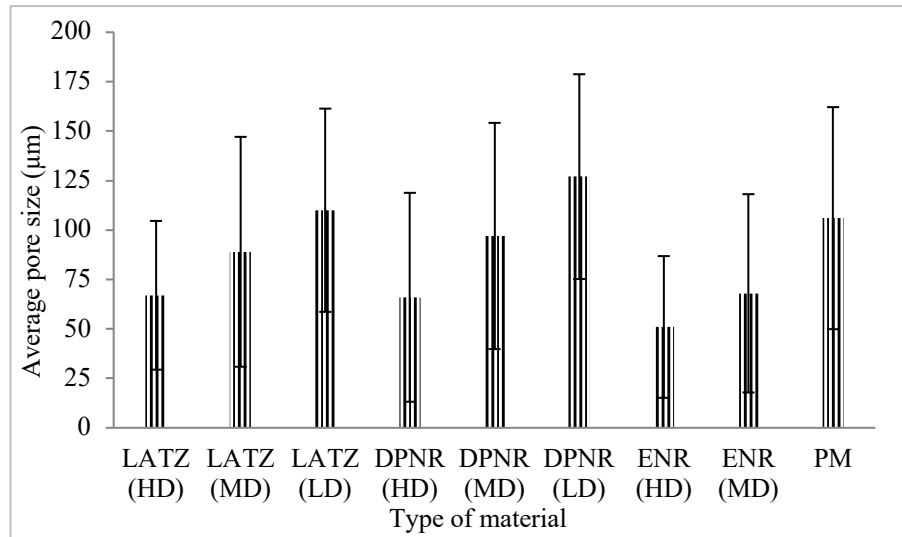


Figure 7.3: Average pore size of foam materials examined in this study.

On the other hand, Figure 7.4 reports the mean pore area and porosity of the latex foams. Mean pore area is the total pore area divided by the total number of pores. On the other hand, to calculate porosity, the total pore area is divided by the total area of the SEM image. As expected, the mean pore area increases as the density of the latex is reduced. The ENR (HD) latex foam had the smallest mean pore area, whereas the DPNR (LD) latex foam had the largest mean pore area. PM foam, on the other hand, has the largest mean pore area among medium-density foams. This suggests that PM foam has the fewest pores overall, but they are extremely large. Figure 7.4 also shows that low-density foams exhibit higher porosity compared to medium-density foams and high-density foams. The most porous material is DPNR (LD), which has a porosity of more than 50%. The least porosity is seen in ENR (HD) latex foam.

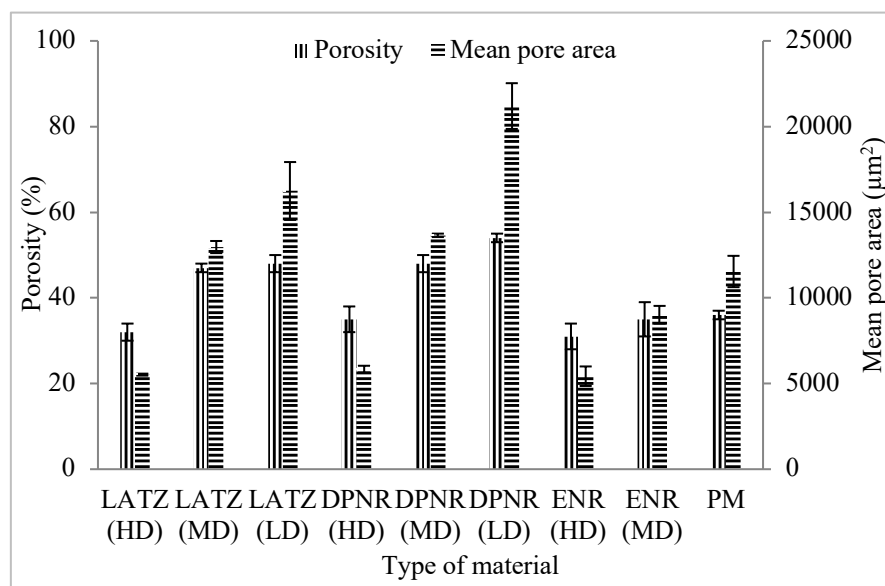


Figure 7.4: Mean pore area and porosity of foam materials examined in this study.

7.2.3 Acoustic properties of SpNR latex foam

7.2.3.1 Effect of density on acoustic properties

Measurements of STL as a function of frequency on latex foam samples with a thickness of 20 mm are shown in Figure 7.5 for the different densities of foam. In general, the STL curve increases with increasing frequency. In all cases, the HD foams show a higher STL value than the MD foams, followed by LD foams. The structure of voids and pores of the latex foams, which acts as the medium of transmissibility of sound wave energy, is one aspect that may cause the STL value of HD foam to be higher than MD and LD foam. It was observed that HD foam has a lower mean pore size than MD and LD foams. This could result in the material having a stronger resistance to sound wave transmissibility, resulting in a higher STL value. This is in line with earlier research,²¹⁶ which found that having a larger surface area per unit volume causes more energy loss due to friction.

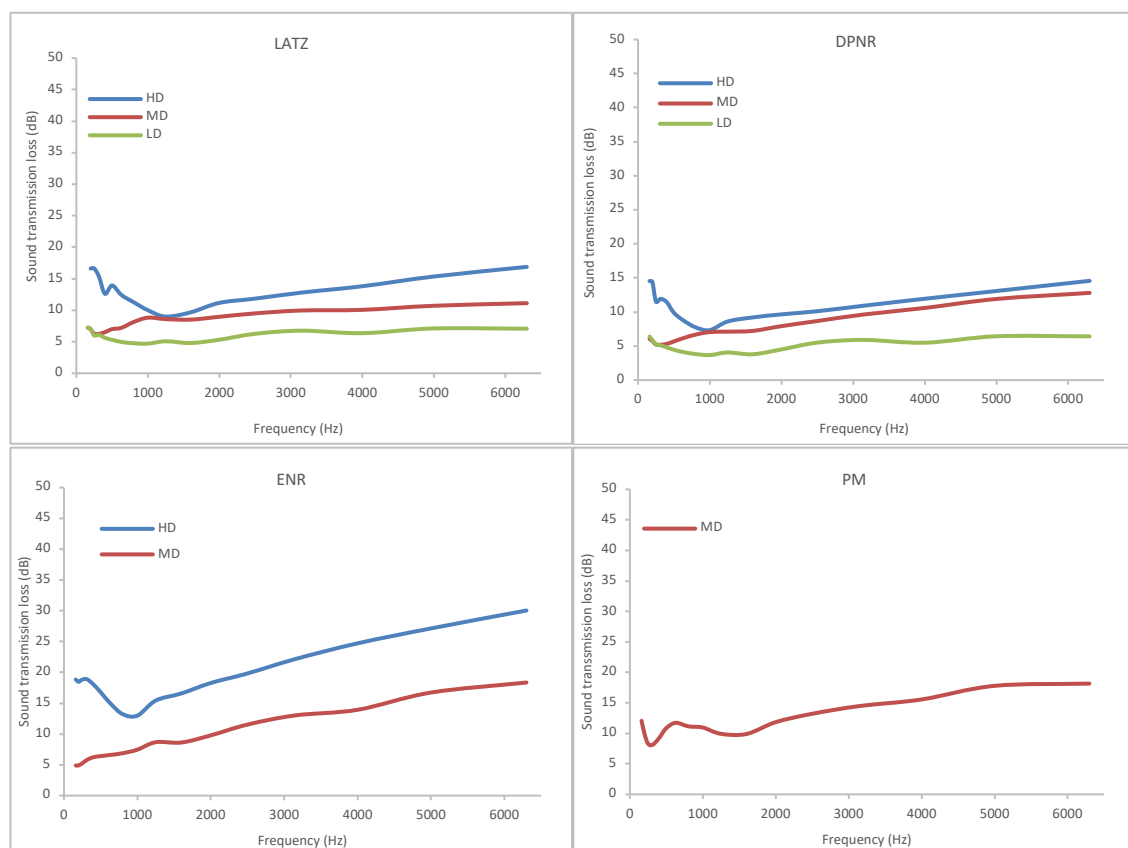


Figure 7.5: Measurements of STL as a function of frequency on 20 mm thick latex foam.

A comparison between ENR, DPNR and LATZ latex foams shows that the ENR foam exhibits the highest STL curve at every density level. This could be a unique property of ENR, possibly due to the inclusion of the epoxy group in the rubber chains boosting both the stiffness and the damping characteristics of the material³⁻⁵. PM foam is a viscoelastic polyurethane foam designed by NASA in the 1960s to serve as an impact absorber for their astronauts¹⁶. PM foam is now used

in a wide variety of products, including sound insulators. This study found that, at a similar density level (MD), PM foam exhibits a higher STL at all frequencies than LATZ and DPNR foams, but a comparable STL to ENR foam. Unfortunately, it was not possible to purchase HD PM foam from the factory to compare with ENR (HD) foam because PM is normally made as MD foam to save cost. As mentioned above, for sound insulation applications, the material should be able to reduce the noise by at least 10 dB. For building acoustic applications, a frequency range from 160 Hz to 3150 Hz is usually investigated as it covers the range from speech tones through to traffic noise²¹⁸. Figure 7.5 shows that the STL value of 20 mm ENR (HD) foam is higher than 10 dB throughout the frequency range, indicating that it meets the specifications for acoustic applications in buildings.

Figure 7.6 shows SAC measurements as a function of frequency on latex foam samples with a thickness of 20 mm for the different densities of foam. It reveals that, in the low-frequency range (160–1800 Hz), both LATZ (HD) and DPNR (HD) samples have higher SAC values than MD and LD samples. According to Chen *et al.*²¹⁵, acoustic resistance has a significant impact on SAC value in the low-frequency range. Low-frequency sound waves have longer wavelengths compared to high-frequency sound waves, making them more difficult to absorb. Therefore, increasing density levels of the latex foams might increase the material's acoustic resistance due to the mass increase, which is helpful in the absorption of low-frequency sound waves²¹⁵. The same study also suggested that the morphological structures of the foam materials influence the SAC performance. The results obtained in Figure 6 indicated that the mean pore size of HD foam is smaller than for MD and LD foams, and the smaller the pore size, the higher the acoustic resistance. This is consistent with a previous study²¹⁹, which found that densely packed foam cell structures increased the airflow resistivity, trapping and dissipating the sound waves within the foam cell structures. In the high-frequency range (> 1600 Hz), the SAC curve of both LATZ (HD) and DPNR (HD) decreased and then increased again. It is also noticeable that the SAC curve of HD foam tended to fluctuate as the frequency was increased. For MD foam, DPNR (MD) shows higher SAC values compared to LATZ (MD), ENR (MD) and PM foams. Additionally, the SAC value of DPNR (MD) was observed to be close to 1 at a frequency range from 3000 Hz to 4000 Hz; this is a critical range that leads to unpleasant sound levels and could cause hearing loss in humans if exposure is on a daily basis at high amplitudes²²⁰. The results also suggest that decreasing the density of the foams from HD foam to MD foam improved SAC performance at high frequencies. This is the reverse of what was observed in STL measurements. According to Zunaidi *et al.*,²¹⁶ at high frequencies the wavelengths are short and the diameter of the pores has limited effect. Setaki *et al.*⁹⁹ on the other hand, claimed that the macro-scale size of pores is generally effective at high

frequencies, allowing sound waves to propagate into the foams to dissipate more sound energy. In this study, as indicated in Figure 7.3, the lower the density, the larger the pore size. Although decreasing the density of the latex foam from HD to MD improved the SAC performance, further decreasing the density from MD foam to LD foam did not show further improvement, suggesting that this correlation may be limited to certain pore sizes and/or densities.

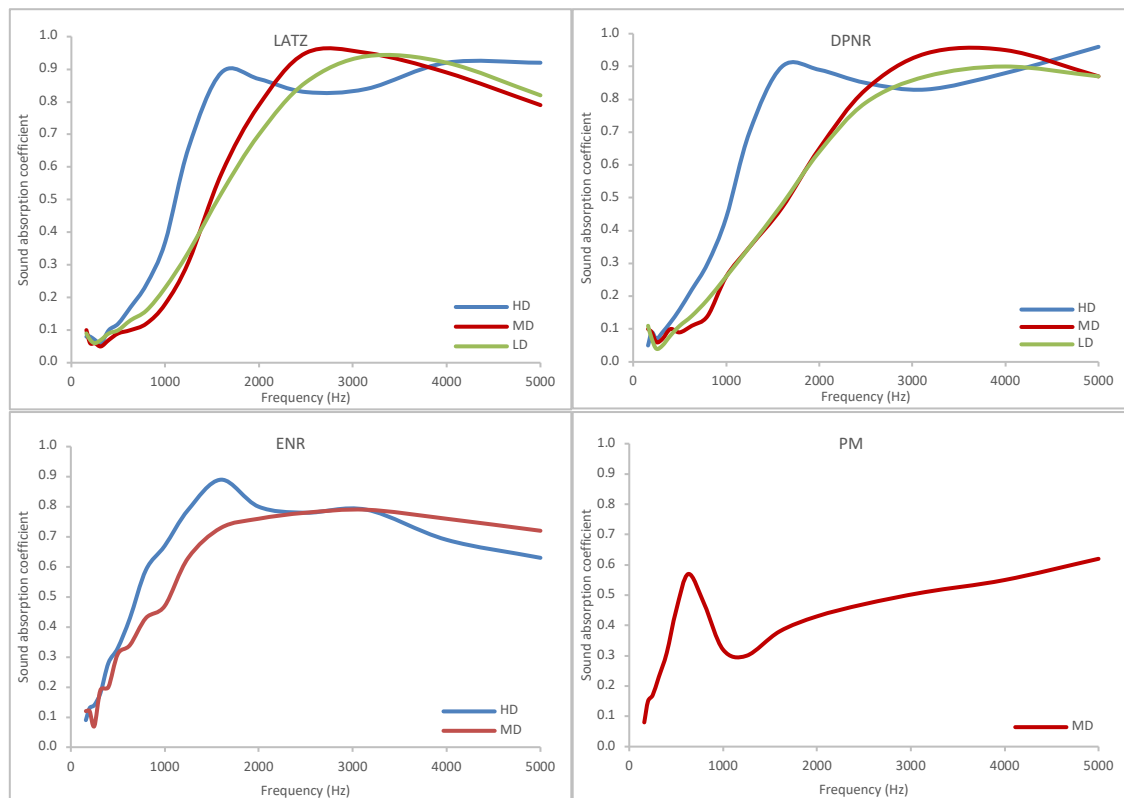


Figure 7.6: Measurements of SAC as a function of frequency on 20 mm thick latex foam.

The noise reduction coefficient (NRC) measurements reported in Table 7.1 are used to evaluate the foam materials' sound absorbing efficiency over a wide acoustic frequency range. An NRC of 0 represents perfect reflection, while an NRC of 1 shows perfect absorption²²¹. The NRC value drops as the density of LATZ and DPNR latex foams is reduced from HD to MD to LD. However, no difference in NRC value was observed when the density of the ENR latex foam was decreased from HD to MD. At similar MD levels, ENR latex foam exhibits a higher NRC value, followed by DPNR, LATZ latex foams, and finally PM foam. The NRC of LD foams of both LATZ and DPNR latex foam are comparable to those of the MD PM foam. It can be concluded that the density of the latex foam plays a vital role in absorbing sound wave propagation. HD foam has a higher STL value than MD and LD foams. HD foam shows a higher SAC value compared to MD and LD latex foams at a low frequency range. However, when it comes to the high frequency range, MD and LD foams show higher SAC values compared to HD foam. This relates

to the wavelength of the sound waves passing through the material²²². HD foam shows a higher NRC value than MD foam, and LD foam, across a wider acoustic frequency range.

Table 7.1: Noise reduction coefficient of 20 mm latex foams

Type of material	LATZ	DPNR	ENR	PM
HD	0.47	0.49	0.49	NA
MD	0.43	0.44	0.49	0.40
LD	0.40	0.39	NA	NA

NA = not available

7.2.3.2 Effect of thickness on acoustic properties

In this section, the effects of thickness levels on STL and SAC curves and NRC values were evaluated. Figures 7.7-7.9 show the effect of thickness levels on the STL curves of HD, MD, and LD foams, respectively. The results indicated that all types of foam materials showed an increase in STL when the sample thickness was increased from 10 mm to 20 mm and finally to 40 mm.

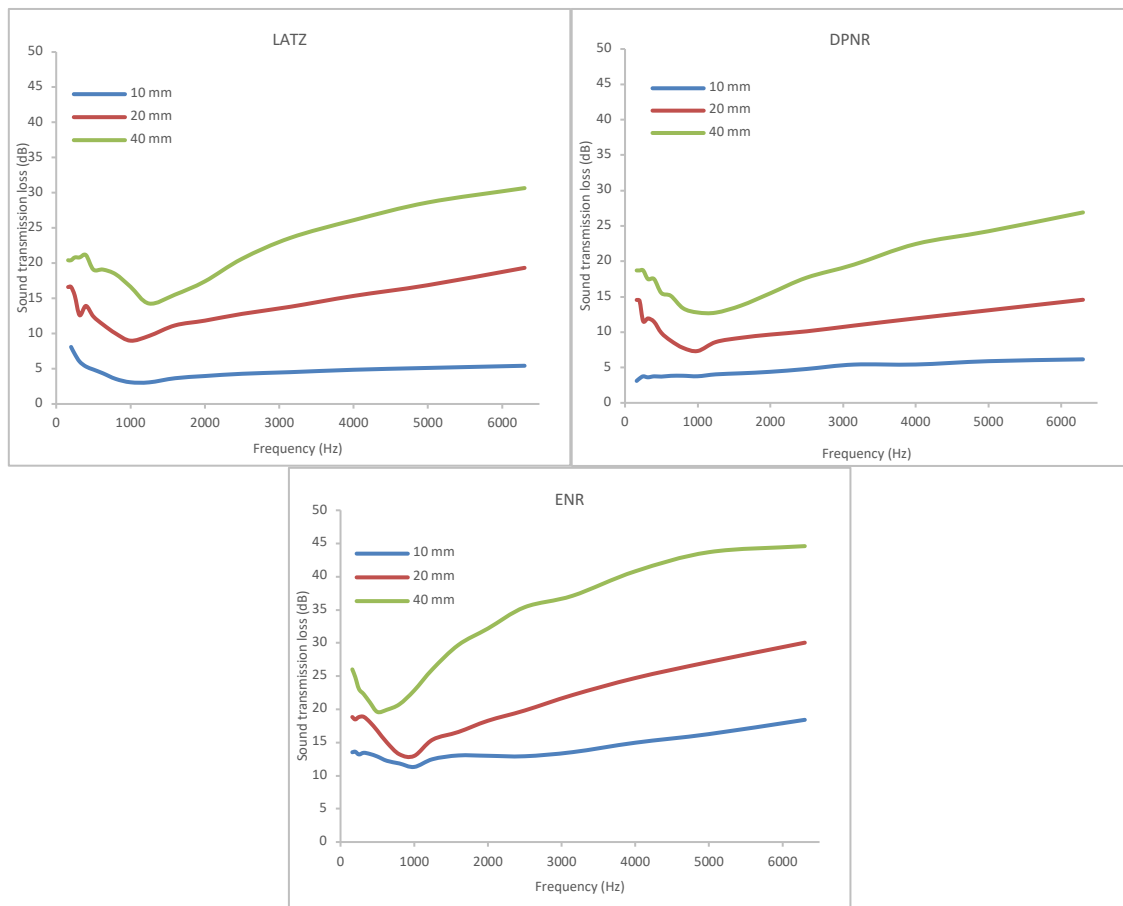


Figure 7.7: Effect of thickness levels on STL curve of HD foam.

This is in line with a previous study¹⁰⁶, which found that STL is related to material thickness and provides more bass sound absorption or damping. The reason for this is that the low-frequency wavelengths are long, meaning that the thicker materials have greater opportunities for sound absorption^{103,223}. Figure 7.7 shows that, for HD foam, the highest STL value was observed on ENR

HD latex foam with a 40 mm thickness, where the sample exhibits a loss of 44 dB at a frequency of 6300 Hz. However, Figure 10 shows that, for MD foam, PM exhibits the highest STL value. The increase in STL of PM when the thickness of the material was increased from 20 mm to 40 mm is quite pronounced, and thus could be a reason why many acoustic PM panels employed in the building and infrastructure industries are 40 mm in thickness. However, it should be noted that the use of thick material for noise control in some applications, such as automotive vehicle cabins, is not recommended because it will reduce the cabin's capacity. There could yet be advantages in selecting ENR (HD) latex foam over PM foam, as this type of material has an even greater STL for the same thickness. On the other hand, for LATZ and DPNR latex foam, it was quite surprising to see that both MD and LD foams demonstrated only moderate increases in STL curves with increasing thickness.

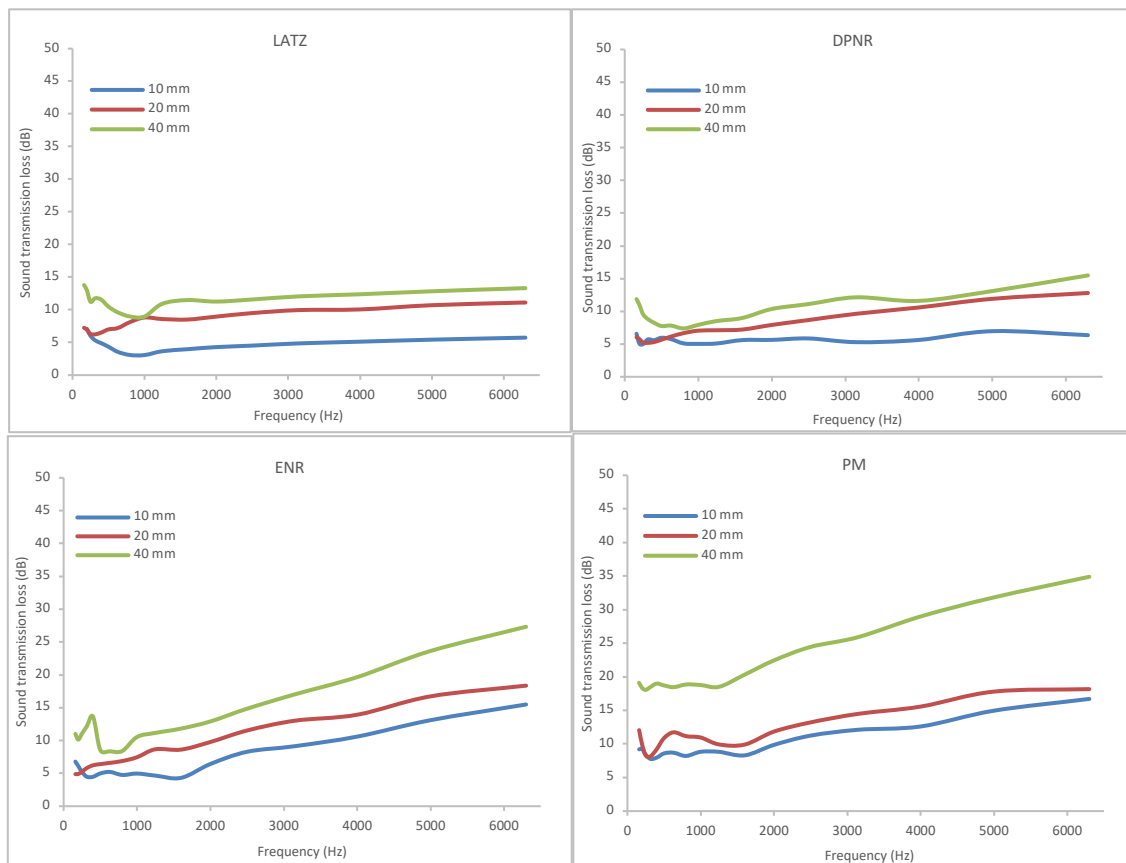


Figure 7.8: Effect of thickness levels on STL curve of MD foam.

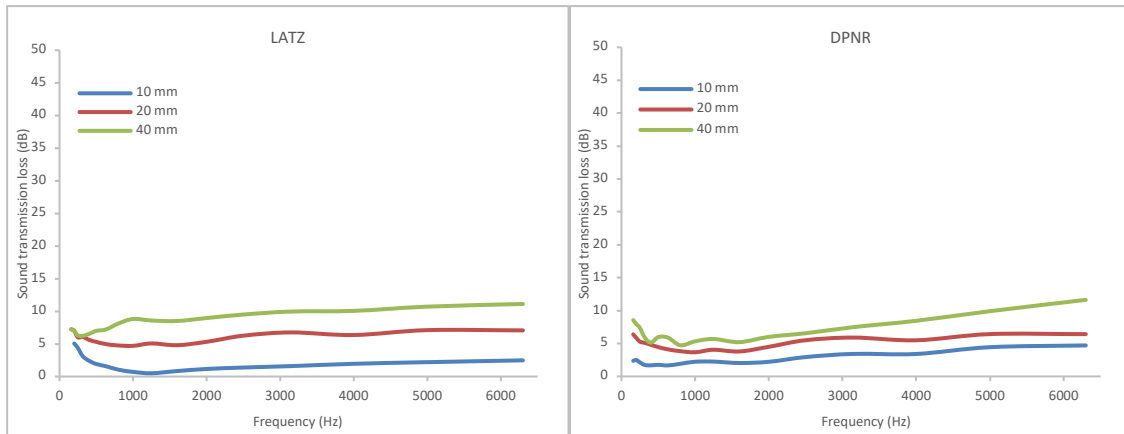


Figure 7.9: Effect of thickness levels on STL curve of LD foam.

Figures 7.10-7.12 show the effect of foam thickness levels on the SAC curves of HD, MD, and LD foams, respectively. It is apparent that increasing the thickness of the foam material from 10 mm to 20 mm to 40 mm broadens the frequency range with a high SAC value, starting at much lower frequencies. It can be observed that, for HD and MD foams that are fabricated at 40 mm, the SAC curves fluctuate as the frequency increases. The SAC curves initially show a gradual increase until they reach a maximum value, then decrease, before increasing again.

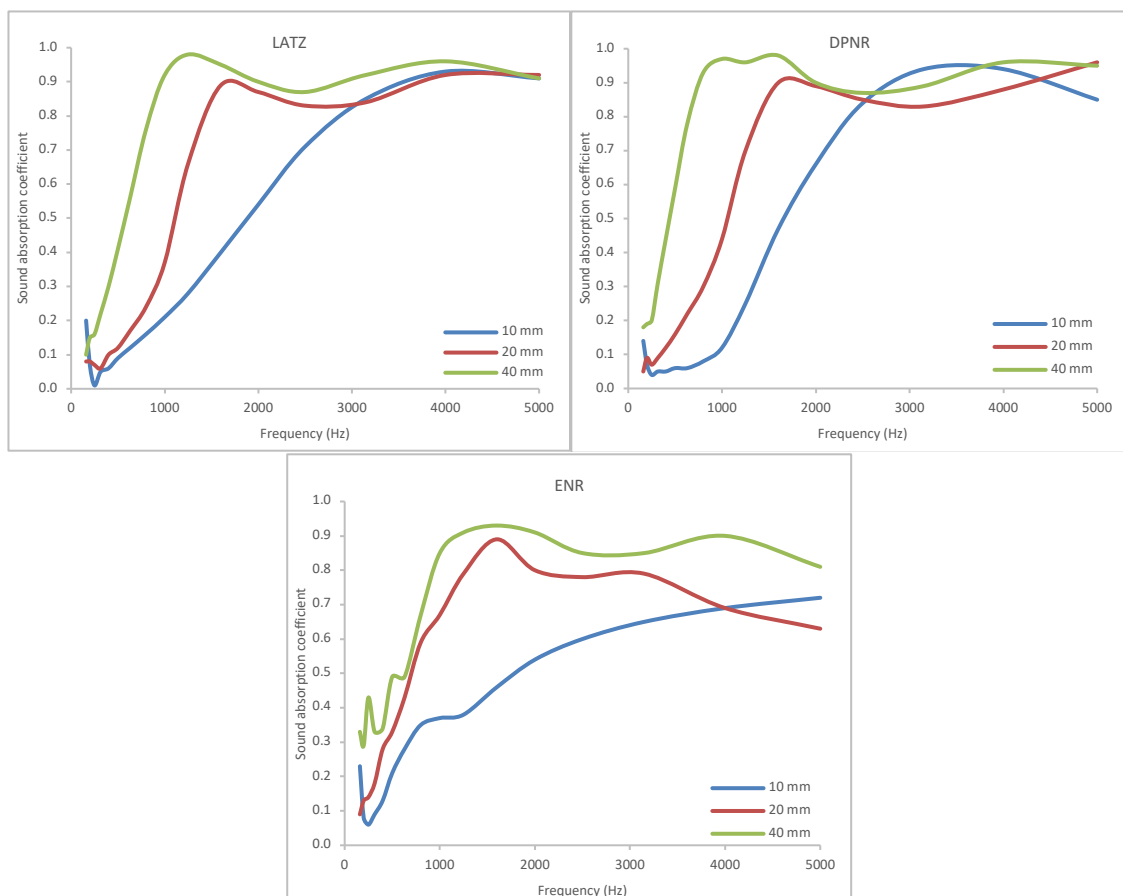


Figure 7.10: Effect of thickness levels on SAC curve of HD foam.

This behavior has been explained by Rienstra and Hirschberg²¹⁵ in terms of the closer match between the acoustic wavelengths and the thickness of the material. The study suggests that SAC value only has a direct relationship with the thickness of foam at low frequencies, but is less affected at high frequencies. At low-frequency range, the higher the thickness, the higher the SAC value. In the LD foam, there was a steady increase in the SAC curve from a low to high-frequency range in each level of thickness. This could be due to the specific morphological characteristics of the material itself in absorbing and reflecting sound wave energy. This is in agreement with previous studies,^{103,222,223} which found that a material's absorption coefficient is influenced not only by the thickness but also by the configuration of the morphological structure and the frequency of the sound wave that strikes the surface structure of the material.

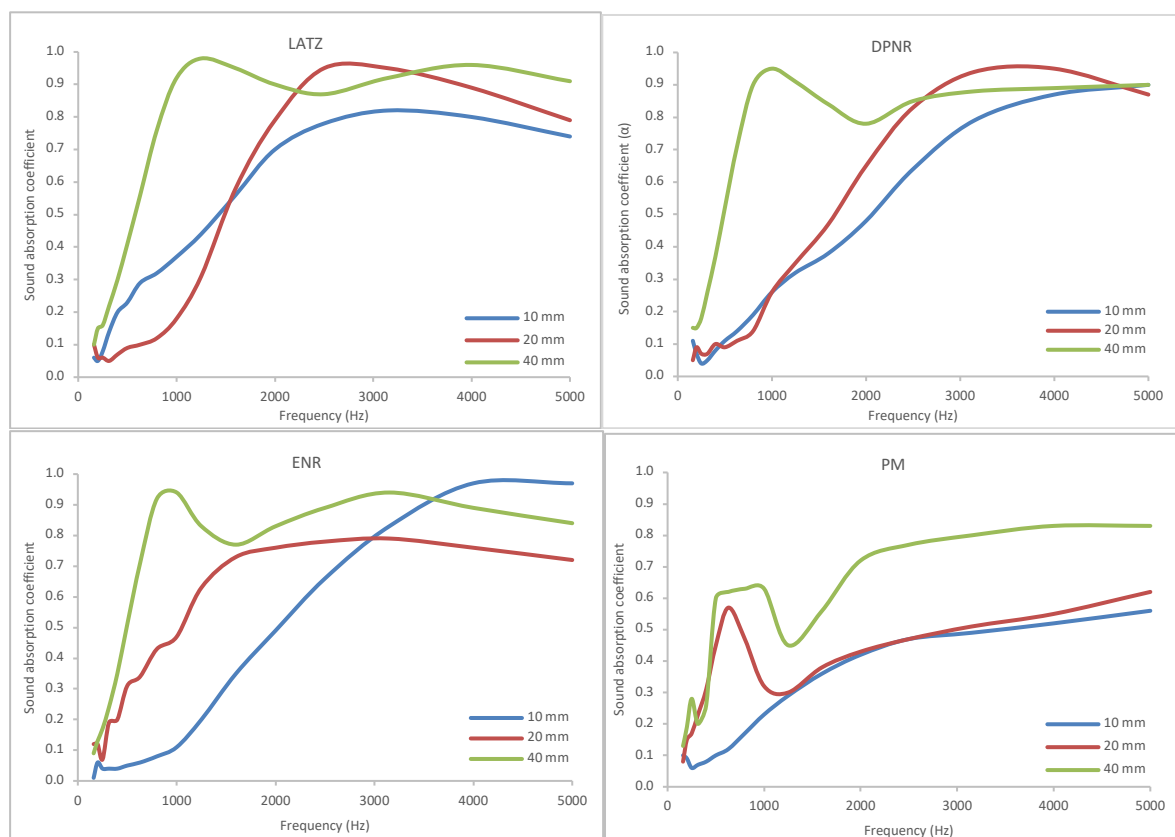


Figure 7.11: Effect of thickness levels on SAC curve of MD foam.

For HD foam, the SAC curve reached a maximum value (the 'peak absorption coefficient') at frequencies of 1200 Hz, 1600 Hz, and 1800 Hz for LATZ, DPNR, and ENR latex foam, respectively. Similarly, to HD foam, 40 mm of MD foam shows excellent absorbing capacity at low-frequency range, but then fluctuates somewhat as the frequency increases.

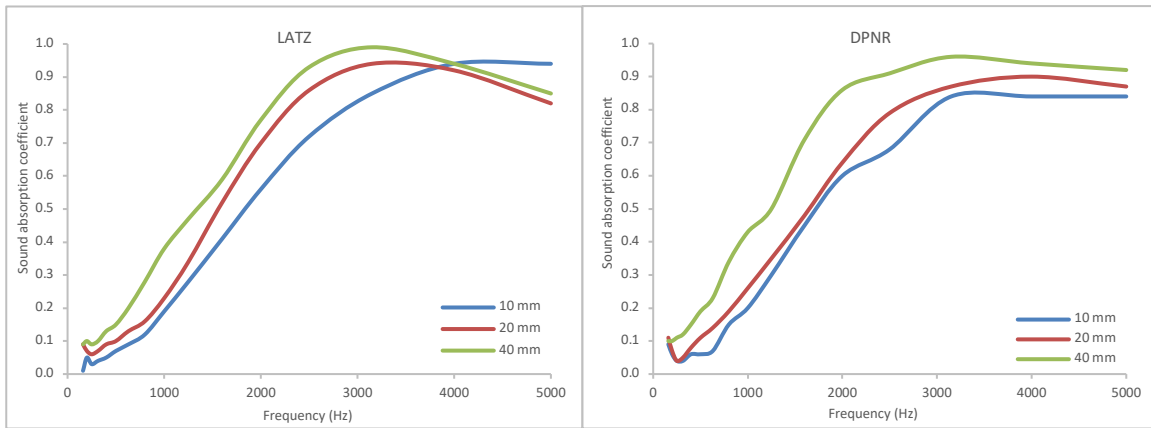


Figure 7.12: Effect of thickness levels on SAC curve of LD foam.

At a frequency between 160 Hz and 1250 Hz, the SAC curves of both LATZ (MD) and DPNR (MD) 40 mm thick latex foams steadily increased. However, beyond 1250 Hz, the SAC curves fluctuate between ~ 0.8 and 1. Nevertheless, foam material with a SAC value of 0.8 or higher is classified as a class A sound absorber.²¹⁶ On the other hand, the SAC curves of 10 mm samples of HD and MD foams are mostly steadily increasing and do not show this same fluctuation. In the PM foam, although the SAC curve is fluctuating a little, an overall increase in the SAC curve was observed with increasing frequency at each level of thickness. For ENR latex foam, the effect of the thickness of the SAC curve is similar to what was observed in LATZ and DPNR latex foams.

To evaluate the acoustics performance of the foam materials, the NRC value was also determined for a range of thicknesses, as shown in Table 7.2. Increasing the thickness of the foam material from 10 mm to 20 mm to 40 mm increases the NRC value for all foams and all densities. This is expected because higher thickness provides better absorption of the incident wave and reflects less energy^{215,216}. The highest NRC was observed on 40mm thick DPNR (HD). Table 6 also indicated that, at 40 mm thickness, the NRC value of HD latex foams is consistently higher than that of MD latex foams.

Table 7.2: Effect of thickness levels on NRC value of latex foams

Thickness	LATZ			DPNR			ENR		PM
	HD	MD	LD	HD	MD	LD	HD	MD	MD
10 mm	0.36	0.40	0.35	0.36	0.35	0.34	0.37	0.30	0.27
20 mm	0.47	0.43	0.40	0.49	0.49	0.39	0.49	0.37	0.38
40 mm	0.70	0.65	0.47	0.72	0.66	0.52	0.70	0.64	0.62

A significant effect of thickness could also be observed in the MD PM foam, the standard acoustic foam material. Increasing the thickness of the PM foam from 10 mm to 20 mm to 40 mm increases the NRC value by 41% and 130% respectively. A comparison between PM and latex foams fabricated in this study shows that the performance of all materials developed in this study are

comparable to, if not better than, PM foam. Since the latex foams are obtained from natural materials, this could offer environmental advantages in the relevant industries.

7.2.3.3 Effect of double-layer foam on acoustic properties

A comparison of STL, SAC, and NRC values between single-layer 20 mm foams and double-layer sandwiches of 10 mm foams was undertaken to further understand whether the acoustic properties of foams could be improved, as shown in Figures 7.13 and 7.14.

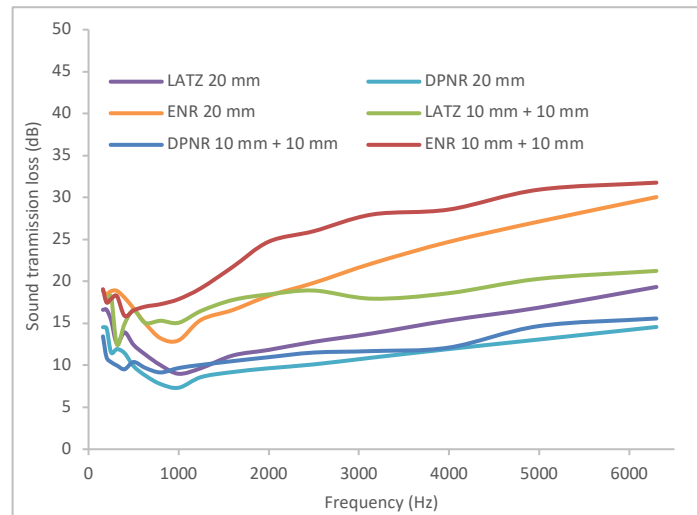


Figure 7.13: The effect of sandwich layer of latex foam on STL curve.

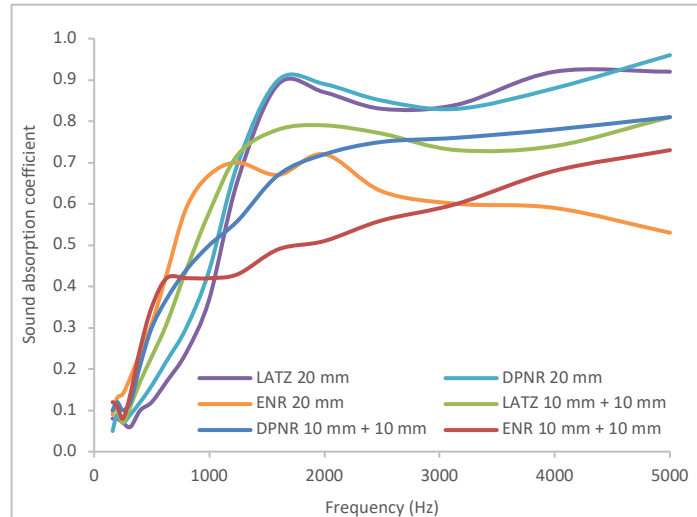


Figure 7.14: The effect of sandwich layer of latex foam on SAC curve.

The double-layer foams exhibit higher STL values compared to the single-layer foams. This could be due to the additional presence of skin layers on each foam, which are likely to raise the resistance to sound wave transmissibility. A similar pattern was observed in terms of SAC values, particularly in the low frequency range. However, in the high frequency range, the single-layer foams exhibit higher SAC values than the double-layer foams. The presence of a skin layer in the middle of the double-layer latex foams is likely to affect the sound wave propagation, which influences the SAC

value at a high frequency range. As shown in Table 7.3, there were no significant differences in NRC values between single-layer and double-layer latex foams.

Table 7.3: Effect of sandwich layer of latex foam on NRC value

	LATZ 10 mm + 10 mm	DPNR 10 mm + 10 mm	ENR 10 mm + 10 mm	LATZ 20 mm	DPNR 20 mm	ENR 20 mm
NRC	0.48	0.48	0.41	0.47	0.49	0.49

7.3 Study on the effect of oil palm trunk biochar as flame retardant filler

Section 7.2 revealed that the acoustic properties of both DPNR latex foam and ENR latex foam are comparable with those of commercial grade synthetic PM foam, making them a strong contender for the next generation of environmentally friendly acoustic foams, especially when the use of natural materials in construction has become a key criterion for sustainable building concepts^{104,224,225}. However, the main challenge with utilizing SpNR latex foam for such applications comes from a safety point of view: whereas the thermal stability of SpNR latex foam must first meet the fire rating requirements^{226,227}. Normally, flame retardant agents are added to acoustic foam material to improve the fire resistance of the material. The most widely used flame retardants are halogen-containing chemicals such as bromine, chlorine, fluorine, and iodine. Although these substances function effectively in imparting flame retardancy to foam materials, they emit dangerous gasses (hydrogen halides, hydrochloric acids, and hydrogen bromides) when burned^{228,229}. The process of manufacturing acoustic foam material from these materials is also hazardous to workers and the environment¹³⁹. Additionally, the use of halogen-based flame retardant for SpNR latex foam also contradicts the purpose of the development of environmentally friendly SpNR latex foam to promote sustainable building concepts.

The purpose of this study is to evaluate the flame retardancy of SpNR latex foam incorporating an eco-friendly filler derived from oil palm trunk biochar (OPTB) filler derived from oil palm trunk (OPT). OPT is a low-cost renewable natural fiber available in large quantities from oil palm plantations in the tropical belt^{230,231}. The economic life of an oil palm tree is about 25 years, which means that 4 % of the planted area is being replanted annually, producing huge amounts of oil palm residue. In Malaysia alone, approximately 18 million tons of OPT are produced per year [23]. Even though OPT can be converted into fiberboard, mulch, or fertilizer, there is still an abundant amount of OPT not being utilized, thus possibly ending up being burnt in the fields by farmers. Therefore, there is an opportunity to investigate the feasibility of using OPT as a flame-retardant filler for SpNR latex foam. This could be done by carbonizing OPT

through pyrolysis, a thermochemical process carried out in the absence of oxygen. This process produces a carbon-rich and thermally stable biochar material with potential as a flame-retardant filler in SpNR latex foam^{97,140}. The utilization of OPTB as a flame-retardant filler may not only improve the thermal stability of the SpNR latex foam but also reduce the overall cost of the material because OPTB is cheaper than the SpNR latex it substitutes. At present, the average cost of biochar is estimated at USD 815 per metric ton, whereas the cost of SpNR latex is three to four times (USD 2,256 – USD 3,760 per metric ton) higher than OPTB²³². It should be noted that SpNR latex is a commodity product whose price depends on the season (raining or drought), supply and demand, as well as the daily price of raw NR and crude oil¹.

OPTB is also a porous material²³³, and therefore the combination of the open-cell structure of SpNR latex foam with the porous structure of OPTB could produce a unique porous composite with advantageous noise control applications. This section reports for the first time the production of an OPTB/SpNR latex foam composite and investigates the effect of OPTB loading on the thermal stability, acoustic properties, and mechanical properties of SpNR latex foam.

7.3.1 Preparation of OPTB/SpNR latex foam composite

7.3.1.1 Preparation of OPTB

The OPT was supplied by Encore Agricultural Industries Sdn. Bhd., Malaysia in the form of dried, chopped short-length fibers, approximately between 10 to 20 mm long. Previous studies^{139,234,235} stated that the main disadvantage of utilizing OPT as a filler polymer is its hydrophilic characteristics, which make it less compatible with hydrophobic polymer matrices. Therefore, in order to ensure good interfacial interaction between OPT and SpNR latex foam, the OPT was subjected to washing and alkaline pretreatment via a method suggested by previous studies^{234,235}. This process is expected to enhance its exterior surface roughness and porous structures as well as reducing its hydrophilicity. In order to improve its thermal stability, OPT was pyrolyzed to produce biochar (OPTB). Four different pyrolysis temperatures were used to identify the temperature that produces the OPTB with the highest thermal stability. Figure 7.15 illustrates the steps involved in the preparation of OPTB. The OPT was ground to a size length below 500 μm using a rotary mill (Fritsch, Model PULVERISETTE-14). Subsequently, approximately 1.0 kg of ground OPT was placed in a fabric case and soaked in hot water at a temperature of 70 °C for 3 hours to remove water-soluble substances and impurities. The OPT was then thoroughly rinsed under flowing tap water and subjected to alkaline treatment by soaking the OPT in 10% (w/v) potassium hydroxide (KOH) overnight at an OPT:KOH ratio of 1:10 w/v.



Figure 7.15: Different stages involved in the preparation of OPTB.

After alkaline treatment, the OPT was thoroughly washed under flowing tap water before being dried in a hot air oven at a temperature of 100 °C until a constant weight was reached. Subsequently, samples of the OPT were heated for 30 minutes to four different pyrolysis temperatures: 300, 400, 500 and 700 °C. A mass m_{OPTB} of approximately 30-35 g of OPT was added to a 150 ml silica crucible, covered with a lid and placed inside a muffle furnace preheated to the desired temperature. After 30 minutes, a mass m_{OPT} of OPTB was recovered, weighed and stored in a desiccator. The yield Y is defined as

$$Y = \frac{m_{OPTB}}{m_{OPT}} \quad (7.1)$$

7.3.1.2 Physical and thermal properties of OPTB

After washing and alkaline treatment, the weight of OPT was reduced by 20 %. This is attributed to the removal of water-soluble minerals and other impurities, as well as KOH-induced dehydration of hemicellulose²³⁴. The dry density of OPT was found to be 0.29 ± 0.05 g/cm³, which is within the range of 0.22 to 0.40 g/cm³ reported in the literature²³⁶. The bulk density of OPTB pyrolyzed at 300 °C (OPTB 300), 400 °C (OPTB 400), 500 °C (OPTB 500) and 700 °C (OPTB 700) was 0.24 ± 0.05 g/cm³, 0.25 ± 0.05 g/cm³, 0.25 ± 0.05 g/cm³, and 0.24 ± 0.05 g/cm³, respectively, which is ~1.16 times lower than OPT. This could be the result of weight loss due to volatilization of hemicellulose, cellulose, and labile lignin²³⁷. Figure 7.16 shows the effect of different pyrolysis temperatures on the OPTB yield. The OPTB yield decreased rapidly between 300 °C (67 ± 1.0 wt.%) and 400 °C (34 ± 0.9 wt.%) and leveled out 500 °C to a value of 30 ± 1.0 wt.%. According to Liu *et al.*²³⁸, the decrease in OPTB yield is due to the release of volatile compounds from the decomposition of holocellulose, which occurs primarily between 250 and

400 °C. Interestingly, the yield of OPTB at 400 °C was approximately half the yield obtained at 300°C, which is in agreement with findings reported by Liu *et al.*²³⁸.

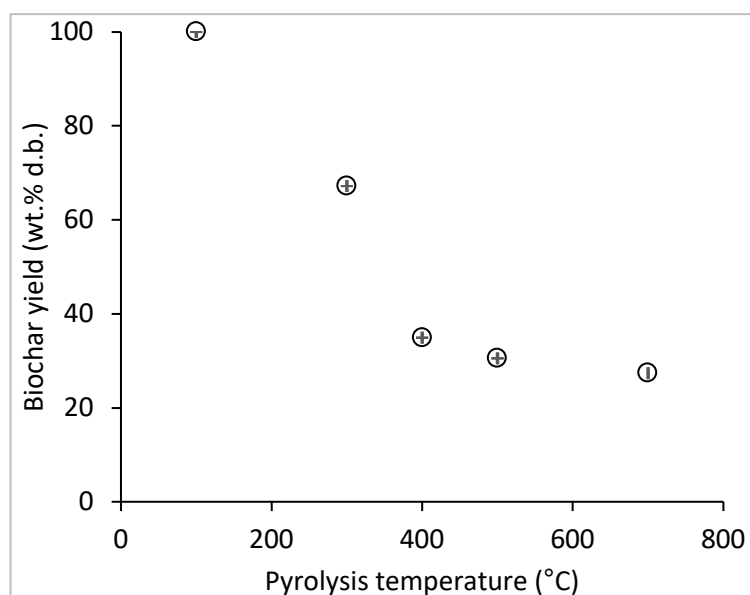


Figure 7.16: Effect of pyrolysis temperature on the yield of OPTB.

Proximate analysis results for untreated and pyrolyzed OPT are summarized in Table 7.4. With an increasing pyrolysis temperature, the volatile matter content decreased, and thus a higher fixed carbon content was obtained. It should be noted that a high concentration of fixed carbon is important because the higher the concentration of fixed carbon, the higher the thermal stability of the material. According to Wu *et al.*²³⁹, volatile matter such as water (H₂O), carbon dioxide (CO₂), carbon monoxide (CO), and ammonia (NH₃), is released during the pyrolysis process. With a further increase in temperature, the release of carbon-rich compounds, such as C_xH_yO_z, from the biochar significantly decreases, whereas other compounds with less carbon (e.g., CO and CO₂) content are continuously released. This results in an increase in the fixed carbon content of OPTB.

Table 7.4: Proximate analysis of OPTB produced at different temperatures

Type of OPTB	Moisture content* (wt. %)	Volatile matter* (wt. % d.b.)	Ash content* (wt. % d.b.)	Fixed carbon* (wt. % d.b.)
OPT	7.6 (2.3)	78.4 (3.0)	4.3 (0.1)	17.3 (2.9)
OPTB 300	3.1 (0.3)	58.5 (0.1)	5.6 (0.2)	35.9 (0.4)
OPTB 400	4.2 (0.3)	33.5 (0.6)	26.9 (0.2)	39.6 (0.5)
OPTB 500	4.64 (0.02)	14.9 (0.3)	10.7 (0.2)	74.4 (0.4)
OPTB 700	5.53 (0.04)	8.6 (0.1)	11.5 (0.2)	79.9 (0.1)

*Average of three replicates. Values in brackets represent the standard deviation.

Figure 7.17 shows the morphological structure of untreated OPT, OPT after washing and alkaline treatment, and OPTB pyrolyzed at different temperatures. The untreated OPT has a comparatively smooth surface (Figure 7.16a), which could be due to a layer of waxes and other

nonstructural substances. Wax is part of the protective layer to prevent water loss²⁴⁰. After washing and alkaline treatment, a rough exterior surface and clean, porous structure were observed on the OPT (Figure 7.17b). In addition, a great number of white spots were observed that are attributed to silica bodies^{234,237,239–241}. Furthermore, according to previous studies^{234,241}, alkaline treatment not only changed the surface structure of OPT, but also caused a decrease in the water absorption property. Such characteristics are important in imparting high interfacial strength and in producing a durable composite with adequate physical properties. After exposure to lower temperature pyrolysis conditions, relatively minor changes in surface structure can be observed between OPT and OPTB 300 (Figure 7.17c) were observed. However, when the pyrolysis temperature was increased, the surface structure started to disintegrate as evidenced by a coarser surface (Figures 7.17d-f). According to Liu *et al.*²³⁹, an increase in pyrolysis temperature liberates more volatile matter from OPTB, producing a char with a coarser surface, more pores, and greater surface area. These characteristics are important because they will increase the surface contact area and are expected to assist in mechanical interlocking bonding mechanisms between OPTB and SpNR latex foam²⁴².

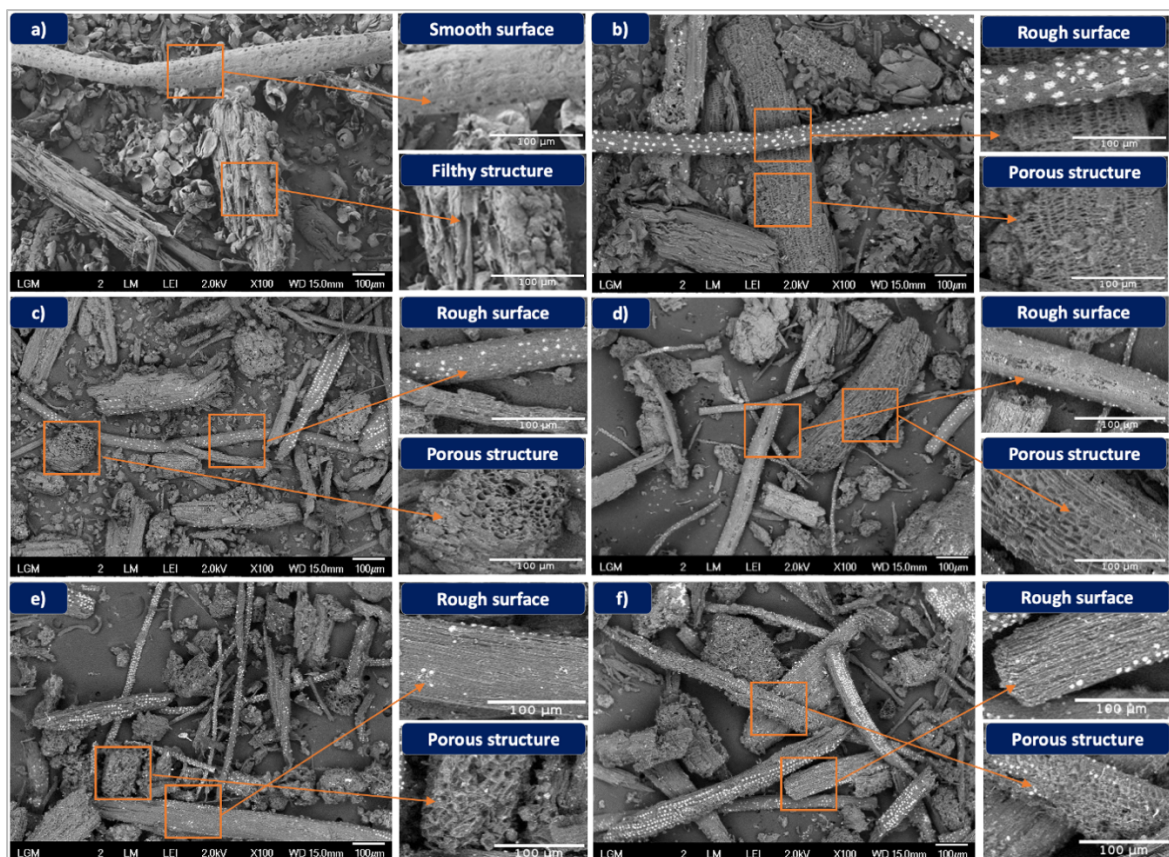


Figure 7.17: SEMs showing the effect of pretreatment and pyrolysis process of OPT.
a) untreated OPT, b) OPT after washing and alkaline treatment, c) OPTB 300, d) OPTB 400, e) OPTB 500, f) OPTB 700.

Figure 7.18 shows the effect of the pyrolysis temperature on the residual weight (TG) and its derivative (DTG) of OPT, OPTB 300, OPTB 400, OPTB 500, and OPTB 700. Figure 7.18 illustrates that OPT and OPTB 300 exhibited three decomposition peaks. The first stage occurs between 35 and 110 °C and is attributed to moisture loss^{97,243}. The shoulder of the second peak of both OPT and OPTB 300 appears at 260 °C, representing the decomposition of hemicellulose²²⁹. The maximum decomposition temperature (T_{max}) of OPT appeared at 340 °C, indicating cellulose decomposition, while the T_{max} of OPTB 300 appeared at 390 °C, indicating crystalline cellulose degradation²⁴³. The decomposition of OPT and OPTB 300 lignin appeared in the third peak with T_{max} at 420 °C and 425 °C, respectively. Prior research on pure lignin observed that it decomposes slowly over a wide temperature range²⁴⁴. OPTB 400 has only two peaks, the first at 370 °C representing the decomposition of residual cellulose, and the second at 430 °C indicating the decomposition of lignin. For OPTB 500 and OPTB 700, a peak appears at ~660°C which could represent the decomposition of whewellite and calcite²⁴⁵.

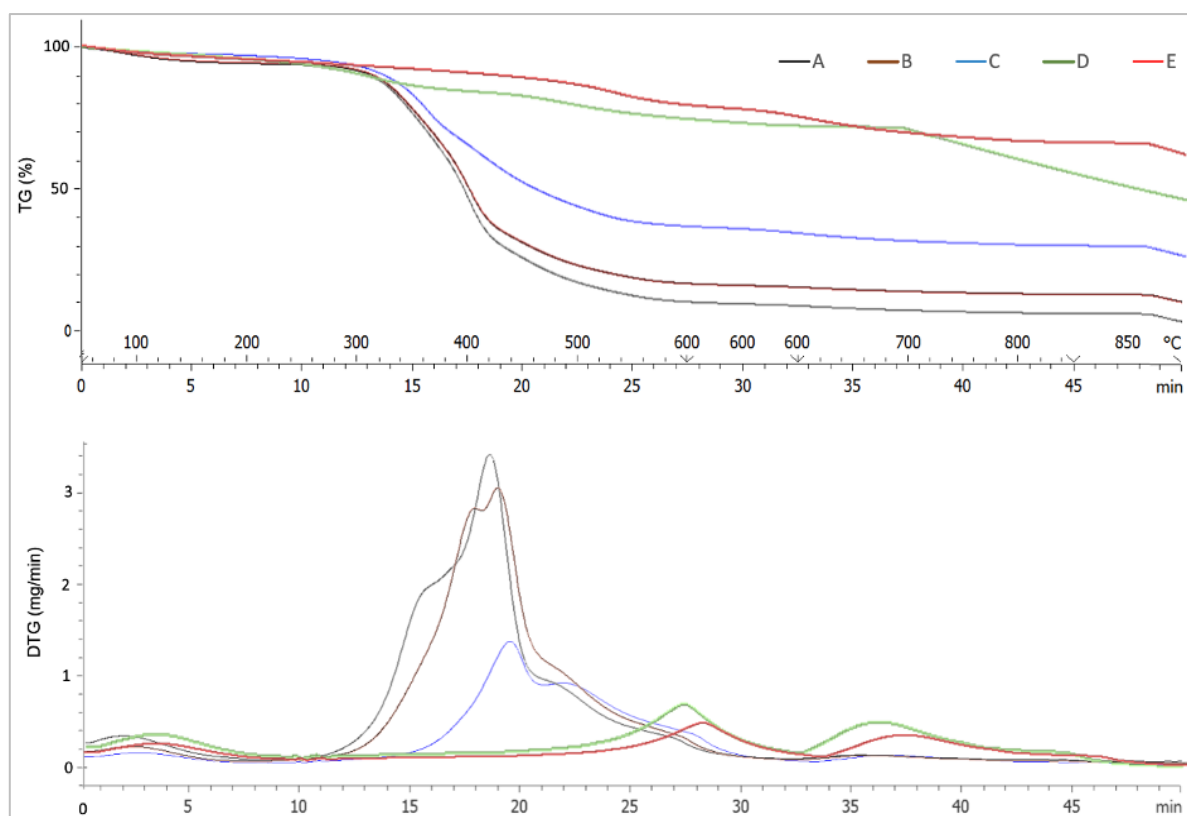


Figure 7.18: Thermogravimetric analysis of OPTB.

A = OPT, B = OPTB 300, C = OPTB 400, D = OPTB 500 and E = OPTB 700

The data derived from the TG and DTG thermogram are presented in Table 7.5. The results indicate the residual weight of the test samples at 100, 425 and 650 °C. At 100 °C, minor weight losses were observed in all samples due to evaporation of water and other highly volatile matter.

Table 7.5: Data evaluated from TG and DTG thermograms of OPTB

Type of OPTB	Decomposition			Residue	
	Stage	Temperature range (°C)	T_{\max} (°C)	Temperature (°C)	Weight (%)
OPT	1 st	35-250	93	100	94.8
	2 nd	260-390	360	425	29.6
	3 rd	400-460	423	600	13.2
OPTB 300	1 st	35-250	97	100	97.0
	2 nd	260-410	395	425	36.2
	3 rd	400-460	425	600	17.1
OPTB 400	1 st	35-350	100	100	97.0
	2 nd	360-470	430	425	59.2
				600	37.8
OPTB 500	1 st	35-390	110	100	96.2
	2 nd	400-620	600	425	86.8
				600	70.2
OPTB 700	1 st	35-390	110	100	95.4
	2 nd	400-650	620	425	91.0
				600	73.4

Higher weight losses occurred at 425 and 650 °C depending on the pyrolysis temperature deployed. The higher the pyrolysis temperature, the lower the weight loss due to the presence of thermally stable fixed carbon (Table 7.4). The results clearly demonstrate that OPTB 700 has the greatest thermal stability, followed by OPTB 500, OPTB 400, OPTB 300 and then OPT. Therefore, OPTB 700 was selected as the flame-retardant filler to fabricate the OPTB/SpNR latex foam composite. To compare and evaluate the effectiveness of OPTB as a flame-retardant filler in improving the thermal stability of SpNR latex foam, an OPT/SpNR latex foam composite was also prepared.

7.3.1.3 Preparation of OPTB/SpNR latex foam composite

The SpNR latex foam composite fabrication process is similar to the SpNR latex foam fabrication process explained in section 5.2. In this work, a high-density (HD) latex foam was used to fabricate the OPTB/SpNR latex foam composite. OPTB was added to the SpNR latex foam after the SpNR latex foam was whipped using a Kenwood mixer and reached the targeted volume marked on the bowl (Figure 7.19). After the gelling ingredients were added, the OPTB/SpNR latex foam is poured into 200 mm × 200 mm × 40 mm (length × width × thickness) square molds with different thickness: 10 mm, 20 mm, and 40 mm. Subsequently, the mold lid was closed and the latex foam was subjected to the vulcanization, washing and drying process. In this section, the effects of different levels of OPTB loading (8 phr, 16 phr, 24 phr and 32 phr) on the SpNR latex foam were investigated.



Figure 7.19: The steps involve the fabrication of the OPTB/SpNR latex foam composite.

During the fabrication process, foam collapse and foam coagulation were observed at the highest level, as shown in Figure 7.20. For DPNR latex, only up to 24 phr OPTB could be added to the latex foam without coagulation. On the other hand, for ENR latex, only 8 phr OPTB could be added to the latex foam, and when 16 phr or more OPTB was added, the latex foam collapsed during the gelling process. The reason for this failure is unclear, and needs further investigation. Nevertheless, at this stage, the focus of this study is to investigate the feasibility of using OPTB as flame retardant filler for SpNR latex foam. Factors influencing the stability of SpNR latex foam as consequent of the addition of OPTB become focal points in the future work.

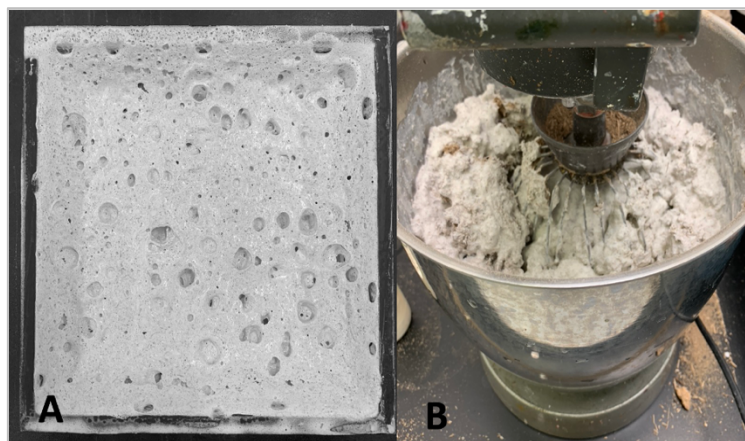


Figure 7.20: Challenge in the fabrication process.
A = foam collapse; B = foam coagulate

7.3.1.4 The appearance of OPTB/SpNR latex foam composite

Figure 7.21 shows the visual appearance of the OPT/SpNR and OPTB/SpNR latex foam composites produced in this work. The color of DPNR latex foam is off-white, while the color of ENR latex foam is yellowish. The addition of OPT and OPTB to DPNR latex foam changes the

color of the DPNR latex foam from off-white to brown and gray, respectively. The addition of OPT and OPTB to the ENR latex foam changes the color of the latex foam from yellowish to brown.

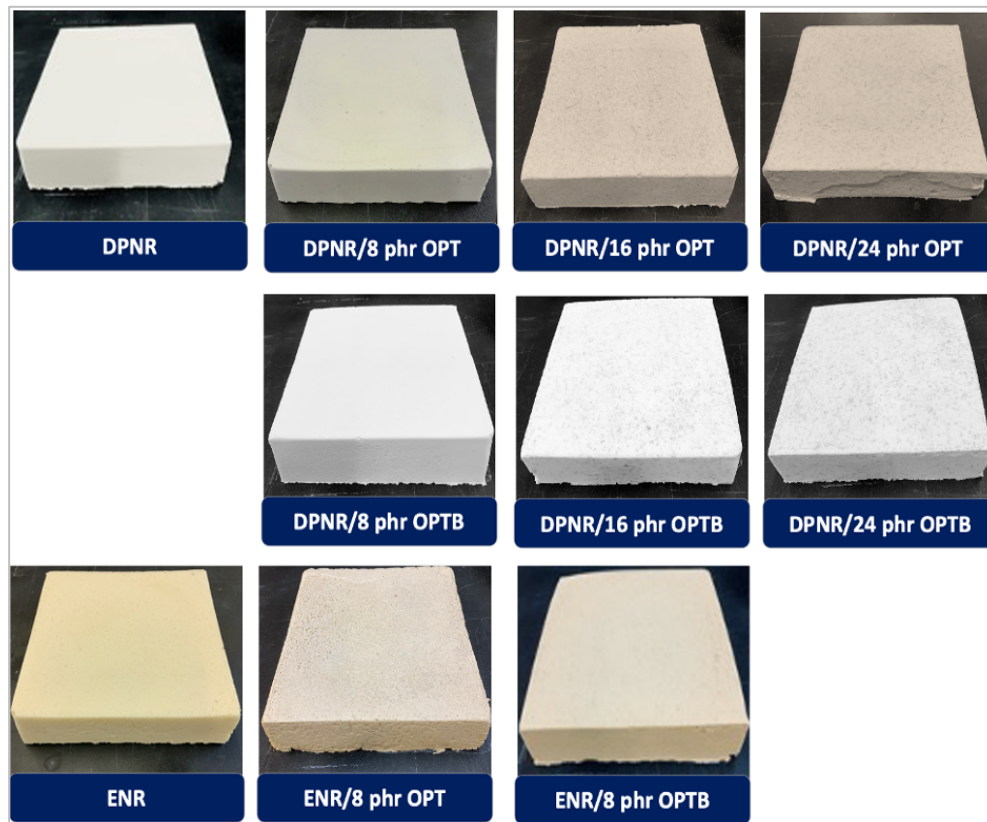


Figure 7.21: The appearance of OPT/SpNR and OPTB/SpNR latex foam composites.

7.3.2 Morphological structure of OPTB/SpNR latex foam composite

Figure 7.22 shows SEM the cross-sectional views of DPNR and ENR latex foams loaded with varying quantities (8 phr, 16 phr, and 24 phr) of OPT and OPTB. Both DPNR and ENR latex foams are open-cell foams interconnected by struts. The addition of the OPT and OPTB is seen to fill into the foam cell, presumably lowering the latex foam porosity. No significant differences in the morphological structure of SpNR latex foam loaded with OPT and OPTB were observed. Both OPT and OPTB are well distributed within the rubber matrix. This could suggest a good interfacial adhesion between the fiber and SpNR latex foam, and therefore a high mechanical strength, as previously observed^{19,242,246}. Figure 7.22 also demonstrates the irregular distribution and orientation of OPT and OPTB within the SpNR latex foam. Additionally, by increasing the concentration of OPT and OPTB loaded into the SpNR latex foam, a higher number of OPT and OPTB particles can be seen in the SEM micrograph. It should be highlighted that OPT and OPTB are themselves also porous materials. The pore structure could be open, partially open, or completely closed^{230,233}. Thus, it might influence the acoustic properties of the latex foam composite.

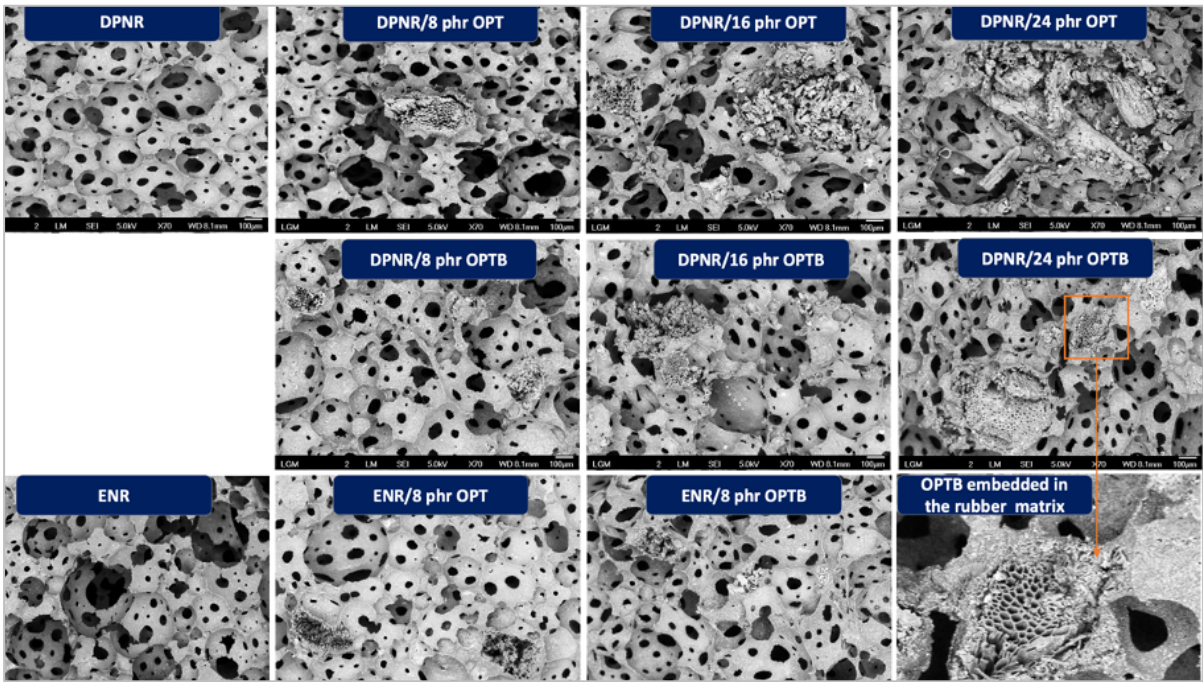


Figure 7.22: Cross-section views of OPTB/SpNR latex foam composites loaded with varying quantities of OPT and OPTB.

7.3.3 Acoustic properties of OPTB/SpNR latex foam composite

The effects of the addition of OPT and OPTB on sound transmission loss (STL) and sound absorption coefficient (SAC) are shown in Figure 7.23 and Figure 7.24, respectively. Figure 7.23a and Figure 7.23b show the effect of the addition of OPT and OPTB on the STL of DPNR latex foam and ENR latex foam, respectively. It is clear that the addition of both OPT and OPTB to DPNR latex foam and ENR latex foam increases the STL value.

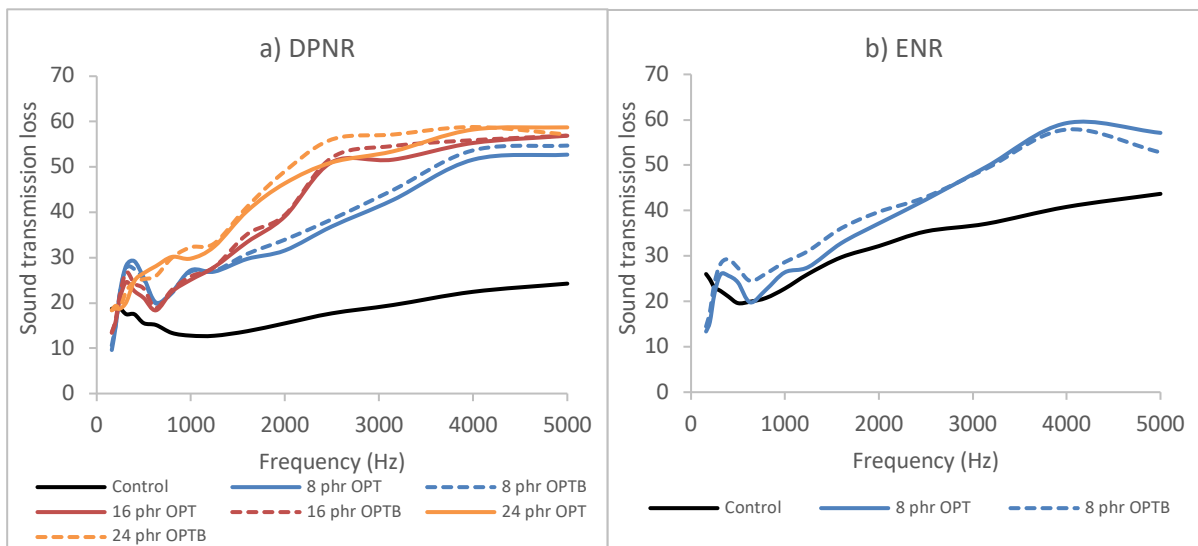


Figure 7.23: Effect of addition of OPTB on STL of SpNR latex foam.

It can be seen that the STL value increases as the frequency increases. The Figures also demonstrate that the STL value increases with concentration of OPT and OPTB for both the

DPNR latex foam and ENR latex foam. This could be the result of latex foam having a higher stiffness and density value, as well as changes in morphological characteristics^{215–217}. Although the stiffness and density were not measured directly here, OPT and OPTB are stiffer materials than latex foam, and the addition of OPT and OPTB is expected to increase the stiffness of the composite foam materials. Additionally, as shown in Figure 7.22, the addition of OPT and OPTB changes the configuration of the foam cell structures of the latex foams, whereby the fibers are seen to be located within the foam cells, which ought to increase the density of the foam material. On the other hand, it should be noted that OPT and OPTB are also porous materials that act as a medium of transmissibility of the sound waves. The open-cell structure of latex foam combined with the porous structure of the OPTB creates a unique porous structure that act as a medium of transmissibility of sound waves²¹⁶. The results show that the higher the concentration of OPT and OPTB loaded, the higher the flow resistance of the latex foam and hence the higher the STL value. According to a recent study²¹⁸, a frequency range of 160 to 3150 Hz is generally examined for the building of acoustic applications since it covers the range from speech tones to traffic noise. The foam material should be able to reduce noise by at least 10 dB. This study found that the STL value of all latex foams is higher than 10 dB throughout the frequency range, indicating that it meets the specifications for acoustic applications in buildings. But a higher concentration of OPT and OPTB offers higher insulation level.

Figure 7.24 shows the negative effect of the addition of OPT and OPTB on the SAC value of the latex foam. The addition of either OPT or OPTB both reduce the SAC value, DPNR latex foam (Figure 7.24a) as well as in ENR latex foam (Figure 7.24b).

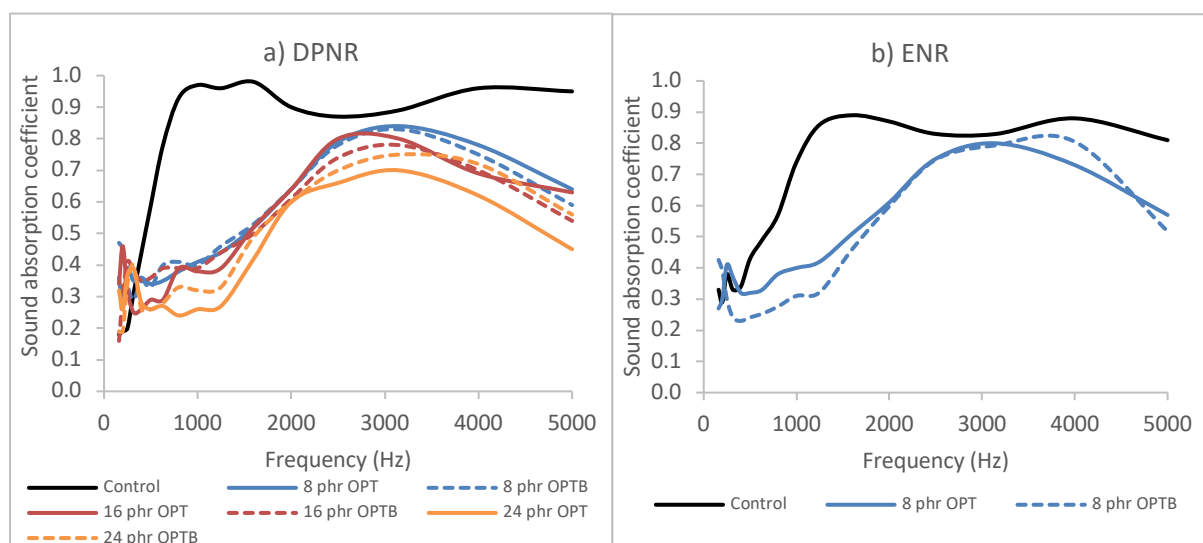


Figure 7.24: Effect of addition of OPTB on SAC of SpNR latex foam.

As explained earlier, the addition of OPT and OPTB to latex foam is likely to produce an increase in the stiffness and density of the foam material. The SEM image shows that the OPT and OPTB

are located within the foam cells, thus lowering the porosity of the latex foam. It is well known that the stiffer the material the more wave energy it reflects rather than absorbs²⁴⁷. Thus, the addition of OPT and OPTB to the SAC of DPNR latex foam has the opposite effect on STL compared with SAC, requiring a compromise. Future studies should be carried out using a statistical analysis, particularly the response surface methodology (RSM) to identify the loading at which acceptable STL and SAC values can be attained. The selection of suitable types and properties of foam materials is crucial because each of them possesses specific characteristics to perform its own function and is not capable of carrying out both tasks, as a sound insulator or a sound absorber. As illustrated in Figure 7.25, sound waves incident on a foam material can be absorbed, reflected, and/or transmitted by the material depending on the type of material. When incident sound waves strike the foam, the air molecules on the surface of the material and within the pores of the material are forced to vibrate due to the changes in the ambient sound pressure.

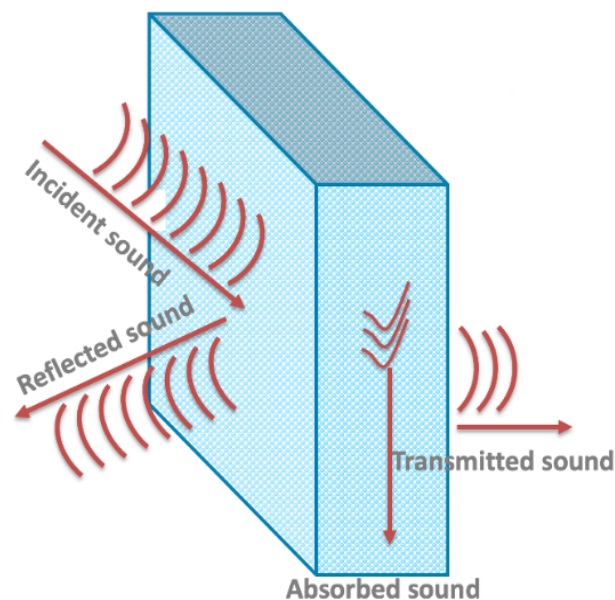


Figure 7.25: Illustration of sound waves propagation in acoustic foam materials.

The sound waves propagate along the foam material, and due to the friction and physical properties of the material such as density and porosity, some sound energy is converted into heat energy and dissipated. The higher the porosity of the foam material, the higher the ability of the foam cell structure to interact with the sound waves so that more energy is transformed into heat by entrapping the sound waves within the pores^{103,222,223,247}. On the other hand, if the porosity is too low, the absorption capability will decrease and the sound waves will be reflected²⁴⁸. Foam materials with high STL values are best for sound insulation applications. Foam materials with a high SAC value, on the other hand, are suitable for use as sound absorbers to control reverberations and echoes. According to a previous study²²⁰, the frequency range of 3000 Hz to 4000 Hz is crucial for

building acoustic applications because it produces unpleasant noise and may cause hearing difficulties in people if exposed to it on a daily basis. The inclusion of OPT and OPTB reduced the SAC value from 0.8 to 0.6; however, the SAC value is still suitable for building acoustic applications, where this material is classified as a class B sound absorber²⁴⁹.

7.3.4 Thermal stability of OPTB/SpNR latex foam composite

Figure 7.26 and Figure 7.27 show the effect of addition of OPT and OPTB into DPNR latex foam and ENR latex foam on TG and DTG, respectively. Thermograms of all samples were relatively similar, with a single major decomposition peak. It can be observed that the TG curves gradually reduced until they reached a point where the SpNR latex foam began to decompose. A dramatic weight loss was observed between 250 and 500 °C indicating the decomposition of SpNR latex foam, with a T_{max} between 380 and 390 °C. The study also observed that the addition of OPT or OPTB slightly altered T_{max} , as reported in Table 7.6. This is consistent with a previous study²⁵⁰, which found that NR undergoes thermal degradation in the temperature range between 287 °C and 400 °C, and where T_{max} was observed at a temperature of 379 °C. According to previous studies^{250,251}, T_{max} is related to the breakdown of the cross-linked network of rubber chains, so a higher T_{max} value corresponds to a higher thermal stability of the material. The addition of OPTB to the DPNR latex foam appears to improve the thermal stability of the DPNR latex foam. As indicated in Table 7.6, the addition of OPTB, especially at 24 phr OPTB, increases the residual weight at T_{max} . This is due to the fact that OPTB has a lower rate of decomposition (Table 7.5) compared to DPNR latex foam. Therefore, when the concentration of OPTB in the latex foam increased, a higher residual weight at T_{max} was observed. OPTB is a biochar that contains lignin with a high concentration of fixed carbon (Table 7.4). Table 7.6 also shows that ENR latex foam has a lower decomposition rate than DPNR latex foam. This is in agreement with previous studies^{138,252} that found that the thermal stability of NR was enhanced when epoxide groups were introduced into its backbone. The improvement in the thermal stability of ENR is because the epoxide groups enlarged the intermolecular attraction and diminished the chain mobility. The addition of 8 phr of OPTB to ENR latex foam slightly decreased the rate of decomposition and increased the residual weight of the OPTB/ENR latex foam composite. However, the changes are considerably lower compared to what has been observed on the effect of the addition of 8 phr of OPTB to the DPNR latex foam.

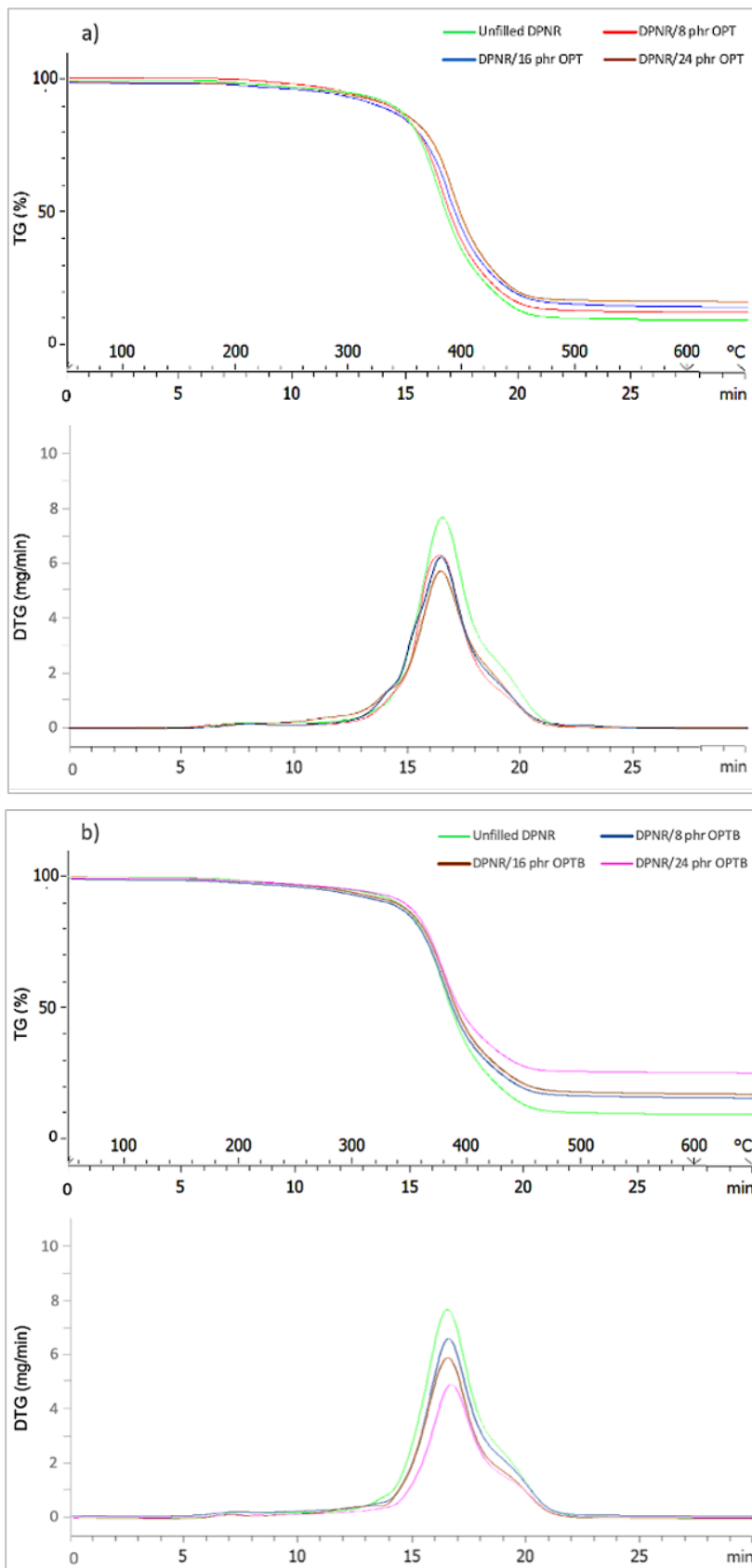


Figure 7.26 Thermogravimetric analysis of the effect of OPT and OPTB on DPNR latex foam
 a) Effect of OPT, b) Effect of OPTB

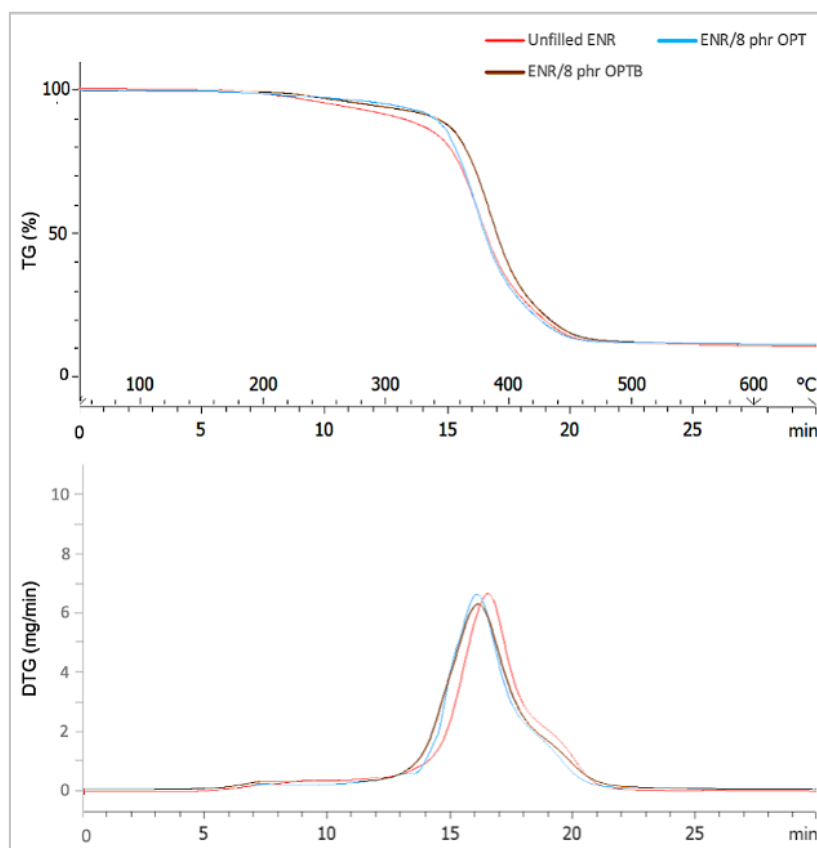


Figure 7.27 Thermogravimetric analysis of the effect of OPT and OPTB on ENR latex foam.

Table 7.6: Data evaluated from TG and DTG thermogram of SpNR latex foam composite

Type of material		T_{max} (°C)	Rate of decomposition (mg/min)	Residual weight (%)
DPNR	Control	387	7.3	8.2
	8 phr OPT	390	6.2	10.8
	16 phr OPT	389	6.1	14.1
	24 phr OPT	389	5.8	17.9
	8 phr OPTB	386	6.4	14.8
	16 phr OPTB	384	5.9	18.9
	24 phr OPTB	386	4.8	24.1
ENR	Control	395	6.6	10.1
	8 phr OPT	385	6.5	10.6
	8 phr OPTB	385	6.4	11.0

Table 7.7 shows the effect of the addition of OPT and OPTB on the burning rate of the SpNR latex foam. The study found that the flame always passed the 125 mm gauge mark. Although the burning rate reduces with increasing OPT and OPTB content, the burning rate of all samples exceeds the allowable maximum of 40 mm/min prescribed in the UL 94 HBF requirements. During the test, the neat SpNR latex foam ignited quickly with a large flame and smoke. The burning rate of the neat DPNR latex foam and the neat ENR latex foam that was measured at 125.59 mm/min and 122.48 mm/min was reduced to 94.30 mm/min and 89.69 mm/min, respectively, when 8 phr of OPTB was loaded. For DPNR latex foam where it was possible to add

24 phr of OPTB, the burning rate was reduced further from 125.6mm/min neat to 68.10 mm/min with 24 phr OPTB.

Table 7.7: Burning rate of OPTB/SpNR latex foam composite

Type of material		Burning velocity rate (mm/min)*
DPNR	Control	125.6 (6.8)
	8 phr OPT	120.1 (5.3)
	16 phr OPT	104.1 (4.0)
	24 phr OPT	88.5 (3.6)
	8 phr OPTB	94.3 (4.0)
	16 phr OPTB	84.8 (2.6)
	24 phr OPTB	68.1 (2.5)
ENR	Control	122.5 (6.1)
	8 phr OPT	120.7 (5.2)
	8 phr OPTB	89.7 (3.1)

*Average of five replicates. Values in brackets represent the standard deviation.

Although OPTB has great flame-retardant characteristics, when employed as a filler, it is insufficient to improve the fire rating of the OPTB/SpNR latex foam composite to meet the requirements for building applications. However, this study found that the utilization of OPTB as an eco-friendly flame-retardant filler in SpNR latex foam does help to reduce the burning rate. If one extrapolates the results obtained for DPNR latex to higher filler content, it is expected that with ~34 phr of OPTB the foam could potentially reach the minimum burning rate stipulated in the standard specification of 40 mm/min (Figure 7.28).

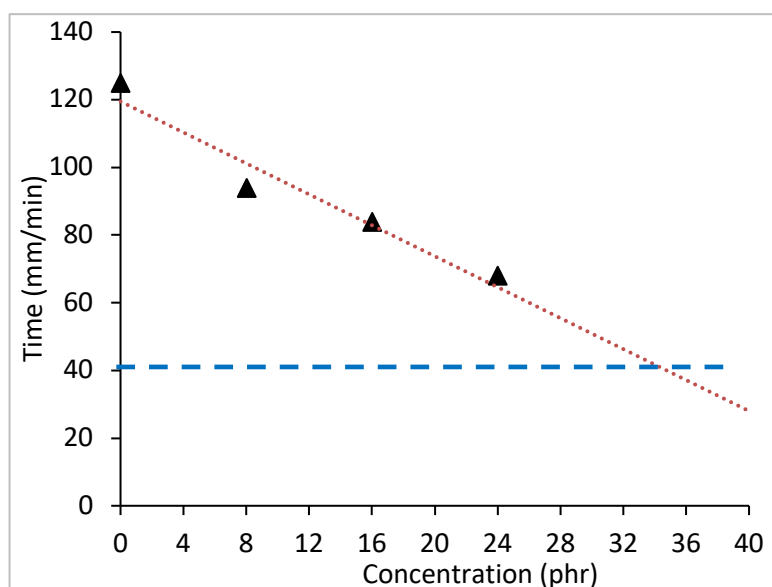


Figure 7.28: Burning rate versus OPTB loading concentration. The line represents linear regression through the data. The target of 40mm/min prescribed in the standard is also shown.

Unfortunately, as mentioned earlier, DPNR latex foam collapsed when 32 phr of OPTB was added. Therefore, it is desirable to find a way to improve the fabrication process in future study in order to enable higher filler content foams.

7.3.5 Physical and mechanical properties of OPTB/SpNR latex foam composite

7.3.5.1 Physical properties of OPTB/SpNR latex foam composite

Figure 7.29 shows the effect of addition of OPTB loading on density, volume shrinkage, hardness and elongation at break of SpNR latex foam. The addition of OPTB as a filler into SpNR latex foam increased the density of both ENR and DPNR latex foam (Figure 7.29a). The higher the concentration of the OPTB, the higher the density was observed. As mentioned earlier, latex foam is a combination of solid phase and air phase. The higher the concentration of air phase the lighter the material, and thus the lower the density. When OPTB is loaded into the SpNR latex foam, the filler occupies the pores of the latex foam as visualized in Figure 7.22.

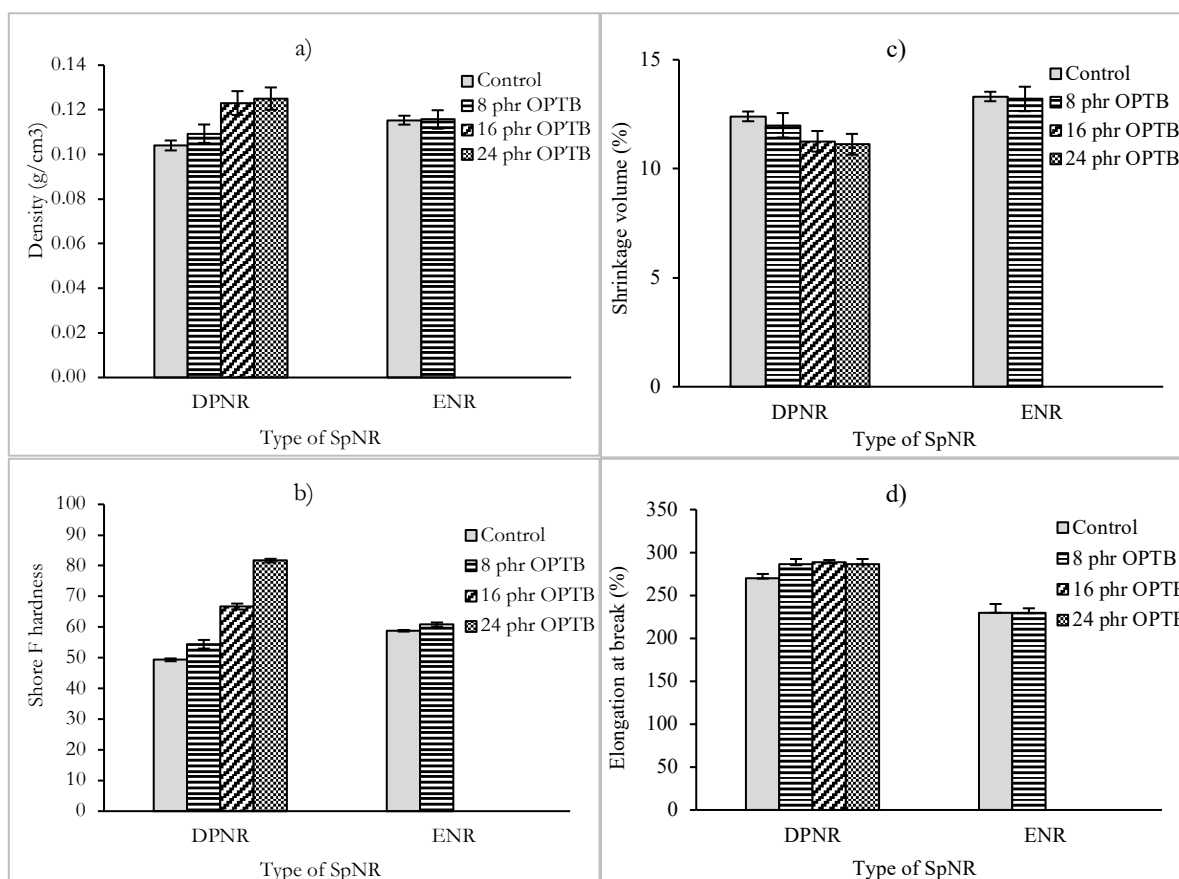


Figure 7.29: Effect of addition of OPTB on physical properties of SpNR latex foam. a) density, b) volume shrinkage, c) hardness and d) elongation at break

Therefore, the higher the amount of OPTB loaded into the SpNR latex foam the higher the OPTB occupying the pores, and hence increasing the concentration of the solid phase than the air phase.

This led to an increase in the density of the SpNR latex foam. Figure 7.29b also shows that the higher the OPTB loading the higher the Shore F hardness value. This is expected because OPTB is harder than SpNR latex foam, thus indirectly increasing the hardness of the SpNR latex foam. The results also show that the higher the concentration of OPTB the harder the material. On the other hand, Figure 7.29c shows that the higher the OPTB loading, the lower the volume shrinkage. Previous studies^{253,254}, stated that soft and elastic materials such as NR tend to shrink more than harder materials after the manufacturing process. Another studies^{255–257} found that the volume shrinkage of NR could be reduced by the addition of harder materials as reinforcing fillers. In this study, the addition of OPTB as a flame-retardant filler reduced the volume shrinkage. During OPTB/SpNR latex foam fabrication process, it was observed that the increase of the fiber loading led to a decrease of the flow behavior of the material during the process, particularly during transferring the foam composite from the bowl mixer to the mold. However, since the addition of OPTB into SpNR latex foam reduced the volume shrinkage, this could lead to better end products. This characteristic is beneficial because it led to better dimensional stability, thus helps the manufacturer to predict the size of the finished products. Thus, it can be drawn that, the higher the OPTB content, the harder the material could be obtained, thus the lower the volume shrinkage. In Figure 7.29b, it can be seen that the neat ENR latex foam has a higher Shore F hardness than neat DPNR latex foam. This could be due to the presence of the epoxy group in the rubber chains that makes the ENR latex foam become harder. Although the hardness of the neat ENR latex foam is higher than the neat DPNR latex foam, the volume shrinkage of the neat ENR latex foam is higher than the neat DPNR latex foam. This indicates that DPNR latex foam and ENR latex foam have different shrinkage characteristics. Figure 7.29d also shows the effect of the addition of OPTB on the elongation at break of SpNR latex foam. The addition of 8 and 16 phr of OPTB into DPNR latex foam increased the elongation at break value. The improved elongation at break for DPNR latex foam loaded with 8 phr of OPTB could be due to good interfacial adhesion between the OPTB filler and the rubber matrix, which has been explained by previous study²⁵⁸. However, no further significant improvements were observed with increased OPTB loading. For ENR latex foam, the addition of 8 phr of OPTB did not show significant changes in the elongation at break value.

7.3.5.2 Compressive stress-strain behavior

Figure 7.30 show the effect of the addition of OPTB on the loading and unloading curves of DPNR and ENR latex foams, respectively. It is obvious that both the neat DPNR and ENR latex foam are viscoelastic materials, and thus create a hysteresis loop during the loading and unloading cycles. The neat ENR latex foam has a bigger gap between the loading and unloading curves

compared to neat DPNR latex foam. Previous studies^{197,199} stated that during loading, the foam cell walls are bent and in contact with specific friction. The air escapes from the foam through the open-cell. During unloading, the air is sucked back into the foam cell structure and thus the recovery rate of the foam cell depends on the breathability or porosity of the foam and the relaxation behavior of the material. Another study²⁵⁹ stated that NR rubber foam exhibits high resistance to the compression force due to its elasticity behavior, thus able to recover its original shape very fast after the compression is released. Therefore, the bigger gap between the loading and unloading curves of ENR latex foam compared to DPNR latex foam is possibly due to the stiffness of the material as a consequence of the epoxidation process that restrict the mobility of the rubber chains. This is in line with a previous study²⁶⁰ that revealed the increase of the hardness of the foam led to higher compression stress value. Figure 7.30 also shows that the addition of OPTB into both DPNR and ENR latex foams increased the stress value, which could be due to the increment of stiffness of the material. The results show that the compressive stress-strain curve of DPNR latex foam loaded with 24 phr has the highest compressive stresses among all other latex foam composites. Further to that, the presence of OPTB in the rubber matrix increases the gap between loading and unloading curves, indicating the reduction of elastic behavior of the latex foam.

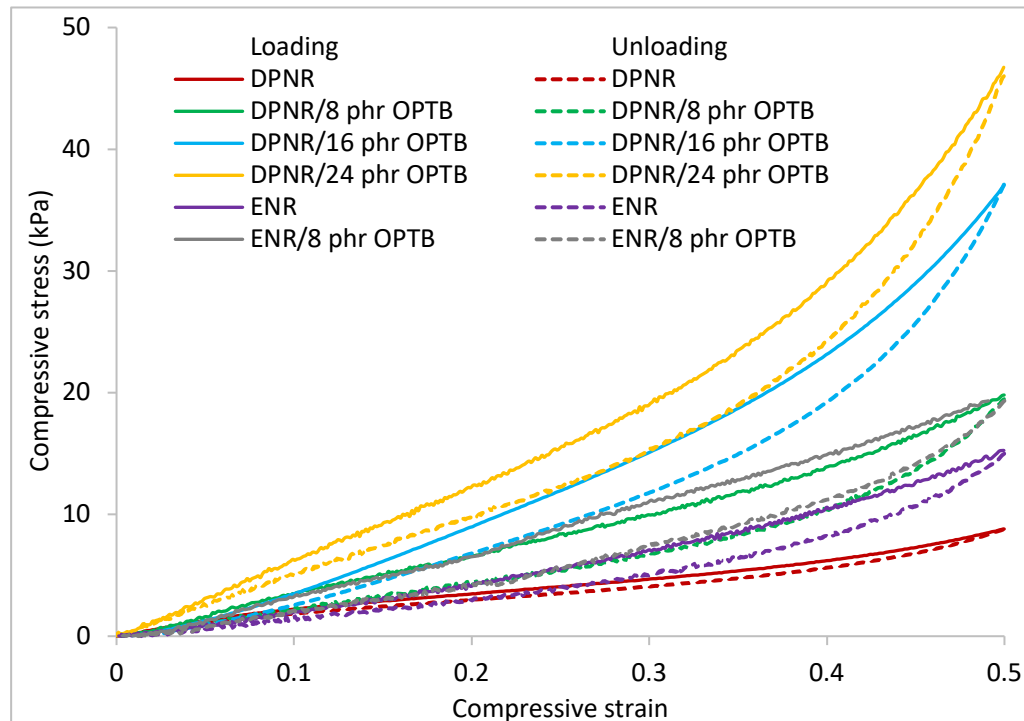


Figure 7.30: Effect of addition of OPTB on stress-strain of SpNR latex foam.

Table 7.8 indicates the elastic behavior of OPTB/SpNR latex foam composite at different strain percentages of 5 %, 15 %, 25 %, and 50 %. It is clear that increasing the strain percentage increases the stress values. The results show that the higher the OPTB loading the higher the stress

value at every strain percentage. This could be the increase in hardness and density of the latex foam (Figure 7.29). Previous study²⁶⁰, claimed that the increase of compressive stress with density is due to the increased contribution of solid material present in the foam cells. This is in line with SEM results shown in Figure 7.22 that visualized OPTB is seen to fill into the foam cell as well as embedded in the rubber matrix, thus increasing the concentration of solid material in the latex foam. Changes in the morphological structures of the latex foam might also affect the deformation behavior of the material, especially when different compression strain rates were applied.

Table 7.8: Stress value of the latex OPTB/SpNR latex foam at different strain

Type of material	Stresses at 5 % strain (kPa)	Stresses at 15 % strain (kPa)	Stresses at 25 % strain (kPa)	Stresses at 50 % strain (kPa)
DPNR (control)	1.293	2.905	4.064	8.804
DPNR/8 phr OPTB	1.297	5.051	8.393	19.813
DPNR/16 phr OPTB	1.612	6.177	12.016	32.023
DPNR/24 phr OPTB	3.148	9.315	15.599	46.734
ENR (control)	0.987	3.162	5.531	15.259
ENR/8 phr OPTB	1.338	4.876	8.797	19.334

In order to better understand the rate sensitivity of latex foam composite cell deformation, the effects of different compression strain frequency on the compressive stress behavior of OPTB/SpNR latex foam composite were investigated in this study. In this work, DPNR latex foam loaded with 16 phr OPTB was used. Strain frequencies of 0.2 Hz, 0.8 Hz, and 1.5 Hz were selected as recommended by previous studies^{123,134,198}. The compressive stress-strain responses of DPNR/16 phr OPTB latex foam composite at different strain frequencies are shown in Table 7.9.

Table 7.9: Effect of strain frequency on stress value

Type of material	Stresses at 5 % strain (kPa)	Stresses at 15 % strain (kPa)	Stresses at 25 % strain (kPa)	Stresses at 50 % strain (kPa)
0.2 Hz	1.297	6.177	12.016	32.023
0.8 Hz	1.587 (+22%)	7.144 (+16%)	12.664 (+5%)	32.750 (+2%)
1.5 Hz	1.686 (+30%)	7.737 (+25%)	13.794 (+15%)	33.946 (6%)

Value in the bracket indicates changes in stress value.

NR latex foam is a unique elastic material. The elasticity behavior of NR follows Hooke's law, and increases with increased strain²⁶¹. Therefore, when applying a compressive strain, the resultant stress will increase with increasing strain rate. Table 7.10 confirmed that when the strain frequency was increased from 0.2 Hz to 0.8 Hz and 1.5 Hz, the stress value was increased. However, it can be seen in Table 7.9, the higher the strain percentage, the lower the increment of the percentage of the stress due to the increase of the strain frequency. According to a previous study²⁶², the higher increment of stress at a lower strain percentage is due to the initial stiff response. As the strain

increased, the stress increased. Stresses at 50 % strain are very high due to the foam cells collapsing to form a higher percentage of rubber, reducing the percentage of air, which then increases the resistance of the material against load.

Another piece of information that can be gained from Figure 7.30 is the hysteresis loss ratio that can be calculated from the hysteresis loop (the gap between the loading and unloading curve) of the foam materials. Hysteresis is defined as the energy loss (dissipation energy) per cycle of deformation¹⁹⁷. It is well understood that, the area under the loading curve is the total mechanical energy input whilst, the area under the unloading curve is the return of stored energy and the area between the two curves is the dissipated energy that is converted to heat¹⁹⁸. The importance of the hysteresis study is that it gives a strong indicator about of material's capability to absorb energy and/or relief pressure²⁰⁴. The hysteresis loss ratio equation is given as follows:

$$Hlr = \frac{H}{E} \quad (7.1)$$

where Hlr is the hysteresis loss ratio, H is the amount of hysteresis (dissipated energy, given by the difference between the area under the uploading and the unloading curve) and E is the supplied energy during uploading (given by the area under the unloading curve).

Figure 7.31 shows the hysteresis loss ratio of SpNR latex foam examined in this study. The hysteresis loss ratio was calculated from the three cycles of the compressive stress-strain curve because it has been recognized as the most stable hysteresis loop¹⁹⁸. Figure 7.31 indicates that DPNR latex foam has the lowest hysteresis loss ratio, whilst DPNR latex foam loaded with 24 phr OPTB has the highest hysteresis loss ratio. As mentioned above, DPNR latex foam is a predominantly elastic material, thus able to store a high amount of energy due to deformation. Previous study²⁰³ revealed that the high hysteresis loss ratio is associated with the energy-consuming mechanisms of foam cell collapse and possibly by friction between the various structural elements of the collapsing foam cell. During compression, the foam cell network produces a resilient force. The resilient force is dependent on reversed effects namely, the relaxation effect, pneumatic effect and adhesive effect^{199,200}. The relaxation effect is the mobility of the chain's network which is related to T_g value and intrinsic elasticity of the material. The pneumatic effect is dependent on the morphological characteristics of the foam material typically porosity. On the other hand, the adhesive effect is the force between struts and foam structures that cause friction. Research findings in this chapter show that the addition of OPTB as filler induced the elastic property of the material. The higher the concentration of OPTB the higher the hysteresis loss ratio. Therefore, the increase of the hysteresis loss ratio of DPNR latex foam loaded with OPTB is mainly influenced by the pneumatic effect. This is because the morphological

characteristic of the foam has been changed, whereas OPTB is distributed within the rubber matrix.

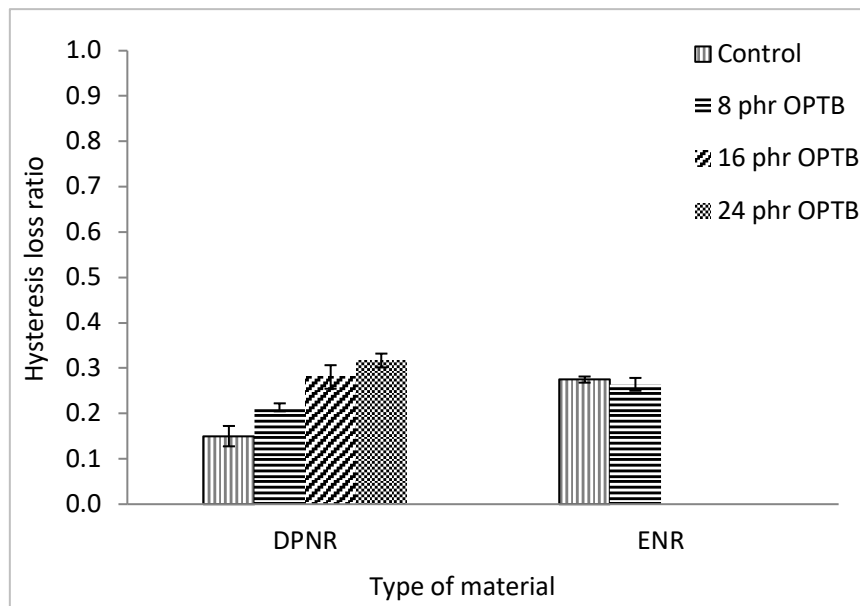


Figure 7.31: Hysteresis loss ratio of OPTB/SpNR latex foam composite.

7.3.5.3 Rebound resilience behavior

Figure 7.32 depicts the relative rebound resilience of the OPTB/SpNR latex foam composites. The study observed that the neat DPNR latex foam shows a higher rebound resilience compared to the neat ENR latex foam. The rebound resilience property was marginally reduced when 8 phr OPTB is added to DPNR latex foam, but not significant for ENR latex foam.

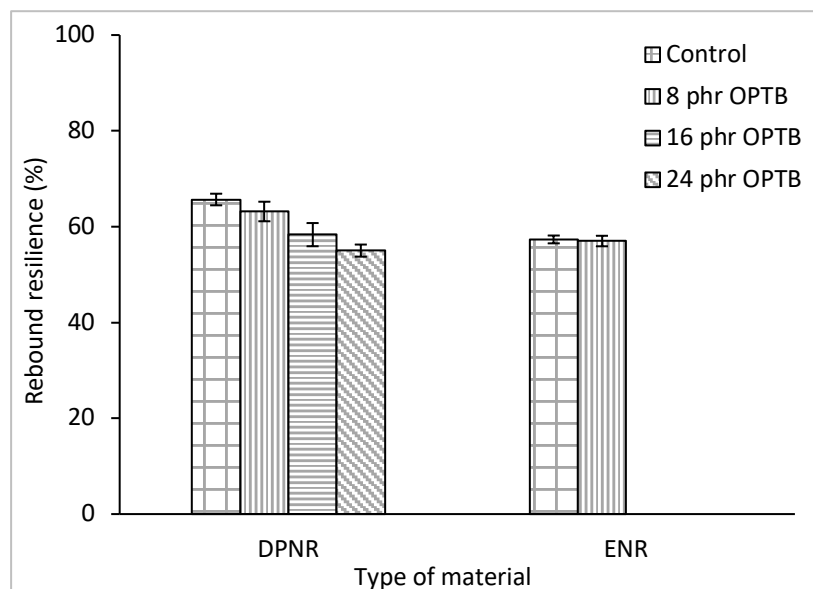


Figure 7.32: Effect of addition of OPTB on rebound resilience of SpNR latex foam.

For DPNR latex foam, the rebound resilience property of DPNR latex foam was further lowered when the OPTB concentration was increased to 16 phr and 24 phr. This finding is consistent with previous study²⁶³, which found that increasing the amount of filler reduced the foam's rebound

resilience. According to ASTM D3574⁵², the resilience property of foam material is proportional to the reaction force applied on the surface of the object. Generally, foam material having a rebound resilience > 40% is categorized as a ‘high resilience foam material.’ Assuming that no energy is lost to air friction, the gravitational potential energy of the steel ball is fully converted to kinetic energy when it is dropped on the surface of the latex foam. Equation 7.2 was used to compute the impact energy of the steel ball,

$$E_i = mgh \quad (7.2)$$

where E_i is the impact energy, m is the ball mass (0.016 kg), g is the gravitational acceleration (9.81 m/s²), and h is the ball drop height (0.5 m). The impact energy was found to be 0.07848 J. Assuming that the kinetic energy returned to the ball from the foam was fully converted to gravitational potential energy during the rebound, the energy returned to the ball was computed using Equation 7.2, where h now represents the rebound height. The ratio of energy returned to the ball is then determined by dividing the ratio of energy returned to the ball by the impact energy of the ball. The ratio of energy returned is proportional to the foam resilience. Thus, the ratio of energy absorbed and the amount of energy absorbed by the foam were calculated using Equations 7.3 and 7.4, respectively.

$$RE_{absorbed} = 1 - \text{resilience} \quad (7.3)$$

$$E_{absorbed} = E_{impact}(RE_{absorbed}) \quad (7.4)$$

where $RE_{absorbed}$ is the ratio of energy absorbed, $E_{absorbed}$ and E_{impact} are the energy absorbed by the foam and ball impact energy respectively.

Table 7.10 tabulates the data gathered in this section. It appears that the higher the resilience property of the foam, the larger the ratio of energy returned to the ball from the foam. As such, the lower the ratio of energy returned to the ball, the higher the ratio of energy absorbed by the foam, indicating a higher ability of the foam to absorb energy. Table 7.10 clearly shows that the energy absorbed of the latex foam was increased when OPTB was loaded to the latex foam. The increase of energy absorbed by DPNR latex foam that was loaded with a higher concentration of OPTB indicates the increase of damping properties of the material, making it appropriate for applications in the transportation industry where a high level of crashworthiness is a key aspect to improve the safety of the transport.

Table 7.10: Effect of addition of OPTB on damping properties of SpNR latex foam

	DPNR				ENR	
	Control	8 phr OPTB	16 phr OPTB	24 phr OPTB	Control	8 phr OPTB
Rebound height (m)	0.328 (0.006)	0.315 (0.010)	0.292 (0.012)	0.275 (0.006)	0.287 (0.004)	0.285 (0.005)
Energy returned (J)	0.051 (0.001)	0.049 (0.002)	0.046 (0.001)	0.043 (0.001)	0.045 (0.001)	0.045 (0.001)
Ratio energy returned	0.657 (0.012)	0.630 (0.020)	0.583 (0.024)	0.550 (0.013)	0.573 (0.008)	0.570 (0.011)
Resilience	0.657 (0.012)	0.630 (0.020)	0.583 (0.024)	0.550 (0.013)	0.573 (0.008)	0.570 (0.011)
Ratio energy absorbed	0.343 (0.012)	0.370 (0.020)	0.417 (0.024)	0.450 (0.013)	0.427 (0.008)	0.430 (0.011)
Energy absorbed (J)	0.027 (0.001)	0.029 (0.002)	0.033 (0.002)	0.035 (0.001)	0.033 (0.001)	0.034 (0.001)

*Average of three replicates. Values in brackets represent the standard deviation.

7.3.5.4 Vibration-damping properties

Figure 7.33 and Figure 7.34 depict the effects of OPTB addition into DPNR and ENR latex foam on the vibration transmissibility, respectively. The vibration transmissibility was plotted as a function of frequency. Two regions can be identified: the amplification region where the value of vibration transmissibility response is more than one, and the isolation region, where the vibration transmissibility response is less than one¹⁹².

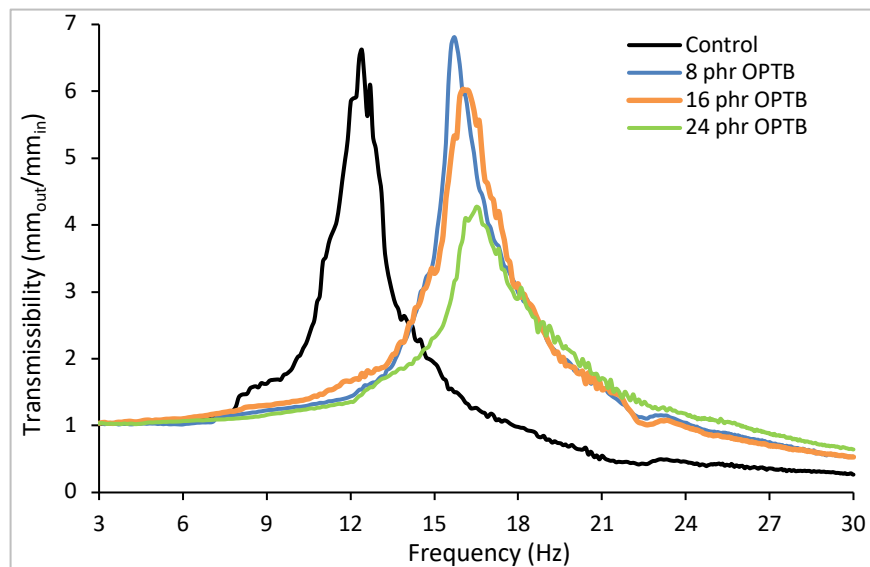


Figure 7.33: Effect of addition of OPTB on vibration transmissibility of DPNR latex foam.

According to Chan *et al.*¹³⁶, the resonance peak corresponds to the vibration-damping property of the material, whereas the lower the resonance peak, the higher the vibration-damping property (Table 7.11). A comparison between the neat DPNR latex foam and the neat ENR latex foam shows that the resonance peak of the neat ENR latex foam is lower than the neat DPNR latex

foam, indicating that the neat ENR latex foam has a greater damping property. The addition of 8 phr of OPTB into both DPNR and ENR latex foams did not show a significant change in resonance peak value but shifted to a greater higher frequency.

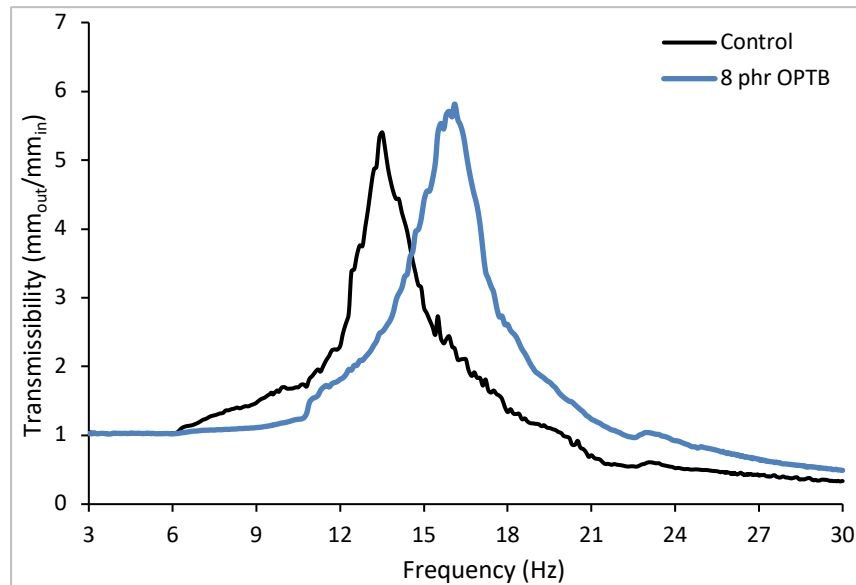


Figure 7.34: Effect of addition of OPTB on vibration transmissibility of ENR latex foam.

According to previous studies¹⁸²⁻¹⁸⁴, the harder the material the stronger the bonds, and the more energy required to cause resonance. This is correlates with results shown in Figure 7.29b, which found an increase in OPTB concentration led to an increase in hardness of the SpNR latex foam. However, the shifts in resonance frequency value to a higher frequency between DPNR latex foam loaded with 8 phr and 16 phr and 24 phr of OPTB appear to be small, contrary to what changes in hardness value indicate. It is hypothesized that OPTB added at 16 and 24 phr did not form noticeable further bonds with the latex but filled up the pores within the matrix instead. Further investigation is required to test this hypothesis. Nevertheless, it can be seen that increasing the concentration of OPTB from 8 to 24 phr has led to a steady decrease in the resonance peak value. This indicates that increasing the concentration of OPTB in the latex foam could result in higher vibration-damping value. This is in agreement with study¹⁹⁴ which found an increase of filler concentration in NR compound increased the damping properties, thus decrease the transmissibility at the resonance frequency. Previous studies^{81,203} stated that seat cushion applications in the transportation industry require material capable of dampening vertical vibration at frequencies below 11 Hz because this is the range that can cause the whole-body vibration syndrome. According to a recent study¹³⁶, the addition of natural fibers to foam material helped to enhance its damping performance. This study found that the vibration transmissibility curve of DPNR latex foam loaded with 24 phr OPTB exhibits the lowest curve at < 11 Hz rendering this combination the most promising damping material for seat cushion applications.

Table 7.11: Effect of addition of OPTB on vibration characteristics of SpNR latex foam

Type of material	Resonance peak	Resonance frequency (Hz)	Resonance value at 11 Hz
DPNR (control)	6.62	12.40	3.45
DPNR/8 phr OPTB	6.79	15.71	1.35
DPNR/16 phr OPTB	6.01	16.21	1.46
DPNR/24 phr OPTB	4.24	16.60	1.28
ENR (control)	5.40	13.51	1.86
ENR/8 phr OPTB	5.71	15.80	1.53

Information obtained from the resonance peak was used to calculate the damping ratio of the material (Table 7.12). As expected, the damping ratio of the DPNR latex foam loaded with 24 phr OPTB was the greatest. This result implies that a higher concentration of OPTB in the latex foam led to an increase in resistance against vibration wave transmissibility. According to Chan *et al.*¹³⁶, the vibrational damping effect of a foam material is further improved when the fibers are well-dispersed in the foam. As visualized in Figure 7.22, the OPTB not only disperses within the rubber matrix but also fills the latex foam-cells. Owing to its good filler-rubber interfacial adhesion, the walls of the foam will move together with the fibers when vibration is applied²⁶⁴. This suggests that the vibrational damping values reported here are close to the maximum achievable due to the good dispersion of OPTB. Additionally, the cellular structure of the OPTB also helps to minimize the vibration transmissibility in the material through dissipating the vibrational energy not only through the air inside the latex foam-cells, but also through the porous structures of OPTB^{136,265}. Nevertheless, while it is very beneficial to have a high damping ratio within the amplification region, an excessive damping ratio hinders the system within the isolation region¹⁹².

Table 7.12: Effect of addition of OPTB on damping ratio of SpNR latex foam

Type of material	Attenuation frequency (Hz)	Damping ratio (α)
DPNR (control)	16.90	0.14
DPNR/8 phr OPTB	24.22	0.15
DPNR/16 phr OPTB	24.01	0.17
DPNR/24 phr OPTB	26.06	0.24
ENR (control)	20.21	0.18
ENR/8 phr OPTB	23.00	0.18

As shown in Table 7.13 the neat DPNR latex foam has the lowest attenuation frequency compared to other material. This is expected because the softer the material the lower the attenuation frequency^{192,266}. However, when OPTB was added into the latex foam, the latex foam became

harder thus delaying its vibration isolation¹⁹³. According to Elmadih²⁶⁷, vibration-damping is different from vibration isolation in the sense that it reduces vibration transmissibility by using high mass or high stiffness material. It reduced the magnitude of vibration transmission in the amplification region, typically the resonance frequency range of the material. On the other hand, vibration isolation reduces the magnitude of vibration transmission by isolating certain frequency ranges through energy absorption resulting in much greater attenuation than damping. These opposing system properties have become a challenging issue for engineers and researchers to address. A stiffer material could lead to very low resonance peaks to become the ideal system in terms of vibration-damping. However, such a system would be delaying the vibration isolation region. The easiest way to determine whether a vibration damper or vibration isolator is needed, it is important to identify the frequencies of concern. Selecting the correct isolator will reduce the resonance peak lower and shift the frequencies of concern into the region of isolation, preventing them from penetrating the system. When the system's resonance peak cannot be reduced further and the frequencies of concern are located near or at the resonance peak, damping is the appropriate method of vibration control. Nevertheless, in many industrial applications, the ability of the material to dampen input vibration over a wide frequency range is important, and thus become a study of interest in future work.

7.4 Conclusion

This study explores the acoustic properties of SpNR latex foam. The results show that the highest STL value was exhibited by ENR (HD) latex foam, where the STL reached 44 dB at 6300 Hz with a 40 mm thick foam layer. Two factors influencing STL value are the density and thickness of the foam. The SAC value in the low-frequency range is governed by the density and thickness levels of the material, which aids in the absorption of low-frequency sound waves. On the other hand, in the high-frequency range, morphological characteristics such as pore size play an important role in determining the SAC value as a result of the shorter wavelengths concerned. As a result, SAC levels fluctuate as sound frequency rises. The NRC measurements revealed that increasing the foam material thickness from 10 mm to 20 mm to 40 mm raised the NRC for all foams, and DPNR (HD) produced the highest NRC value. In order to meet the fire rating requirements for acoustic foam for building applications, OPTB which was treated with alkaline and carbonized at 700 °C was added into the latex foam as a flame-retardant filler. However, the maximum volume of OPTB can be added is 24 phr. The addition of OPTB improved the STL value. The addition of OPTB to the SAC of SpNR latex foam, on the other hand, produced the opposite effect. This could be attributed to a decrease in porosity and an increase in material stiffness, two parameters

that influence the SAC value of acoustic foam materials. The addition of OPTB into SpNR latex foam decreased the burning velocity rate but the addition of OPTB up to 24 phr still did not meet the fire rating requirements for building applications. The effects of the addition of OPTB on the physical and mechanical properties of SpNR latex foam were investigated to explore the potential application of the material. The study found that the addition of OPTB improved physical properties such as hardness, elongation at break and dimensional stability of the latex foam. A hysteresis loss ratio study suggested that the addition of OPTB to SpNR latex foam enhanced the damping properties, making it suitable for applications that require significant impact absorption. A ball-rebound resilience study indicates that the addition of OPTB reduces the bouncing effect. As a result, the damping property of SpNR latex foam was improved. A vibration transmissibility study confirmed that the latex foam is suitable for vibration damping applications typically for high-frequency applications.

Chapter 8

Conclusions and recommendation for future work

8.1 Summary

The first part of the study demonstrates the method and composition for producing SpNR latex directly from field NR latex. In order to produce a 60 % TSC concentrated latex, ultrafiltration using membrane separation technology was used. Physicochemical properties of SpNR latex were found to be comparable with commercial LATZ latex except for viscosity value. ENR latex exhibits highest viscosity followed by DPNR and LATZ. This study also found that LATZ and DPNR latex behave more like viscous liquids, whilst ENR latex is more like an elastic solid. The non-ionic surfactant used during the preparation and modification process influenced the flow and deformation behavior of the ENR and DPNR latex. This study discovered that SpNR latex and normal latex (LATZ) have different levels of foamability. The foamability of SpNR latex is lower compared to normal latex (LATZ). Nevertheless, this study proved that both ENR latex and DPNR latex are suitable for the production of latex foam products. Foam collapse and foam coagulation are two main challenges in the production of SpNR latex foam which can be solved by altering the foaming levels and gelling ingredients. This study also found that foam density influenced the gelling time and volume shrinkage of the SpNR latex foam. In this study, an ideal compounding, foaming and gelling formulations to produce SpNR latex foam have been developed. The production of SpNR latex foam was carried out using the Dunlop batch foaming process.

In the second part of the study, SpNR latex was used to produce latex foam products. DPNR latex was used to produce a dual-density cervical shape latex foam pillow prototype, whereas the pillow has a lower density at the upper part and higher density at the lower part. The physical properties of the pillow also comply with the requirements stipulated in standard specifications. Pressure-mapping visualizes that a combination of dual density and cervical shape structure help to reduce the peak pressure value, thus expected to offer better pressure-relief performance compared to a normal pillow. The advantages of DPNR latex foam pillow not only offer excellent physical properties and good pressure-relief performance, but is also hypoallergenic.

Besides pillows, the DPNR latex was used to produce seat cushions for the transportation industry. Two major characteristics were examined which are pressure-relief performance and vibration transmissibility. The study found that the DPNR latex foam seat cushions has both excellent pressure-relief and vibration-isolation performance, suitable for the transportation industry that require isolation of higher frequency vibrations such as high-speed crafts, trains, and trucks.

Morphological study visualized the SpNR latex foam is an open-cell structure, which is beneficial for sound and vibration control applications. Therefore, in the third part of the study, SpNR latex was used to develop latex foam for acoustic foam for building applications. The study found that the thickness and density of the latex foam play a major role in influencing the sound transmission loss (STL) value. The highest STL is shown by the ENR latex foam (HD) with a foam layer 40 mm thick, whereas the STL value reached 44 dB at 6300 Hz. On the other hand, the sound absorption coefficient (SAC) value in the low-frequency range is governed by the density and thickness levels of the material, but in the high-frequency range, morphological characteristics such as pore size play an important role in determining the SAC value. As a result, the SAC levels fluctuate as the sound frequency increases. The noise reduction coefficient (NRC) measurement was used to represent a measure of the ability of a material to absorb noise over a broad frequency range. It was found that the NRC values increased as the foam material thickness increased from 10 mm to 20 mm to 40 mm. DPNR (HD) shows the highest NRC value. OPTB was used as a flame-retardant filler to improve the flame retardancy of the SpNR latex foam to meet the fire rating requirement for building applications. The addition of OPTB to SpNR latex foam up to 24 phr improved the thermal stability of the material, but was not sufficient to meet fire rating requirements for building applications. However, the study found that the addition of OPTB to SpNR latex foam increased the dimensional stability, elongation at break, and hardness of the SpNR latex foam. In addition to that, the OPTB/SpNR latex foam composite also has a high-damping property, making it appropriate for applications that require impact absorption, for example, in the transportation industry, where a high level of crashworthiness is a key aspect to improving the safety of the transport vehicle.

8.2 Study limitation and recommendation for future work

ENR latex only can be used to fabricate HD and MD latex foam. Therefore, ENR latex is not suitable for manufacturing latex foam pillow which requires a soft latex foam. The high density of ENR latex foam is also not suitable for the transportation industry because for the transportation

industry seat cushions need to be produced with low density (low weight) material, to ensure effective fuel or energy consumption. For sound and vibration control typically for building applications, both ENR and DPNR show excellent acoustics properties, but must first fulfill the fire rating requirements. The addition of OPTB as a flame-retardant filler improves the thermal stability of the foam but is not sufficient enough to meet the fire rating requirements. Using Forecast in Microsoft Excel, it is predicted that the OPTB/SpNR latex foam composite will meet the standard requirement if 32 phr of OPTB is loaded in the latex foam. However, in this study it was observed that the SpNR latex foam collapsed when 32 phr of OPTB was added. Therefore, in future work it is important to find a way to improve the fabrication process so that a higher concentration of OPTB can be loaded into the SpNR latex foam.

References

- ¹ S.A.R. Mahmud Iskandar, Epoxidized Natural Rubber in Vibration and Noise Control Applications, PhD Thesis, University of Sheffield, U.K., 2019.
- ² D.C. Blackley, *Polymer Latices and Technology. Volume 2: Types of Latices*, 2nd ed. (Chapman & Hall, London, U.K., 1997).
- ³ M.R. Fatimah Rubaizah, M.Y. Amir Hashim, Y. Nurul Hayati, A. Mohamad Asri, R. Roslim, and A.B. Rohani, *Rubber World* **259**, 32 (2018).
- ⁴ H. Rosniza, Structural Study of Epoxidized Natural Rubber (ENR-50) and Its Derivatives Synthesized via Epoxide Ring-Opening Reactions Using NMR Techniques, PhD Thesis, Universiti Sains Malaysia, 2015.
- ⁵ S. Siti Salina, A.A. Azira, C.A. Ahmad Kifli, A.R. Rohaidah, and N.I. Nik Intan, *J. Polym. Sci. Technol.* **2**, 36 (2017).
- ⁶ W. Ariyawiryanan, J. Nuinu, K. Sae-Heng, and S. Kawahara, *Energy Procedia* **34**, 728 (2013).
- ⁷ J. Yunyongwattanakorn, Y. Tanaka, S. Kawahara, W. Klinklai, and J. Sakdapipanich, *Rubber Chem. Technol.* **76**, 1228 (2003).
- ⁸ K. Shamsul, A.F. Ramly, N. Mohd Shukri, A.G. Bakri, and Q. Fourier, in *Int. Rubber Conf.* (Kuala Lumpur, Malaysia, 2019).
- ⁹ M. Bianchi and F. Scarpa, *Smart Mater. Struct.* **22**, (2013).
- ¹⁰ F. Fazli, B. Farahmand, F. Azadinia, and A. Amiri, *Med. J. Islam. Repub. Iran* **32**, 470 (2018).
- ¹¹ D. Cafuta, M. Abu-Rous, S. Jary, M. Scheffelmeyer, and T. Rijavec, *Text. Res. J.* **89**, 3722 (2019).
- ¹² L.J. Soal, C.M. Bester, B.S. Shaw, and C. Yelverton, *Heal. SA Gesondheid* **24**, 1 (2019).
- ¹³ X.Y. Lin and F.G. Wu, *Procedia Manuf.* **3**, 4429 (2015).
- ¹⁴ S.M. Halliwell, *Polymers in Building and Construction* (Rapra Technology Limited, Shawbury, U.K., 2002).
- ¹⁵ K.C. Frisch, *J. Macromol. Sci. Part A - Chem.* **15**, 1089 (1981).
- ¹⁶ S. Berezvai, Visco-Hyperelastic Characterization of Polymeric Foams, MSc. Thesis, Budapest University of Technology and Economics, Hungary, 2015.
- ¹⁷ V.G. Nuno, F. Artur, and B.T. Ana, *Materials (Basel)*. **11**, 1 (2018).
- ¹⁸ Z. Yang, H. Peng, W. Wang, and T. Liu, *J. Appl. Polym. Sci.* **116**, 2658 (2010).
- ¹⁹ S.N.I. Kudori and H. Ismail, *Cell. Polym.* **39**, 57 (2020).
- ²⁰ Y. Jongeun, *Indian J. Sci. Technol.* **8**, 135 (2015).
- ²¹ D.P. Strchan and I.M. Carey, *BMJ Open* **311**, 1053 (1995).
- ²² C. Jessica, *Wellness Fam.* 1 (2012).
- ²³ F.M. Casati, J.M. Sonney, H. Misprouve, A. Fanget, R. Herrington, and J. Tu, in *API 2001 Proc.* (2001).
- ²⁴ R.A. Lavin, M. Pappagallo, and K. V. Kuhlemeier, *Arch. Phys. Med. Rehabil.* **78**, 193 (1997).
- ²⁵ T.M. Tuan Muhammad, *Rubber Plantation and Processing Technologies* (Malaysian Rubber Board, Kuala Lumpur, Malaysia, 2009).
- ²⁶ The Malaysian Rubber Producers' Research Association, *The Natural Rubber Formulary and Property* (Inprint of Luton Limited, London, U.K., 1984).
- ²⁷ D.C. Blackley, *Polymer Latices and Technology. Volume 3: Applications of Latices*, 2nd ed. (Chapman & Hall, London, U.K., 1997).
- ²⁸ K. Xu, C. He, Y. Wang, Y. Luo, S. Liao, and Z. Peng, *Adv. Mater. Res.* **396–398**, 478 (2012).
- ²⁹ Y. Tanaka and L. Tarachiwin, *Rubber Chem. Technol.* **82**, 283 (2009).
- ³⁰ L.M. Wu, S.Q. Liao, P. Qu, R.J. Zhou, and B.X. Wang, *Adv. Mater. Res.* **1052**, 231 (2014).
- ³¹ M.Y. Amir Hashim, R. Roslim, and M.W. Rosni, *J. Rubber Res.* **15**, 243 (2012).
- ³² R. Roslim and M.Y. Amir Hashim, *J. Rubber Res.* **13**, 125 (2010).
- ³³ T. Akabane, *Int. Polym. Sci. Technol.* **43**, 369 (2016).
- ³⁴ Malaysian Rubber Council, *Natural Rubber Statistics 2020* (Kuala Lumpur, Malaysia, 2020).

- ³⁵ M.Y. Amir Hashim and A. Ikram, in *Int. Symp. Green Technol. Glob. Carbon Cycle Asia* (Nagaoka, Japan, 2009).
- ³⁶ M.Y. Amir Hashim and M.W. Rosni, in *IRRDB Rubber Technol. Semin.* (Ho Chi Minh City, Vietnam, 2009).
- ³⁷ R. Roslim, K.L. Mok, M.R. Fatimah Rubaizah, K. Shamsul, K.S. Tan, and M.Y. Amir Hashim, *J. Rubber Res.* **21**, 277 (2018).
- ³⁸ R.A. Bakar and A. Mustafa, *J. Acad.* **8**, 58 (2020).
- ³⁹ C. Burkhart, J. Schloemer, and M. Zirwas, *Cutis* **96**, 369 (2015).
- ⁴⁰ J.J. Condemni, *J. Allergy Clin. Immunol.* **110**, 107 (2002).
- ⁴¹ E.W. Madge, *Latex Foam Rubber* (MacLaren and Sons Ltd., London, U.K., 1962).
- ⁴² S. Norhazariah, A.R. Azura, A. Baharin, and R. Sivakumar, in *3rd Adv. Mater. Conf.* (Langkawi Island, Malaysia, 2016).
- ⁴³ R. Roslim, M.Y. Amir Hashim, and P.T. Augurio, *J. Eng. Sci.* **8**, 15 (2012).
- ⁴⁴ R. Roslim, M.R. Fatimah Rubaizah, K. Shamsul, K.L. Mok, and M.Y. Amir Hashim, *J. Eng. Appl. Sci.* **12**, 5560 (2017).
- ⁴⁵ E. David, *Handbook of Polymer Foams* (Rapra Technology Ltd., Shawbury, Shropshire, UK, 2004).
- ⁴⁶ R. Roslim, *Rubber Foam: Unpublished MRB Quarterly Report* (2019).
- ⁴⁷ STALAM, (2020).
- ⁴⁸ W. Kaewsakul, K. Sahakaro, W.K.. Dierkes, and J.W.M. Noordermeer, *KGK Kautschuk Gummi Kunststoff* **66**, 33 (2013).
- ⁴⁹ J. Nienaber, *Rubber Plast. News* 14 (2013).
- ⁵⁰ The European Standard, *DIN EN 1957: Furniture - Beds and Mattresses - Test Methods for the Determination of Functional Characteristics and Assessment Criteria* (2012).
- ⁵¹ International Organization for Standardization, *ISO 2439: Flexible Cellular Polymeric Materials - Determination of Hardness (Indentation Technique)* (2008).
- ⁵² American Society for Testing and Materials, *ASTM D3574: Standard Test Methods for Flexible Cellular Materials — Slab, Bonded, and Molded Urethane Foams* (2012).
- ⁵³ Malaysian Standard, *Malaysian Standard MS679: 2011. Specification for Latex Foam Rubber Mattresses for Domestic and General Use* (Department of Standards Malaysia, 2011).
- ⁵⁴ B. Martin, G. Miroslav, G. Milan, and R. Daniel, *Wood Res.* **61**, 1003 (2016).
- ⁵⁵ S. Ramasamy, H. Ismail, and Y. Munusamy, *BioResources* **8**, 4258 (2013).
- ⁵⁶ K. Prasad Rajan, D.B. Dhilipraj, R. Manikandan, and N.R. Veena, *Cell. Polym.* **30**, 13 (2011).
- ⁵⁷ S.J. Gordon, K.A. Grimmer-Somers, and P.H. Trott, *J. Pain Res.* **3**, 137 (2010).
- ⁵⁸ D.M. Margarida Gaspar, M. Adilson, G. Tania, and P. Teresa, *Heal. Educ. Care* **2**, 1 (2017).
- ⁵⁹ C.M. Chow, *Int. J. Environ. Res. Public Health* **17**, 17 (2020).
- ⁶⁰ R. Jackson, *Clin. Orthop. Relat. Res.* **468**, 1739 (2010).
- ⁶¹ S. Ren, D.W.C. Wong, H. Yang, Y. Zhou, J. Lin, and M. Zhang, *PeerJ* **4**, 1 (2016).
- ⁶² J.G. Her, D.H. Ko, J.H. Woo, and Y.E. Choi, *J. Phys. Ther. Sci.* **26**, 377 (2014).
- ⁶³ S. Liu, Y.L. Ms, and J.L. Ms, *J. Chiropr. Med.* **10**, 229 (2011).
- ⁶⁴ N. Shields, N. Taylor, T. Polak, and J. Capper, *New Zeal. J. Physiother.* **34**, 3 (2006).
- ⁶⁵ M.Y. Jeon, H.C. Jeong, S.W. Lee, W. Choi, J.H. Park, S.J. Tak, D.H. Choi, and J. Yim, *Toboku J. Exp. Med.* **233**, 183 (2014).
- ⁶⁶ K. Georgios, S. Arlindo, and F. Mihail, *Compos. Part B Eng.* **49**, 120 (2019).
- ⁶⁷ S. Poulidikou, *Integration of Design for Environment in the Vehicle Manufacturing Industry in Sweden: Focus on Practices and Tools*, PhD Thesis, KTH, Royal Institute of Technology, Sweden, 2013.
- ⁶⁸ T. Eduardo, *Polymer Composite Materials Based on Bamboo Fibres*, PhD Thesis, KU Leuven, Belgium, 2014.
- ⁶⁹ Grand View Research, *Mark. Anal. Rep.* (2019).
- ⁷⁰ H.M. Lim and M.Y. Amir Hashim, *J. Rubber Res.* **14**, 41 (2011).

- ⁷¹ Malaysian Standard, *Malaysian Standard MS 2623: 2016. Rubber - Identification of β -Sitosterol in Natural Rubber* (Department of Standards Malaysia, 2016).
- ⁷² B.E. Boor, M.P. Spilak, J. Laverge, A. Novoselac, and Y. Xu, *Build. Environ.* **125**, 528 (2017).
- ⁷³ A. Capíková, D. Tesařova, J. Hlavaty, A. Ekielski, and P.K. Mishra, *Adv. Polym. Technol.* **2019**, 1 (2019).
- ⁷⁴ P. Fitzharris, R. Siebers, and J. Crane, *Clin. Exp. Allergy* **29**, 429 (1999).
- ⁷⁵ S. Miri, Z. Pourpak, A. Zarinara, M. Heidarzade, A. Kazemnejad, G. Kardar, A. Firooz, and A. Moin, in *Allergy Asthma Proc.* (2007), pp. 557–563.
- ⁷⁶ H. Chardin, F.X. Desvaux, C. Mayer, H. Sénéchal, and G. Peltre, *Int. Arch. Allergy Immunol.* **119**, 239 (1999).
- ⁷⁷ M. Leuzzi, C. Vincenzi, A. Sechi, C. Tomasini, D. Giuri, B.M. Piraccini, and M. La Placa, *Contact Dermatitis* **81**, 404 (2019).
- ⁷⁸ Y. Yamamoto, P.T. Nghia, W. Klinklai, T. Saito, and S. Kawahara, *J. Appl. Polym. Sci.* **107**, 2329 (2008).
- ⁷⁹ K. Cornish, G. M. Bates, J.L. Slutzky, A. Meleshchuk, W. Xie, K. Sellers, R. Mathias, M. Boyd, R. Castaneda, M. Wright, and L. Borel, *Biol. Med.* **11**, 1 (2019).
- ⁸⁰ K.M. George, G. Rajammal, G. Amma, and N.M. Mathew, *J. Rubber Res.* **10**, 171 (2007).
- ⁸¹ M. Kolich, S.D. Essenmacher, and J.T. McEvoy, *J. Sound Vib.* **281**, 409 (2005).
- ⁸² X. Zhang, Y. Qiu, and M.J. Griffin, *Int. J. Ind. Ergon.* **48**, 36 (2015).
- ⁸³ O. Shechtman, C.S. Hanson, D. Garrett, and P. Dunn, *Occup. Ther. J. Res.* **21**, 29 (2001).
- ⁸⁴ H. Iftekhhar, R.M.W. Ullah Khan, M.A. Asghar, A. Qadeer, M. Umair, Y. Nawab, and S.T.A. Hamdani, *J. Automob. Eng.* **234**, 645 (2020).
- ⁸⁵ J.M. Neil, *Human Response to Vibration* (CRC Press, Washington, D.C., USA, 2005).
- ⁸⁶ S. Foteini, T. Martin, V.T. Arjan, and T. Michela, in *Inter Noise* (San Francisco, California, USA., 2015).
- ⁸⁷ C. Gambino, (2015).
- ⁸⁸ C. Bermano, D. Boote, T. Pais, and S. McCartan, 13 (2015).
- ⁸⁹ S. Shafizah, Sound Absorption Characteristics of Natural Fiber Filled in Flexible Foam Upon UV Irradiation Exposure, MSc. Thesis, Universiti Tun Hussein Onn Malaysia, 2016.
- ⁹⁰ A. Abbad, K. Jaboviste, M. Ouisse, and N. Dauchez, *J. Cell. Plast.* **54**, 651 (2018).
- ⁹¹ M. Sararat, Acoustic and Thermal Properties of Recycled Porous Media, PhD Thesis, University of Bradford, 2011.
- ⁹² K. V Horoshenkov, in *22 Int. Congr. Sound Vib.* (2015), pp. 12–16.
- ⁹³ A.A. Lamyaa, R. Raja Ishak, and A.R. Roslan, *Am. J. Appl. Sci.* **10**, 1307 (2013).
- ⁹⁴ A.L. Hanif, Y. Musli Nizam, Z. Izzudding, S. Mathan, G. Mohd. Imran, and M.H. Mohamed Nasrul, *J. Eng. Appl. Sci.* **11**, 7670 (2016).
- ⁹⁵ B. Muhammad Khusairy, Investigation of Acoustical and Mechanical Properties of Epoxy Based Natural Fibre Composites, MSc. Thesis, Swinburne University of Technology, Malaysia, 2015.
- ⁹⁶ H. Kim, Hybrid Composites with Natural Fibres, MSc. Thesis. University of Birmingham, U.K., 2014.
- ⁹⁷ M. Vinay and S. Anshuman, *Org. Med. Chem.* **4**, 8 (2017).
- ⁹⁸ X. Zhu, B.J. Kim, Q.W. Wang, and Q. Wu, *BioResources* **9**, 1764 (2014).
- ⁹⁹ F. Setaki, M. Tenpierik, A. Van Timmeren, and M. Turrin, in *44th Int. Congr. Expo. Noise Control Eng.* (California, USA, 2015).
- ¹⁰⁰ S.E. Roper, A Room Acoustics Measurement System Using Non-Invasive Microphone Arrays, PhD Thesis. University of Birmingham, U.K., 2009.
- ¹⁰¹ S. Palk, M. De Geest, and K. Vansant, *Sound Vib.* **47**, 10 (2013).
- ¹⁰² C. Okolieocha, D. Raps, K. Subramaniam, and V. Altstädt, *Eur. Polym. J.* **73**, 500 (2015).
- ¹⁰³ T.G. Hawkins, Studies and Research Regarding Sound Reduction Materials, Master thesis, California Polytechnic State University, USA, 2014.

- ¹⁰⁴ R. Roslim, K. Shamsul, M.R. Fatimah Rubaizah, K.L. Mok, and A.H. Aziana, *Malaysian Rubber Technol. Dev.* **18**, 38 (2018).
- ¹⁰⁵ W.H. Tan, E.A. Lim, H.G. Chuah, E.M. Cheng, and C.K. Lam, *Int. J. Mech. Mechatronics Eng.* **16**, 33 (2016).
- ¹⁰⁶ W.H. Tan and C.F. Sin, *Int. J. Automot. Mech. Eng.* **15**, 6001 (2018).
- ¹⁰⁷ J.Y. Chen, in (Woodhead Publishing Limited, 2010), pp. 184–201.
- ¹⁰⁸ C.S.L. Baker, I.R. Gelling, and R. Newell, *Rubber Chem. Technol.* **58**, 67 (1985).
- ¹⁰⁹ S.P. Vernekar, M.B. Sabne, S.D. Patil, A.S. Patil, S.B. Idage, C. V. Avadhani, and S. Sivaram, *J. Appl. Polym. Sci.* **44**, 2107 (1992).
- ¹¹⁰ V. Devaraj, M.N. Zairossani, S. Pretibaa, and I. Aimi Izyana, Malaysian Patent Application Number: PI 2012004868 (2012).
- ¹¹¹ M.R. Fatimah Rubaizah, V. Devaraj, A.R. Mohamad Akmal, M.N. Zairossani, D. Dazylah, and A.A. Azira, Malaysian Patent Application Number: PI2017700457 (2017).
- ¹¹² Y.A. Veerasamy, Devaraj, Nik Meriam Sulaiman, J. Nambiar, *J. Rubber Res.* **6**, 12 (2003).
- ¹¹³ V. Devaraj, M.N. Zairossani, and S. Pretibaa, *J. Appl. Mem. Sci. Technol.* **4**, 13 (2006).
- ¹¹⁴ M. Ahmad Khairul, *Malaysian Rubber Technol. Dev.* **1**, 14 (2016).
- ¹¹⁵ International Organization for Standardization, *ISO 1652: Rubber Latex - Determination of Apparent Viscosity by the Brookfield Test Method* (2011).
- ¹¹⁶ International Organization for Standardization, *ISO 35: Natural Rubber Latex Concentrate — Determination of Mechanical Stability Time* (2004).
- ¹¹⁷ H. Hasma, *J. Nat. Rubber Res.* **7**, 102 (1992).
- ¹¹⁸ A.J. Durbateki and C.M. Miles, *Anal. Chem.* **37**, 1231 (1965).
- ¹¹⁹ H. Fatin and H.C. Chin, in *Flex. Stretchable Electron. Compos.* (2016), pp. 37–59.
- ¹²⁰ Malaysian Rubber Board, *MRB In-House Test Method UPB/P/022-Determination of Epoxidised Level via Proton Nuclear Magnetic Resonance Spectroscopy* (2017).
- ¹²¹ American Society for Testing and Materials, *ASTM D5712-15: Standard Test Method for Analysis of Aqueous Extractable Protein in Latex, Natural Rubber, and Elastomeric Products Using the Modified Lowry Method* (2009).
- ¹²² E.L. Ong, in *Latex 2001 Conf.* (Munich, Germany, 2001).
- ¹²³ M.S.N.O.R. Qamarina, K.L. Mok, A.Y. Tajul, and R.N.U.R. Fadilah, *J. Rubber Res.* **13**, 240 (2019).
- ¹²⁴ Malaysian Rubber Board, *MRB In-House Test Method UPB/P/003a-Identification and Quantification of Residual Chemicals* (2017).
- ¹²⁵ K. Hillier, D.A. King, and C. Henneuse, *Cell. Polym.* **28**, 113 (2009).
- ¹²⁶ K. Hillier, T. Schupp, and I. Carney, *Cell. Polym.* **22**, 237 (2003).
- ¹²⁷ N. Yoganandan, F.A. Pintar, J. Zhang, and J.L. Baisden, *J. Biomech.* **42**, 1177 (2009).
- ¹²⁸ TECAM, *Accessed Novemb. 2020* (n.d.).
- ¹²⁹ International Organization for Standardization, *ISO 12219-2:2012. Interior Air of Road Vehicles- Part 2: Screening Method for the Determination of the Emissions of Volatile Organic Compounds from Vehicle Interior Parts and Materials- Bag Method* (2012).
- ¹³⁰ American Society for Testing and Materials, *ASTM D2240: Standard Test Methods for Rubber Property - Durometer Softness* (2003).
- ¹³¹ International Organization for Standardization, *ISO 10534-2: Determination of Sound Absorption Coefficient and Impedance in Impedance Tubes - Part 2: Transfer-Function Method* (1998).
- ¹³² J.P. Guyer, F. Asce, and F. Aei, *An Introduction to Building Acoustics and Noise Control* (CED, Inc., California, USA, 2009).
- ¹³³ A. Giovanni, *Vibro-Acoustic* (SCS & Partners, Padova, Italy, 2015).
- ¹³⁴ S. Kamaruddin, Long-Term Mechanical Properties of Rubber, PhD. Thesis. University of Southampton, Southampton, U.K., 2013.
- ¹³⁵ American Society for Testing and Materials, *Standard Test Methods for Vibration (Vertical Linear Motion) Test of Products* (2022).

- ¹³⁶ W.S. Chan, G. Mohd Imran, and I.I. Maizlinda, *Int. J. Automot. Mech. Eng.* **7**, 1031 (2013).
- ¹³⁷ I. Zaman, A.L. Mohd Tobi, B. Manshoor, A. Khalid, and N.A. Mohd Amin, *ARPN J. Eng. Appl. Sci.* **11**, 2308 (2016).
- ¹³⁸ S. Chuayjuljit, P. Mungmeechai, and A. Boonmahitthisud, *J. Elastomers Plast.* **49**, 99 (2017).
- ¹³⁹ G.F. Sandra, Improving the Fire Behavior of Flexible Polyurethane Foams Using Eco-Friendly Fillers, PhD thesis. Universidad del Pais Vasco, Leioa, Spain., 2018.
- ¹⁴⁰ M.R. Ketabchi, M. Khalid, and R. Walvekar, *J. Eng. Sci. Technol.* **12**, 797 (2017).
- ¹⁴¹ International Organization for Standardization, *ISO 9772: Cellular Plastics - Determination of Horizontal Burning Characteristics of Small Specimens Subjected to a Small Flame* (2001).
- ¹⁴² V. Jaya Kumar, M.Y. Khairul Muis, A. Mohamed Kheireddine, and S. Nik Meriam, International Publication Number: WO 2016/204601 AI (2016).
- ¹⁴³ V. Devaraj, Fouling Studies on Natural Rubber Skim Latex Concentration Using Integrated Ultrafiltration Membrane System, PhD Thesis. Universiti Teknologi Malaysia, Malaysia, 2015.
- ¹⁴⁴ K. Nawamawat, J.T. Sakdapipanich, and C.C. Ho, *Macromol. Symp.* **288**, 95 (2010).
- ¹⁴⁵ T. Jitladda and P. Rojruthai, in *Biotechnol. - Mol. Stud. Nov. Appl. Improv. Qual. Hum. Life*, edited by R. Sammour (Intechopen, Rijeka, Croatia, 2012), pp. 213–238.
- ¹⁴⁶ L. Tarachiwin, J.T. Sakdapipanich, and Y. Tanaka, *Rubber Chem. Technol.* **78**, 694 (2005).
- ¹⁴⁷ A.J. Chan, K. Steenkeste, M. Eloy, D. Brosson, F. Gaboriaud, and M.P. Fontaine-Aupart, *Rubber Chem. Technol.* **88**, 248 (2015).
- ¹⁴⁸ M. Singh, T.F. Tadros, C. Solans, K. Booten, B. Leveck, and J. Esquena, *Langmuir* **35**, 16978 (2019).
- ¹⁴⁹ D.T.N. Chen, Q. Wen, P.A. Janmey, J.C. Crocker, and A.G. Yodh, *Annu. Rev. Condens. Matter Phys.* **1**, 301 (2010).
- ¹⁵⁰ S. Jatuporn, Rheological Properties of Natural Rubber Latex, PhD Thesis, Suranaree University of Technology, Thailand, n.d.
- ¹⁵¹ S. Manroshan and M.R. Fatimah Rubaizah, *J. Rubber Res.* **22**, 153 (2019).
- ¹⁵² C.A. Ruslimie, M.Y. Norhanifah, M.R. Fatimah Rubaizah, and M. Asrul, in *3rd Int. Conf. Chem. Agric. Med. Sci.* (Singapore, 2015).
- ¹⁵³ D. Dazylah and M.S. Ma'zam, *Pertanika J. Sci. Technol.* **18**, 421 (2010).
- ¹⁵⁴ M. Siti Nor Qamarina, M.R. Fatimah Rubaizah, A. Nurul Suhaira, and M.Y. Norhanifah, *AIP Conf. Proc.* **1901**, (2017).
- ¹⁵⁵ R. Yoksan, *Kasetsart J. (Nat. Sci.)* **42**, 325 (2008).
- ¹⁵⁶ P. Rojruthai, T. Kantaram, and J. Sakdapipanich, *J. Rubber Res.* **23**, 353 (2020).
- ¹⁵⁷ C. Huang, J. Zhang, X. Cai, G. Huang, and J. Wu, *J. Polym. Res.* **27**, (2020).
- ¹⁵⁸ J. Tangpakdee and Y. Tanaka, *Rubber Chem. Technol.* **70**, 1851 (1997).
- ¹⁵⁹ P. Sollich, F. Lequeux, P. Hébraud, and M.E. Cates, *Phys. Rev. Lett.* **78**, 2020 (1997).
- ¹⁶⁰ K.K. Sasidharan, R. Joseph, S. Palaty, K.S. Gopalakrishnan, G. Rajammal, and P.V. Pillai, *J. Appl. Polym. Sci.* **97**, 1804 (2005).
- ¹⁶¹ International Organization for Standardization, *ISO 126: Natural Rubber Latex Concentrate - Determination of Dry Rubber Content* (2005).
- ¹⁶² S. Mathew and S. Varghese, *Rubber Sci.* **31**, 249 (2018).
- ¹⁶³ Arvind Mafatal Group, *NR Latex & Latex Products* (Nocil Limited, Gujarat, India, 2010).
- ¹⁶⁴ Q. Sun, L. Tan, and G. Wang, *Int. J. Mod. Phys. B* **22**, 2333 (2008).
- ¹⁶⁵ M. Safouane, A. Saint-Jalmes, V. Bergeron, and D. Langevin, *Eur. Phys. J. E* **19**, 195 (2006).
- ¹⁶⁶ D.J. McKeand, *Ind. Eng. Chem.* **43**, 415 (1951).
- ¹⁶⁷ C.R. Hall, B.L. Campbell, B.K. Behe, C. Yue, R.G. Lopez, and J.H. Dennis, *HortScience* **45**, 583 (2010).
- ¹⁶⁸ V. Albino, A. Balice, and R.M. Dangelico, *Bus. Strateg. Environ.* **18**, 83 (2009).
- ¹⁶⁹ L. Simão and A. Lisboa, *Procedia Manuf.* **12**, 183 (2017).
- ¹⁷⁰ W.G.I.U. Rathnayake, H. Ismail, A. Baharin, I.M.C.C.D. Bandara, and S. Rajapakse, *J. Appl. Polym. Sci.* **131**, 1 (2014).

- ¹⁷¹ Z. Chen, Y. Li, R. Liu, D. Gao, Q. Chen, Z. Hu, and J. Guo, *PLoS One* **9**, 1 (2014).
- ¹⁷² M.S. Thomas, A Comparative Analysis of Air-Inflated and Foam Seat Cushions for Truck Seats, Master thesis. Virginia Polytechnic Institute and State University, USA, 2002.
- ¹⁷³ K. Oz, B. Merav, S. Sara, and D. Yael, *Environ. Sci. Technol.* **53**, 9171 (2019).
- ¹⁷⁴ S. Sirikulchaikij, B. Nooklay, R. Kokoo, and M. Khangkhamano, *Mater. Sci. Forum* **962**, 96 (2019).
- ¹⁷⁵ B. Nancy, *Appl. Nurs. Res.* **10**, 111 (1997).
- ¹⁷⁶ A.B. Othman, G.A.W. Murray, and A.W. Birley, *J. Rubber Res.* **11**, 183 (1996).
- ¹⁷⁷ V.A. Lucille, The Effect of Proteins on the Aging Properties of Radiation Vulcanized Natural Rubber Latex, MSc. thesis. University of Santo Tomas, Philippine., 1993.
- ¹⁷⁸ C. Bendjaouahdou and S. Bensaad, *Int. J. Ind. Chem.* **9**, 345 (2018).
- ¹⁷⁹ D. Lhamo and C. McMahan, *Rubber Chem. Technol.* **90**, 387 (2017).
- ¹⁸⁰ S. Tuampoemsab, J. Sakdapipanich, and Y. Tanaka, *Rubber Chem. Technol.* **80**, 159 (2007).
- ¹⁸¹ A.R. Azura, An Investigation of the Effect of Ageing on the Physical Properties of Natural Rubber, PhD Thesis. Queen Mary University of London, London, U.K., 2003.
- ¹⁸² G.Y. Li and J.L. Koenig, *Rubber Chem. Technol.* **78**, 355 (2005).
- ¹⁸³ R. Roslim, K.S. Tan, and J. Jefri, *J. Rubber Res.* **21**, 1 (2018).
- ¹⁸⁴ A. Samsuri, *Shreir's Corrosion. Volume 3: Degradation of Natural Rubber and Synthetic Elastomers* (Elsevier, Amsterdam, 2010).
- ¹⁸⁵ S. Sirikulchaikij, R. Kokoo, and M. Khangkhamano, *Mater. Lett.* **260**, 1 (2020).
- ¹⁸⁶ C.W. Lung, T.D. Yang, B.A. Crane, J. Elliott, B.E. Dicianno, and Y.K. Jan, *Biomed Res. Int.* **2014**, (2014).
- ¹⁸⁷ R. Xie, C. Ulven, and B. Khoda, *Procedia Manuf.* **26**, 132 (2018).
- ¹⁸⁸ L. Yu-Chi, L. Chih-Yun, and W. Mao-Jiun, *Int. J. Ind. Ergon.* **78**, 102979 (2020).
- ¹⁸⁹ A. Radwan, P. Fess, D. James, J. Murphy, J. Myers, M. Rooney, J. Taylor, and A. Torii, *Sleep Heal.* **1**, 257 (2015).
- ¹⁹⁰ N. V. Gama, A. Ferreira, and A. Barros-Timmons, *Materials (Basel)*. **11**, 1 (2018).
- ¹⁹¹ S. Bergstrand, Preventing Pressure Ulcers by Assessment of the Microcirculation in Tissue Exposed to Pressure, PhD. Thesis, Linköping University, Sweden, 2014.
- ¹⁹² H. Janik, Low-Frequency Vibration Attenuation Using Multi Degree of Freedom Quasi-Zero Stiffness Systems, Msc. Thesis. The University of Guelph, Toronto, Canada, 2022.
- ¹⁹³ N. Ab Latif and A.Z.M. Rus, *J. Mech. Eng. Sci.* **6**, 772 (2014).
- ¹⁹⁴ J.S. Ronald, in *Handb. Ind. Polyethyl. Technol.* (2016), pp. 381–410.
- ¹⁹⁵ X. Xie, J. Diao, Y. Xu, and Z. Zhang, *J. Low Freq. Noise Vib. Act. Control* **37**, 1164 (2018).
- ¹⁹⁶ K. Olausson, On Evaluation and Modelling of Human Exposure to Vibration and Shock on Planing High-Speed Craft, PhD Thesis. KTH Royal Institute of Technology, Stockholm, Sweden., 2015.
- ¹⁹⁷ N.J. Mills, *Cell. Polym.* **25**, 293 (2006).
- ¹⁹⁸ A.B. Chai, S. Kamaruddin, K.Y. Tshai, I. Kong, B.J.H. Tay, and S.Y. Ch'ng, *J. Eng. Appl. Sci.* **11**, 128 (2016).
- ¹⁹⁹ M.F. Alzoubi, E.Y. Tanbour, and R. Al-Wakedb, *ASME 2011 Int. Mech. Eng. Congr. Expo.* **9**, 101 (2011).
- ²⁰⁰ M. Krebs and R. Hubel, in *CPI Conf.* (American Chemistry Council, 2016).
- ²⁰¹ Ł. Piszczyk, M. Danowska, A. Mietlarek-Kropidłowska, M. Szyszka, and M. Strankowski, *J. Therm. Anal. Calorim.* **118**, 901 (2014).
- ²⁰² S. Adnan, M.T.I. Tuan Noor, N.H. Ain, K.P.P. Devi, N.S. Mohd, Y. Shoot Kian, Z.B. Idris, I. Campara, C.M. Schiffman, K. Pietrzyk, V. Sendijarevic, and I. Sendijarevic, *J. Appl. Polym. Sci.* **134**, 1 (2017).
- ²⁰³ F.M. Casati, R.M. Herrington, R. Broos, and Y. Miyazaki, *J. Cell. Plast.* **34**, 430 (1998).
- ²⁰⁴ M.L. Ju, H. Jmal, R. Dupuis, and E. Aubry, *Polym. Eng. Sci.* **55**, 1795 (2015).
- ²⁰⁵ M.L. Ju, S. Mezghani, H. Jmal, R. Dupuis, and E. Aubry, *Cell. Polym.* **32**, 21 (2013).

- ²⁰⁶ R. Roslim, K.L. Mok, M.R. Fatimah Rubaizah, K. Shamsul, and K.S. Tan, *J. Phys. Chem. Mater.* **7**, 1 (2020).
- ²⁰⁷ H.O. Ahmed, J.H. Dennis, O. Badran, M. Ismail, S.G. Ballal, A. Ashoor, and D. Jerwood, *Ann. Occup. Hyg.* **45**, 371 (2001).
- ²⁰⁸ I. Croy, M.G. Smith, and K.P. Waye, *BMJ Open* **3**, 1 (2013).
- ²⁰⁹ B. Groothoff, *Physical Hazards: Noise and Vibration* (Safety Institute of Australia Ltd., Victoria, Australia, 2012).
- ²¹⁰ O.S. Hong, M.J. Kerr, G.L. Poling, and S. Dhar, *Disease-a-Month* **59**, 110 (2013).
- ²¹¹ K.P. Waye, *Encycl. Environ. Heal.* 240 (2011).
- ²¹² S.K. Jain, P. Shrivage, and N. V Karanth, in *Automot. Mater. Conf.* (Pune, India, 2010).
- ²¹³ S. Abdollahi Baghban, M. Khorasani, and G.M.M. Sadeghi, *J. Appl. Polym. Sci.* **135**, (2018).
- ²¹⁴ B. Merillas, F. Villafañe, and Á. Miguel, *Polymers (Basel)*. (2022).
- ²¹⁵ W. Chen, S. Liu, L. Tong, and S. Li, *Theor. Appl. Mech. Lett.* **6**, 42 (2016).
- ²¹⁶ S. Amares, E. Sujatmika, T.W. Hong, R. Durairaj, and H.S.H.B. Hamid, in *Int. Conf. Adv. Des. Manuf. Eng.* (Shenzhen, China, 2017).
- ²¹⁷ L.Q.N. Tran, K. Huang, A.V. Rammohan, W.S. Teo, and H.P. Lee, in *17th Eur. Conf. Compos. Mater.* (Munich, Germany, 2016).
- ²¹⁸ M. Neri, E. Levi, E. Cuerva, F. Pardo-Bosch, A.G. Zabaleta, and P. Pujadas, *Appl. Sci.* **11**, 1 (2021).
- ²¹⁹ D. Balasubramanian, S. Rajendran, B. Srinivasan, and N. Angamuthu, *Materials (Basel)*. **13**, 1 (2020).
- ²²⁰ N. Rastegar, A. Ershad-Langroudi, H. Parsimehr, and G. Moradi, *Iran. Polym. J.* (2022).
- ²²¹ E. Jayamani, S. Hamdan, and N.B. Suid, *Appl. Mech. Mater.* **315**, 577 (2013).
- ²²² T. Yamashita, K. Suzuki, S. Nishino, and Y. Tomota, *Mater. Trans.* **49**, 345 (2008).
- ²²³ C. Fan, Y. Tian, Z.Q. Wang, J.K. Nie, G.K. Wang, and X.S. Liu, in *Glob. Conf. Polym. Compos. Mater.* (Guangzhou, China, 2017).
- ²²⁴ R. Roslim, M.R. Fatimah Rubaizah, K. Shamsul, K.L. Mok, and M.Y. Amir Hashim, Malaysian Patent Application Number: 2018700712 (2018).
- ²²⁵ F. Asdrubali, S. Schiavoni, and K. V. Horoshenkov, *J. Build. Acoust.* **19**, 283 (2012).
- ²²⁶ M. Ranjbar, in *4th Int. Symp. Railw. Syst. Eng.* (Karabuk, Turkey, 2018).
- ²²⁷ D. Wennberg, Multi-Functional Composite Design Concepts for Rail Vehicle Car Bodies, PhD thesis. KTH Royal Institute of Technology, Sweden., 2013.
- ²²⁸ B.P. Chang, S. Thakur, A.K. Mohanty, and M. Misra, *Sci. Rep.* **9**, 1 (2019).
- ²²⁹ Z. Kovačević, S. Flinčec Grgac, and S. Bischof, *Polymers (Basel)*. **13**, 1 (2021).
- ²³⁰ C.K. Abdullah, M. Jawaid, H.P.S. Abdul Khalil, A. Zaidon, and A. Hadiyane, *BioResources* **7**, 2948 (2012).
- ²³¹ N. Hamzah, K. Tokimatsu, and K. Yoshikawa, *Sustain.* **11**, 1 (2019).
- ²³² FGV Holdings Berhad, (n.d.).
- ²³³ R. Kalaivani, L.S. Ewe, O.S. Zaroog, H.S. Woon, and I. Zawawi, *Int. J. Adv. Appl. Sci.* **5**, 88 (2018).
- ²³⁴ N.A. Latip, A.H. Sofian, M.F. Ali, S.N. Ismail, and D.M.N.D. Idris, *Mater. Today Proc.* **17**, 1105 (2019).
- ²³⁵ T. Gurunathan, S. Mohanty, and S.K. Nayak, *Compos. Part A Appl. Sci. Manuf.* **77**, 1 (2015).
- ²³⁶ S. Srivaro, N. Matan, and F. Lam, *J. Wood Sci.* **64**, (2018).
- ²³⁷ L.N. Megashah, H. Ariffin, M.R. Zakaria, and M.A. Hassan, in *Wood Biofiber Int. Conf.* (2017).
- ²³⁸ Z. Liu, W. Niu, H. Chu, T. Zhou, and Z. Niu, *BioResources* **13**, 3429 (2018).
- ²³⁹ J.L. Wu, J. Hong, and Q.Y. Han, *Chem. Rev.* **115**, 12251 (2015).
- ²⁴⁰ N.S. Rosli, S. Harun, J.M. Jahim, and R. Othaman, *Malaysian J. Anal. Sci.* **21**, 188 (2017).
- ²⁴¹ N.M. Nurazzi, M.R.M. Asyraf, M. Rayung, M.N.F. Norrrahim, S.S. Shazleen, M.S.A. Rani, A.R. Shafi, H.A. Aisyah, M.H.M. Radzi, F.A. Sabaruddin, R.A. Ilyas, E.S. Zainudin, and K. Abdan, *Polymers (Basel)*. **13**, (2021).

- ²⁴² R. Ramli, R.M. Yunus, M.D.H. Beg, and D.M.R. Prasad, *J. Compos. Mater.* **46**, 1275 (2012).
- ²⁴³ Z. Khan, S. Yusup, and M.M. Ahmad, *Int. J. Renew. Energy Res.* **1**, 7 (2011).
- ²⁴⁴ C. Rodriguez Correa, T. Otto, and A. Kruse, *Biomass and Bioenergy* **97**, 53 (2017).
- ²⁴⁵ T. Wang, M. Camps-Arbestain, B.P. Singh, R. Calvelo-Pereira, and C. Wang, *Soil Res.* **52**, 495 (2014).
- ²⁴⁶ A.F. Abdul Karim, H. Ismail, and Z. Mohamad Ariff, *IOP Conf. Ser. Mater. Sci. Eng.* **374**, (2018).
- ²⁴⁷ M.R. Anika Zafiah, M.A. M. Shafiq, K. Shaharuddin, B.S. Leong, Z. M. Taufiq, and M.L.F. Ahraz Sadrina, in *4th Int. Conf. Adv. Mater. Nanotechnol.* (Selangor, Malaysia, 2016).
- ²⁴⁸ N. Martin, S. Franntisek, F. Roman, T. Peter, J. Jaroslav, M. Natalia, and K. Jaroslav, *Met. Foam.* **1**, 15 (2017).
- ²⁴⁹ International Organization for Standardization, *ISO 11654: Acoustic – Sound Absorbers for Use in Building- Rating of Sound Absorption* (1997).
- ²⁵⁰ V. Rao and J. Johns, *J. Therm. Anal. Calorim.* **92**, 801 (2008).
- ²⁵¹ K. Damampai, S. Pichaiyut, S. Mandal, S. Wießner, A. Das, and C. Nakason, *Polymers (Basel)* **13**, (2021).
- ²⁵² N.A. Yunus, S.A. Mazlan, Ubaidillah, S.A. Abdul Aziz, S.T. Shilan, and N.A. Abdul Wahab, *Int. J. Mol. Sci.* **20**, 1 (2019).
- ²⁵³ A.E. Juve and J.R. Beatty, *Rubber Chem. Technol.* **28**, 1141 (1955).
- ²⁵⁴ T. Prasopdee and W. Smitthipong, *Polymers (Basel)* **12**, 1 (2020).
- ²⁵⁵ M.Y. Amir Hashim and A. Ikram, in *Int. Symp. Green Technol. Glob. Carbon Cycle Asia* (Nagaoka University of Technology, Japan., n.d.).
- ²⁵⁶ M. Asrul, M. Othman, M. Zakaria, Fauzi, and 4, *Int. J. Eng. Sci. Invent.* **2**, 38 (2013).
- ²⁵⁷ A.F.A. Karim, H. Ismail, and Z.M. Ariff, *BioResources* **11**, 1080 (2016).
- ²⁵⁸ J.S. Yeo, J.H. Lee, and S.H. Hwang, *Compos. Part B Eng.* **130**, 167 (2017).
- ²⁵⁹ C. Thongpin, A. Muanwong, J. Yanyongsak, and P. Lorphaitoon, *Mater. Sci. Forum* **889 MSF**, 45 (2017).
- ²⁶⁰ M.S.F. Samsudin, Z.M. Ariff, and A. Ariffin, *AIP Conf. Proc.* **1835**, (2017).
- ²⁶¹ C. Blanchard, T. Weisser, R. Barbeau, E. Aubry, A.-I. Mallet-da Costa, and A.-I. Mallet-Da Costa, in *Surveillance, Vishno AVE Conf.* (INSA-Lyon, Université de Lyon, France, 2019).
- ²⁶² H.J. Qi and M.C. Boyce, *Mech. Mater.* **37**, 817 (2005).
- ²⁶³ M. Dalen and S. Mador, *Int. Res. J. Pure Appl. Chem.* **14**, 1 (2017).
- ²⁶⁴ C.H. Sung, K.S. Lee, J.H. Kim, M.S. Kim, and H.M. Jeong, *Macromol. Res.* **15**, 443 (2007).
- ²⁶⁵ G.V.F. Henrique, Displacement and Force Transmissibility in Structures and Multilayer Supports with Applications to Vibration Isolation, MSc. Thesis. Universidade Tecnica De Lisboa, Lisbon, Portugal, 2011.
- ²⁶⁶ C.R. Mehta and V.K. Tewari, *J. Terramechanics* **47**, 401 (2010).
- ²⁶⁷ W. Elmadih, Additively Manufactured Lattice Structures for Vibration Attenuation, PhD thesis. University of Nottingham, Nottingham, UK., 2019.